



DISSERTATION

Synthesis and reactivity of molybdenum, iron, and palladium complexes with mono-, bi- and tridentate phosphorus and nitrogen donor ligands

ausgeführt
zum Zwecke der Erlangung des akademischen Grades
eines Doktors der technischen Wissenschaften

unter der Leitung von
Ao. Univ. Prof. Dipl.-Ing. Dr. techn. Karl Kirchner
E163 – Institut für Angewandte Synthesechemie
Abteilung Metallorganische Chemie

eingereicht an der Technischen Universität Wien
Fakultät für Technische Chemie

von
DI Julia Wiedermann
Matrikelnummer 9725682
Ulmenweg 11
2301 Groß-Enzersdorf

Wien, am 25. März 2008

Abstract

The first part of this work describes the synthesis of two classes of ligands. First, the concept of aminophosphine-based tridentate PNP pincer ligands was extended to include tridentate PNP ligands based on N-heterocyclic diamines such as 1,3,5-triazine and bidentate PN ligands based on 2-aminopyridine. In most cases these compounds react readily with electrophilic chlorophosphines and –phosphites in the presence of base. The respective chlorophosphines are commercially available, the chlorophosphites are easily derived from PCl_3 and the corresponding diols. Employing this methodology even chiral derivatives can be obtained when *e.g.* dimethyl tartrate is used as diol. The second class covers ligands prepared *via* a condensation reaction of 2,5-thiophenedicarboxaldehyde and 2-thiophenecarboxaldehyde with various amines.

The second part of this work comprises the synthesis, characterisation and reactivity of molybdenum, iron, and palladium complexes of these ligands.

In the case of molybdenum, octahedral tricarbonyl PNP complexes were obtained under mild conditions by reaction of $\text{Mo(CO)}_3(\text{CH}_3\text{CN})_3$ (prepared *in situ* by refluxing Mo(CO)_6 in acetonitrile) with the respective pincer ligands. These zerovalent complexes undergo oxidative addition with halogens leading to heptacoordinated monocationic complexes. Tetracarbonyl complexes with the bidentate PN ligands were obtained by heating equimolar amounts of Mo(CO)_6 and the ligand in toluene. These complexes show enhanced reactivity towards iodine—which results in the cleavage of all carbonyl ligands—and undergo oxidative addition with allyl bromide. Attempts to obtain vinylidene compounds by reacting the complexes with phenylacetylene failed as well as the reaction with methyl iodide or crotyl bromide.

Upon reaction of the PNP pincer ligands with $[\text{Fe(H}_2\text{O)}_6](\text{BF}_4)_2$ dicationic octahedral tris(acetonitrile) complexes were obtained. Up to three of the acetonitrile ligands are labile and can be replaced by chelating nitrogen donor ligands or carbon monoxide. The catalytic activity of the complexes was tested in the coupling of aromatic aldehydes with ethyl diazoacetate. It was found that the formation of 3-hydroxyacrylates is favoured in comparison to the β -ketoester. In addition, a plausible mechanism for the catalytic cycle was proposed supported by mechanistic investigations based on DFT/B3LYP calculations.

Starting from Pd(cod)Cl₂ and PNP pincer ligands tetracoordinated, cationic palladium complexes with different counterions could be obtained. The 2,5-thiophenedicarboxaldehyde-based ligands proved to be too rigid to coordinate in a tridentate fashion. When reacted with Pd(cod)Cl₂ two 2-thiophenecarboxaldehyde-based ligands were observed to coordinate only *via* the imine or amine nitrogen atom, forming neutral square planar complexes. The catalytic activity of these compounds in the Suzuki-Miyaura coupling of aryl bromides with phenyl boronic acid was investigated and was found to be comparable to related α - and β -diimine systems. Qualitatively, it was found that complexes with imine ligands featuring sterically demanding substituents such as mesityl are clearly better catalysts.

Kurzfassung

Der erste Teil dieser Arbeit beschreibt die Synthese zweier Ligandenklassen. Zunächst wurde das Konzept der auf Aminophosphinen basierenden tridentaten PNP Pincer-Liganden erweitert und schließt nun auch auf N-heterozyklischen Diaminen wie z. B. 1,3,5-Triazin basierende tridentate PNP-Liganden und auf 2-Aminopyridin basierende bidentate PN-Liganden ein. Diese Verbindungen reagieren in Gegenwart von Base in vielen Fällen bereitwillig mit elektrophilen Chlorphosphinen und -phosphiten. Die entsprechenden Chlorphosphine sind käuflich zu erwerben, die Chlorphosphite können leicht aus PCl_3 und dem jeweiligen Diol hergestellt werden. Bei der Verwendung von z. B. Dimethyltartrat sind auf diese Weise auch chirale Derivate einfach zugänglich. Die zweite Klasse umfasst Liganden, die über eine Kondensationsreaktion von 2,5-Thiophendicarboxaldehyd und 2-Thiophencarboxaldehyd mit verschiedenen Aminen hergestellt wurden.

Der zweite Teil dieser Arbeit umfasst die Synthese, Charakterisierung und Reaktivität von Molybdän-, Eisen- und Palladiumkomplexen dieser Liganden.

Im Falle von Molybdän wurden oktaedrische Tricarbonyl-PNP-Komplexe unter milden Bedingungen durch Reaktion von $\text{Mo(CO)}_3(\text{CH}_3\text{CN})_3$ (*in situ* hergestellt durch Erhitzen von Mo(CO)_6 in Acetonitril) mit den entsprechenden Pincer-Liganden erhalten. Diese Komplexe mit Molybdän der Oxidationsstufe Null gehen oxidative Additionsreaktionen mit Halogenen ein, was zur Bildung von heptakoordinierten monokationischen Komplexen führt. Aus den bidentaten PN-Liganden wurden durch Erhitzen äquimolarer Mengen von Mo(CO)_6 und Ligand in Toluol Tetracarbonyl-Komplexe hergestellt. Diese Komplexe zeigen verstärkte Reaktivität gegenüber Iod – was zur Abspaltung aller Carbonylliganden führt – und gehen eine oxidative Additionsreaktion mit Allylbromid ein. Versuche zur Herstellung von Vinylidenkomplexen über eine Reaktion mit Phenylacetylen scheiterten ebenso wie die Reaktion mit Methyljodid oder Crotylbromid.

Durch Reaktion der PNP-Pincer-Liganden mit $[\text{Fe(H}_2\text{O)}_6](\text{BF}_4)_2$ wurden dikationische oktaedrische Tris(Acetonitril)-Komplexe erhalten. Bis zu drei der Acetonitril-Liganden sind labil und können durch chelatisierende Stickstoff-Donor-Liganden oder Kohlenstoffmonoxid substituiert werden. Die katalytische Aktivität dieser Komplexe in der Kupplung von aromatischen Aldehyden mit Ethyldiazoacetat wurde untersucht. Es

wurde festgestellt, dass die Bildung von 3-Hydroxyacrylaten vor jener der β -Ketoester begünstigt ist. Zusätzlich wurde ein plausibler Mechanismus für den Katalysezyklus vorgeschlagen, der sich auf mechanistische Untersuchungen mithilfe von DFT/B3LYP-Berechnungen stützt.

Ausgehend von $\text{Pd}(\text{cod})\text{Cl}_2$ und PNP-Pincer-Liganden wurden tetrakoordinierte, kationische Palladiumkomplexe mit verschiedenen Gegenionen erhalten. Die auf 2,5-Thiophendicarboxaldehyd basierenden Liganden stellten sich als zu unflexibel heraus, so dass keine tridentate Koordination beobachtet werden konnte. Lässt man $\text{Pd}(\text{cod})\text{Cl}_2$ mit zwei auf 2-Thiophencarboxaldehyd basierenden bidentaten Liganden reagieren, koordinieren diese nur über das Imin- oder Amin-Stickstoffatom und bilden neutrale quadratisch-planare Komplexe. Die katalytische Aktivität dieser Verbindungen in der Suzuki-Miyaura-Kupplung von Arylbromiden mit Phenylboronsäure wurde untersucht und als mit verwandten α - und β -Diiminsystemen vergleichbar erkannt. Qualitativ wurde festgestellt, dass Komplexe, die sterisch anspruchsvolle Iminliganden beinhalten, sich deutlich besser als Katalysatoren eignen.

Contents

1	Introduction and scope	1
2	General considerations	5
2.1	Pincer ligands	5
2.2	Phosphines	7
2.3	Transition metal pincer complexes	8
2.3.1	Binding modes and coordination geometries	8
2.3.2	Binding modes of thiophene	10
2.3.3	Synthetic approaches to transition metal pincer complexes	10
3	Results and discussion	13
3.1	Ligands	13
3.1.1	Introduction	13
3.1.2	Building blocks	16
3.1.3	1,3,5-Triazine-based PNP ^T pincer ligands	17
3.1.4	Pyrimidine-based PNP ^P pincer ligands	19
3.1.5	Pyridine-based PNP pincer ligands	20
3.1.6	Pyridine-based PN ligands	21
3.1.7	Thiophene-based NSN pincer ligands	24
3.1.8	Thiophene-based imine SN ligands	26
3.1.9	Thiophene-based amine SN ligands	27
3.2	Molybdenum complexes	28
3.2.1	Introduction	28
3.2.2	Molybdenum(0) PNP ^T complexes	30
3.2.3	Molybdenum(0) PNP ^P complexes	31
3.2.4	Molybdenum(0) PN complexes	32
3.2.5	Reactivity of Molybdenum(0) complexes	41
3.3	Iron complexes	48
3.3.1	Introduction	48
3.3.2	Iron(II) PNP ^T complexes	49
3.3.3	Iron(II) PNP ^P complexes	55
3.3.4	Lability of the acetonitrile ligands	56
3.3.5	Iron(II) catalysed coupling of aromatic aldehydes with ethyl diazoacetate . .	59

3.4	Palladium complexes	63
3.4.1	Introduction	63
3.4.2	Palladium(II) PNP ^T complexes	64
3.4.3	Palladium(II) PNP complexes	65
3.4.4	Palladium(II) NSN complexes	68
3.4.5	Palladium(II) imine SN complexes	68
3.4.6	Palladium(II) amine SN complexes	72
3.4.7	Palladium catalysed Suzuki-Miyaura coupling	72
4	Summary	79
5	Experimental	80
5.1	General remarks	80
5.2	Building blocks and precursors	81
5.3	Ligands	86
5.3.1	PNP ^T ligands	86
5.3.2	PNP ^P ligands	89
5.3.3	PN ligands	90
5.3.4	NSN ligands	96
5.3.5	SN imine ligands	99
5.3.6	SN amine ligands	101
5.4	Molybdenum complexes	102
5.4.1	Molybdenum PNP ^T complexes	102
5.4.2	Molybdenum PNP ^P complexes	105
5.4.3	Molybdenum PN complexes	106
5.5	Iron complexes	114
5.5.1	Iron PNP ^T complexes	114
5.5.2	Iron PNP ^P complexes	118
5.6	Palladium complexes	120
5.6.1	Palladium PNP ^T complexes	120
5.6.2	Palladium SN imine complexes	121
5.6.3	Palladium SN amine complexes	124
5.7	Catalytic reactions	125
5.7.1	Iron(II) catalysed coupling of aromatic aldehydes with EDA	125
5.7.2	Palladium(II) catalysed Suzuki-Miyaura coupling	125
A	List of abbreviations	127
B	Crystallographic data	128
	References	132

List of Figures

1.1	General structure of pincer complexes	1
2.1	Schematic structure of pincer ligands	5
2.2	Examples of different types of pincer ligands	6
2.3	Molecular orbitals of phosphines and phosphine complexes	6
2.4	Classification of different phosphines and phosphites	7
2.5	Binding modes of NCN pincer complexes	9
2.6	Coordination geometries of pincer complexes	9
2.7	Known types of thiophene binding in transition metal complexes	10
3.1	Examples of PNP ligands	15
3.2	<i>N</i> -alkylated PNP ligands	15
3.3	Chlorophosphites prepared from PCl ₃ and the respective diol	16
3.4	1,3,5-Triazine-based PNP ^{TR} -Ph pincer ligands	18
3.5	Pyrimidine-based PNP ^{PCl} -R pincer ligands	20
3.6	Pyridine-based PN-R ligands	22
3.7	Thiophene based NSN-R pincer ligands	25
3.8	Thiophene-based imine SN-R ligands	26
3.9	Mo(PNP)(L _n) and Mo(PN)(L _n) complexes	28
3.10	Mo(PNP ^{TR} -Ph)(CO) ₃ complexes	31
3.11	Phosphine Mo(PN-R)CO ₄ complexes	33
3.12	Phosphite Mo(PN-R)CO ₄ complexes	33
3.13	Stretching vibrations of the basal and apical carbonyl ligands	36
3.14	Structural view of Mo(PN-Ph)(CO) ₄	37
3.15	Structural view of Mo(PN- ⁱ Pr)(CO) ₄	38
3.16	Structural view of Mo(PN- ^t Bu)(CO) ₄	39
3.17	Structural view of Mo(PN-ETOL)(CO) ₄	40
3.18	Examples for achiral and chiral Schrock catalysts	41
3.19	Structural view of Mo(O-PN-Ph)(O)I ₄	44
3.20	Structural view of Mo(PN- ⁱ Pr)(η^3 -allyl)(CO) ₂ Br	46
3.21	First examples of NNN iron complexes with catalytic activities in ethylene polymerisation	48
3.22	[Fe(PNP ^{TR} -Ph)(CH ₃ CN) ₃](BF ₄) ₂ complexes	50

3.23	Structural view of $[\text{Fe}(\text{PNP}^{\text{TPh}}\text{-Ph})(\text{CH}_3\text{CN})_3](\text{BF}_4)_2$	52
3.24	Structural view of $[\text{Fe}(\text{PNP}^{\text{TMe}}\text{-Ph})(\text{CH}_3\text{CN})_3](\text{BF}_4)_2$	53
3.25	Structural view of $[\text{Fe}(\text{PNP}^{\text{TOEt}}\text{-Ph})(\text{CH}_3\text{CN})_3](\text{BF}_4)_2$	54
3.26	$[\text{Fe}(\text{PNP}^{\text{PCl}}\text{-R})(\text{CH}_3\text{CN})_3](\text{BF}_4)_2$ complexes	56
3.27	Examples of palladium pincer complexes	63
3.28	Examples of palladium thiophene imine complexes	64
3.29	Structural view of $[\text{Pd}(\text{PNP}\text{-Ph})\text{Cl}]\text{Cl}$	67
3.30	Pd imine complexes $\text{Pd}(\text{SN}\text{-R})_2\text{Cl}_2$	69
3.31	Structural view of $\text{Pd}(\text{SN}\text{-Mes})_2\text{Cl}_2$	70
3.32	Structural view of $\text{Pd}(\text{SN}\text{-}^n\text{Pr})_2\text{Cl}_2$	71
3.33	Structural view of $\text{Pd}(\text{SN}^{\text{H}}\text{-Ph})_2\text{Cl}_2$	73

List of Tables

2.1	$^{31}\text{P}\{^1\text{H}\}$ NMR chemical shifts and cone angles of phosphines and phosphites	8
3.1	$^{31}\text{P}\{^1\text{H}\}$ NMR shifts of the PN-R ligands and ClPR_2	23
3.2	Selected ^1H NMR shifts of the PN-R ligands	24
3.3	Selected NMR shifts of the NSN-R ligands	25
3.4	Selected NMR shifts of the SN-R ligands	27
3.5	Selected ^1H NMR shifts of the $\text{Mo}(\text{PN-R})(\text{CO})_4$ complexes	34
3.6	$^{31}\text{P}\{^1\text{H}\}$ NMR shifts of the $\text{Mo}(\text{PN-R})(\text{CO})_4$ complexes	35
3.7	Selected $^{13}\text{C}\{^1\text{H}\}$ NMR shifts of the $\text{Mo}(\text{PN-R})(\text{CO})_4$ complexes	35
3.8	Calculated stretching vibration frequencies of CO ligands	36
3.9	Yields of the coupling of aromatic aldehydes with EDA	60
3.10	Selected NMR shifts of the $\text{Pd}(\text{SN-R})_2\text{Cl}_2$ complexes	71
3.11	Reaction conditions for the Suzuki-Miyaura coupling	76
3.12	Yields of the Suzuki coupling catalysed by $\text{Pd}(\text{SN-R})_2\text{Cl}_2$ complexes	77
3.13	Yields of the Suzuki coupling catalysed by $\text{Pd}(\text{SN-Mes})_2\text{Cl}_2$	78
A.1	List of abbreviations	127
B.1	Details for structure determination 1	128
B.2	Details for structure determination 2	129
B.3	Details for structure determination 3	130
B.4	Details for structure determination 4	131

List of Schemes

1.1	Goals of this work 1	3
1.2	Goals of this work 2	4
2.1	Direct metalation of pincer ligands	11
2.2	Synthetic routes to ECE pincer complexes	11
3.1	Synthesis of methylene bridged PNP ligands	13
3.2	Synthesis of amino bridged PNP ligands	14
3.3	One-step synthesis of chlorophosphites	16
3.4	Synthesis of 1,3,5-triazine-based PNP ^{TR} -Ph pincer ligands	17
3.5	Synthesis of pyrimidine-based PNP ^{PCl} -R pincer ligands	19
3.6	Synthesis of the pyridine-based 2PN2P-Ph ligand	21
3.7	Synthesis of pyridine-based PN-R ligands	21
3.8	Synthesis of thiophene-based NSN-R pincer ligands	24
3.9	Synthesis of thiophene-based imine SN-R ligands	26
3.10	Synthesis of the amine ligand SN ^H -Ph	27
3.11	Preparation of zerovalent molybdenum complexes <i>mer</i> -Mo(PNP-R)(CO) ₃ . .	29
3.12	Mo(L)(CO) ₃ complexes with facial and meridional arrangement of the carbonyl ligands	29
3.13	Synthesis of the Mo(PNP ^{TR} -Ph)(CO) ₃ complexes	30
3.14	Synthesis of the Mo(PNP ^{PCl} -Ph)(CO) ₃ complex	31
3.15	Synthesis of Mo(PN-R)(CO) ₄ complexes	32
3.16	Reaction of Mo(PNP- ⁱ Pr)(CO) ₃ with halogens	42
3.17	Reaction of Mo(PN-Ph)(CO) ₄ with iodine	43
3.18	Reaction of Mo(PN- ⁱ Pr)(CO) ₄ with various substrates	45
3.19	Synthesis of [Fe(H ₂ O) ₆](BF ₄) ₂	49
3.20	Synthesis of [Fe(PNP ^{TR} -Ph)(CH ₃ CN) ₃](BF ₄) ₂ complexes	49
3.21	Synthesis of [Fe(PNP ^{PCl} -R)(CH ₃ CN) ₃](BF ₄) ₂ complexes	55
3.22	Lability of the acetonitrile ligands of [Fe(PNP-Ph)(CH ₃ CN) ₃](BF ₄) ₂	57
3.23	Lability of the acetonitrile ligands of [Fe(PNP ^{TPH} -Ph)(CH ₃ CN) ₃](BF ₄) ₂	58
3.24	Lewis acid catalysed formation of 3-hydroxyacrylates and β -ketoesters	59
3.25	Proposed mechanism for the coupling of aromatic aldehydes with EDA	61
3.26	Synthesis and counterion exchange of [Pd(PNP ^{TPH} -Ph)Cl] ⁺	65

3.27	Reaction of the 2PN2P ligand with Mo(CO) ₄ (ndb)	66
3.28	Unexpected formation of [Pd(PNP-Ph)Cl]Cl	67
3.29	Attempts for the synthesis of Pd NSN complexes	68
3.30	Synthesis of Pd imine complexes Pd(SN-R) ₂ Cl ₂	68
3.31	Attempts to synthesise palladacyclic complexes	70
3.32	Synthesis of the Pd amine complex Pd(SN ^H -Ph) ₂ Cl ₂	72
3.33	General mechanism of the Suzuki-Miyaura coupling	75
3.34	The Suzuki-Miyaura coupling of aryl bromides with phenyl boronic acid	76

1 Introduction and scope

Pincer type ligands and complexes were first synthesised in the late 1970s by Bernard L. Shaw and coworkers and have ever since received considerable interest in organic as well as organometallic chemistry.^{1,2} Their importance has been pointed out in several reviews.³⁻⁵

The general structure of these tridentate so-called pincer ligands, named after their particular coordination mode to metal centres, typically features an aromatic backbone (benzene, pyridine) bound to two-electron donor groups **E** by a spacer **A**. Pincer ligands coordinate to the metal centre *via* the two-electron donor groups and metal-carbon (benzene-based pincer complexes) or metal-nitrogen (pyridine-based pincer complexes) σ -bonds (Figure 1.1).

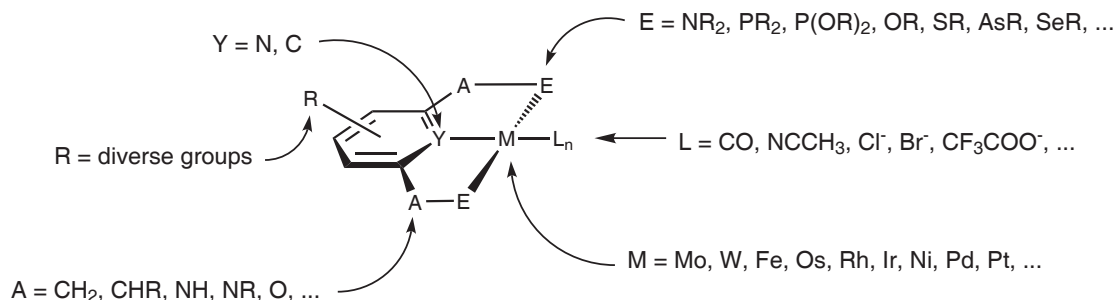


Figure 1.1: General structure of pincer complexes

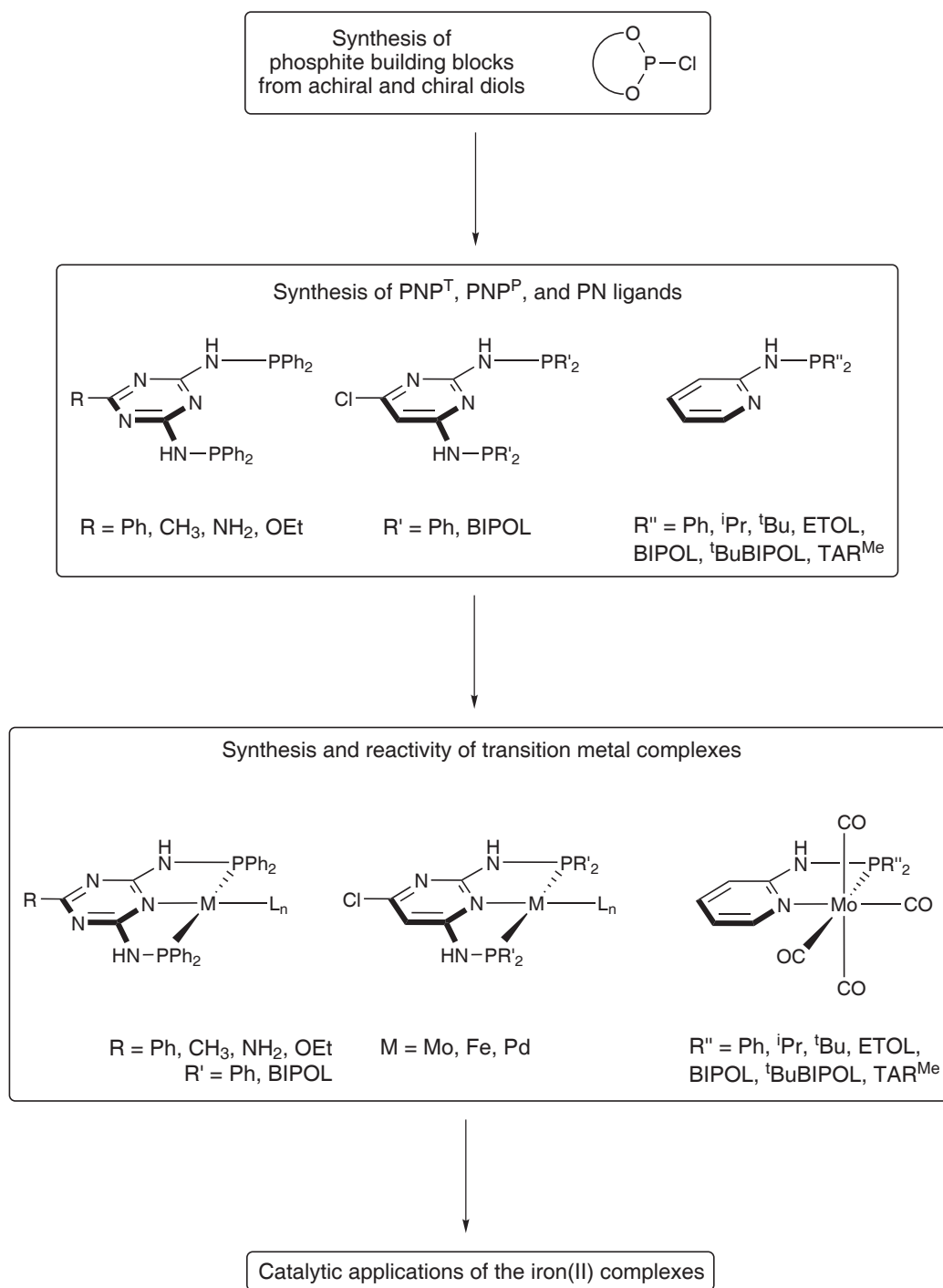
By variation of the aromatic backbone, the donor groups **E** or the spacer groups **A** the steric, electronic, and stereochemical parameters of pincer ligands can be tuned. Moreover, different metals and counterions provide further access to an enhancement of the complex reactivity, stability, or reaction selectivity.

Throughout this work ligands will be named primarily after their coordinating atoms, thus the pincer ligand depicted in Figure 1.1 would be of EYE-type. The ligands with *N*-heterocyclic backbones and phosphorus donor atoms described in here are of the PNP-type and are specified with a superscript letter "T" for 1,3,5-triazine and "P" for pyrimidine. Furthermore, the superscript contains information on the *p*-substituent of

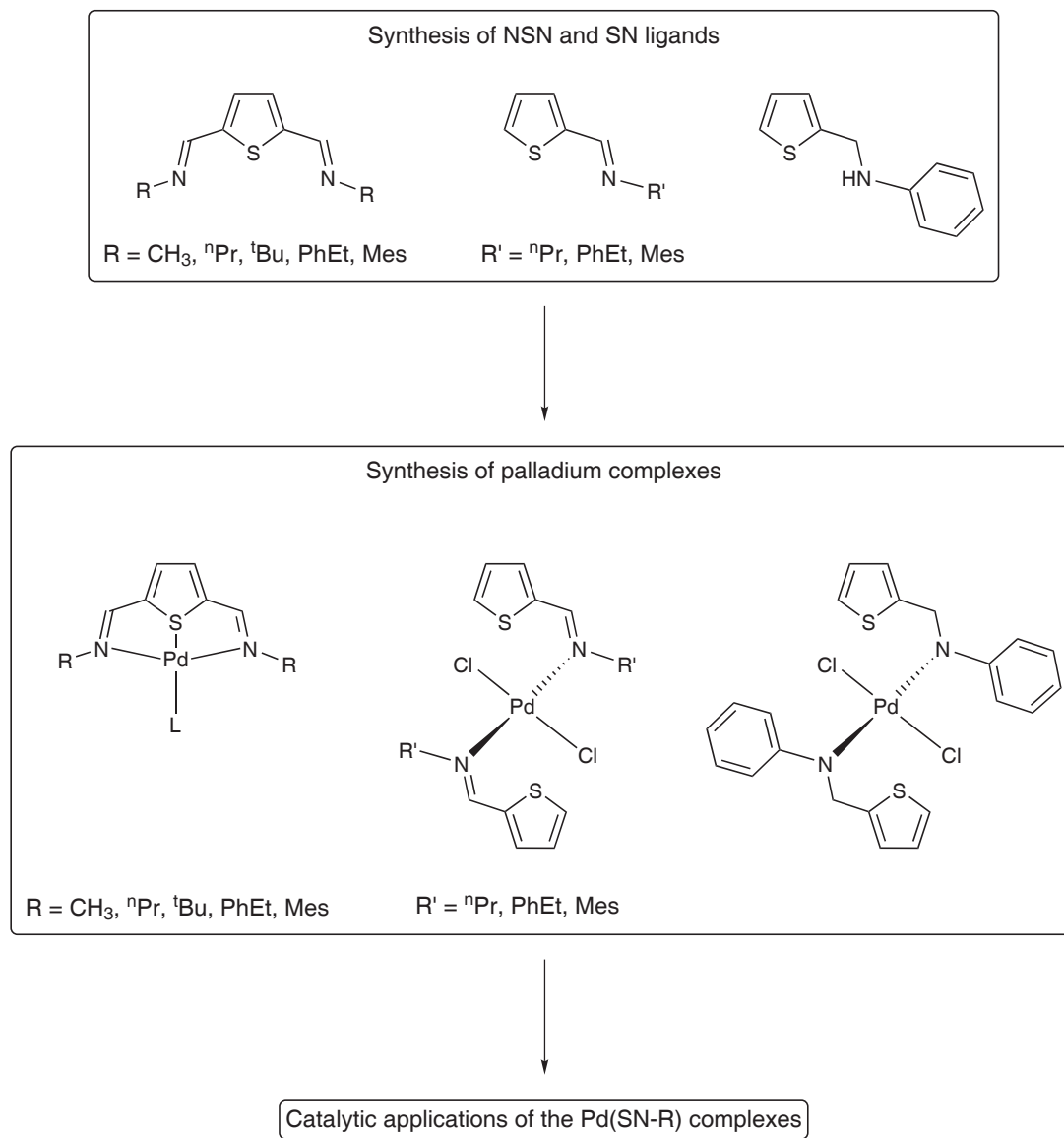
this heterocycle. Separated by a hyphen follows the description of the phosphine. In the case of the thiophene-based ligands the nomenclature follows the same pattern with the substituent on the imine nitrogen separated by a hyphen.

The objectives of this work are depicted in Schemes 1.1 and 1.2. With respect to *N*-heterocyclic-based ligands and complexes the first task was to prepare chlorophosphite building blocks from achiral and chiral diols. These electrophilic phosphites and commercially available phosphines were to be reacted with different aromatic backbones, such as 1,3,5-triazine, pyrimidine, 2,6-diaminopyridine, and 2-aminopyridine in order to synthesise and characterise an array of tridentate PNP^T, PNP^P, and 2PN2P pincer ligands and of bidentate PN ligands. Consecutively, the reactivity of these ligands towards different molybdenum, iron, and palladium precursors was to be investigated. The reactivity of some of the molybdenum complexes in oxidative addition reactions and the catalytic activity of the iron pincer complexes in the Lewis acid catalysed coupling of aromatic aldehydes with ethyl diazoacetate was to be screened.

Thiophene-based ligands were to be prepared from thiophenemono- or dialdehyde by reaction with various amines. The ligands were to be reacted with several palladium precursors and screened with respect to their coordination behaviour. Additionally, the catalytic activity of some of the complexes was to be investigated in the Suzuki-Miyaura coupling of aryl halides with phenylboronic acid.



Scheme 1.1: Goals of this work 1



Scheme 1.2: Goals of this work 2

2 General considerations

2.1 Pincer ligands

Pincer ligands consist of an aromatic backbone, coordinating to the metal *via* the *ipso* carbon or nitrogen atom, which is *ortho*, *ortho*-disubstituted with two two-electron donor heteroatom groups **E**, which coordinate to the metal centre themselves (Figure 2.1). The substituents **E** can be connected to the central aromatic backbone by different spacer groups **A**, such as methylene groups ($-\text{CH}_2-$), amines ($-\text{NH}-$ or $-\text{NR}-$) or oxygen atoms ($-\text{O}-$). The aromatic ring can be either a pyridine ring ($\text{Y} = \text{N}$) or a benzene ring ($\text{Y} = \text{C}$) with optional substituents, particularly in the *p*-position; thus, both neutral and anionic pincer ligands are accessible. As for the neutral lone pair donors **E**, they are typically amines ($-\text{NR}_2$), phosphines ($-\text{PR}_2$), phosphites ($-\text{P}(\text{OR})_2$), ethers ($-\text{OR}$), thioethers ($-\text{SR}$), arsines ($-\text{AsR}_2$), selenoethers ($-\text{SeR}$) and even *N*-heterocyclic carbenes (NHC). The donor groups can be identical, anyway, systems with two different donor atoms **E** have been reported.⁶⁻⁸

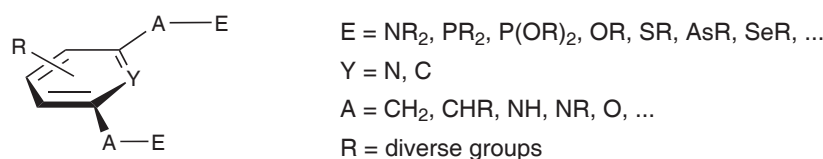


Figure 2.1: Schematic structure of pincer ligands

Variation of either of these groups **E**, **A**, and **Y** gives access to a wide variety of PCP, NCN, PNP, CNC, PCN, ... pincer ligands⁹⁻¹¹ which in combination with the appropriate metal precursor can be customised for catalytic applications, reactivity examinations and explorative chemistry. Some examples for different types of pincer ligands are depicted in Figure 2.2.^{2,9-12}

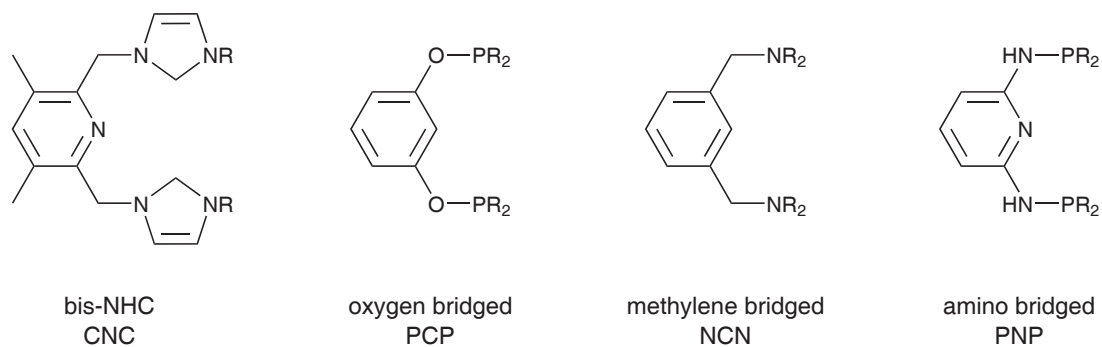


Figure 2.2: Examples of different types of pincer ligands

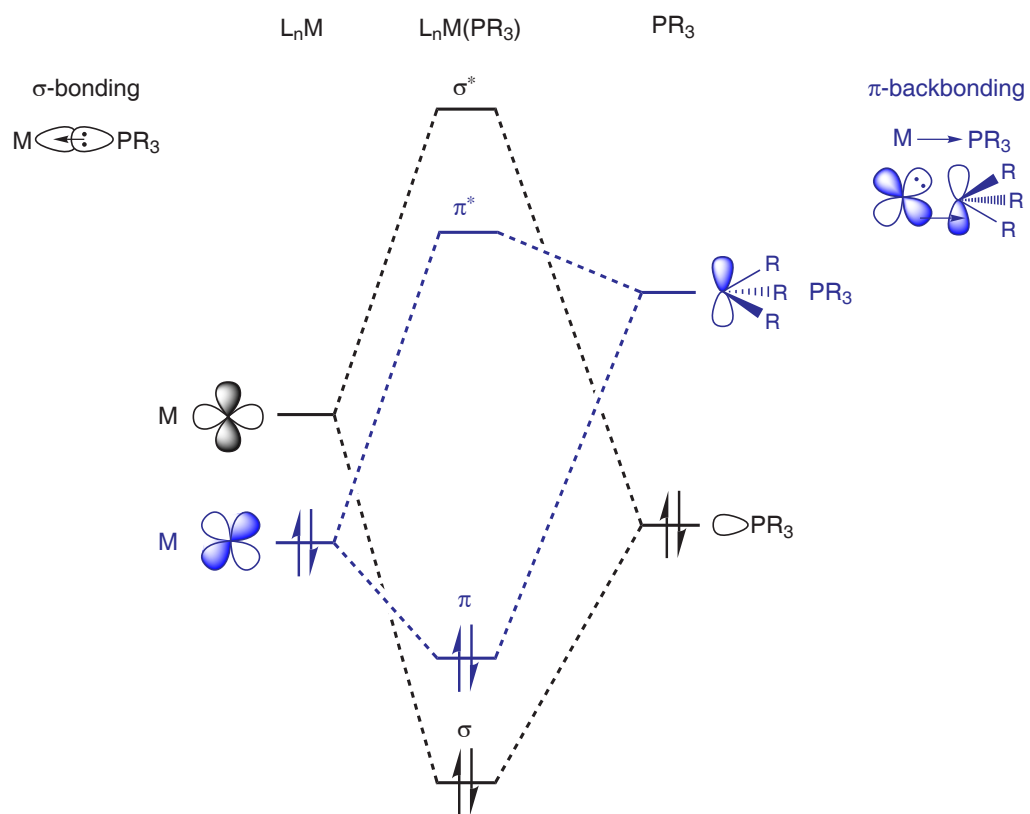


Figure 2.3: Molecular orbitals of phosphines and phosphine complexes

2.2 Phosphines

In organometallic chemistry, tertiary phosphines of the type PR_3 ($\text{R} = \text{alkyl, aryl, OR}', \text{NR}'_2, \text{Cl, Br, H}$) were found to be important coligands in catalytic reactions. Upon appropriate choice of the substituents the electronic, steric and stereochemical properties of the phosphine ligands can be tuned.

These ligands act as neutral two-electron σ -donor/ π -acceptor with the σ -bonding being developed between the lone pair of the ligand and an empty d-orbital of the metal. A π -backbonding similar to that of carbonyl ligands comes about between an occupied d-orbital of the metal and an empty σ^* -orbital of the ligand (Figure 2.3).

Along with the electronic properties of the substituents R on the tertiary phosphine the donor/acceptor properties of the ligands are modified. Electron withdrawing substituents on the phosphine decrease its σ -donation capacity and strengthen the π -backbonding by reducing the energy of the π^* -orbital. Thus, phosphines can be arranged according to their increasing π -acidity and decreasing σ -donating properties (Figure 2.4). Alkylphosphines form the strongest σ -bonds to the metal centre, and trifluorophosphine, PF_3 , is a strong π -acceptor comparable to carbon monoxide.

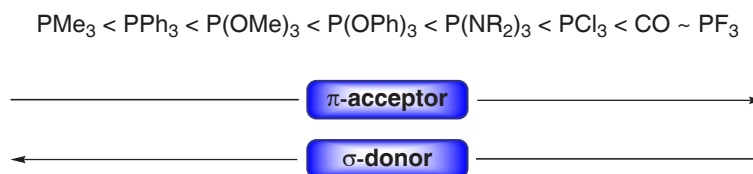


Figure 2.4: Classification of different phosphines and phosphites according to their donor/acceptor properties

A classification in which the donor/acceptor properties of a great number of monodentate phosphines were investigated was published by Tolman in 1977.¹³ By substituting one carbonyl group of Ni(CO)_4 with different phosphines and by comparing the stretching frequencies of the remaining carbonyl groups with infrared spectroscopy, it is possible to reason about the electron density at the metal centre, and therefore about the π -backbonding. The stronger the backbonding, the weaker becomes the C-O triple bond, and the carbonyl stretching is shifted towards smaller wave numbers.

This paper also contains the implementation of a parameter to describe the space occupied by a coordinated phosphine (Tolman's cone angle Θ). For symmetric ligands, this parameter is defined as the apex angle of a cylindrical cone, centered 2.28 Å from the centre of the phosphorus atom, which just touches the van der Waals radii of the out-

ermost atoms of the model. These cone angles range from 87 ° for PH₃ to 182 ° for the sterically demanding P^tBu₃.

Another important advantage of phosphines is their detectability by ³¹P{¹H} NMR spectroscopy. The NMR active isotope is a spin- $\frac{1}{2}$ -nucleus and because of its 100 % natural occurrence this method is highly sensitive, despite the fact that the sensitivity of the nucleus is only 6.6% of the one of ¹H. When coordinated to a metal centre the phosphorus is normally deshielded and in combination with the coupling to ¹H and ¹³C nuclei NMR spectroscopy is a powerful instrument for the characterization of phosphine containing ligands and complexes. Noticeably, the ³¹P{¹H} NMR shift of phosphines depends on the steric parameter Θ ; the cone angles increase with a downfield shift of δ (³¹P). The values of the cone angles and of the ³¹P{¹H} NMR resonances of several phosphines and phosphites are summarised in Table 2.1.

Entry	PR ₃	³¹ P{ ¹ H} NMR (δ [ppm])	Θ °
1	PH ₃	−240	87
2	PF ₃	97	104
3	PMe ₃	−62	118
4	PCl ₃	220	124
5	PEt ₃	−20	132
6	PPr ₃	−33	132
7	PPh ₃	−6	145
8	P ⁱ Pr ₃	17	160
9	PCy ₃	11	170
10	P ^t Bu ₃	61	182
11	P(OMe) ₃	140	107
12	P(OEt) ₃	138	109
13	P(O ⁱ Pr) ₃	137	130
14	P(O ^t Bu) ₃	138	172

Table 2.1: ³¹P{¹H} NMR chemical shifts and cone angles of phosphines and phosphites

2.3 Transition metal pincer complexes

2.3.1 Binding modes and coordination geometries

Pincer ligands, being tridentate ligands, in most cases coordinate in a terdentate mode to the metal centre. For NCN pincer complexes binding modes other than terdentate have

been observed, reaching from $\kappa^1\text{-C}$ over $\kappa^2\text{-N,C}$ to $\kappa^3\text{-N,C,N}$.^{3,14–16} If those NCN ligands coordinate in a ternary mode, they usually adopt meridional geometry; only in very few cases a facial geometry has been observed. Examples for the different binding modes in NCN pincer complexes are depicted in Figure 2.5.

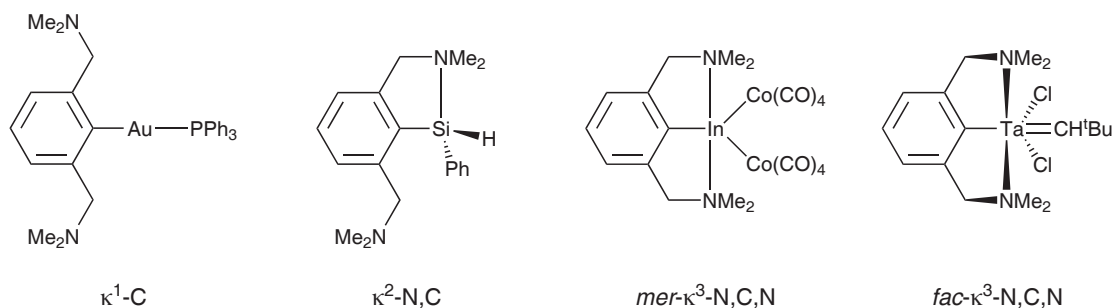


Figure 2.5: Binding modes of NCN pincer complexes

In the case of the PNP ligands described in this work, the most frequently observed coordination mode is the meridional $\kappa^3\text{-PNP}$ mode, in which the ligand binds to the metal centre in a terdentate manner as a six electron donor. In this geometry the two phosphorus atoms are *trans* to each other and the aromatic backbone is forced into a conformation coplanar to the coordination plane of d^8 square-planar metal centres (Ni^{II} , Pd^{II} , Pt^{II}) or to the central plane of d^6 octahedral metal geometries (Mo^0 , Fe^{II} , Ru^{II} , Ir^{III}) (see Figure 2.6).

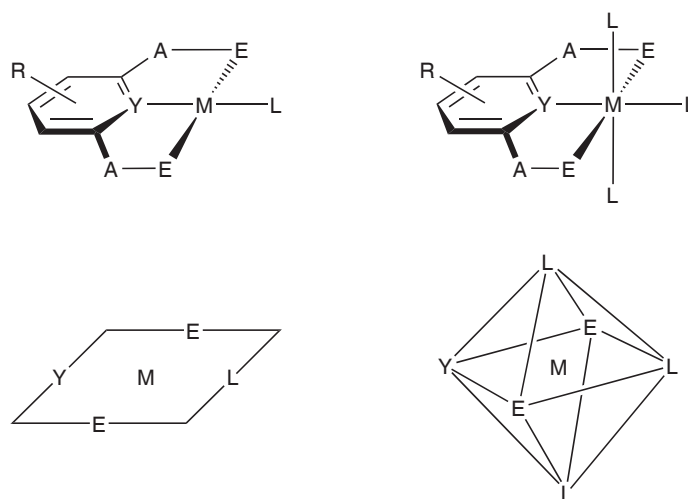


Figure 2.6: Coordination geometries of pincer complexes

2.3.2 Binding modes of thiophene

Thiophene is known to be able to coordinate in various modes to transition metals. In mononuclear complexes S-bound, η^2 -bound, η^4 -bound, and η^5 -bound thiophene has been observed. Moreover, also bridging modes with two (η^4 , S- μ^2 -bound) or three (η^4 , S- μ^3 -bound) metal centres are described in the literature.^{17,18} In some cases, the transition metal is inserted into a thiophene C-S bond.¹⁹

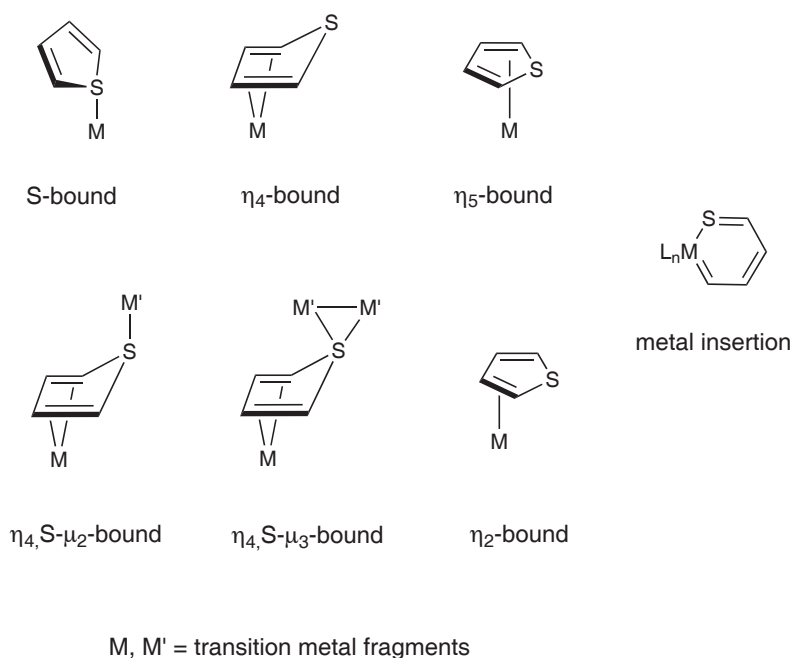


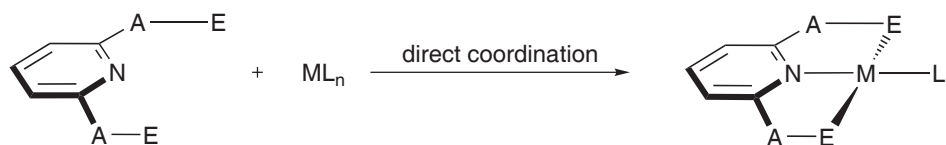
Figure 2.7: Known types of thiophene binding in transition metal complexes

Thiophene based pincer ligands are hardly found in the literature. In most cases the thiophene sulfur is not coordinated to the metal centre but the thiophene moiety acts as spacer group.²⁰

2.3.3 Synthetic approaches to transition metal pincer complexes

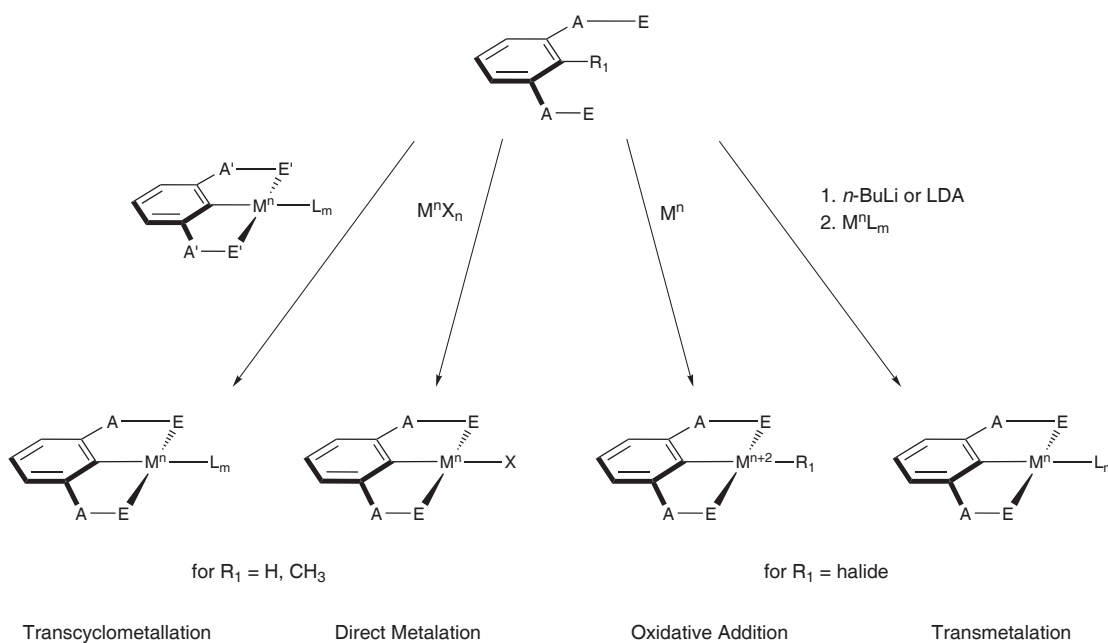
For the metalation of pincer ligands several methods have been developed. The appropriate method depends strongly on the transition metal and the donor groups of the pincer ligand. In the case of neutral PNP ligands, the use of a suitable metal precursor with labile coligands is sufficient for most direct metalation processes. Due to the chelat-

ing coordination mode of the pincer ligands, the metal precursor coligands are easily displaced and the coordination usually takes place in short reaction times under mild conditions (Scheme 2.1).



Scheme 2.1: Direct metalation of pincer ligands

In the case of the metalation of anionic ECE ligands which require the cleavage of a C-R₁ bond (R₁ = H, CH₃, SiR₃, Li, Cl, Br, I...), the reaction conditions are sometimes harsher; Scheme 2.2 provides an overview of established methods.



Scheme 2.2: Synthetic routes to ECE pincer complexes

The direct metalation is one of the most often applied synthetic methods. It has become very attractive because prefunctionalisation of the ligand is not required in order to achieve regioselectivity. The metalation is in most cases straightforward and involves the reaction of a suitable metal precursor (*e.g.* metal halide salts or complexes with labile ligands) with the ligand.

The oxidative addition method relies on the ability of many transition metals to switch easily between different oxidation states from M^n to M^{n+2} . During this process, a C-halide bond containing ligand is added to the metal centre without liberation of acid. Therefore this method may be suitable for sensitive ligands.

In the transmetalation method metal M^1 which is bound to the ligand on only one site is exchanged by metal M^2 which then ligates in a terdentate mode. This method requires the preparation of a prefunctionalised ligand which is accomplished in most cases with lithium reagents such as *n*-BuLi or LDA. Due to the lithiation step being not regioselective in the case of methylene-bridged pincer ligands this method is not as straightforward as those mentioned before.

Transcyclometalation has been developed recently as a novel method for the preparation of pincer complexes. The term is used to describe the substitution of one cyclometalated ligand by another without the formation of detectable amounts of inorganic salts. The driving force for this reaction is apparently the bond strength—the free ligand must coordinate stronger to the metal centre than the one of the parent complex.

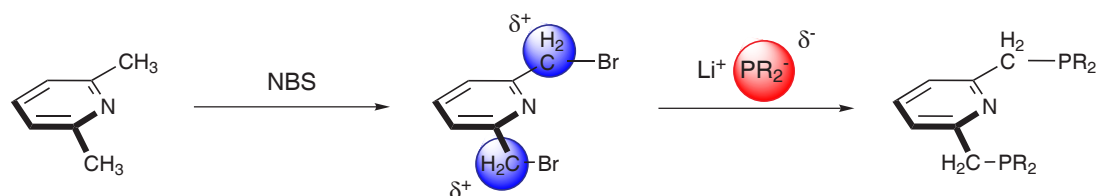
3 Results and discussion

3.1 Ligands

3.1.1 Introduction

Pincer ligands and their complexes with several transition metals have been first reported in the late 1970s by Bernard L. Shaw.¹ Right after their discovery minor attention has been paid to this new class of ligands. This has changed dramatically for in the last decade pincer ligands have attracted increasing interest of research groups covering many topics in modern organometallic chemistry. The fields in which pincer complexes are employed range from explorative chemistry over catalytic applications to supramolecular chemistry.

The synthetic pathway to PNP pincer ligands with a methylene spacer group between the aromatic backbone and the phosphine donors involves a nucleophilic substitution of the bromine atom of 2,6-bis(bromomethyl)pyridine by treatment with phosphides (Scheme 3.1).



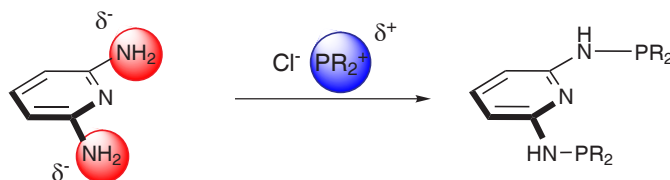
Scheme 3.1: Synthesis of methylene bridged PNP ligands

Although widely used, this synthetic route has some drawbacks: On the one hand, although commercially available, the starting material 2,6-bis(bromomethyl)pyridine is rather expensive^a. This can be circumvented, however, by starting with radical bromi-

^a5 g: 123.50 € (Aldrich)

nation of the much cheaper^b 2,6-lutidine—which adds another step to the synthesis. On the other hand, in the nucleophilic substitution the phosphide acts as nucleophile which limits the range of applicable phosphines to aryl and alkyl derivatives. Finally, the modification of stereochemical parameters often requires time-consuming multi-step syntheses.

The ligands presented in this work feature an amino bridging group between the aromatic backbone and the phosphine donors. The first example of this class of ligands (*viz.* PNP-Ph) was reported by Haupt²¹ in 1987.



Scheme 3.2: Synthesis of amino bridged PNP ligands

Starting from commercially available and inexpensive^c 2,6-diaminopyridine the synthesis involves the nucleophilic attack of the amino groups on an electrophilic chlorophosphine (Scheme 3.2). In this case of polarity the nature of the electrophile is not limited to phosphines but can be extended to phosphites as well. The modular design of these ligands allows for the modification of the steric, electronic and stereochemical properties. Moreover, it provides easy access to chiral derivatives when chiral phosphite building blocks are utilised.

Some examples of PNP ligands that have been prepared in our group^{12,22} by employing this methodology are depicted in Figure 3.1. The phosphine or phosphite moiety features sterically demanding groups as well as chiral derivatives.

As shown in Figure 3.2, the amino bridging groups can be alkylated to circumvent possible problems derived from the acidity of the NH protons. In addition, the use of functionalised alkyl chains as substituents offers the possibility of immobilising the ligand through a covalent linker to a soluble or heterogeneous support.²³

^b500 mL: 50.30 € (Aldrich)

^c500 g: 89.00 € (Aldrich)

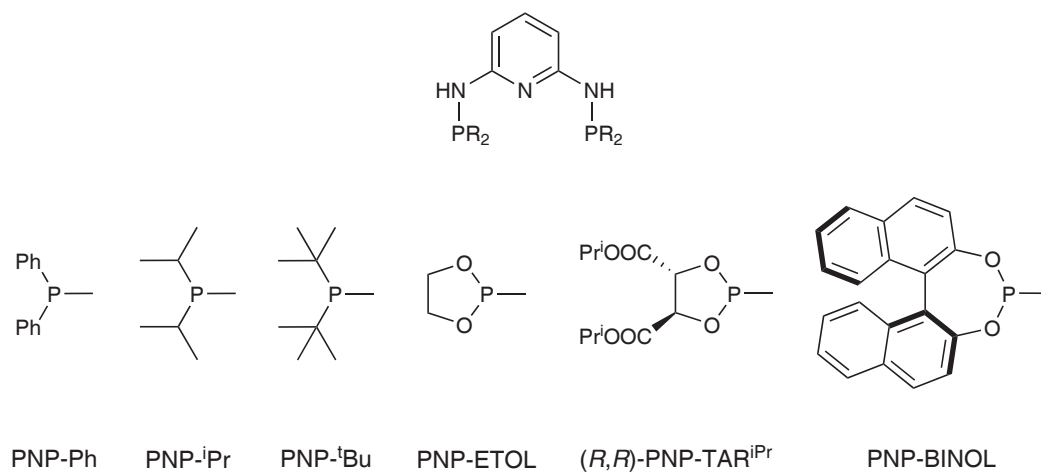


Figure 3.1: Examples of PNP ligands

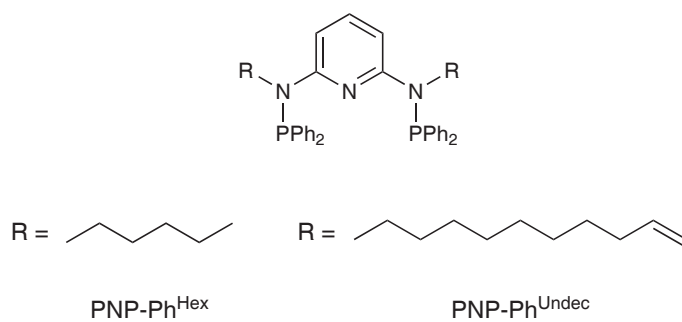
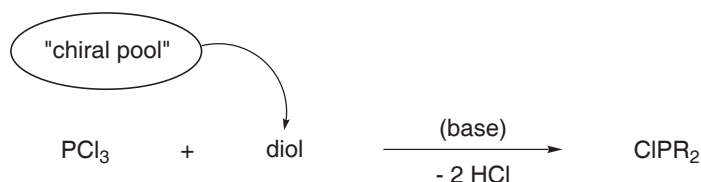


Figure 3.2: N-alkylated PNP ligands

3.1.2 Building blocks

Chlorophosphites

Unlike dialkyl or diaryl phosphines the chlorophosphite building blocks are in most cases not commercially available. This is especially true when it comes to chiral derivatives. A convenient one-step synthesis of chlorophosphites is depicted in Scheme 3.3. It involves the reaction of PCl_3 and the corresponding diol in the presence of base, if necessary.



Scheme 3.3: One-step synthesis of chlorophosphites

All the chlorophosphites used in this work (Figure 3.3) are known in the literature and were prepared according to published procedures.^{24–26} The formation of ETOL-PCl proceeded without addition of base, in the case of BIPOL-PCl and TAR^{Me} -PCl 10 mol % of *N*-methylpyrrolidone were used, and for the synthesis of $^t\text{BuBIPOL-PCl}$ excess triethylamine was employed as base.

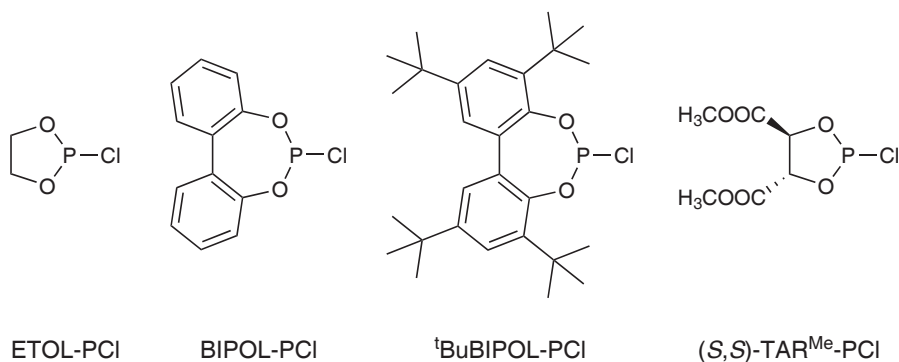


Figure 3.3: Chlorophosphites prepared from PCl_3 and the respective diol

All compounds were obtained as colourless to pale yellow solids in 65–87 % yield and proved to be quite sensitive to moisture and were therefore stored under inert conditions. The chlorophosphites were identified by ^1H NMR and $^{31}\text{P}\{^1\text{H}\}$ NMR spectroscopy. In

the $^{31}\text{P}\{^1\text{H}\}$ NMR spectra they give rise to a single resonance in the range of 169 to 179 ppm.

2,5-Thiophenedicarboxaldehyde

Although commercially available 2,5-thiophenedicarboxaldehyde is quite expensive and was thus synthesised using a well-established one-pot methodology.²⁷ Treatment of thiophene with *n*-BuLi and quenching with DMF afforded 2,5-thiophenedicarboxaldehyde in 78 % yield.

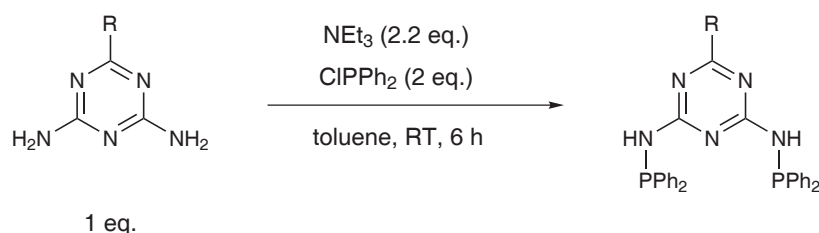
2,6-Diamino-4-ethoxy-1,3,5-triazine²⁸

A suspension of 2,6-diamino-4-chlor-1,3,5-triazine in ethanol was treated with excess KOH and heated to reflux for 20 h. The product was obtained as a white solid in 82 % yield.

3.1.3 1,3,5-Triazine-based PNP^{T} pincer ligands

Synthesis

While the chemistry of 2,6,-diaminopyridine-derived PNP pincer ligands has been studied by Haupt and coworkers^{21,29} and our group^{22,30} no examples of PNP pincer ligands based on 1,3,5-triazine have been known in the literature. Phosphine and phosphide derivatives of 1,3,5-triazine are mainly found in polymer science and consequentially in the patent literature but not in organometallic chemistry. Thus, the concept of pincer ligands was extended to this type of N-heterocyclic diamines.



Scheme 3.4: Synthesis of 1,3,5-triazine-based PNP^{TR} -Ph pincer ligands

In a typical procedure, a toluene or THF solution of one equivalent of 2,6-diamino-triazine was treated with 2.2 equivalents of triethylamine and, after cooling to 0 °C, with

two equivalents of ClPPh_2 (Scheme 3.4). The reactions then proceeded at room temperature with the ligands obtained as colourless to pale yellow solids in 64–95 % yield after filtration of $\text{NEt}_3\cdot\text{HCl}$ (Figure 3.4).

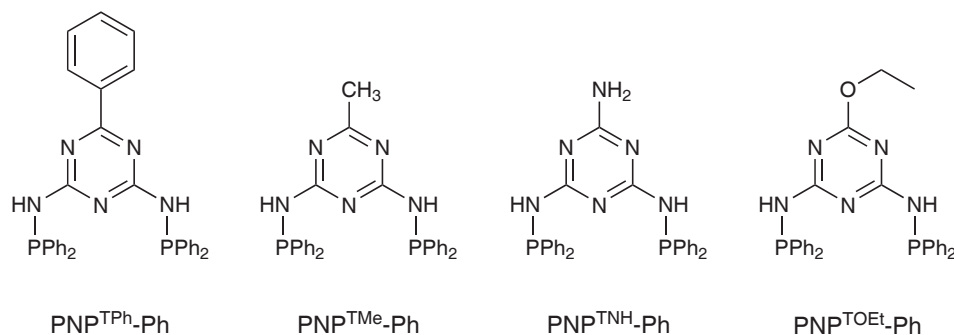


Figure 3.4: 1,3,5-Triazine-based $\text{PNP}^{\text{TR}}\text{-Ph}$ pincer ligands

It has to be pointed out that the reaction did not proceed when ClP^iPr_2 was used. Although the reaction conditions have been varied systematically (*i.e.* THF or toluene as solvent, triethylamine and/or *n*-BuLi as base, addition of the chlorophosphine neat or in solution, the reaction carried out at room temperature or at reflux) the *iso*-propyl derivative $\text{PNP}^{\text{TPh-}i\text{Pr}}$ could not be obtained cleanly. This may be due to the varied electronic conditions in this pair of reactants. On the one hand, the *iso*-propyl groups exert an electron-releasing inductive effect (" +I effect") which reduces the electrophilicity of the phosphorus. On the other hand, triazine is considered to be electron-deficient for it undergoes nucleophilic rather than electrophilic aromatic substitution. This electron-withdrawing effect may render the amino groups less nucleophile. So in sum, no reaction takes place between the less electrophilic phosphorus and the less nucleophilic nitrogen.

Mechanistic investigations based on DFT calculations to explain these experimental findings are currently in progress. First of all, it has been found that the formation of the P–N bond does not proceed *via* SN_1 or SN_2 mechanisms. The suggested reaction pathway involves the transfer of a proton from the amino group to the phosphorus as initial step. Simplified, this may result in an amide anion and a phosphonium cation. As a consequence the energy level of the antibonding orbitals of the phosphorus would be dropped and the one of the binding orbitals of the amine would be lifted concomitantly, so in sum, the energy gap would be narrowed. The reason why this proton transfer pathway is preferred to "classic" SN mechanisms is under investigation. Although the role of the base and in particular the exact moment of its intervention in the course of the reaction is not fully understood yet, it is clear on any account, that it facilitates the elimination of HCl from the phosphorus.

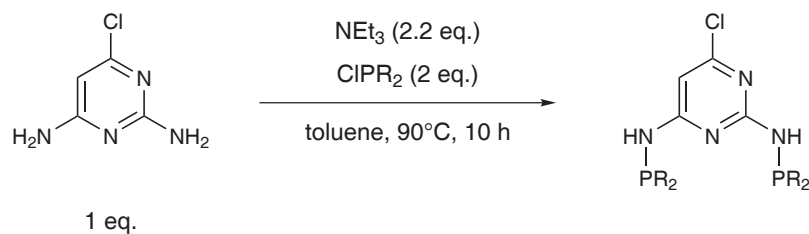
Characterisation

The PNP^T-Ph pincer ligands were fully characterised by ¹H NMR, ¹³C{¹H} NMR, and ³¹P{¹H} NMR spectroscopy with the ³¹P{¹H} NMR spectra being the most significant. The course of the condensation reaction can easily be monitored via ³¹P{¹H} NMR spectroscopy, for the single resonance of the diphenylchlorophosphine disappears along with the appearance of a single product peak. The resonance for this class of ligands lies within the expected range of 27 to 30 ppm. Due to the fact that the PNP^T-Ph ligands bear a large number of aromatic protons the ¹H NMR spectra show multiple signal overlaps. The NH protons, however, are sufficiently resolved and give rise to singlets between 5.65 and 6.33 ppm.

In the ¹³C{¹H} NMR spectra the triazine⁴ carbon atoms exhibit single or double resonances from 171.9 to 176.6 ppm while the triazine^{2,6} carbons give rise to singlets or doublets from 167.6 to 168.7 ppm. Of the diphenylphosphine carbon atoms the one adjacent to the phosphorus is shifted downfield the farthest and gives rise to doublets in the range of 138.6 to 139.6 ppm with coupling constants *J*_{CP} between 13.0 and 15.8 Hz. The Ph^{2,6} carbons exhibit doublets varying only in a small interval from 131.6 to 131.7 ppm with coupling constants *J*_{CP} from 21.5 to 22.1 Hz. The Ph⁴ carbon atoms give rise to singlets in the range of 129.1 to 129.5 ppm. Finally, the Ph^{3,5} carbons show doublets from 128.5 to 128.6 ppm with coupling constants *J*_{CP} between 6.5 and 6.9 Hz.

3.1.4 Pyrimidine-based PNP^P pincer ligands

Synthesis



Scheme 3.5: Synthesis of pyrimidine-based PNP^{PCl}-R pincer ligands

PNP pincer ligands comprising a pyrimidine-based aromatic backbone have not been described in the literature so far. They can be prepared by adding two equivalents of chlorophosphine or -phosphite to a toluene solution of one equivalent of 2,6-diamino-4-chloropyrimidine and 2.2 equivalents of triethylamine (Scheme 3.5). Heating the mix-

ture to 90 °C and subsequent filtration of $\text{NEt}_3\cdot\text{HCl}$ afforded the ligands as off-white solids in 89 % yield in the case of $\text{PNP}^{\text{PCl}}\text{-Ph}$ and 67 % yield in the case of $\text{PNP}^{\text{PCl}}\text{-BIPOL}$ (Figure 3.5).

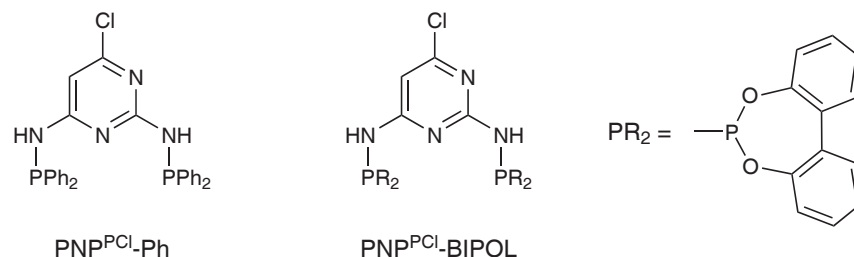


Figure 3.5: Pyrimidine-based $\text{PNP}^{\text{PCl}}\text{-R}$ pincer ligands

Characterisation

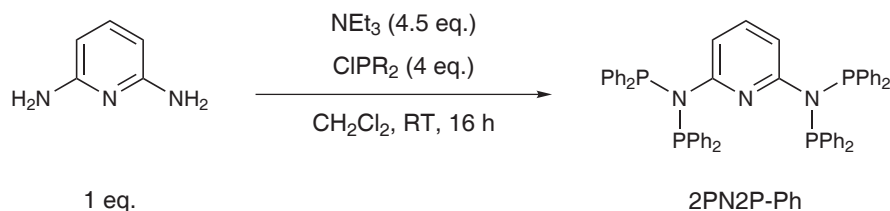
The PNP^{P} ligands were characterised by ^1H NMR, $^{13}\text{C}\{^1\text{H}\}$ NMR, and $^{31}\text{P}\{^1\text{H}\}$ NMR spectroscopy. Similar to the related PNP^{T} ligands the course of the reaction was monitored by $^{31}\text{P}\{^1\text{H}\}$ NMR spectroscopy. The $^{31}\text{P}\{^1\text{H}\}$ NMR spectrum of $\text{PNP}^{\text{PCl}}\text{-Ph}$ exhibits a single resonance at 27.97 ppm while the one of $\text{PNP}^{\text{PCl}}\text{-BIPOL}$ shows a doublet at 146.06 ppm with a coupling constant J_{CP} of 42.2 Hz. In the ^1H NMR spectra the aromatic protons show wide-stretched signal overlaps. The NH protons, however, which are not symmetrical in this type of compounds give rise to a broad singlet and a doublet or two doublets, respectively, with signals in the range of 6.07 from 6.73 ppm and coupling constants J between 4.6 and 7.7 Hz.

In the $^{13}\text{C}\{^1\text{H}\}$ NMR spectra the pyrimidine^{2,4,6} carbon atoms give rise to signals in the range of 158.5–166.0 ppm while the pyrimidine⁵ carbon exhibits a characteristic signal at 95.7 or 95.8 ppm. The carbon atoms of the phosphine and phosphite moiety lie within the expected range.

3.1.5 Pyridine-based PNP pincer ligands

Synthesis

Based on the findings of Haupt and coworkers²⁹ who reported the synthesis of *N,N*-bis(diphenylphosphino)-2-aminopyridine from one equivalent of 2-aminopyridine and two equivalents of ClPPh_2 in toluene Dyson and coworkers³¹ have synthesised the poly-



Scheme 3.6: Synthesis of the pyridine-based 2PN2P-Ph ligand

dentate ligand 2PN2P-Ph (Scheme 3.6) which offers interesting coordination possibilities.

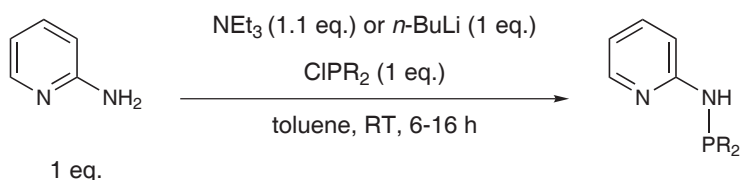
According to the published procedure a methylene chloride solution of one equivalent of 2,6-diaminopyridine was treated with 4.5 equivalents of triethylamine and, under cooling, four equivalents of ClPPh₂. The mixture was allowed to reach room temperature, stirred for another 10 h, filtered and the solvent removed. The ligand was obtained as white solid in 82 % yield.

Characterisation

The compound was identified by ¹H NMR and ³¹P{¹H} NMR spectroscopy with the spectral data being identical to those of the authentic sample reported.³¹

3.1.6 Pyridine-based PN ligands

Synthesis



Scheme 3.7: Synthesis of pyridine-based PN-R ligands

While the first synthesis of PN-Ph published in 1967³² employed two equivalents of 2-aminopyridine—one equivalent acting as scavenger for hydrogen chloride—the synthetic methodology established for PNP ligands with NEt₃ as additional base can also be

applied to the synthesis of PN ligands. When NEt_3 instead of 2-aminopyridine—which is a solid—is used as the hydrogen chloride scavenger any excess of base can easily be removed *in vacuo*.

Accordingly, a cooled solution of one equivalent of 2-aminopyridine was mixed with 1.1 equivalents of NEt_3 and treated with an equimolar amount of the respective chlorophosphine or -phosphite (Scheme 3.7). The reactions then proceeded at room temperature affording, after filtration of the generated $\text{NEt}_3\cdot\text{HCl}$, the ligands in good to excellent yields (85–95 %) with purities > 97 % (Figure 3.6).

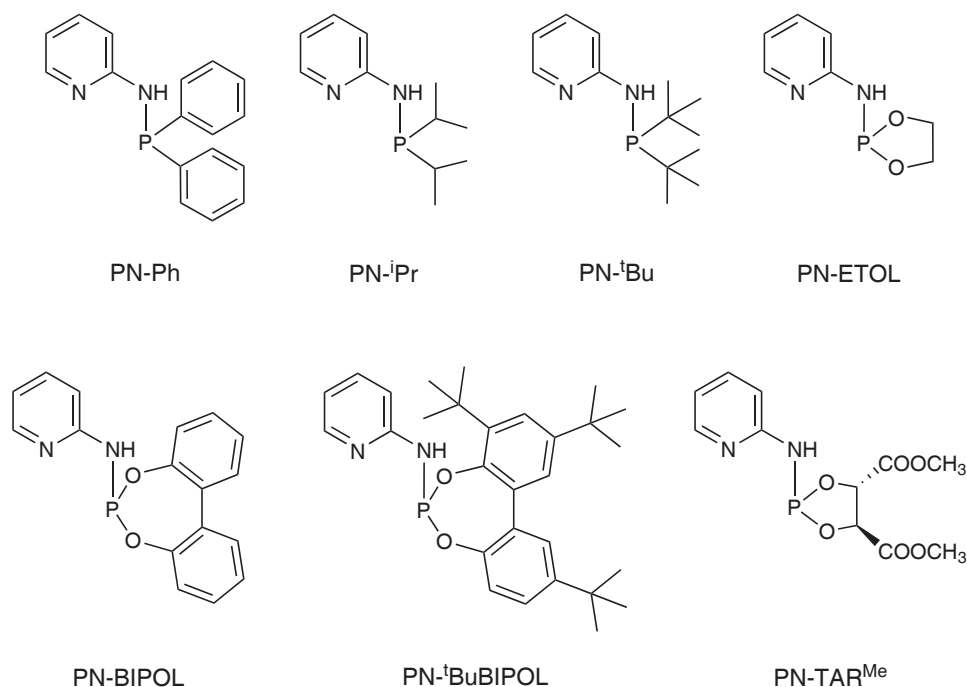


Figure 3.6: Pyridine-based PN-R ligands

It has to be noted that in the case of $\text{PN-}^t\text{Bu}$ the reaction failed when only NEt_3 was used. As for the synthesis of the corresponding tridentate $\text{PNP-}^t\text{Bu}$ ligand deprotonation was only successful when both NEt_3 and *n*-BuLi were utilised.²² Thus, in order to prepare $\text{PN-}^t\text{Bu}$, equimolar amounts of NEt_3 and *n*-BuLi were added to a cooled solution of 2-aminopyridine in toluene. Subsequent heating to 80 °C and filtration of $\text{NEt}_3\cdot\text{HCl}$ afforded $\text{PN-}^t\text{Bu}$ in 68 % yield.

Characterisation

The formation of the PN ligands can easily be monitored via $^{31}\text{P}\{^1\text{H}\}$ NMR spectroscopy for both the starting compounds (*i.e.* the chlorophosphines and -phosphites) and the ligands exhibit a single resonance. In comparison to the signals of the chlorophosphines the resonances of the ligands are shifted upfield considerably thus leading to resonances of the PN ligands between 27.4 and 61.2 ppm. Likewise, the signals of the chlorophosphite derived ligands are shifted upfield when compared to the starting materials albeit in a narrower range, the resulting resonances of the ligands varying from 129.7 to 147.3 ppm. The $^{31}\text{P}\{^1\text{H}\}$ NMR shifts of the starting chlorophosphines and -phosphites and the resulting PN ligands are reported in Table 3.1.

CIPR ₂	$^{31}\text{P}\{^1\text{H}\}$ NMR	PN ligand	$^{31}\text{P}\{^1\text{H}\}$ NMR
CIPPh ₂	83.3	PN-Ph	27.4
CIP ⁱ Pr ₂	135.6	PN- ⁱ Pr	50.0
CIP ^t Bu ₂	147.3	PN- ^t Bu	61.2
ETOL-PCl	169.0	PN-ETOL	129.7
BIPOL-PCl	179.6	PN-BIPOL	147.3
^t BuBIPOL-PCl	173.0	PN- ^t BuBIPOL	140.9
TAR ^{Me} -PCl	176.3	PN-TAR ^{Me}	142.6

Table 3.1: $^{31}\text{P}\{^1\text{H}\}$ NMR shifts of the PN-R ligands and the corresponding chlorophosphines and -phosphites (δ [ppm], CD₃Cl, 20 °C)

In the ^1H NMR spectra (Table 3.2) the py⁶ proton gives rise to doublets in the range of 7.93 to 8.17 ppm with coupling constants $J = 4.0\text{--}5.0$ Hz. Regarding the signal multiplicity the py⁴ proton appears inconsistently as doublet, virtual triplet or doublet of doublets with signals in the range of 7.33 to 7.93 ppm. Furthermore, in the PN ligands with other aromatic moieties (*i.e.* PN-Ph and PN-BIPOL) these signals were not resolved. The py³ proton exhibits doublet signals varying from 6.70 to 7.39 ppm with coupling constants $J = 8.2\text{--}8.5$ Hz. In the case of PN-ETOL and PN-BIPOL there were overlaps between the signals of py³ and py⁵. The latter show virtual triplets or doublets of doublets in the range of 6.57 to 7.29. Finally, the NH proton appears as singlet or doublet within the range of 4.94 to 6.38 ppm.

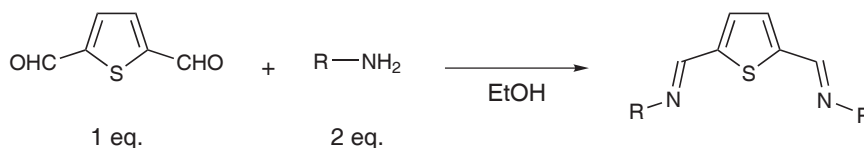
Compound	py ⁶ (1H)	py ⁴ (1H)	¹ H NMR		NH (1H)
			py ³ (1H)	py ⁵ (1H)	
PN-Ph	7.93	7.36–7.33 ^a	7.06	6.64	5.93
PN- ⁱ Pr	7.97	7.38	7.05	6.57	4.94
PN- ^t Bu	8.03	7.43	7.13	6.62	5.02
PN-ETOL	8.03	7.43	6.79–6.74 ^b	6.79–6.74 ^b	6.06
PN-BIPOL	8.12	7.54–7.47 ^a	7.39–7.24 ^b	7.39–7.24 ^b	6.38
PN- ^t BuBIPOL	8.17	7.93	6.89	6.78	6.15
PN-TAR ^{Me}	8.13	7.48	6.70	6.80	6.60

^asignal overlaps with other aromatic signals^bsignal overlaps between py³ and py⁵Table 3.2: Selected ¹H NMR shifts of the PN-R ligands (δ [ppm], CD₃Cl, 20 °C)

3.1.7 Thiophene-based NSN pincer ligands

Synthesis

The general procedure for the synthesis of thiophene based NSN pincer ligands is depicted in Scheme 3.8. It involves the reaction of one equivalent of 2,5-thiophenedicarboxaldehyde with two equivalents of amine.³³ The reactions proceeded smoothly at room temperature with ethanol as a solvent. In some cases the products precipitated during the course of the reaction and could thus be isolated by filtration, otherwise the solvent had to be removed *in vacuo*. The desired diimines were obtained as off-white solids in high yields (82–97 %).



Scheme 3.8: Synthesis of thiophene-based NSN-R pincer ligands

Characterisation

The NSN ligands were characterised by ¹H NMR and ¹³C{¹H} NMR spectroscopy. The ¹H NMR spectra bear no unusual features. With the exception of the NSN-Me ligand—which gives a double resonance at 8.29 ppm with a coupling constant $J = 1.6$ Hz—all

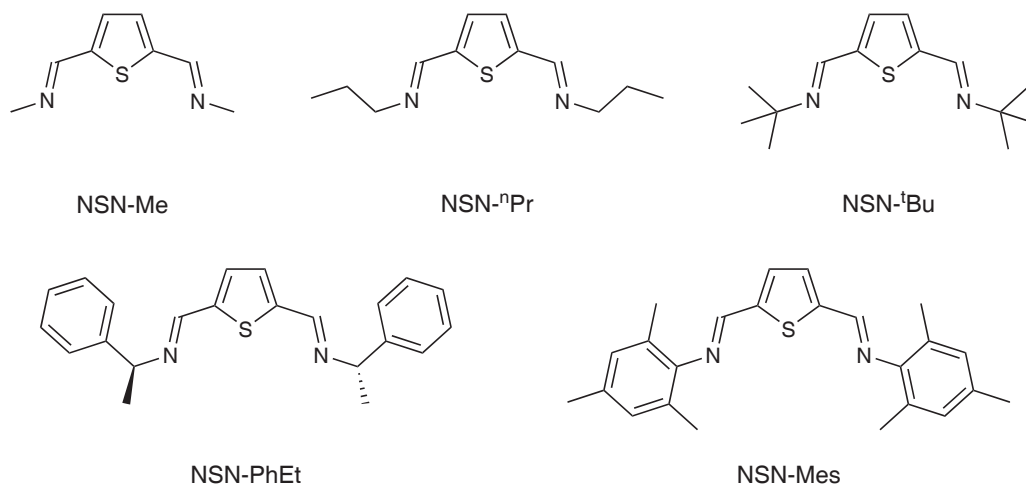


Figure 3.7: Thiophene based NSN-R pincer ligands

protons of the imine $\text{N}=\text{CH}$ moiety give rise to a characteristic singlet that lies within the range of 8.21 to 8.39 ppm. For all ligands the thiophene protons exhibit a single resonance between 7.21 and 7.34 ppm. Likewise, in the $^{13}\text{C}\{^1\text{H}\}$ NMR spectra the imine carbon atoms give rise to resonances between 148 and 155 ppm. Selected shifts of the diimine ligands are summarised in Table 3.3.

Ligand	^1H NMR		$^{13}\text{C}\{^1\text{H}\}$ NMR
	$\text{N}=\text{CH}$	thiophene ^{3,4}	$\text{N}=\text{CH}$
NSN-Me	8.29	7.21	155.5
NSN- ⁿ Pr	8.29	7.23	153.7
NSN- ^t Bu	8.28	7.21	148.3
NSN-PhEt	8.39	7.44–7.23 ^a	152.4
NSN-Mes	8.21	7.34	155.3

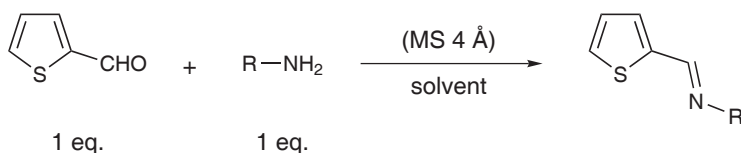
^asignal overlaps with other aromatic signals

Table 3.3: Selected ^1H NMR and $^{13}\text{C}\{^1\text{H}\}$ NMR shifts of the NSN-R pincer ligands (δ [ppm], CD_3Cl , 20 °C)

3.1.8 Thiophene-based imine SN ligands

Synthesis

The thiophene-based imine SN-R ligands were prepared according to procedures described in the literature from equimolar amounts of 2-thiophenecarboxaldehyde and amine (Scheme 3.9). For the synthesis of SN-Mes, which is not known in the literature, the same method as for the related thiophene-based NSN pincer ligands discussed in Section 3.1.7, *viz.* ethanol as a solvent, was employed.



Scheme 3.9: Synthesis of thiophene-based imine SN-R ligands

The synthesis of SN-ⁿPr³⁴ was carried out in methylene chloride with 4 Å molecular sieve and SN-PhEt³⁵ was synthesised using methanol as solvent. The imine SN-R ligands were obtained as yellow solids (SN-Mes) or orange to brown oils (SN-ⁿPr and SN-PhEt) in 71–95 % yield (Figure 3.8).

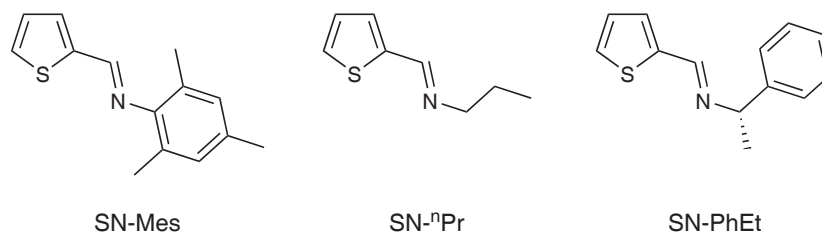


Figure 3.8: Thiophene-based imine SN-R ligands

Characterisation

The ligands were fully characterised by ¹H NMR and ¹³C{¹H} NMR spectroscopy. Like the spectra of the related NSN diimine ligands described in Section 3.1.7 the imine N=CH protons exhibit a characteristic single resonance within the range of 8.32 to 8.46 ppm in the ¹H NMR spectrum. Likewise, the imine N=CH carbon atoms give rise to signals varying from 152.8 to 155.6 ppm (Table 3.4).

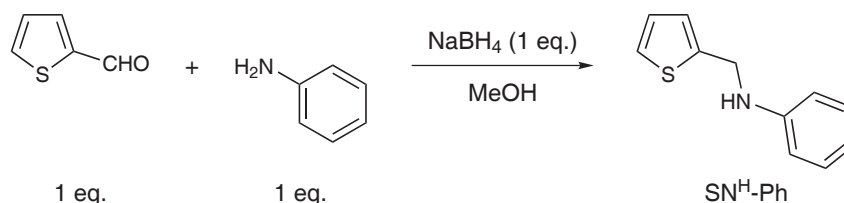
Ligand	^1H NMR N=CH	$^{13}\text{C}\{^1\text{H}\}$ NMR N=CH
SN-Mes	8.32	155.6
SN- n Pr	8.35	154.0
SN-PhEt	8.46	152.8

Table 3.4: Selected ^1H NMR and $^{13}\text{C}\{^1\text{H}\}$ NMR shifts of the imine SN-R ligands (δ [ppm], CD_3Cl , 20 °C)

3.1.9 Thiophene-based amine SN ligands

Synthesis

For comparison of the properties of thiophene-based imine and amine complexes an amine SN ligand was prepared by mixing one equivalent of 2-thiophenecarboxaldehyde and one equivalent of aniline under cooling. Dilution with methanol followed by reduction with NaBH_4 ³⁶ afforded, after workup, $\text{SN}^{\text{H}}\text{-Ph}$ in 97 % yield (Scheme 3.10).



Scheme 3.10: Synthesis of the amine ligand $\text{SN}^{\text{H}}\text{-Ph}$

Characterisation

The compound was identified by ^1H NMR and $^{13}\text{C}\{^1\text{H}\}$ NMR spectroscopy. Spectral data were identical with those of the authentic sample reported.³⁶

3.2 Molybdenum complexes

3.2.1 Introduction

In contrast to pincer complexes of late transition metals molybdenum derivatives are scarcely found in the literature. Although complexes of group VI metals were among the first examples of aminophosphine-based PNP pincer complexes that have been published no more investigations have been carried out on this topic so far.

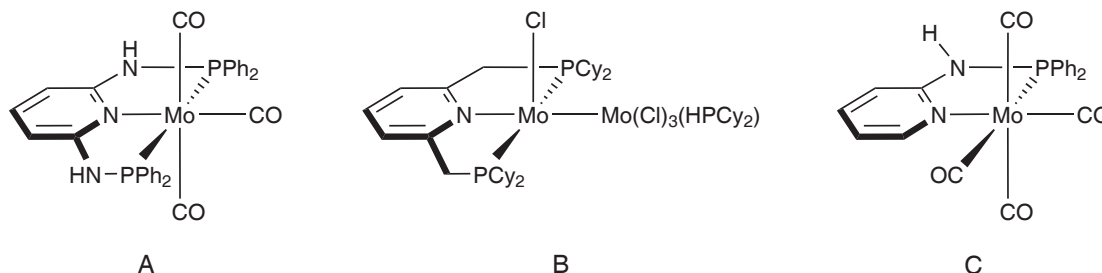
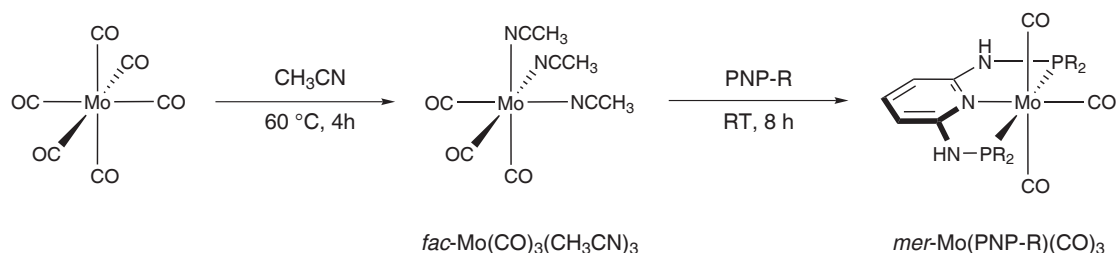


Figure 3.9: Mo(PNP)(L_n) and Mo(PN)(L_n) complexes

In 1987, Haupt and coworkers²¹ published the synthesis of PNP pincer ligands based on 2,6-diaminopyridine and neutral tricarbonyl chromium, molybdenum, and tungsten complexes thereof (**A**, Figure 3.9). The second example for molybdenum PNP pincer ligands is the dinuclear complex Mo(PNP)(Cl)–Mo(HPCy₂)Cl₃ with PNP = 2,6-bis(dicyclohexylphosphinomethyl)pyridine (**B**, Figure 3.9) which has been published by Walton and coworkers in 2002.³⁷ Basically the same holds true for molybdenum PN complexes. Only the synthesis and kinetic studies of ring-opening reactions of Mo(PN-Ph)(CO)₄ (**C**, Figure 3.9) have been reported by Angelici in 1973.^{38,39} However, complexes comprising the PN-Ph ligand and other transition metals (*e.g.* Cr, Mn, Fe, Co, Ni, Pd, Cu) have been synthesised.^{40–43}

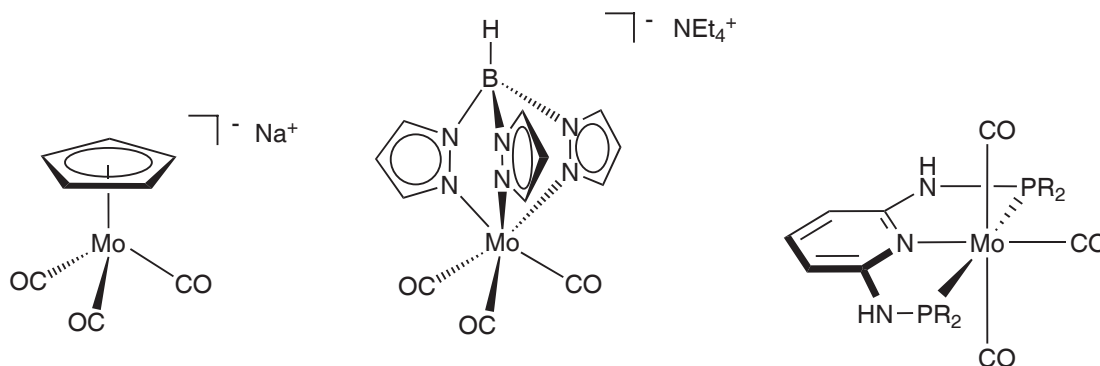
For the preparation of zerovalent molybdenum complexes Mo(CO)₆ and its nitrile derivatives have proven to be excellent precursors. This results from the fact that end-on coordinated nitriles are considered to be moderate σ -donors and π -acceptors toward transition metals⁴⁴ and can thus be displaced easily. The synthesis of *fac*-Mo(CO)₃(CH₃CN)₃ by refluxing Mo(CO)₆ in acetonitrile was first reported in 1962 by Tate *et. al.*⁴⁵

When refluxed in acetonitrile the first and second carbonyl ligand are replaced readily by acetonitrile ligands. For the substitution of a third carbonyl longer reaction times are required. Due to the *trans*-effect the carbonyl as well as the acetonitrile ligands are coordinated in a facial arrangement. Acetonitrile represents a stronger σ -donor and weaker



Scheme 3.11: Preparation of zerovalent molybdenum complexes $\text{mer-Mo(PNP-R)(CO)}_3$

π -acceptor than carbon monoxide and therefore strengthens the π -backdonation from the metal centre to the carbonyl ligand. Once the chelating PNP ligand is added and coordinates to the metal centre the carbonyl ligands are enforced to a meridional arrangement (Scheme 3.11). The meridional coordination geometry is quite uncommon for molybdenum tricarbonyl complexes; in the vast majority of published examples they adopt a facial arrangement with $\text{Cp}^{46,47}$ and Tp^{48-51} coligands (Scheme 3.12).

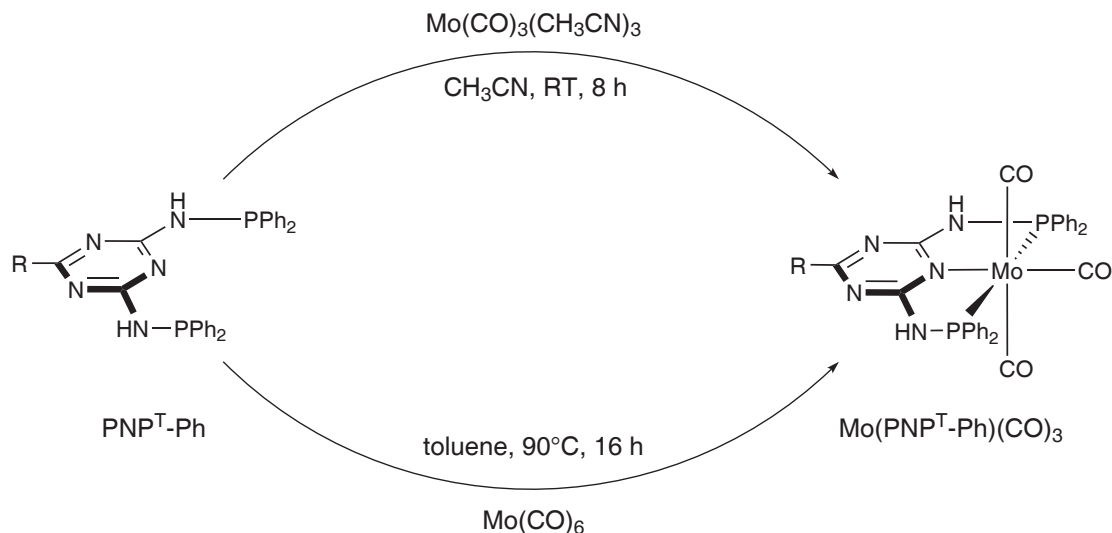


Scheme 3.12: Mo(L)(CO)_3 complexes with facial and meridional arrangement of the carbonyl ligands

Another pathway leading to zerovalent molybdenum pincer complexes involves the thermally activated displacement of three of the carbonyl ligands without an intermediate that can be isolated. By refluxing equimolar amounts of Mo(CO)_6 and the PNP ligand in higher boiling non-coordinating solvents such as toluene or *n*-heptane the carbonyl ligands are replaced one after another by the chelating, strong σ -donating PNP ligand. However, this pathway requires rather harsh conditions which not every ligand may endure.

3.2.2 Molybdenum(0) PNP^T complexes

Synthesis



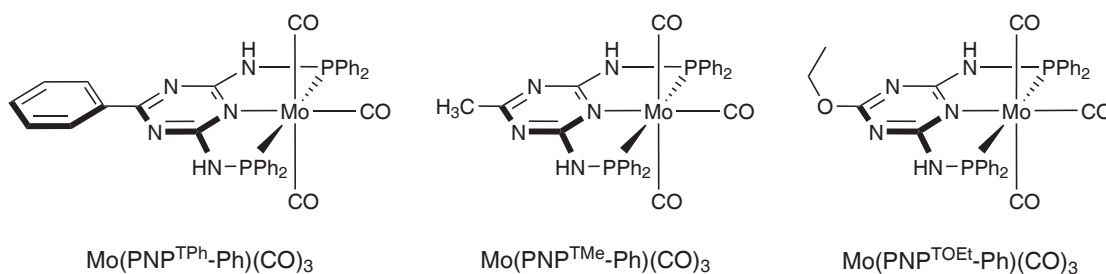
Scheme 3.13: Synthesis of the $\text{Mo(PNP}^{\text{TR}}\text{-Ph)(CO)}_3$ complexes

The PNP^T ligands proved to be thermally robust so that either of the synthetic routes outlined in Section 3.2.1 could be applied for the synthesis of the tricarbonyl Mo PNP^T complexes (Scheme 3.13). It has to be noted, however, that the yields decreased when the "direct" method with toluene as the solvent was utilised. The complexes were obtained as yellow solids in 68–81 % yield (Figure 3.10) and are air stable to some extent so that they can be purified by flash chromatography. To avoid decomposition they should be stored under inert conditions.

Characterisation

All complexes were characterised by ^1H NMR, $^{13}\text{C}\{^1\text{H}\}$ NMR, and $^{31}\text{P}\{^1\text{H}\}$ NMR spectroscopy. Due to the large number of aromatic protons, the ^1H NMR spectra show wide-stretched signal overlaps. The NH protons, however, give a characteristic broad single resonance in the range of 7.05 to 7.31 ppm. The $^{31}\text{P}\{^1\text{H}\}$ NMR spectra exhibit a singlet in the range of 103.3 to 105.7 ppm.

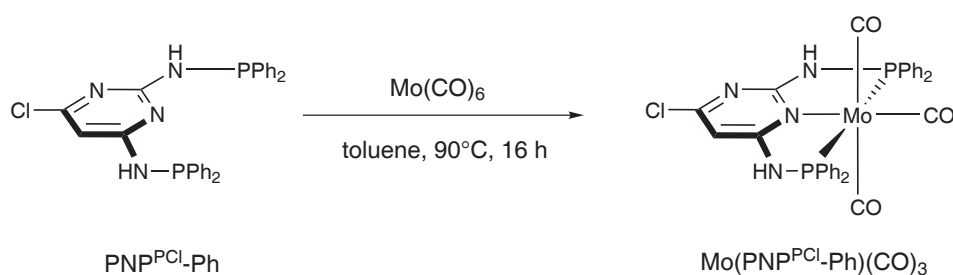
In the $^{13}\text{C}\{^1\text{H}\}$ NMR spectra the two different types of carbonyl ligands give rise to

Figure 3.10: $\text{Mo}(\text{PNP}^{\text{TR}}\text{-Ph})(\text{CO})_3$ complexes

weak signals from 226.4 to 226.6 ppm and to triplets between 210.7 and 210.8 ppm with coupling constants J_{CP} from 9.9 to 10.1 Hz. The triazine⁴ carbon atom exhibits single or triple resonances from 168.7 to 174.3 ppm while the triazine^{2,6} carbons give rise to triplets from 169.5 to 170.4 ppm with coupling constants J_{CP} between 13.2 and 13.4 Hz. The shifts of the diphenylphosphine carbon atoms are not much affected by the nature of the p-substituent on the triazine backbone and therefore vary only in a small interval. The carbon atom adjacent to the phosphorus gives rise to triplets in the range of 139.0 to 139.1 ppm with coupling constants J_{CP} between 19.3 and 19.4 Hz. The Ph^{2,6} carbons exhibit doublets varying from 130.6 to 130.7 ppm with a coupling constant J_{CP} of 7.8 Hz. The Ph⁴ carbon atom gives rise to singlets in the range of 130.1 to 130.2 ppm and the Ph^{3,5} carbons show triplets at 128.4 ppm with a coupling constant J_{CP} of 5.2 Hz.

3.2.3 Molybdenum(0) PNP^{P} complexes

Synthesis

Scheme 3.14: Synthesis of the $\text{Mo}(\text{PNP}^{\text{PCL}}\text{-Ph})(\text{CO})_3$ complex

The pyrimidine-based PNP^{P} complex was prepared by heating equimolar amounts of

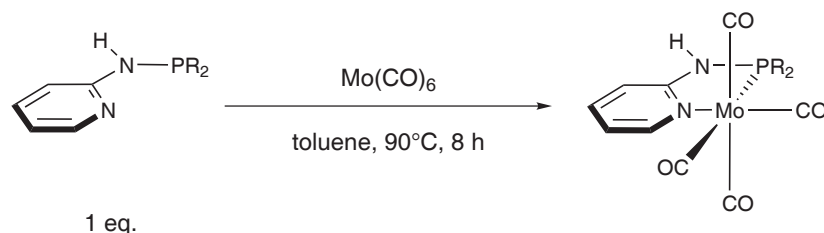
$\text{Mo}(\text{CO})_6$ and the $\text{PNP}^{\text{P}}\text{-Ph}$ ligand in toluene for 16 h. The product was obtained as a yellow solid in 54 % yield which slowly decomposed when exposed to air (Scheme 3.14). As has been observed with related PNP ligands¹² attempts to synthesise the phosphite complex $\text{Mo}(\text{PNP}^{\text{PCl}}\text{-BIPOL})(\text{CO})_3$ from $\text{PNP}^{\text{PCl}}\text{-BIPOL}$ and $\text{Mo}(\text{CO})_6$ resulted in no clean product formation.

Characterisation

The complex was characterised by ^1H NMR, $^{13}\text{C}\{^1\text{H}\}$ NMR, and $^{31}\text{P}\{^1\text{H}\}$ NMR spectroscopy. In the ^1H NMR spectrum the NH protons give rise to two doublets at 6.92 and 6.80 ppm, respectively, with coupling constants J 5.2 and 5.4 Hz while the pyrimidine⁵ proton appears as singlet at 6.42 ppm. The $^{31}\text{P}\{^1\text{H}\}$ NMR spectrum shows a single resonance at 102.09 ppm. In the $^{13}\text{C}\{^1\text{H}\}$ NMR spectrum the carbonyl ligands give rise to doublets and virtual triplets at 205.8, 210.4, and 227.0 ppm, respectively. The pyrimidine^{2,4,6} carbon atoms appear as doublet or doublet of doublets between 159.0 and 164.8 ppm, while the pyrimidine⁵ carbon atom exhibits a characteristic double signal at 95.8 ppm with a coupling constant J_{CP} of 7.4 Hz. With respect to the diphenylphosphine carbon atoms the $^{13}\text{C}\{^1\text{H}\}$ NMR spectrum is similar to those of the related $\text{Mo}(\text{PNP}^{\text{T}}\text{-Ph})$ complexes.

3.2.4 Molybdenum(0) PN complexes

Synthesis



Scheme 3.15: Synthesis of $\text{Mo}(\text{PN-R})(\text{CO})_4$ complexes

The synthetic methodologies discussed for the preparation of $\text{Mo}(\text{PNP-R})(\text{CO})_3$ complexes (Section 3.2.1) are also applicable to the synthesis of $\text{Mo}(\text{PN-R})(\text{CO})_4$ complexes. In order to prepare tetracarbonyl complexes it seems more reasonable to pursue the strategy of performing the reaction in a non-coordinating solvent (Scheme 3.15). Due to the fact that three of the carbonyl ligands are labile more than two carbonyls may be

displaced when performing the reaction in acetonitrile. Another advantage of the first method is the avoidance of the oxygen-sensitive intermediate $\text{Mo(CO)}_3(\text{CH}_3\text{CN})_3$.

Thus, the Mo(PN-R)(CO)_4 complexes were obtained as yellow solids in 66–74 % yield for the phosphine complexes (Figure 3.11) and 65–81 % yield for the phosphite complexes (Figure 3.12). The compounds are air stable to some extent but are best stored under an inert atmosphere of argon.

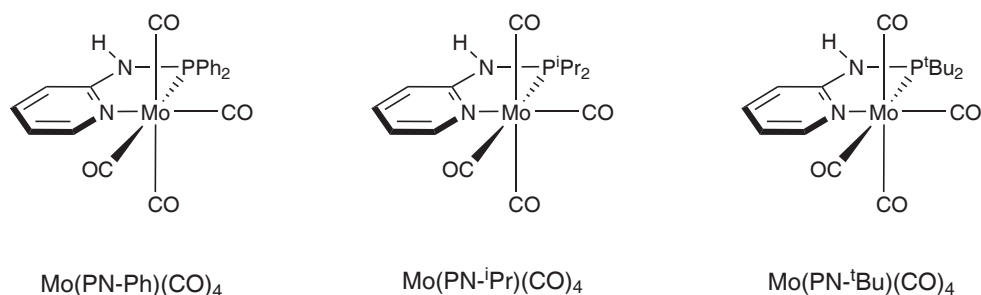


Figure 3.11: Phosphine Mo(PN-R)CO_4 complexes

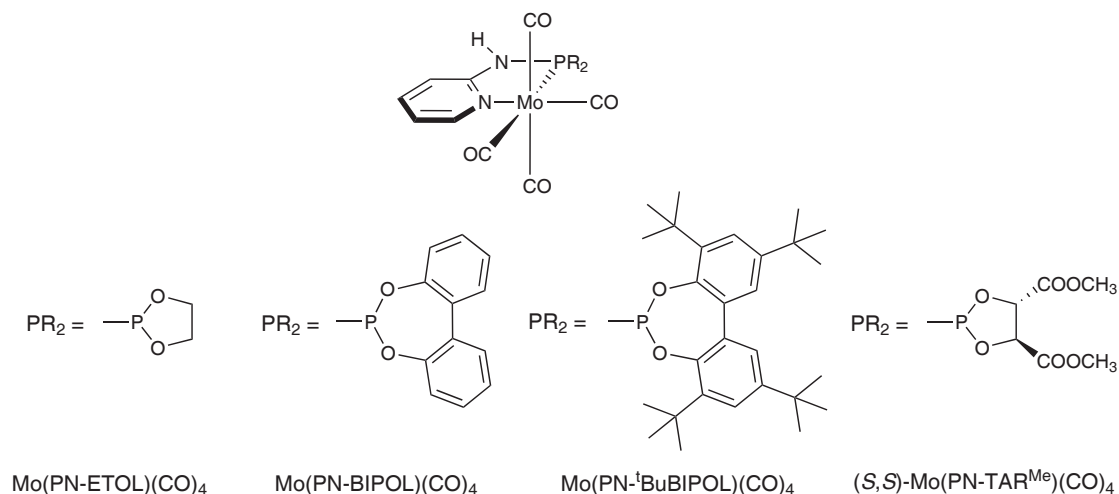


Figure 3.12: Phosphite Mo(PN-R)CO_4 complexes

Characterisation

The Mo(PN-R)CO_4 complexes were fully characterised by ^1H NMR, $^{13}\text{C}\{^1\text{H}\}$ NMR, $^{31}\text{P}\{^1\text{H}\}$ NMR, and IR spectroscopy. In comparison to the PN-R ligands (Figure 3.6)

the complexes' ^1H NMR spectra show a downfield shift of all signals. The strongest influence is observed at the protons adjacent to the metal centre. Whereas the signal of py^6 is shifted downfield by about 0.4–0.5 ppm, the change for the py^5 proton is rather neglectable. Thus, the py^6 proton exhibits single or double resonances in the range of 8.39 to 8.52 ppm. The other pyridine protons show wide-stretched signal overlaps and are not discussed further (Table 3.5).

Compound	^1H NMR				
	py^6 (1H)	py^4 (1H)	py^3 (1H)	py^5 (1H)	NH (1H)
$\text{Mo}(\text{PN-Ph})(\text{CO})_4$	8.51	7.66–7.50 ^a	6.91	6.69	6.18
$\text{Mo}(\text{PN-}^i\text{Pr})(\text{CO})_4$	8.41	7.49	6.75	6.58	5.45
$\text{Mo}(\text{PN-}^t\text{Bu})(\text{CO})_4$	8.39	7.49	6.87	6.59	5.54
$\text{Mo}(\text{PN-ETOL})(\text{CO})_4$	8.42	7.56	6.75–6.69 ^b	6.75–6.69 ^b	6.75–6.69 ^b
$\text{Mo}(\text{PN-BIPOL})(\text{CO})_4$	8.52	7.64–7.08 ^a	6.82–6.79 ^c	6.82–6.79 ^c	6.60–6.52
$\text{Mo}(\text{PN-}^t\text{BuBIPOL})(\text{CO})_4$	8.52	7.55–7.12 ^a	7.74–6.59 ^b	7.74–6.59 ^b	7.74–6.59 ^b
$\text{Mo}(\text{PN-TAR}^{\text{Me}})(\text{CO})_4$	8.44	7.59 ^d	7.59 ^d	6.84–6.74 ^e	6.84–6.74 ^e

^asignal overlaps with other aromatic signals

^bsignal overlaps between py^3 , py^5 , and NH

^csignal overlaps between py^3 and py^5

^dsignal overlaps between py^4 and py^3

^esignal overlaps between py^5 and NH

Table 3.5: Selected ^1H NMR shifts of the $\text{Mo}(\text{PN-R})(\text{CO})_4$ complexes (δ [ppm], CD_2Cl_2 , 20 °C)

The course of the reaction was monitored by $^{31}\text{P}\{^1\text{H}\}$ NMR spectroscopy. As in the ligands' spectra the complexes exhibit a single resonance in the $^{31}\text{P}\{^1\text{H}\}$ NMR spectra that lies in the range of 87.50 to 127.89 ppm for the phosphine complexes and 180.27 to 192.57 ppm for the phosphite complexes (Table 3.6).

From the $^{13}\text{C}\{^1\text{H}\}$ NMR spectra (Table 3.7) it is obvious that four carbonyl ligands are still present around the metal centre. The carbonyl ligand *cis* to the pyridine nitrogen atom exhibits the strongest downfield shift with doublet signals in the range of 222.2 to 218.5 ppm and coupling constants J_{CP} from 6.9 to 11.5 Hz. The carbonyl *cis* to the phosphorus atom exhibits doublets between 214.4 and 216.4 with coupling constants J_{CP} from 33.4 to 56.9 Hz.

Except for the complex (*S, S*)- $\text{Mo}(\text{PN-TAR}^{\text{Me}})(\text{CO})_4$ the carbonyl ligands *trans* to each other give rise to a doublet signal ranging from 205.8 to 211.4 ppm with coupling constants J_{CP} from 8.3 to 13.2 Hz. In the chiral complex the carbonyls *trans* to each other are not equal and therefore exhibit two double signals at 205.8 and 205.6 ppm, respectively,

Complex	$^{31}\text{P}\{^1\text{H}\}$ NMR
$\text{Mo}(\text{PN-Ph})(\text{CO})_4$	87.50
$\text{Mo}(\text{PN-}^i\text{Pr})(\text{CO})_4$	114.44
$\text{Mo}(\text{PN-}^t\text{Bu})(\text{CO})_4$	127.89
$\text{Mo}(\text{PN-ETOL})(\text{CO})_4$	180.27
$\text{Mo}(\text{PN-BIPOL})(\text{CO})_4$	186.37
$\text{Mo}(\text{PN-}^t\text{BuBIPOL})(\text{CO})_4$	183.90
$\text{Mo}(\text{PN-TAR}^{\text{Me}})(\text{CO})_4$	192.57

Table 3.6: $^{31}\text{P}\{^1\text{H}\}$ NMR shifts of the $\text{Mo}(\text{PN-R})(\text{CO})_4$ complexes (δ [ppm], CD_2Cl_2 , 20 °C)

the coupling constant J_{CP} being 13.8 Hz.

The signals of the pyridine carbon atoms lie within the expected range with the py^2 carbon exhibiting the strongest downfield shift and giving rise to doublet signals from 157.4 to 161.5 ppm with coupling constants J_{CP} from 10.6 to 20.7 Hz. The resonances of the other pyridine atoms are not much affected by the nature of the phosphine or phosphite moiety. The py^6 atom exhibits doublets in the range between 153.2 and 153.9 ppm with coupling constants J_{CP} from 4.5 to 5.2 Hz. The py^4 and py^5 carbon atoms give rise to single resonances in the range from 138.8 to 139.4 ppm and from 115.0 to 116.8 ppm, respectively. The py^3 carbon exhibits doublets between 110.6 and 111.4 ppm with coupling constants J_{CP} from 4.6 to 6.9 Hz.

Complex				$^{13}\text{C}\{^1\text{H}\}$ NMR				
	CO	CO	CO	py^2	py^6	py^4	py^5	py^3
$\text{Mo}(\text{PN-Ph})(\text{CO})_4$	220.7	216.1	208.1	160.0	153.6	139.0	115.7	111.2
$\text{Mo}(\text{PN-}^i\text{Pr})(\text{CO})_4$	221.5	215.7	209.6	161.0	153.4	138.8	114.8	110.6
$\text{Mo}(\text{PN-}^t\text{Bu})(\text{CO})_4$	222.2	216.4	211.4	161.5	153.2	138.9	115.0	111.1
$\text{Mo}(\text{PN-ETOL})(\text{CO})_4$	219.1	214.8	206.1	157.8	153.4	139.1	116.3	110.9
$\text{Mo}(\text{PN-BIPOL})(\text{CO})_4$	218.5	214.4	206.2	157.8	153.9	139.4	116.8	111.2
$\text{Mo}(\text{PN-}^t\text{BuBIPOL})(\text{CO})_4$	219.2	215.2	206.7	157.5	153.7	139.4	116.4	111.0
$\text{Mo}(\text{PN-TAR}^{\text{Me}})(\text{CO})_4$	218.5	214.8	205.8, 205.6 ^a	157.4	153.3	139.2	116.6	111.4

^a*trans* carbonyls give two signals due to the chiral ligand

Table 3.7: Selected $^{13}\text{C}\{^1\text{H}\}$ NMR-shifts of the $\text{Mo}(\text{PN-R})(\text{CO})_4$ complexes (δ [ppm], CD_2Cl_2 , 20 °C)

IR spectra of the complexes were recorded. The possible symmetric and asymmetric basal and apical carbonyl stretching modes are depicted in Figure 3.13. In order to ex-

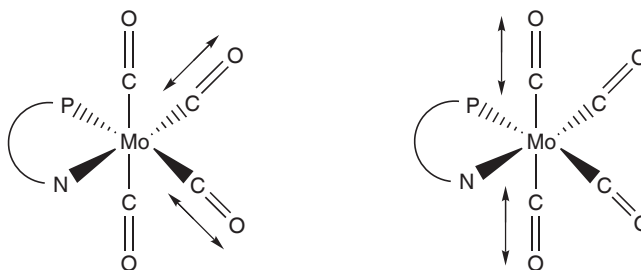


Figure 3.13: Stretching vibrations of the basal and apical carbonyl ligands

plain the observed infrared absorptions commonly assigned to the coordinated carbonyl ligands, frequency calculations were carried out for $\text{Mo}(\text{PN-ETOL})(\text{CO})_4$ and $\text{Mo}(\text{PN-Ph})(\text{CO})_4$. In the case of $\text{Mo}(\text{PN-ETOL})(\text{CO})_4$ with an almost planar arrangement of the octahedral plane the asymmetric apical CO stretching and the symmetric basal CO stretching are almost degenerate. Geometric data were taken from the experimentally obtained structures and a scale factor of 0.9608 was applied to the calculated frequencies. These are listed in Table 3.8.

Complex	Basal CO		Apical CO	
	$\nu_{\text{C=O}}$ (asym.)	$\nu_{\text{C=O}}$ (sym.)	$\nu_{\text{C=O}}$ (asym.)	$\nu_{\text{C=O}}$ (sym.)
$\text{Mo}(\text{PN-ETOL})(\text{CO})_4$	1919	1948	1946	2027
$\text{Mo}(\text{PN-Ph})(\text{CO})_4$	1906	1934	1923	2015

Table 3.8: Calculated stretching vibration frequencies of the carbonyl ligands of $\text{Mo}(\text{PN-ETOL})(\text{CO})_4$ and $\text{Mo}(\text{PN-Ph})(\text{CO})_4$ [cm^{-1}]

Additionally, the structures of several complexes were confirmed by X-ray crystallography. Structural views of $\text{Mo}(\text{PN-Ph})(\text{CO})_4$ (Figure 3.14), $\text{Mo}(\text{PN-}^i\text{Pr})(\text{CO})_4$ (Figure 3.15), $\text{Mo}(\text{PN-}^t\text{Bu})(\text{CO})_4$ (Figure 3.16), and $\text{Mo}(\text{PN-ETOL})(\text{CO})_4$ (Figure 3.17) are shown along with selected bond lengths and angles reported in the captions. For all complexes yellow crystals were obtained by slow diffusion of *n*-pentane into a saturated dichloromethane solution of the compound.

The structure of $\text{Mo}(\text{PN-Ph})(\text{CO})_4$ (Figure 3.14) comprises one molecule of dichloromethane as crystallisation solvent which is highly disordered. Due to the immediate loss of solvent the crystals were not stable in air. A hydrogen bond between the nitrogen bound proton and the O(2) oxygen atom of another molecule's carbonyl ligand is observed which results in the formation of infinite chains.

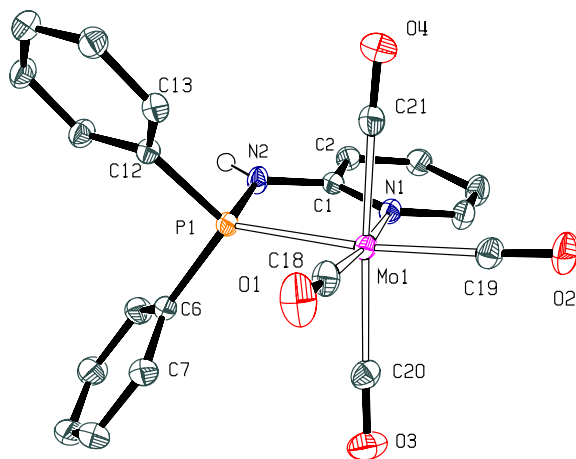


Figure 3.14: Structural view of $\text{Mo}(\text{PN-Ph})(\text{CO})_4$ showing 50 % thermal ellipsoids (C-bound hydrogen atoms and crystallisation solvent omitted for clarity). Selected bond lengths (\AA), bond angles and torsion angles ($^\circ$): $\text{Mo}(1)\text{--N}(1)$ 2.2822(10), $\text{Mo}(1)\text{--P}(1)$ 2.4803(3), $\text{Mo}(1)\text{--C}(18)$ 1.9675(14), $\text{Mo}(1)\text{--C}(19)$ 1.9821(13), $\text{Mo}(1)\text{--C}(20)$ 2.0643(13), $\text{Mo}(1)\text{--C}(21)$ 2.0263(13); $\text{C}(18)\text{--Mo}(1)\text{--N}(1)$ 173.41(4), $\text{C}(19)\text{--Mo}(1)\text{--P}(1)$ 170.01(4), $\text{C}(21)\text{--Mo}(1)\text{--C}(20)$ 174.19(5), $\text{N}(1)\text{--Mo}(1)\text{--P}(1)$ 75.89(3), $\text{C}(20)\text{--Mo}(1)\text{--N}(1)$ 94.98(4), $\text{C}(20)\text{--Mo}(1)\text{--P}(1)$ 94.46(4), $\text{C}(21)\text{--Mo}(1)\text{--N}(1)$ 89.43(5), $\text{C}(21)\text{--Mo}(1)\text{--P}(1)$ 90.29(4); $\text{N}(1)\text{--Mo}(1)\text{--P}(1)\text{--N}(2)$ $-12.26(5)$, $\text{P}(1)\text{--N}(2)\text{--C}(1)\text{--N}(1)$ $-9.26(15)$.

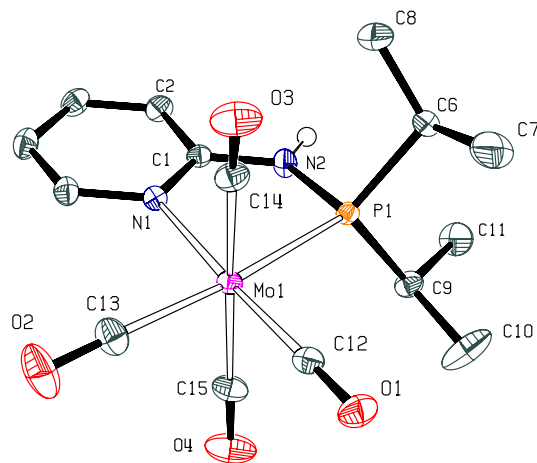


Figure 3.15: Structural view of $\text{Mo}(\text{PN}^i\text{Pr})(\text{CO})_4$ showing 50 % thermal ellipsoids (C-bound hydrogen atoms omitted for clarity). Selected bond lengths (\AA), bond angles and torsion angles ($^\circ$): Mo(1)–N(1) 2.2962(9), Mo(1)–P(1) 2.4912(3), Mo(1)–C(12) 1.9631(11), Mo(1)–C(13) 1.9951(13), Mo(1)–C(14) 2.0505(12), Mo(1)–C(15) 2.0347(12); C(12)–Mo(1)–N(1) 176.38(4), C(13)–Mo(1)–P(1) 170.46(4), C(14)–Mo(1)–C(15) 172.52(4), N(1)–Mo(1)–P(1) 76.31(2), C(14)–Mo(1)–N(1) 94.55(4), C(14)–Mo(1)–P(1) 94.39(3), C(15)–Mo(1)–N(1) 92.42(4), C(15)–Mo(1)–P(1) 89.91(3); N(1)–Mo(1)–P(1)–N(2) $-3.96(4)$, P(1)–N(2)–C(1)–N(1) $-7.56(15)$.

Large prismatic crystals of $\text{Mo}(\text{PN}^i\text{Pr})(\text{CO})_4$ were obtained, one of them being collected and shaped for structure determination. Similar to $\text{Mo}(\text{PN-Ph})(\text{CO})_4$ the nitrogen bound proton generates a hydrogen bond to the O(1) of another molecule. Due to the non-linearity of this bond the N(2) nitrogen exhibits a slight pyramidal coordination. The same holds true for $\text{Mo}(\text{PN}^t\text{Bu})(\text{CO})_4$ with the hydrogen bond being established to the O(2) oxygen atom.

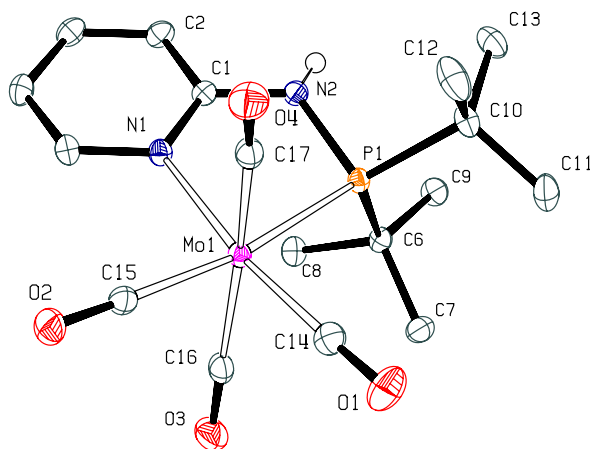


Figure 3.16: Structural view of $\text{Mo}(\text{PN}^t\text{Bu})(\text{CO})_4$ showing 50 % thermal ellipsoids (C-bound hydrogen atoms omitted for clarity). Selected bond lengths (Å), bond angles and torsion angles (°): Mo(1)–N(1) 2.2874(9), Mo(1)–P(1) 2.5596(3), Mo(1)–C(14) 1.9793(12), Mo(1)–C(15) 1.9666(11), Mo(1)–C(16) 2.0567(12), Mo(1)–C(17) 2.0280(11); C(14)–Mo(1)–N(1) 172.33(4), C(15)–Mo(1)–P(1) 170.35(3), C(16)–Mo(1)–C(17) 166.49(5), N(1)–Mo(1)–P(1) 75.22(2), C(17)–Mo(1)–N(1) 90.97(4), C(17)–Mo(1)–P(1) 96.36(3), C(16)–Mo(1)–N(1) 98.00(4), C(16)–Mo(1)–P(1) 95.70(3); N(1)–Mo(1)–P(1)–N(2) 15.01(4), P(1)–N(2)–C(1)–N(1) 15.80(14).

In all four complexes the molybdenum centre displays a distorted octahedral coordination geometry. The PN ligands occupy two sites of the octahedral plane while the four carbonyl ligands are located in the remaining two positions of the octahedral plane and in the two apical positions. Whereas the Mo–P(1) bonds range from 2.4092(6) to 2.5596(3) Å, the Mo–N(1) bonds are significantly shorter varying between 2.2732(18) and 2.2962(9) Å. The bond distances between the metal centre and the carbonyl ligands in the octahedral plane lie in the range of 1.9631(11) to 1.997(2) Å and are shorter than those between molybdenum and the apical carbonyls which vary from 2.0263(13) to 2.0643(13) Å.

Concerning the bond angles around the metal it is obvious that the P(1)–Mo(1)–C(*trans*-P) angle is not affected by the nature of the substituent on the phosphorus atom varying

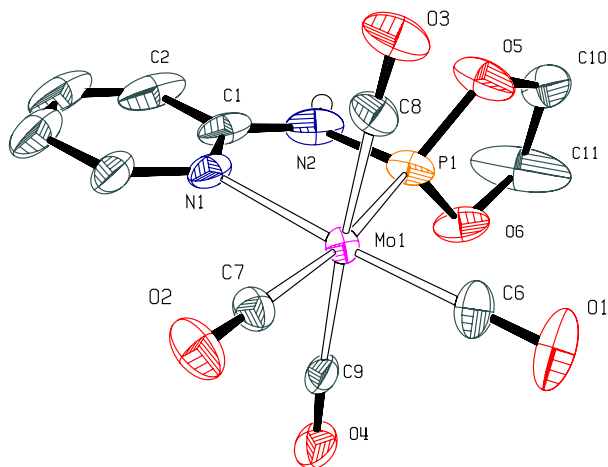


Figure 3.17: Structural view of $\text{Mo}(\text{PN-ETOL})(\text{CO})_4$ showing 50 % thermal ellipsoids (C-bound hydrogen atoms omitted for clarity). Selected bond lengths (\AA), bond angles and torsion angles ($^\circ$): $\text{Mo}(1)\text{--N}(1)$ 2.2732(18), $\text{Mo}(1)\text{--P}(1)$ 2.4092(6), $\text{Mo}(1)\text{--C}(6)$ 1.965(2), $\text{Mo}(1)\text{--C}(7)$ 1.997(2), $\text{Mo}(1)\text{--C}(8)$ 2.031(2), $\text{Mo}(1)\text{--C}(9)$ 2.050(2); $\text{C}(6)\text{--Mo}(1)\text{--N}(1)$ 175.18(9), $\text{C}(7)\text{--Mo}(1)\text{--P}(1)$ 170.81(6), $\text{C}(8)\text{--Mo}(1)\text{--C}(9)$ 174.43(8), $\text{N}(1)\text{--Mo}(1)\text{--P}(1)$ 76.64(6), $\text{C}(8)\text{--Mo}(1)\text{--N}(1)$ 92.70(8), $\text{C}(8)\text{--Mo}(1)\text{--P}(1)$ 91.66(6), $\text{C}(9)\text{--Mo}(1)\text{--N}(1)$ 92.60(7), $\text{C}(9)\text{--Mo}(1)\text{--P}(1)$ 91.22(6); $\text{N}(1)\text{--Mo}(1)\text{--P}(1)\text{--N}(2)$ $-4.35(8)$, $\text{P}(1)\text{--N}(2)\text{--C}(1)\text{--N}(1)$ $-3.0(3)$, $\text{O}(5)\text{--C}(10)\text{--C}(11)\text{--O}(6)$ $-13.2(5)$.

only in a narrow interval between $170.01(4)^\circ$ and $170.81(6)^\circ$. This is presumably due to the fact that the carbonyl ligand points in the direction opposite to the phosphine or phosphite moiety so that no influence is exerted. The $\text{N}(1)\text{--Mo}(1)\text{--C}(\text{trans-N})$ angles, however, are influenced by the substituent on the phosphorus and range from $172.33(4)^\circ$ for $\text{P-}^t\text{Bu}$ to $176.38(4)^\circ$ for $\text{P-}^i\text{Pr}$.

The nature and therefore the size of the phosphine or phosphite becomes effective when the $\text{C--Mo}(1)\text{--C}$ angle between the two carbonyl ligands *trans* to each other is looked upon closer: This angle decreases from $174.43(8)^\circ$ (P-ETOL) and $174.19(5)^\circ$ (P-Ph) via $172.52(4)^\circ$ ($\text{P-}^i\text{Pr}$) to $166.49(5)^\circ$ ($\text{P-}^t\text{Bu}$) emphasising the sterical demand of the *tert.*-butyl substituent. The same holds true for the torsion angles $\text{N}(1)\text{--Mo}(1)\text{--P}(1)\text{--N}(2)$ and $\text{P}(1)\text{--N}(2)\text{--C}(1)\text{--N}(1)$. While in $\text{Mo}(\text{PN-ETOL})(\text{CO})_4$ both angles lie in the range of $3\text{--}4^\circ$ indicating a planar geometry the value increases to about 15° for $\text{Mo}(\text{PN-}^t\text{Bu})(\text{CO})_4$.

3.2.5 Reactivity of Molybdenum(0) complexes

Molybdenum compounds are found to be stable in a wide variety of oxidation states ($\text{Mo}^0\text{--Mo}^{\text{VI}}$) and because of the possibility to switch easily between these oxidation states they are commonly used in catalytic applications. A very important reaction that can be efficiently catalysed by molybdenum containing "Schrock catalysts" is olefin metathesis.⁵² The Schrock catalysts comprise a Mo^{IV} metal centre, an alkylidene ligand, an imidoaryl ligand and two single or one chelating achiral or chiral alkoxide ligand(s) (Figure 3.18).

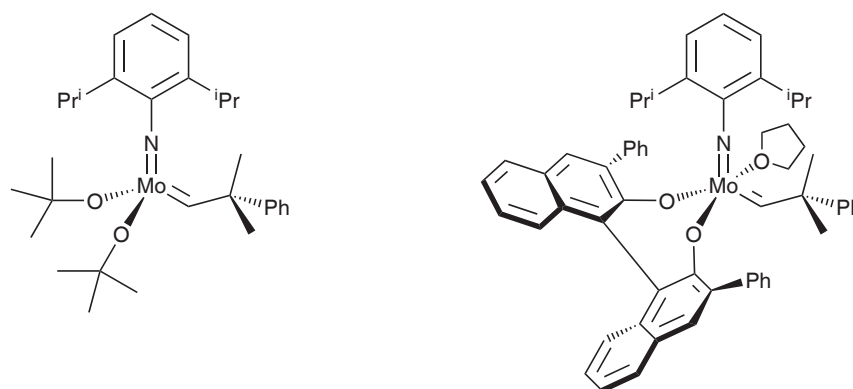
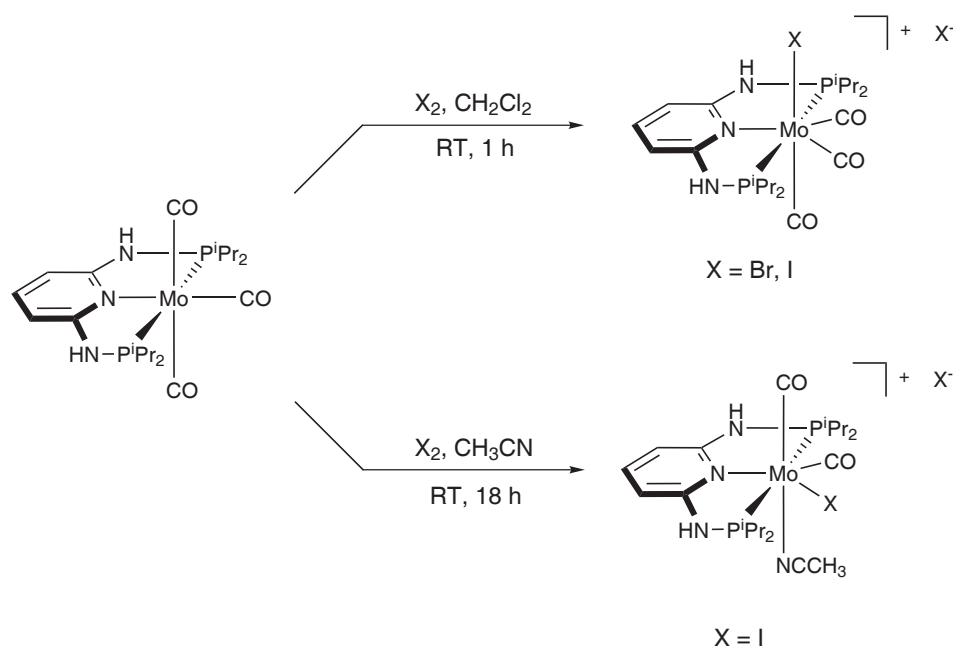


Figure 3.18: Examples for achiral (left) and chiral (right) Schrock catalysts

Other catalytic applications of molybdenum complexes include olefin epoxidation^{53–55} and, very recently, the fixation and activation of dinitrogen.⁵⁶ Moreover, zerovalent

molybdenum complexes are known to undergo oxidative addition reactions.⁵⁷ In this context, the reactivity of $\text{K}[\text{MoTp}(\text{CO})_3]$ towards methyl iodide, acetic acid and allyl bromide has been studied.⁴⁹ Upon oxidative addition of these reactants, this model complex was found to give neutral, bivalent hepta-coordinated compounds.

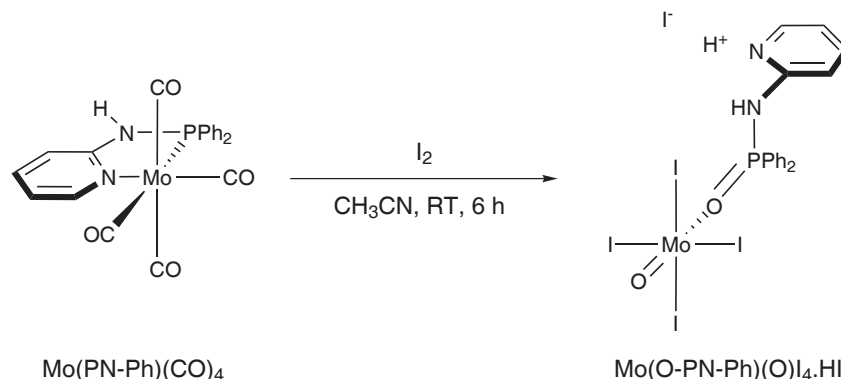
Investigations that have been carried out in our group^{12,58} revealed that molybdenum PNP complexes can be reacted with halogens to form the first hepta-coordinated molybdenum pincer complexes reported in the literature. It has been found that $\text{Mo}(\text{PNP-}^i\text{Pr})(\text{CO})_3$ reacts readily with one equivalent of Br_2 or I_2 in CH_2Cl_2 to afford the hepta-coordinated complex $[\text{Mo}(\text{PNP-}^i\text{Pr})(\text{CO})_3\text{X}]\text{X}$ ($\text{X} = \text{Br}, \text{I}$). Additionally, when treated with two equivalents of I_2 $\text{Mo}(\text{PNP-}^i\text{Pr})(\text{CO})_3$ forms the compound $[\text{Mo}(\text{PNP-}^i\text{Pr})(\text{CO})_3\text{I}]\text{I}_3$. These two hepta-coordinated complexes differ only in the nature of the counterion, *i.e.*, iodide versus triiodide. On the other hand, performing the reaction in CH_3CN results in the formation of the mono-acetonitrile complex $[\text{Mo}(\text{PNP-}^i\text{Pr})(\text{CO})_2(\text{CH}_3\text{CN})\text{I}]\text{I}$ (Scheme 3.16).



Scheme 3.16: Reaction of $\text{Mo}(\text{PNP-}^i\text{Pr})(\text{CO})_3$ with halogens

Molybdenum complexes with P–N bond containing ligands (*e.g.* dialkylaminodifluorophosphine $[\text{PF}_2\text{NR}_2]$) are found to be reactive towards hydrogen halides resulting in the cleavage of the P–N bond.^{59–62} Apart from these investigations the reactivity of such compounds has not been examined. Accordingly, one of the goals of this work was to study the reactivity of the $\text{Mo}(\text{PN-R})(\text{CO})_4$ complexes towards several substrates. For

this purpose $\text{Mo}(\text{PN-Ph})(\text{CO})_4$ and $\text{Mo}(\text{PN-}^i\text{Pr})(\text{CO})_4$ were chosen as the model complexes.



Scheme 3.17: Reaction of $\text{Mo}(\text{PN-Ph})(\text{CO})_4$ with iodine

When compared to $\text{Mo}(\text{PNP-}^i\text{Pr})(\text{CO})_3$ the complex $\text{Mo}(\text{PN-Ph})(\text{CO})_4$ shows enhanced reactivity towards iodine, which results in the cleavage of all carbonyl ligands rather than the formation of a heptacoordinated complex (Scheme 3.17). An equimolar amount of iodine (neat or in solution) was added to a cooled acetonitrile solution of $\text{Mo}(\text{PN-Ph})(\text{CO})_4$ whereupon gas evaporation was observed. After work-up the product was obtained as brown solid in 38 % yield. From the $^{13}\text{C}\{^1\text{H}\}$ NMR spectroscopic data it is obvious that all carbonyl ligands have been displaced, additionally, the $^{31}\text{P}\{^1\text{H}\}$ NMR spectrum exhibits a single resonance at 99.32 ppm. Apart from that the NMR spectra bear no unusual features.

Crystals of $\text{Mo}(\text{O-PN-Ph})(\text{O})\text{I}_4$ were obtained by evaporation of a 1,2-dichloroethane solution of the compound. A structural view is depicted in Figure 3.19 along with selected bond lengths and angles reported in the captions. The crystal structure features an extra aminopyridine molecule. The position of the N(2)-bonded proton was inferred from the N(2)–I(5) distance which represents the shortest N–I(5) distance (3.457 Å) of all nitrogen atoms. This indicates the presence of a significant N–H–I hydrogen bond. However, it cannot be ruled out that the acid proton is distributed between N(2) of the $\text{Mo}(\text{O-PN-Ph})(\text{O})\text{I}_4$ complex and N(4) of the free aminopyridine molecule because the aromatic C–N bonds in both pyridine rings do not differ significantly. The coordination geometry around the molybdenum centre can be described as distorted octahedron with the Mo(1)–I bonds being significantly longer than the Mo(1)–O bonds (2.760 to 2.810 *vs.* 1.659 to 2.174 Å, respectively). Finally, it is worth mentioning that the substituents on the phosphorus are arranged in a tetrahedral geometry.

$\text{Mo}(\text{PN-}^i\text{Pr})(\text{CO})_4$ undergoes oxidative addition of allyl bromide with concomitant loss

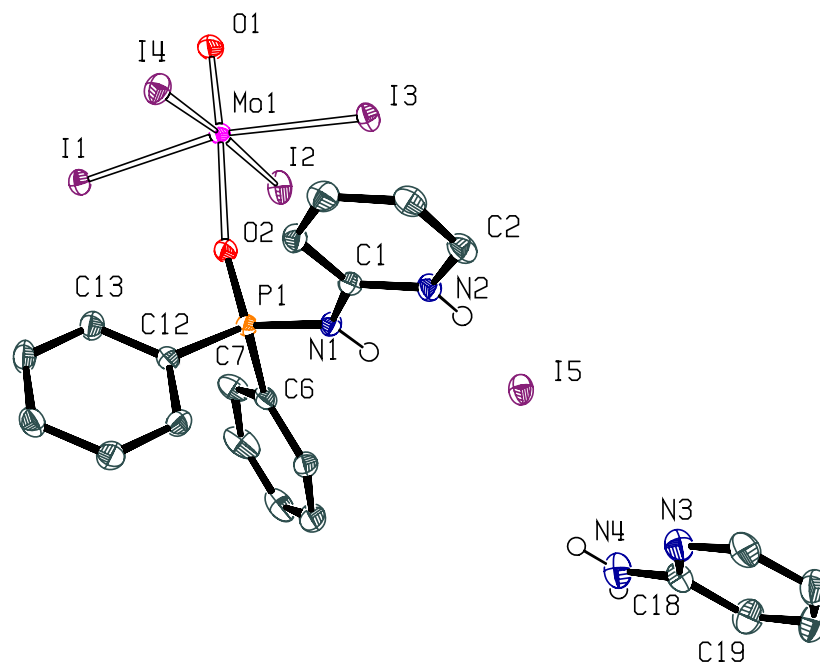
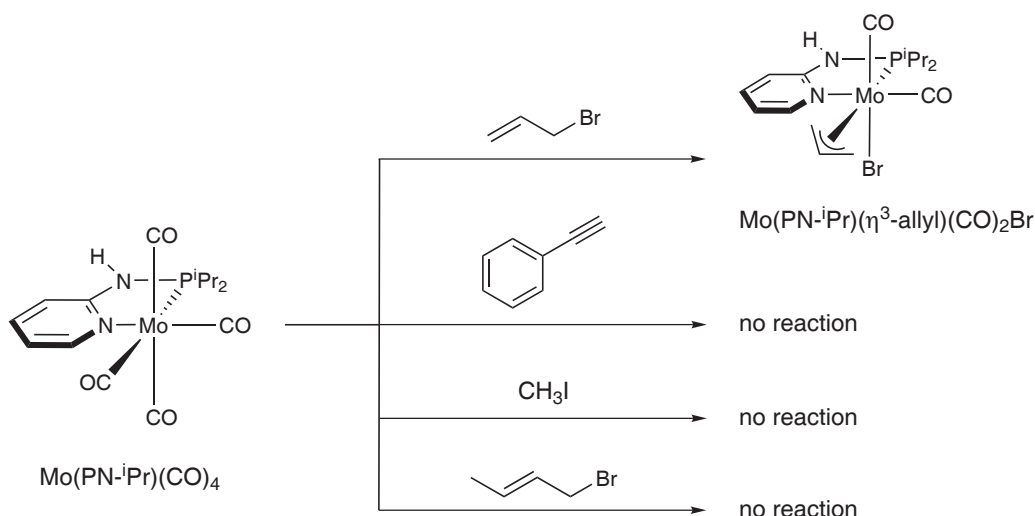


Figure 3.19: Structural view of $\text{Mo}(\text{O-PN-Ph})(\text{O})\text{I}_4$ showing 50 % thermal ellipsoids (C-bound hydrogen atoms omitted for clarity). Selected bond lengths (Å), and angles (°): Mo(1)–I(1) 2.810, Mo(1)–I(2) 2.760, Mo(1)–I(3) 2.764, Mo(1)–I(4) 2.762, Mo(1)–O(1) 1.659, Mo(1)–O(2) 2.174, O(2)–P(1) 1.499; I(1)–Mo(1)–I(3) 167.75, I(2)–Mo(1)–I(4) 174.00, O(1)–Mo(1)–O(2) 176.50, Mo(1)–O(2)–P(1) 165.25, O(2)–P(1)–C(6) 112.31, O(2)–P(1)–C(12) 108.44, O(2)–P(1)–N(1) 114.87.

Scheme 3.18: Reaction of $\text{Mo}(\text{PN}^i\text{Pr})(\text{CO})_4$ with various substrates

of two carbonyl ligands (Scheme 3.18). Heating equimolar amounts of $\text{Mo}(\text{PN}^i\text{Pr})(\text{CO})_4$ and allyl bromide in toluene gives the allyl complex as an orange solid in 82 % yield. Attempts to obtain vinylidene complexes—which are very useful substrates in various fields of organometallic and synthetic organic chemistry—by reacting the complex with phenylacetylene failed as well as the reaction with methyl iodide or crotyl bromide. A possible explanation for these findings is the instance that the carbonyl ligands are bound very strongly to the electron rich molybdenum centre due to the powerful π -backbonding exerted by the metal. The chelating PN ligand with two σ -donating groups even enhances this effect. As a consequence, substrates like methyl iodide prove to be too unreactive to undergo oxidative addition—this requires strong oxidising agents such as iodine.

The structure of $\text{Mo}(\text{PN}^i\text{Pr})(\eta^3\text{-allyl})(\text{CO})_2\text{Br}$ was confirmed by X-ray crystallography and is depicted in Figure 3.20 along with selected bond lengths and angles reported in the captions. Crystals were obtained by slow diffusion of *n*-pentane into a saturated dichloromethane solution of the compound. The bromine atom is slightly disordered and distributed among the *trans*-positions in a ratio 93:7. The coordination geometry around the molybdenum centre can be described as distorted octahedron. The PN ligand occupies two sites of the octahedral plane while the other positions of the octahedral plane are filled with the allyl-cation and a carbonyl ligand, respectively. The apical positions are occupied with bromide and another carbonyl.

Concerning the bond lengths around the metal centre the Mo–P(1) bond is the longest of the bonds to the ligands in the octahedral plane with 2.5215(5) Å. The Mo–N(1) bond lies

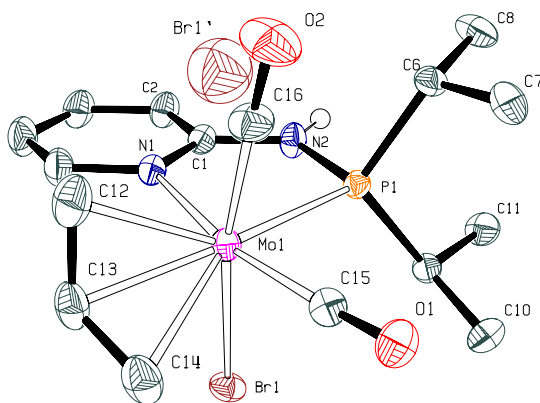


Figure 3.20: Structural view of $\text{Mo}(\text{PN}^i\text{Pr})(\eta^3\text{-allyl})(\text{CO})_2\text{Br}$ showing 50 % thermal ellipsoids (C-bound hydrogen atoms omitted for clarity). Selected bond lengths (Å), bond angles and torsion angles (°): Mo(1)–N(1) 2.3288(14), Mo(1)–P(1) 2.5215(5), Mo(1)–C(12) 2.328(2), Mo(1)–C(13) 2.2233(18), Mo(1)–C(14) 2.3507(19), Mo(1)–C(15) 1.9568(18), Mo(1)–C(16) 1.935(2), Mo(1)–Br(1′) 2.514(7), Mo(1)–Br(1) 2.6863(3); C(15)–Mo(1)–N(1) 166.81(6), C(12)–Mo(1)–P(1) 146.13(6), C(13)–Mo(1)–P(1) 163.46(5), C(14)–Mo(1)–P(1) 152.39(6), Br(1)–Mo(1)–C(16) 169.08(6), Br(1)–Mo–Br(1′) 169.83(13), N(1)–Mo(1)–P(1) 75.20(4), C(16)–Mo(1)–N(1) 98.65(8), C(16)–Mo(1)–P(1) 86.75(6), Br(1′)–Mo(1)–N(1) 88.41(14), Br(1′)–Mo(1)–P(1) 91.14(13), Br(1)–Mo(1)–N(1) 82.11(4), Br(1)–Mo(1)–P(1) 82.907(11), C(12)–C(13)–C(14) 115.1(2), C(12)–Mo(1)–C(14) 61.11(8); N(1)–Mo(1)–P(1)–N(2) –1.73(7), P(1)–N(2)–C(1)–N(1) 3.6(2).

in the same range as the Mo–C(allyl) bonds which vary from 2.2233(18) to 2.3507(19) Å. The bond angles display a strong deviation from the idealised geometry with the C(15)–Mo(1)–N(1) bond being 166.81(6)° and the Br(1)–Mo(1)–C(16) bond being 169.08(6)°. This may be due to the sterically demanding allyl-cation. However, no deviation from planarity of the PN-ⁱPr ligand is observed.

3.3 Iron complexes

3.3.1 Introduction

Although the first reports concerning iron (and cobalt) complexes of pincer-type bis-(imino)pyridine ligands date back to the 1950s it was only a decade ago that they established themselves as a class of powerful compounds in organometallic chemistry.⁶³

In 1998 and 1999 the groups of Brookhart⁶⁴ and Gibson⁶⁵ independently reported the synthesis of a series of iron(II) pincer complexes comprising bis(arylimino)pyridine moieties with very high catalytic activities for ethylene polymerisation (**A**, Figure 3.21). Consecutively, Chirik and coworkers have prepared several iron bis(dinitrogen)- and carbonyl complexes which can be used in olefin and alkyne hydrogenation, hydrosilylation and polymerisation reactions.^{66–69}

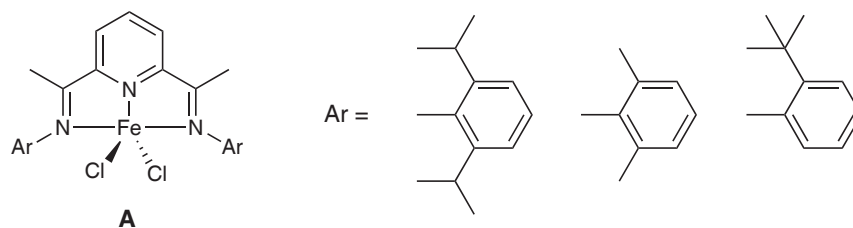
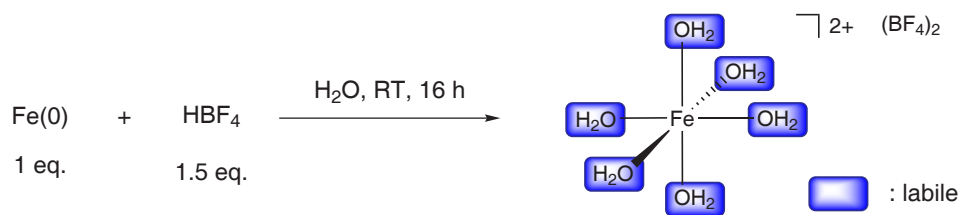


Figure 3.21: First examples of NNN iron complexes with catalytic activities in ethylene polymerisation

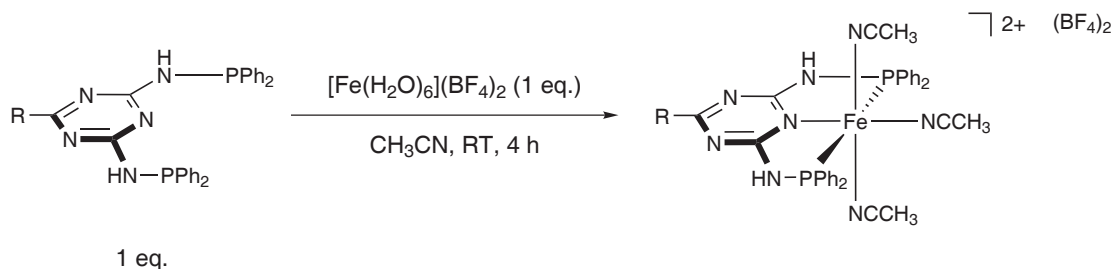
For the preparation of the iron complexes presented in this work hexaaquoiron(II) tetrafluoroborate⁷⁰ proved to be an excellent precursor. This compound can be synthesised in large quantities and very good yields from metallic iron powder and tetrafluoroboric acid (Scheme 3.19). The advantage of this precursor is that all aquo ligands are labile and can be displaced by other coordinating solvents. It may be of no minor concern for the stability of the ligands that during the course of the complexation reaction up to six equivalents of water are released for each equivalent of the iron precursor.

Scheme 3.19: Synthesis of $[\text{Fe}(\text{H}_2\text{O})_6](\text{BF}_4)_2$

3.3.2 Iron(II) PNP^T complexes

Synthesis

Equimolar amounts of the PNP^T ligands described in Section 3.1.3 and $[\text{Fe}(\text{H}_2\text{O})_6](\text{BF}_4)_2$ were reacted in acetonitrile to yield iron PNP^T complexes (Scheme 3.20).

Scheme 3.20: Synthesis of $[\text{Fe}(\text{PNP}^{\text{TR}}\text{-Ph})(\text{CH}_3\text{CN})_3](\text{BF}_4)_2$ complexes

Addition of the iron(II) precursor to a solution of the corresponding ligand in acetonitrile at room temperature afforded the complexes in 77–89 % yield (Figure 3.22). Due to the high lability of all of the H_2O ligands the reaction proceeds very fast. Once the iron precursor is added to the solution of the ligand, an immediate colour change from colourless/pale yellow to deep orange is observed. Removal of the solvent after four hours gives the crude iron complexes which in some cases contained paramagnetic impurities. The latter could be removed by flash chromatography. Interestingly, the release of six equivalents of water during the course of the reaction does not seem to affect the formation of the complexes.

It has to be noted that the synthesis of the melamine derived analogue $[\text{Fe}(\text{PNP}^{\text{TNH}}\text{-Ph})(\text{CH}_3\text{CN})_3](\text{BF}_4)_2$ was unsuccessful. Treatment of the corresponding ligand $\text{PNP}^{\text{TNH}}\text{-Ph}$

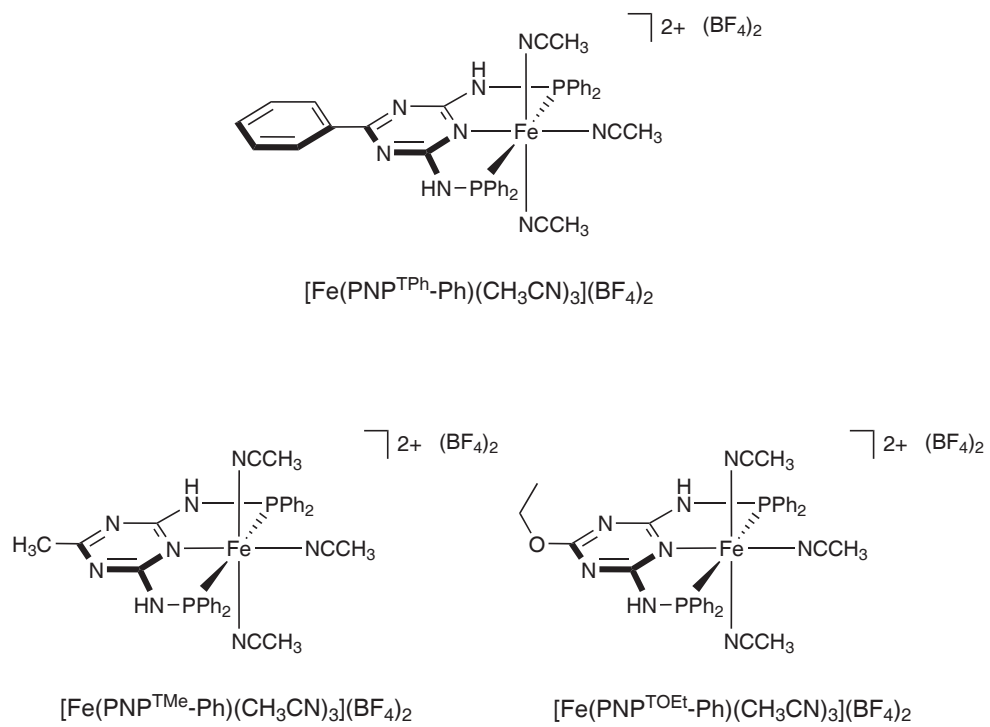


Figure 3.22: [Fe(PNP^{TR}-Ph)(CH₃CN)₃](BF₄)₂ complexes

Ph with $[\text{Fe}(\text{H}_2\text{O})_6](\text{BF}_4)_2$ did not result in the formation of a clean product. This may be due to the fact that this ligand can also coordinate *via* the amino group which may lead to a mixture of products.

Characterisation

The complexes were characterised by ^1H NMR, $^{13}\text{C}\{^1\text{H}\}$ NMR, and $^{31}\text{P}\{^1\text{H}\}$ NMR spectroscopy and X-ray crystallography. The ^1H NMR spectra bear no unusual features and are dominated by wide-stretched signal overlaps between the aromatic signals. The *NH* protons, however, are resolved and give a characteristic broad singlet in the range of 8.11 to 8.79 ppm. In a similar fashion, the methyl group of CH_3CN exhibits a broad single resonance between 1.94 and 1.97 ppm. The $^{31}\text{P}\{^1\text{H}\}$ NMR spectra exhibit a singlet in the range of 98.5 to 101.5 ppm.

In the $^{13}\text{C}\{^1\text{H}\}$ NMR spectra the triazine^{2,6} carbons give rise to singlets or triplets from 174.8 to 178.7 ppm while the triazine⁴ carbon atom exhibits a single resonance from 170.7 to 174.4 ppm. The carbon atom adjacent to the phosphorus gives rise to singlets in the range of 135.9 to 137.3 ppm. As observed in the Mo PNP^{T} complexes the shifts of the other diphenylphosphine carbon atoms are very similar for each compound. The Ph^4 carbon atom gives rise to singlets in the range of 131.9 to 132.1 ppm. The $\text{Ph}^{2,6}$ carbons exhibit singlets or triplets at 131.2 ppm with a coupling constant J_{CP} of 6.2 Hz and the $\text{Ph}^{3,5}$ carbons show triple resonances from 129.3 to 129.4 ppm with a coupling constant J_{CP} of 5.1 Hz.

$[\text{Fe}(\text{PNP}^{\text{TPh}}\text{-Ph})(\text{CH}_3\text{CN})_3](\text{BF}_4)_2$ (Figure 3.23) is the first triazine-based PNP complex that has been characterised by X-ray crystallography. The crystals were obtained as red air-stable prisms by slow evaporation of a concentrated 1,2-dichloroethane solution of the compound. Apart from two tetrafluoroborate counterions the structure comprises three molecules of the crystallising solvent and one molecule of water derived from air moisture. One counterion and two of the solvent molecules are highly disordered. As observed in related complexes the water molecule forms hydrogen bonds to the N(5) nitrogen atoms.

Orange crystals of the complexes $[\text{Fe}(\text{PNP}^{\text{TMe}}\text{-Ph})(\text{CH}_3\text{CN})_3](\text{BF}_4)_2$ (Figure 3.24) and $[\text{Fe}(\text{PNP}^{\text{TOEt}}\text{-Ph})(\text{CH}_3\text{CN})_3](\text{BF}_4)_2$ (Figure 3.25) were obtained by slow diffusion of diethyl ether into a saturated acetonitrile solution of the complexes. In the structure of the former the tetrafluoroborate counterions are moderately disordered, the latter features two molecules of acetonitrile as crystallising solvent.

The X-ray structures of the complexes reveal the distorted octahedral geometry around the iron centre. The PNP^{T} ligands coordinate in a meridional fashion occupying three sites of the octahedral plane. The three *N*-coordinated acetonitrile ligands are located

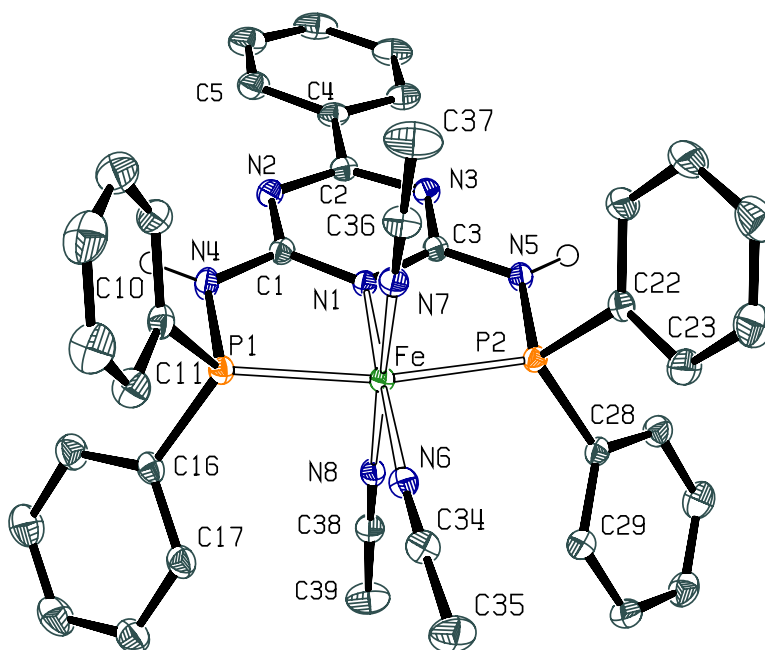


Figure 3.23: Structural view of $[\text{Fe}(\text{PNP}^{\text{TPH}}\text{-Ph})(\text{CH}_3\text{CN})_3](\text{BF}_4)_2 \cdot 3 \text{C}_2\text{H}_4\text{Cl}_2 \cdot \text{H}_2\text{O}$ showing 50 % thermal ellipsoids (C-bound hydrogen atoms, counterions, crystallisation solvent, and water omitted for clarity). Selected bond lengths (\AA), bond angles and torsion angles ($^\circ$): Fe–P(1) 2.2430(4), Fe–P(2) 2.2409(4), Fe–N(1) 1.9566(12), Fe–N(6) 1.9419(13), Fe–N(7) 1.9144(13), Fe–N(8) 1.9152(13); P(2)–Fe–P(1) 165.436(16), N(6)–Fe–N(1) 178.70(5), N(7)–Fe–N(8) 178.61(5); P(1)–N(4)–C(1)–N(1) $-3.40(18)$, P(2)–N(5)–C(3)–N(1) 1.72(17).

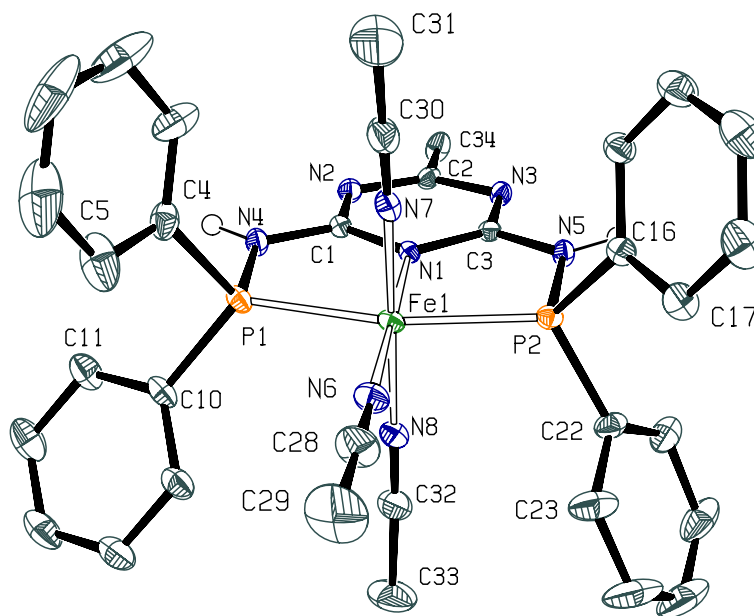


Figure 3.24: Structural view of $[\text{Fe}(\text{PNP}^{\text{TMc}}\text{-Ph})(\text{CH}_3\text{CN})_3](\text{BF}_4)_2$ showing 50 % thermal ellipsoids (C-bound hydrogen atoms and counterions omitted for clarity). Selected bond lengths (Å), bond angles and torsion angles (°): Fe–P(1) 2.2571(9), Fe(1)–P(2) 2.2397(8), Fe(1)–N(1) 1.958(2), Fe(1)–N(6) 1.928(3), Fe(1)–N(7) 1.912(3), Fe(1)–N(8) 1.928(3); P(2)–Fe(1)–P(1) 165.54(3), N(6)–Fe(1)–N(1) 179.60(11), N(7)–Fe(1)–N(8) 176.46(11); P(1)–N(4)–C(1)–N(1) $-2.5(3)$, P(2)–N(5)–C(3)–N(1) $5.1(3)$.

in the fourth site of the octahedral plane and in the two apical positions, respectively. Arising from the fact that the complexes differ only in the nature of the 4-substituent of the triazine ring the respective bond lengths and angles are very similar to each other.

Considering the coordination sphere around the iron centre the Fe–P bonds are the longest ones ranging from 2.2397(8) to 2.2571(9) Å. The Fe–N(1) distances—between the iron atom and the pincer ligands' central coordinating atom—are significantly shorter varying from 1.9566(12) to 1.9579(11) Å. Finally, it is worth mentioning that the Fe–N distances to the acetonitrile *trans* to the PNP^T nitrogen atom are generally longer than the ones *cis* to the PNP^T nitrogen (1.928(3)–1.9419(13) *vs.* 1.912(3)–1.928(3) Å).

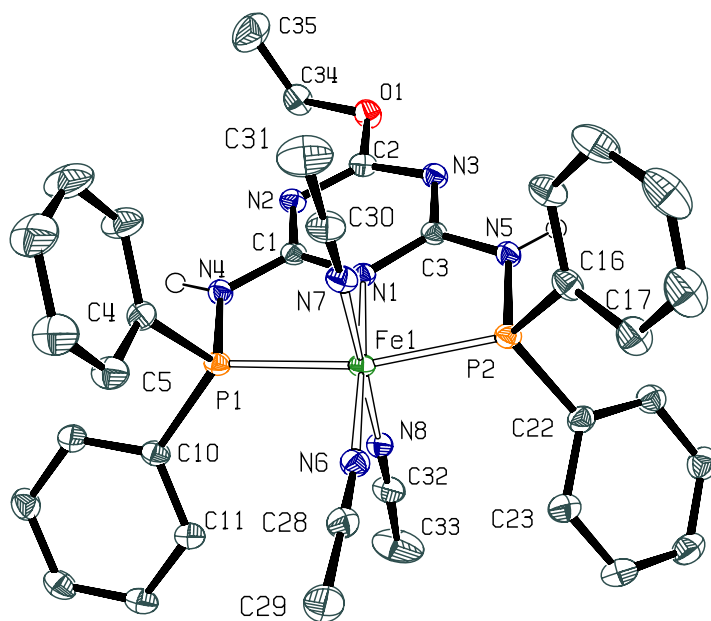


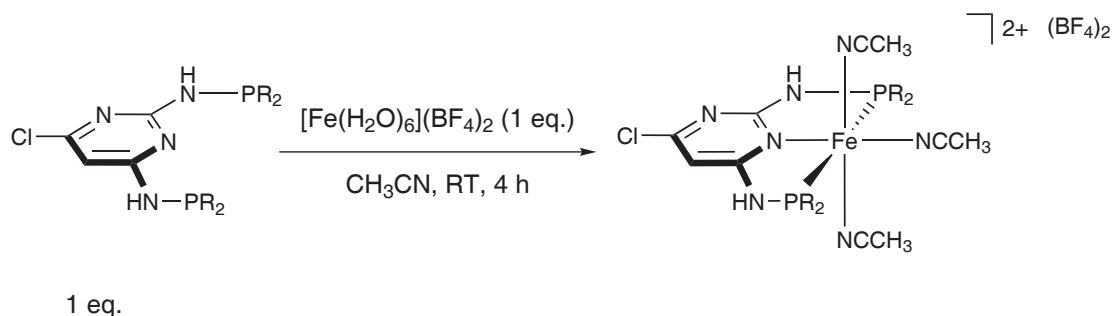
Figure 3.25: Structural view of $[\text{Fe}(\text{PNP}^{\text{TOEt-Ph}})(\text{CH}_3\text{CN})_3](\text{BF}_4)_2 \cdot 2 \text{CH}_3\text{CN}$ showing 50 % thermal ellipsoids (C-bound hydrogen atoms, counterions, and crystallisation solvent omitted for clarity). Selected bond lengths (Å), bond angles and torsion angles ($^\circ$): Fe(1)–P(1) 2.2452(4), Fe(1)–P(2) 2.2506(4), Fe(1)–N(1) 1.9579(11), Fe(1)–N(6) 1.9298(11), Fe(1)–N(7) 1.9142(12), Fe(1)–N(8) 1.9211(11); P(2)–Fe(1)–P(1) 165.523(14), N(6)–Fe(1)–N(1) 177.64(4), N(7)–Fe(1)–N(8) 179.78(5); P(1)–N(4)–C(1)–N(1) 3.10(15), P(2)–N(5)–C(3)–N(1) 0.93(16).

The distortion of the octahedral geometry is obvious when bond angles are looked upon closer: While the N–Fe–N angles (N being triazine as well as acetonitrile nitrogen atoms) are close to 180° in all complexes the P(1)–Fe–P(2) angles lie between $165.436(16)^\circ$ and

165.54(3)° showing that the iron atom is not located in the centre of the octahedral plane defined by the PNP^T ligand. No distinct deviation from the planarity of the ligand is observed, the respective torsion angles P(1)–N(4)–C(1)–N(1) and P(2)–N(5)–C(3)–N(1) range from 0.93(16)° to 5.1(3)°.

3.3.3 Iron(II) PNP^P complexes

Synthesis



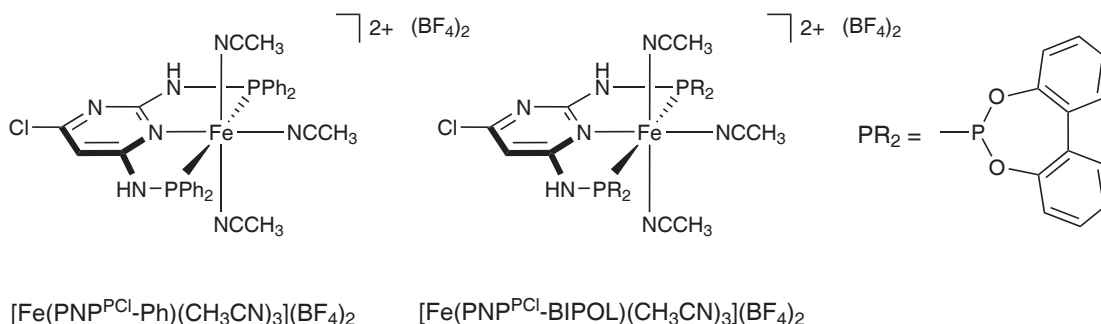
Scheme 3.21: Synthesis of $[\text{Fe}(\text{PNP}^{\text{P}^{\text{Cl}}}\text{-R})(\text{CH}_3\text{CN})_3](\text{BF}_4)_2$ complexes

Tris(acetonitrile) complexes of the pyrimidine-based PNP^P^{Cl}-R ligands were prepared from equimolar amounts of $[\text{Fe}(\text{H}_2\text{O})_6](\text{BF}_4)_2$ and the corresponding ligand. Like in the case of the triazine-based complexes the reactions proceeded very fast (Scheme 3.21). Thus, the complexes were obtained as brown solids in 76 % yield in the case of PNP^P^{Cl}-Ph and 71 % yield in the case of PNP^P^{Cl}-BIPOL (Figure 3.26).

Characterisation

The complexes were characterised by ^1H NMR, $^{13}\text{C}\{^1\text{H}\}$ NMR, and $^{31}\text{P}\{^1\text{H}\}$ NMR spectroscopy. The $^{31}\text{P}\{^1\text{H}\}$ NMR spectrum of $[\text{Fe}(\text{PNP}^{\text{P}^{\text{Cl}}}\text{-Ph})(\text{CH}_3\text{CN})_3](\text{BF}_4)_2$ exhibits a single resonance at 99.29 ppm while the one of $[\text{Fe}(\text{PNP}^{\text{P}^{\text{Cl}}}\text{-BIPOL})(\text{CH}_3\text{CN})_3](\text{BF}_4)_2$ shows two singlets at 176.73 and 181.05 ppm, respectively. In the ^1H NMR spectra the NH protons, which are not symmetrical in this type of compounds give rise to two broad singlets at 8.46 and 8.96 ppm for the phenyl derivative and a multiplet from 6.99 to 7.07 ppm and a singlet at 6.85 ppm for the BIPOL derivative, respectively.

In the $^{13}\text{C}\{^1\text{H}\}$ NMR spectra the pyrimidine^{2,4,6} carbon atoms give rise to signals in the

Figure 3.26: $[\text{Fe}(\text{PNP}^{\text{P}^{\text{Cl}}-\text{R}})(\text{CH}_3\text{CN})_3](\text{BF}_4)_2$ complexes

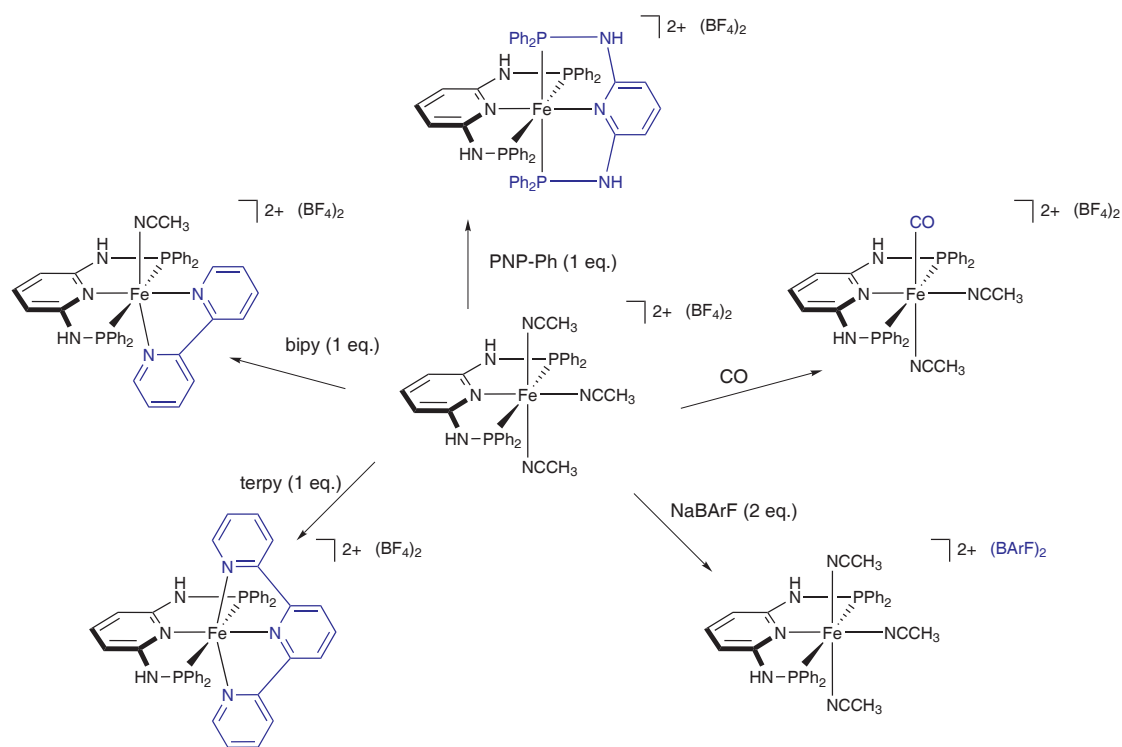
range of 159.7 to 176.9 ppm while the pyrimidine⁵ carbon exhibits a characteristic signal at 95.8 or 97.4 ppm. The carbon atoms of the phosphine and phosphite moiety lie within the expected range.

3.3.4 Lability of the acetonitrile ligands

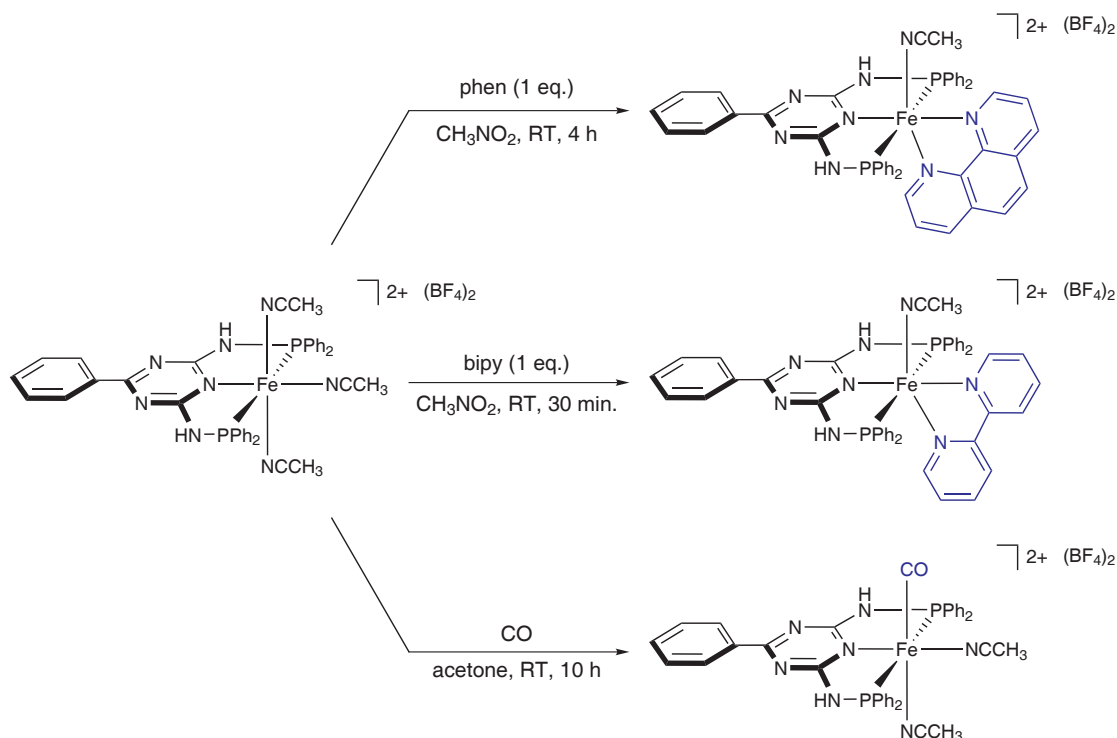
In exploring the chemistry of aminophosphine-based iron pincer ligands our group has examined their reactivity towards other ligands competing to acetonitrile.^{12,22} The lability of the three acetonitrile ligands has been studied on the related complex $[\text{Fe}(\text{PNP}^{\text{P}^{\text{Cl}}-\text{Ph}})(\text{CH}_3\text{CN})_3](\text{BF}_4)_2$. It has been shown that up to three of these ligands can be readily replaced by chelating nitrogen donors such as 2,2'-bipyridine or 2,2':6',2''-terpyridine. It is also possible to obtain bis-PNP complexes by adding another PNP-Ph ligand to a solution of the complex. Only one acetonitrile ligand is substituted when using carbon monoxide as competing ligand. Finally, the counterion can also be replaced by the non-coordinating anion BArF^- (Scheme 3.22).

Synthesis

Based on these findings the iron complexes with PNP^{T} ligands presented in this work were also examined with respect to their substitutional behaviour. For these investigations, $[\text{Fe}(\text{PNP}^{\text{TPh}}-\text{Ph})(\text{CH}_3\text{CN})_3](\text{BF}_4)_2$ was chosen as the model complex. As expected, displacement of the acetonitrile ligands with chelating nitrogen donor ligands proceeded very smoothly at room temperature. Upon addition of equimolar amounts of 1,10-phenanthroline or 2,2'-bipyridine to a solution of $[\text{Fe}(\text{PNP}^{\text{TPh}}-\text{Ph})(\text{CH}_3\text{CN})_3](\text{BF}_4)_2$ in nitromethane the colour changed immediately from orange to deep red. After removal of the solvent and a purification step the substituted complexes $[\text{Fe}(\text{PNP}^{\text{TPh}}-\text{Ph})(\text{CH}_3\text{CN})_2(\text{phen})](\text{BF}_4)_2$ and $[\text{Fe}(\text{PNP}^{\text{TPh}}-\text{Ph})(\text{CH}_3\text{CN})(\text{bipy})](\text{BF}_4)_2$ were obtained as

Scheme 3.22: Lability of the acetonitrile ligands of $[\text{Fe}(\text{PNP-Ph})(\text{CH}_3\text{CN})_3](\text{BF}_4)_2$

deep red, air-stable solids in 77-97 % yield (Scheme 3.23). When carbon monoxide is bubbled through an acetone solution of the complex $[\text{Fe}(\text{PNP}^{\text{TPh}}\text{-Ph})(\text{CH}_3\text{CN})_3](\text{BF}_4)_2$ for 15 min. and left to stir at room temperature for 10 h, the colour of the solution changes only slightly from orange to brown. After work-up the (bis)acetonitrile mono CO complex $[\text{Fe}(\text{PNP}^{\text{TPh}}\text{-Ph})(\text{CH}_3\text{CN})_2(\text{CO})](\text{BF}_4)_2$ is obtained in 82 % yield.



Scheme 3.23: Lability of the acetonitrile ligands of $[\text{Fe}(\text{PNP}^{\text{TPh}}\text{-Ph})(\text{CH}_3\text{CN})_3](\text{BF}_4)_2$

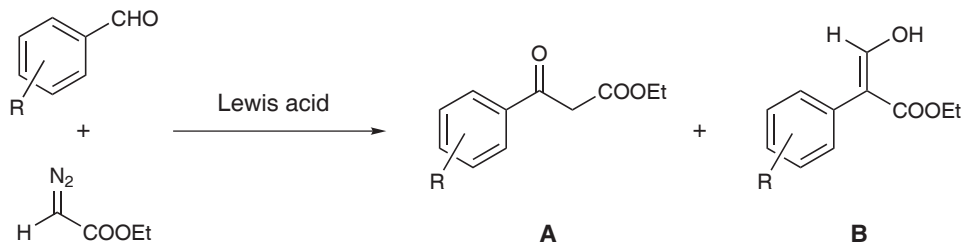
Characterisation

The complexes were characterised by ^1H NMR, $^{13}\text{C}\{^1\text{H}\}$ NMR, and $^{31}\text{P}\{^1\text{H}\}$ NMR spectroscopy. While the ^1H NMR spectra show signal overlaps that are even more developed in the compounds with additional aromatic protons, in the $^{31}\text{P}\{^1\text{H}\}$ NMR spectra, the signals of the substituted complexes appear shifted to the high field when compared to those of the original tris(acetonitrile) complex. In all cases a single resonance from 95.2 to 98.6 ppm was observed. Also the $^{13}\text{C}\{^1\text{H}\}$ NMR spectra appear shifted to the high field with spectra similar to those of the parent complex. In $[\text{Fe}(\text{PNP}^{\text{TPh}}\text{-Ph})(\text{CH}_3\text{CN})_2(\text{CO})](\text{BF}_4)_2$ the carbonyl gives rise to a weak signal at 213.7 ppm.

3.3.5 Iron(II) catalysed coupling of aromatic aldehydes with ethyl diazoacetate

Despite the fact that iron is a non-toxic, inexpensive and highly abundant transition metal the number of reactions that can actually be catalysed by iron complexes was limited for a long time. In the last few years the interest in iron-catalysed reactions increased due to its economical and ecological advantages. An important milestone was the discovery of the iron-catalysed polymerisation of ethylene mediated by the Brookhart-Gibson pyridine-diimine catalysts.^{64,65} Since then, very efficient catalytic processes have emerged which include asymmetric catalysis⁷¹ as well cross-coupling reactions of Grignard reagents with aryl, heteroaryl and alkyl chlorides.^{72–75}

Lewis acids such as BF_3 , ZnCl_2 , AlCl_3 , GeCl_2 , and SnCl_4 are known to catalyse the reaction of aromatic aldehydes with ethyl diazoacetate to give mainly 3-oxo-3-arylpropanoic acid ethyl esters (β -ketoesters) (**A**, Scheme 3.24) in high yields.^{76–80} Quite recently, Hos-sain and coworkers have discovered that the cyclopentadienyl dicarbonyl Lewis acid $[\text{FeCp}(\text{CO})_2(\text{THF})](\text{BF}_4)_2$ is an active catalyst for the coupling of aromatic aldehydes with ethyl diazoacetate to afford 3-hydroxy-2-arylacrylic acid ethyl esters (3-hydroxyacrylates) (**B**, Scheme 3.24) as the main product.^{81,82} This complex has consecutively found application in the synthesis of a Naproxen precursor, a highly valued antiinflammatory drug.⁸² A drawback of this catalyst is the need for slow addition of ethyl diazoacetate over a period of 6–7 h at low temperatures. Furthermore, mixtures of β -ketoesters and 3-hydroxyacrylates are obtained.



Scheme 3.24: Lewis acid catalysed formation of 3-hydroxyacrylates and β -ketoesters

To investigate the catalytic activity of the iron tris(acetonitrile) PNP^{T} complexes made within this work some coupling reactions with an array of aromatic aldehydes and ethyl diazoacetate and $[\text{Fe}(\text{PNP}^{\text{TPh}}\text{-Ph})(\text{CH}_3\text{CN})_3](\text{BF}_4)_2$ as catalyst were performed. In a typical procedure, aldehyde (1 eq.) and ethyl diazoacetate (1 eq.) were added at room temperature to a CH_3NO_2 or CH_2Cl_2 solution of the catalyst (10 mol%). The reaction mixture was then stirred for 16 h. Afterwards, the solvent was removed and the crude product purified by flash chromatography. The substrates and the product ratio are listed in Table 3.9.

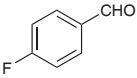
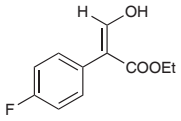
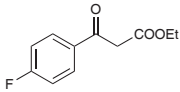
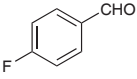
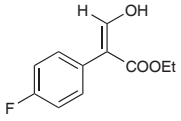
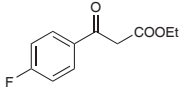
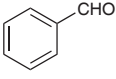
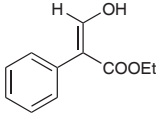
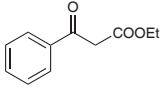
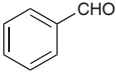
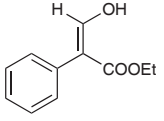
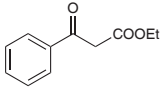
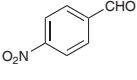
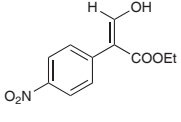
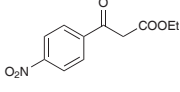
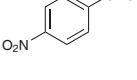
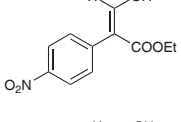
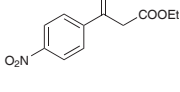
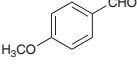
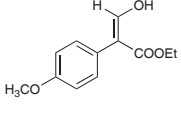
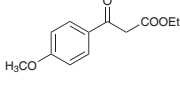
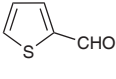
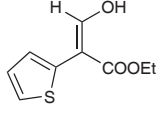
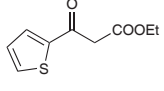
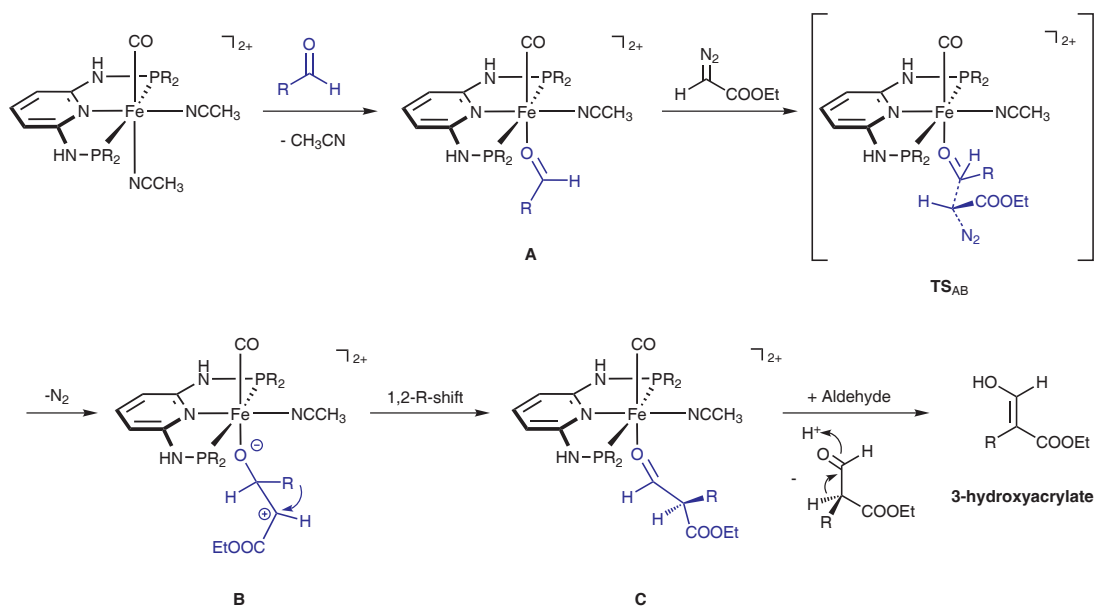
Entry	Solvent	Aldehyde	3-Hydroxy-acrylate	Yield	β -Ketoester	Yield
1	CH ₃ NO ₂			63		11
2	CH ₂ Cl ₂			43		18
3	CH ₃ NO ₂			56		12
4	CH ₂ Cl ₂			67		20
5	CH ₃ NO ₂			26		18
6	CH ₂ Cl ₂			43		39
7	CH ₃ NO ₂			44		5
8	CH ₂ Cl ₂			11		8

Table 3.9: Yields of the coupling of aromatic aldehydes with EDA

It can be seen from Table 3.9 that the formation of 3-hydroxyacrylates is favoured with all substrates and in most cases with a product ratio similar or better than those published by Hossain and coworkers.⁸³ Major advantages of the procedure presented here are the mild reaction conditions and the avoidance of slow addition of ethyl diazoacetate at low temperature.

It has to be noted that with the related $[\text{Fe}(\text{PNP-}^i\text{Pr})(\text{CH}_3\text{CN})_2\text{CO}](\text{BF}_4)_2$ complex up to 90 % of 3-hydroxyacrylates with amounts of β -ketoester less than 5 % are obtained. In the case of the triazine-based PNP^{T} complexes the preparation of the isopropyl derivative was not successful until now but it is believed that this complex shows enhanced catalytic activity.

Mechanistic investigations based on DFT/B3LYP calculations led to the proposal of a plausible mechanism for the catalytic cycle which is depicted in Scheme 3.25. Due to the stronger *trans*-effect exerted by the carbonyl ligand the initial displacement of acetonitrile by the aldehyde (which is present in a large excess under the catalytic conditions) may take place on the coordination site *trans* to the carbonyl which results in the formation of complex **A**. Nucleophilic attack of ethyl diazoacetate on the coordinated aldehyde via a $\text{S}_{\text{N}}2$ -type mechanism would yield, *via* the transition state TS_{AB} and liberation of N_2 , intermediate **B**.



Scheme 3.25: Proposed mechanism for the coupling of aromatic aldehydes with EDA

The preferential [1,2]-shift of the aromatic substituent over a hydride migration might lead to intermediate complex **C**, which comprises a $\kappa^1(\text{O})$ -coordinated aldehyde ester molecule. This might be displaced by an incoming unreacted aldehyde molecule and then tautomerise to yield the corresponding thermodynamically more stable 3-hydroxyacrylate. Thus, the catalytic process can be seen as an equilibrium reaction in which the product is subject to the displacement by unreacted aromatic aldehyde, which shows enhanced coordination properties. At the start of the catalytic reaction, a large excess of aldehyde is present to displace the produced 3-hydroxyacrylate; however, when conversions of around 80% are achieved, the amount of aldehyde is too small to release the product. Taking this into account, it seems reasonable that the catalytic reaction stops at around 90 % conversion and that the yields never reach 100 %.

3.4 Palladium complexes

3.4.1 Introduction

Together with nickel and platinum complexes palladium compounds were among the first transition metal pincer complexes published in the literature.^{1,2,84–86} Ever since, the discovery of their many applications in catalytic processes has made their study one of the major research fields in modern organometallic chemistry.^{3–5}

Palladium pincer complexes can be prepared by different metalation procedures with pincer ligands comprising a wide variety of backbones, spacer and donor groups. Some examples are depicted in Figure 3.27 illustrating the high versatility of this class of compounds.

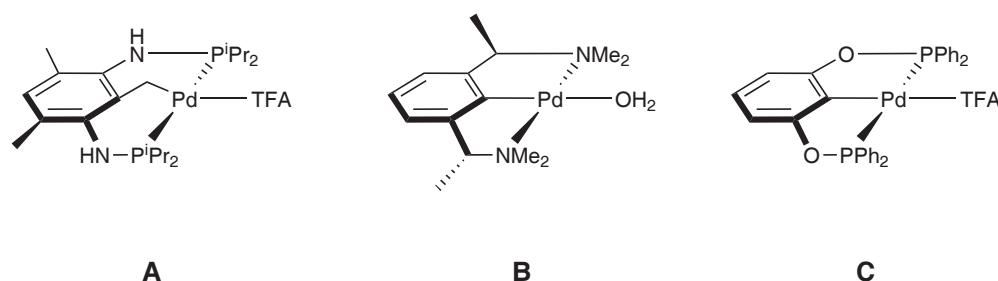


Figure 3.27: Examples of palladium pincer complexes

Within the large number of transition metal compounds that are catalytically active, palladium complexes play a very important role. The great diversity of their catalytic applications has been pointed out in several reviews.^{87–94} They are known to catalyze C–C bond forming reactions (Suzuki,^{95,96} Heck,^{97–100} and Sonogashira¹⁰¹ couplings), cyclopropanation reactions,¹⁰² aldol reactions¹⁰³ and Michael addition reactions.¹⁰⁴ Additionally, they have also been reported to promote C–C and C–H bond activation processes.³

Palladium complexes featuring thiophene imine moieties are found less often in the literature.^{105–107} The synthesis of $\text{Pd}(\text{SN}^{\text{n}}\text{Pr})_2\text{Cl}_2$ (**A**, Scheme 3.28) has been described elsewhere but no spectroscopical or X-ray data have been presented.³⁴ Additionally, the synthesis and characterisation along with one X-ray structure of related dichlorobis-*N*-[*N*-(2-thienylmethylene)-aniline]palladium(II) complexes (**B**, Scheme 3.28) has been published recently.¹⁰⁸

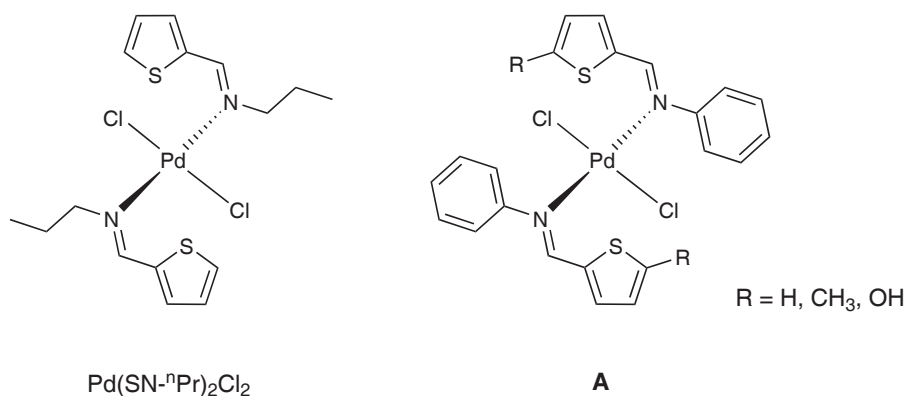


Figure 3.28: Examples of palladium thiophene imine complexes

3.4.2 Palladium(II) PNP^T complexes

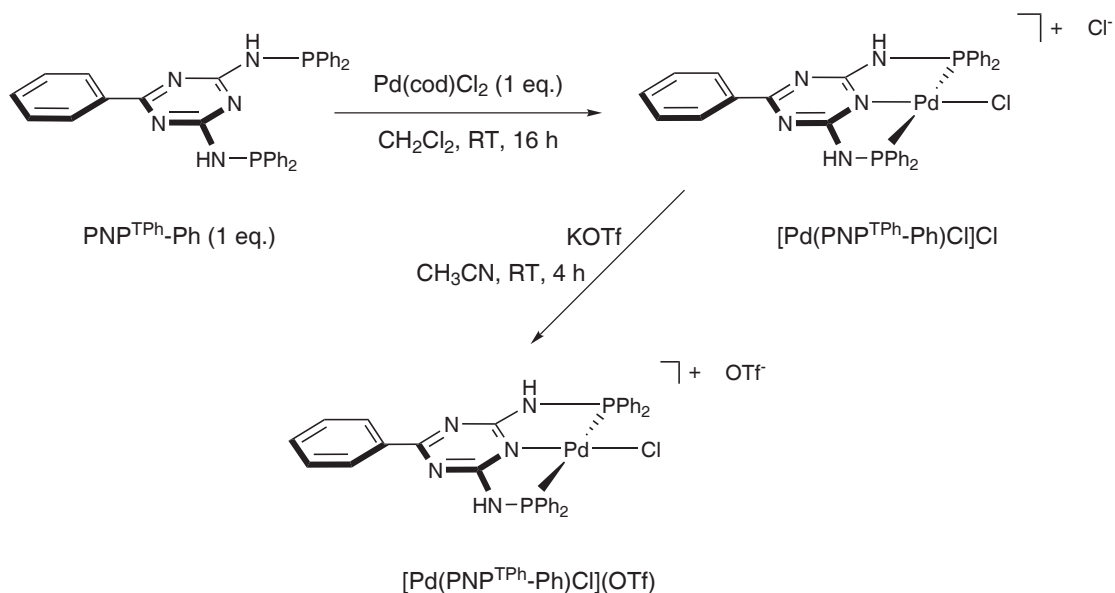
Synthesis

The PNP^T ligands described in this work can also be transformed into their palladium(II) complexes. Thus, a CH₂Cl₂ solution of one equivalent of the ligand PNP^{TPh}-Ph was reacted with one equivalent of Pd(cod)Cl₂ to afford, after workup, complex [Pd(PNP^{TPh}-Ph)Cl]Cl in 87 % yield. It turned out that this complex had only moderate solubility in common solvents, hence it was transferred into the more soluble [Pd(PNP^{TPh}-Ph)Cl]OTf complex. The exchange of the counterion was performed with potassium trifluoromethanesulfonate (KOSO₂CF₃) in acetonitrile at room temperature to yield 92 % (Scheme 3.26).

Characterisation

Due to the constrained solubility of [Pd(PNP^{TPh}-Ph)Cl]Cl it was only possible to record ¹H NMR and ³¹P{¹H} NMR spectra of this compound. The ¹H NMR spectrum is unremarkable with wide-stretched signal overlaps which include the NH protons as well as the aromatic signals. The ³¹P{¹H} NMR signal shows a singlet resonance at 62.7 ppm.

After exchange of the counterion the complex was sufficiently soluble and therefore fully characterised by ¹H NMR, ¹³C{¹H} NMR, and ³¹P{¹H} NMR spectroscopy. In the ¹H NMR spectrum the compound [Pd(PNP^{TPh}-Ph)Cl]OTf exhibits a doublet resonance at 8.27 ppm for the NH protons with a coupling constant *J* = 7.1 Hz. Again, the signals of the aromatic protons are not resolved.



Scheme 3.26: Synthesis and counterion exchange of $[\text{Pd}(\text{PNP}^{\text{TPh-Ph}})\text{Cl}]^+$

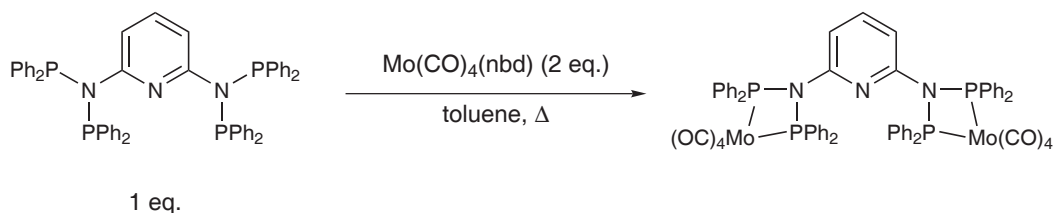
In the $^{13}\text{C}\{^1\text{H}\}$ NMR spectrum the phenyl carbons adjacent to the phosphorous atom give rise to triplet resonances at 132.5 ppm with a coupling constant $J_{\text{CP}} = 8.3$ Hz for the carbon atoms *ortho* and 129.5 ppm and $J_{\text{CP}} = 6.2$ Hz for the carbon atoms *meta* to the phosphorus. The *para*-carbon atom exhibits only a singlet resonance at 133.1 ppm. No resonance of the P-bound carbon could be detected. In comparison to the signal of $[\text{Pd}(\text{PNP}^{\text{TPh-Ph}})\text{Cl}]\text{Cl}$ the singlet resonance in the $^{31}\text{P}\{^1\text{H}\}$ NMR spectrum is shifted to the high field and is located at 60.7 ppm.

3.4.3 Palladium(II) PNP complexes

Synthesis

When reacted with the pyridine-based 2PN2P ligand, molybdenum was found to form four membered Mo–P–N–P metallacycles (Scheme 3.27) rather than coordinate in a tridentate fashion.³¹ No evidence for dimers, higher oligomers or other species was detected.

We were interested in whether palladium complexes show a similar coordination be-

Scheme 3.27: Reaction of the 2PN2P ligand with $\text{Mo(CO)}_4(\text{nbd})$

haviour, that is, if also four membered metallacycles are formed or if the ligand coordinates in a tridentate fashion. If the tridentate coordination mode was favoured, the additional free diphenylphosphino groups could then be reacted with other metal precursors to yield trinuclear complexes. Accordingly, a solution of one equivalent of the ligand in acetonitrile was treated with one equivalent of Pd(cod)Cl_2 at 60 °C for 10 h. After that the solvent was removed and the product was washed with diethyl ether.

Characterisation

The complex was characterised by ^1H NMR and $^{31}\text{P}\{^1\text{H}\}$ NMR spectroscopy and X-ray crystallography. From the $^{31}\text{P}\{^1\text{H}\}$ NMR spectrum it was evident that the ligand had indeed coordinated in a tridentate fashion; in accordance with spectral data presented in the literature²¹ a single resonance at 68.62 ppm was assigned to the existence of two five-membered palladacycles. A second signal was detected at 28.22 ppm. However, if free diphenylphosphino groups were still present in the complex, the resonance of the coordinated phosphines would not be exactly the same as those of the $[\text{Pd}(\text{PNP-Ph})\text{Cl}]\text{Cl}$ complex reported in the literature.

To determine the structure the compound was characterised by X-ray crystallography. Crystals were obtained by evaporation of a 1,2-dichloroethane solution. A structural view is presented in Figure 3.29 along with selected geometric data reported in the captions. From the structure it is obvious that the P–N bond of the non-coordinating phosphine groups were hydrolysed and that $[\text{Pd}(\text{PNP-Ph})\text{Cl}]\text{Cl}$ was formed (Scheme 3.28). This seems remarkable, since in other cases (*e.g.* the formation of the related $[\text{Fe}(\text{PNP}^{\text{TR}}\text{-Ph})(\text{CH}_3\text{CN})_3](\text{BF}_4)_2$ with $[\text{Fe}(\text{H}_2\text{O})_6](\text{BF}_4)_2$, where six equivalents of water are set free in the course of the reaction) the P–N bond proved to be very stable.

The structure of $[\text{Pd}(\text{PNP-Ph})\text{Cl}]\text{Cl}$ additionally comprises one molecule of crystallisation solvent and one molecule of water. An interesting feature of this structure are the three hydrogen bonds to the water molecule: one is formed between the oxygen atom of the water molecule a N–H bond of the pincer ligand while the others are developed between the hydrogen atoms of the water molecule and the chloride counterion.¹⁰⁹

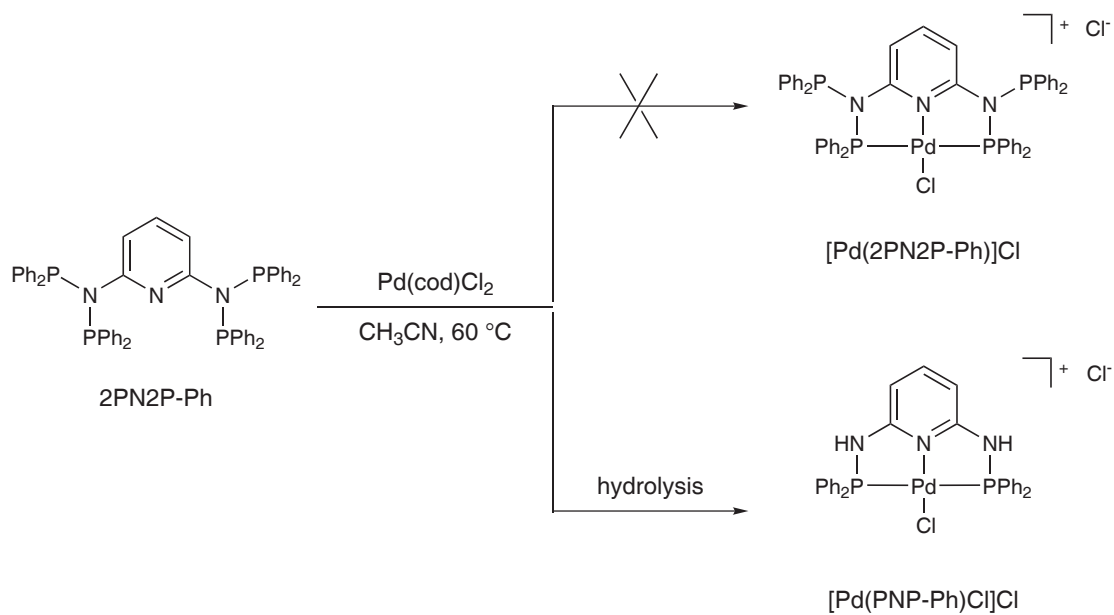
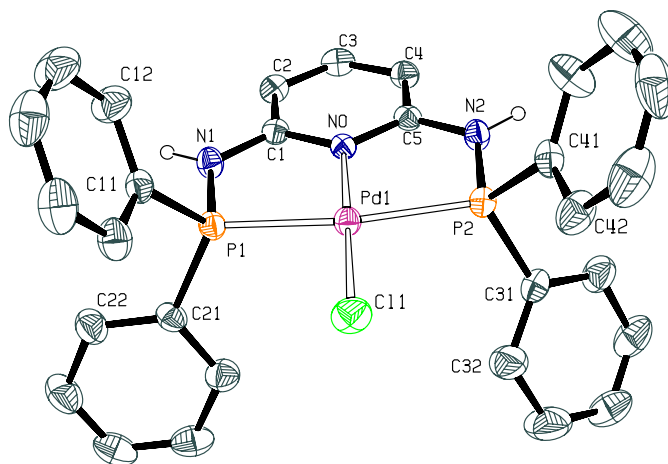
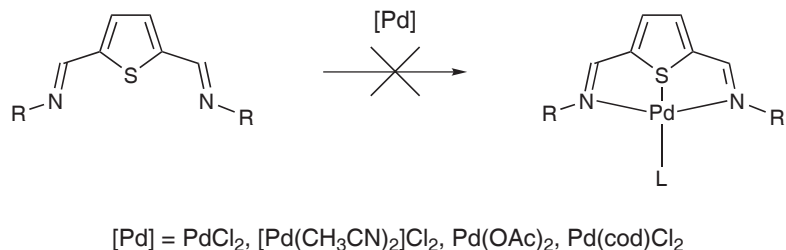
Scheme 3.28: Unexpected formation of $[\text{Pd}(\text{PNP-Ph})\text{Cl}]\text{Cl}$ 

Figure 3.29: Structural view of $[\text{Pd}(\text{PNP-Ph})\text{Cl}]\text{Cl}$ showing 30 % thermal ellipsoids (hydrogen atoms and crystallisation solvent omitted for clarity). Selected bond lengths (\AA) and angles ($^\circ$): Pd–P(1) 2.2705(7), Pd–P(2) 2.2750(7), Pd–N(1) 1.677(2), Pd–Cl(1) 2.3002(6), P(1)–N(1) 1.677(2), P(2)–N(2) 1.681(2); P(1)–Pd–P(2) 166.39(2), N(0)–Pd–Cl(1) 179.32(6).

3.4.4 Palladium(II) NSN complexes

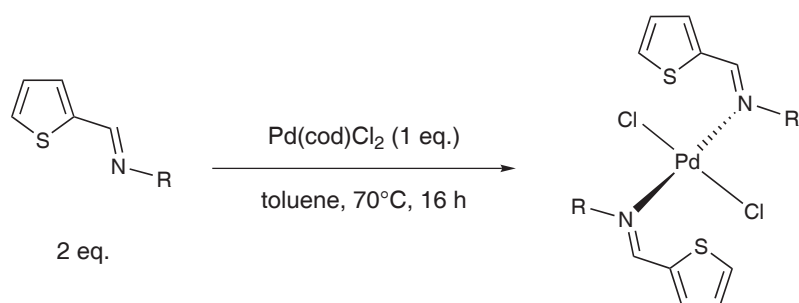


Scheme 3.29: Attempts for the synthesis of Pd NSN complexes

The thiophene-based NSN ligands were reacted with several palladium precursors such as PdCl₂, [Pd(CH₃CN)₂]Cl₂, Pd(OAc)₂, and Pd(cod)Cl₂. In none of the reactions a defined product could be obtained (Scheme 3.29). Moreover, the resulting compounds were characterised by bad solubility which could not be enhanced by exchange of the counterion. These findings are attributed to steric constraints of the ligands; the two imine moieties may be too rigid so that the cavity for a tridentate metal coordination is too small. As a consequence, the formation of oligomers is favoured which would in addition explain the solubility behavior.

3.4.5 Palladium(II) imine SN complexes

Synthesis



Scheme 3.30: Synthesis of Pd imine complexes Pd(SN-R)₂Cl₂

Treatment of one equivalent of Pd(cod)Cl₂ with two equivalents of the SN-R ligands (R = mesityl, *n*-propyl, and phenylethyl) in toluene for 16 h afforded the complexes cleanly

in high isolated yields (85–87 %) as yellow solids (Scheme 3.30). Higher reaction temperatures (70 °C) were needed to displace the bidentate 1,5-cyclooctadiene with the weak σ -donating imine ligands. All complexes are thermally robust and stable to air both in the solid state and in solution. In contrast to the findings of another working group¹⁰⁸ the reaction with Pd(cod)Cl₂ at elevated temperature was successful. However, it turned out that the reaction did not proceed cleanly when precursors other than Pd(cod)Cl₂ were employed: The use of PdCl₂ in acetonitrile as well as palladium acetate in THF led to several products which were not identified.

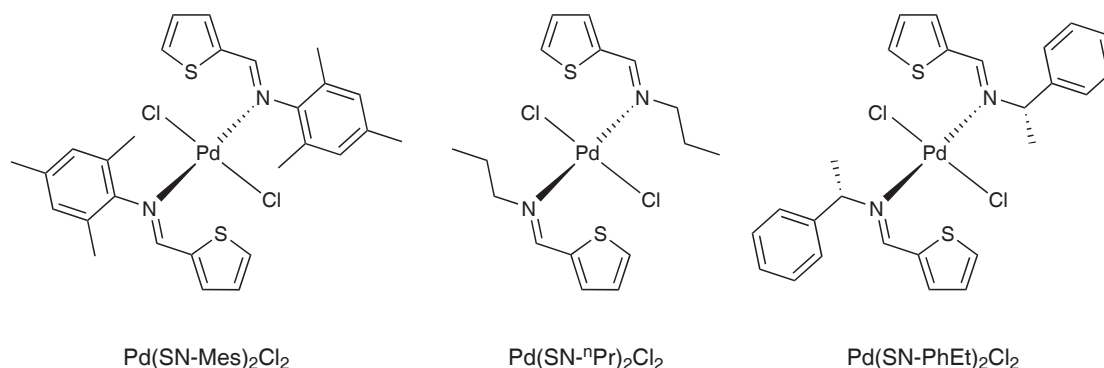


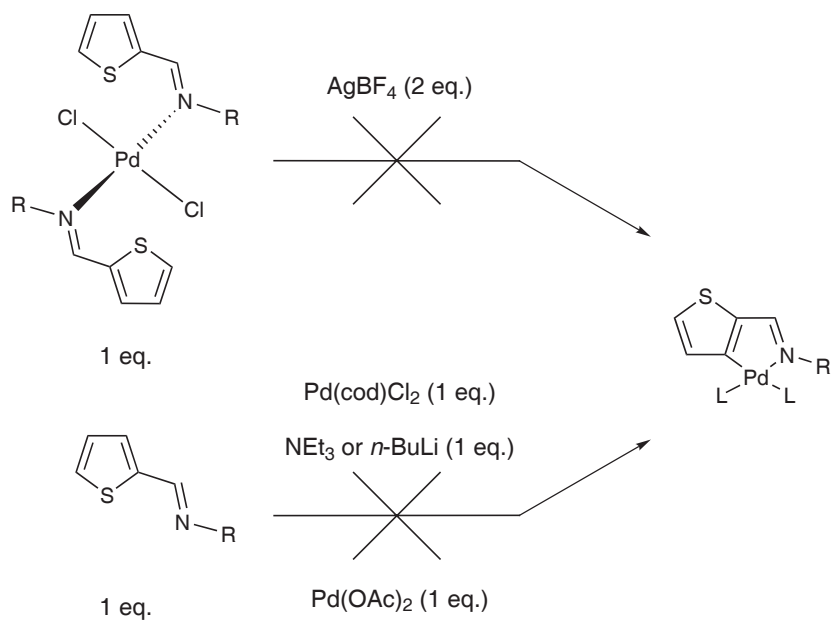
Figure 3.30: Pd imine complexes Pd(SN-R)₂Cl₂

Attempts to obtain a chelating κ^2 -C,N bound imine ligand, as has been frequently observed in related systems^{83,110–117} were not successful (Scheme 3.31). In fact, neither the use of base (*n*-BuLi or NEt₃) nor the employment of palladium acetate—a precursor that is commonly used for this purpose—led to palladacyclic compounds. Likewise, treatment of the complex with the chloride abstracting reagent silver tetrafluoroborate did not result in orthopalladated systems. These findings are consistent with results reported elsewhere.¹⁰⁸

Characterisation

The identity of the compounds was established by ¹H NMR and ¹³C{¹H} NMR spectroscopy. Consistent with the ligands, the complexes exhibit a characteristic singlet resonance for the imine moiety both in the ¹H NMR and ¹³C{¹H} NMR spectra. The shifts range from 7.75 to 9.09 ppm for the ¹H NMR and 161 to 165 ppm for the ¹³C{¹H} NMR spectra, respectively (Table 3.10).

Additionally, X-ray structures of the complexes Pd(SN-Mes)₂Cl₂ and Pd(SN-ⁿPr)₂Cl₂ have been determined. They are depicted in Figures 3.31 and 3.32, respectively, along with selected geometric data reported in the captions.



Scheme 3.31: Attempts to synthesise palladacyclic complexes

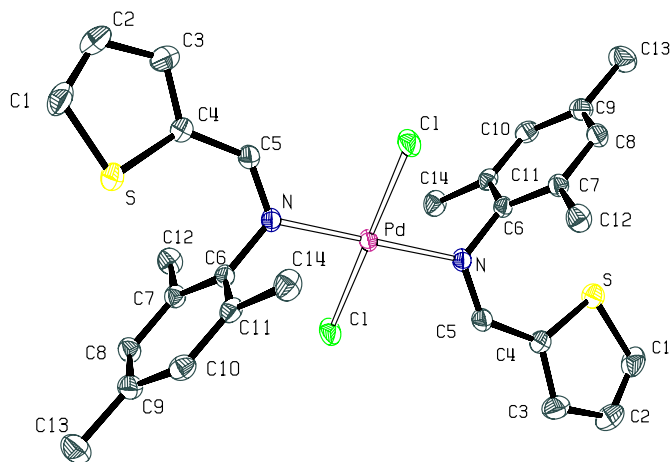


Figure 3.31: Structural view of Pd(SN-Mes)₂Cl₂ · C₂H₄Cl₂ showing 50% thermal ellipsoids (hydrogen atoms and crystallisation solvent omitted for clarity). Selected bond lengths (Å) and angles (°): Pd–N = Pd–N' 2.054(2), Pd–Cl = Pd–Cl' 2.3010(4), N–C(5) 1.289(2), N–C(6) 1.442(2); Cl–Pd–Cl' = N–Pd–N' 180.0, Cl–Pd–N = Cl'–Pd–N' 89.16(4).

Complex	^1H NMR N=CH	$^{13}\text{C}\{^1\text{H}\}$ NMR N=CH
$\text{Pd}(\text{SN-Mes})_2\text{Cl}_2$	9.09	165.5
$\text{Pd}(\text{SN-}^i\text{Pr})_2\text{Cl}_2$	8.03	161.2
$\text{Pd}(\text{SN-PhEt})_2\text{Cl}_2$	7.75	162.1

Table 3.10: Selected ^1H NMR and $^{13}\text{C}\{^1\text{H}\}$ NMR shifts of Pd imine complexes $\text{Pd}(\text{SN-R})_2\text{Cl}_2$ (δ [ppm], CDCl_3 , 20 °C)

The complexes are in their *trans* form with the imine ligands coordinating via the nitrogen atoms in monodentate fashion. The molecules display the usual square-planar coordination around the palladium centre and are centrosymmetric with respect to the metal. The Pd–N bonds are typically shorter than Pd–Cl (2.1 *vs.* 2.3 Å). Virtually no deviation from square planarity is observed with the N–Pd–N' and Cl–Pd–Cl' angles being 180.0° and the N–Pd–Cl angles close to 90°.

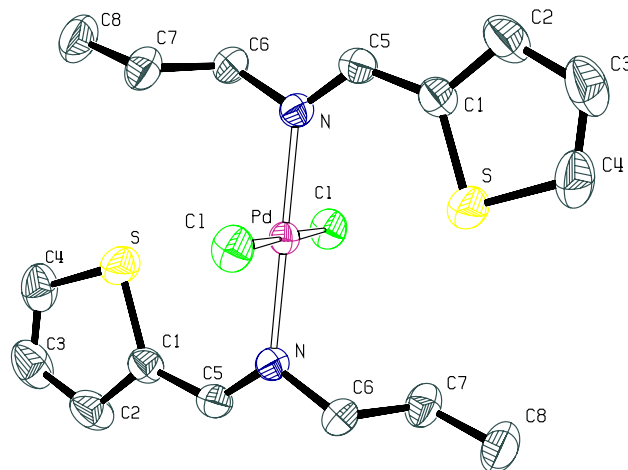
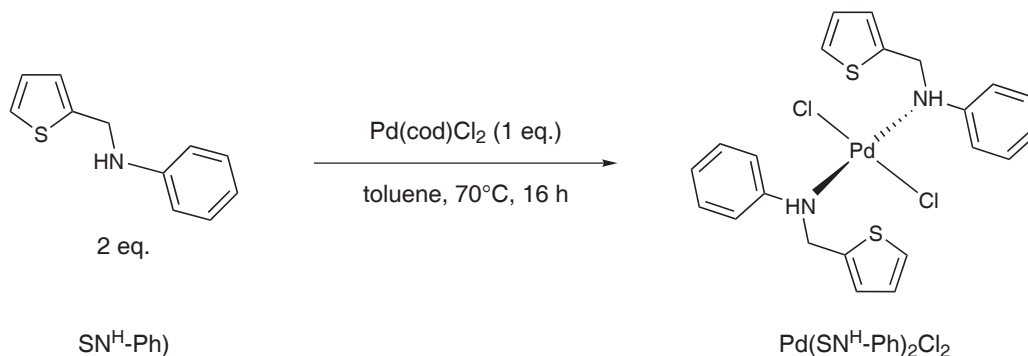


Figure 3.32: Structural view of $\text{Pd}(\text{SN-}^i\text{Pr})_2\text{Cl}_2 \cdot \text{C}_2\text{H}_4\text{Cl}_2$ showing 50% thermal ellipsoids (hydrogen atoms and crystallisation solvent omitted for clarity). Selected bond lengths (Å) and angles (°): Pd–N = Pd–N' 2.018(1), Pd–Cl = Pd–Cl' 2.3043(4), N–C(5) 1.276(2), N–C(6) 1.473(2); Cl–Pd–Cl' = N–Pd–N' 180.0, Cl–Pd–N' = Cl'–Pd–N 89.51(4).

3.4.6 Palladium(II) amine SN complexes

Synthesis

The synthesis of the related compound $\text{Pd}(\text{SN}^{\text{H}}\text{-Ph})_2\text{Cl}_2$ was accomplished analogously to the imine complexes. Thus, one equivalent of $\text{Pd}(\text{cod})\text{Cl}_2$ and two equivalents of the $\text{SN}^{\text{H}}\text{-Ph}$ ligand yielded 81 % of the palladium complex which was obtained as yellow solid and showed thermal and air stability equal to the imine complexes (Scheme 3.32).



Scheme 3.32: Synthesis of the Pd amine complex $\text{Pd}(\text{SN}^{\text{H}}\text{-Ph})_2\text{Cl}_2$

Characterisation

In the ^1H NMR spectrum the N-CH_2 moiety gives rise to signals in the range of 4.94 to 4.78 and 4.26 to 4.18 ppm. The $^{13}\text{C}\{^1\text{H}\}$ NMR spectrum exhibits a singlet resonance at 51.7 ppm for the respective carbon atom N-CH_2 . The structure has also been determined by X-ray crystallography (see Figure 3.33 and the caption for selected geometric data), revealing a square planar coordination similar to the imine complexes. Analogously, the amine molecules act as monodentate ligands with the nitrogen atoms as coordinating sites. Interestingly, this complex shows a more distinct deviation from the idealised geometry, the Cl-Pd-N angle being $86.38(7)^\circ$.

3.4.7 Palladium catalysed Suzuki-Miyaura coupling

The development of compounds that can act as selective and efficient catalysts to afford functional molecules from simple substrates in high yields is a central topic in modern organic and organometallic chemistry. Palladium pincer complexes are among the most utilised transition metal compounds as catalysts for several C-C and C-N bond

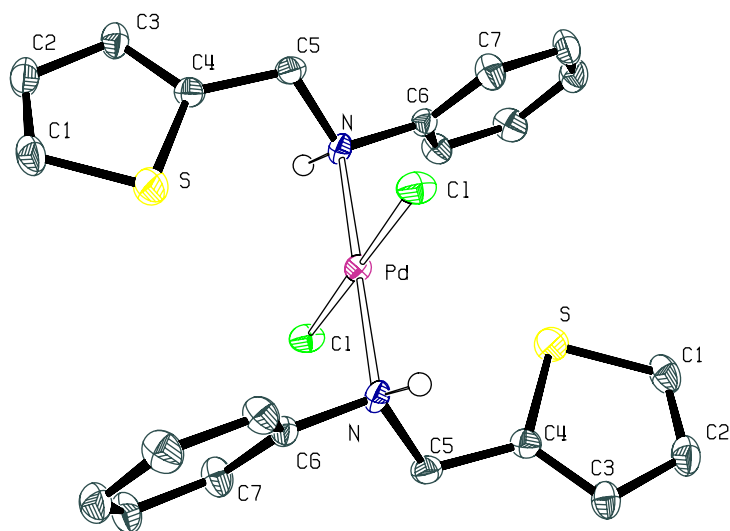


Figure 3.33: Structural view of $\text{Pd}(\text{SN}^{\text{H}}\text{-Ph})_2\text{Cl}_2$ showing 50% thermal ellipsoids. Selected bond lengths (Å) and angles (°): $\text{Pd-N} = \text{Pd-N}'$ 2.054(2), $\text{Pd-Cl} = \text{Pd-Cl}'$ 2.3090(7), N-C(5) 1.455(3), N-C(6) 1.499(3); $\text{Cl-Pd-Cl}' = \text{N-Pd-N}'$ 180.0, $\text{Cl-Pd-N} = \text{N'-Pd-Cl}'$ 86.38(7).

forming reactions, such as the Suzuki-Miyaura coupling,⁹¹ the Heck reaction,¹¹⁸ or the Sonogashira coupling.¹⁰¹

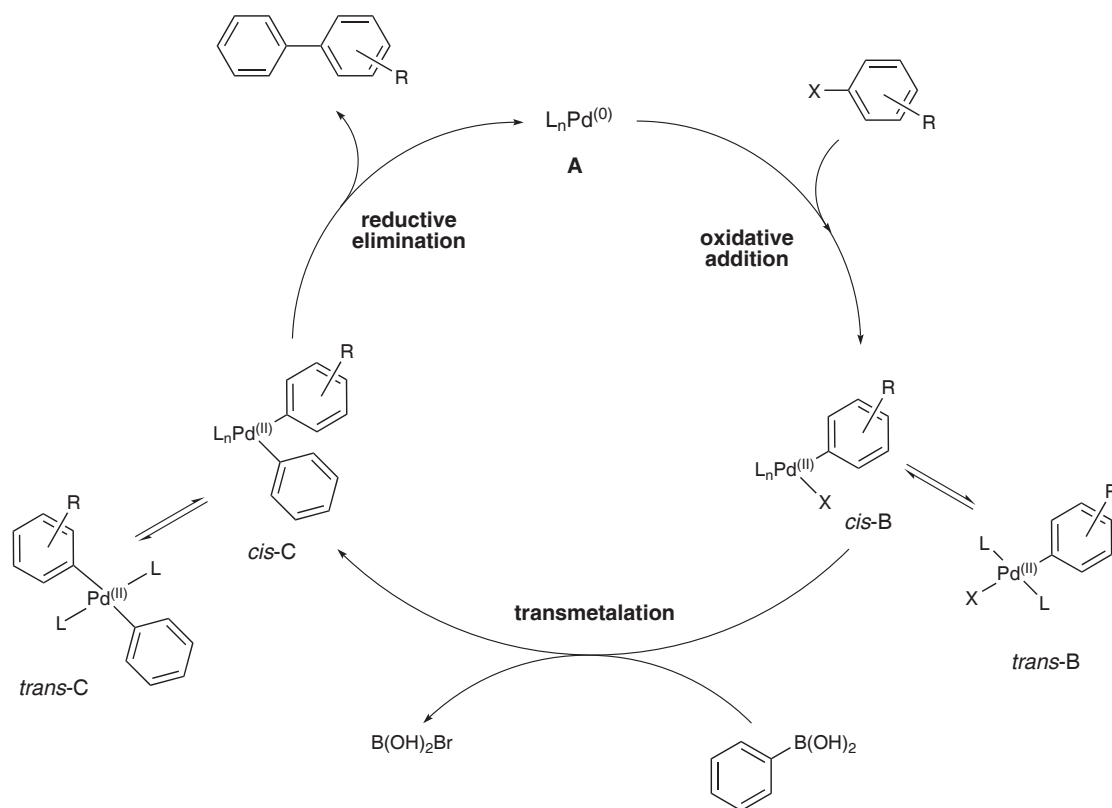
Among the palladium catalysed C–C bond forming reactions the cross-coupling of organic halides with organoboron compounds, the Suzuki-Miyaura coupling,⁹¹ is the most widely used. Its main advantage is the application of non-toxic organoboron reagents, which are generally thermally stable and inert towards air and moisture. However, their nucleophilicity is not sufficient to make them react directly with electrophiles such as aryl and/or vinyl halides. To increase their nucleophilicity the use of a base as additive is required; by coordinating to the boron atom the base increases the negative charge of the adjacent carbon atom and facilitates its migration to an electrophilic centre. The presence of a metal centre in the catalytic process is also necessary for the transmetalation step (see mechanism below).

The general mechanism for the Suzuki-Miyaura coupling of aryl halides with phenyl boronic acid is depicted in Scheme 3.33. It comprises three key steps, *viz.* oxidative addition of the aryl halide to the Pd(0) species, transmetalation, and reductive elimination of the coupling product. Thus, during the course of a catalytic cycle the palladium centre changes its oxidation state from 0 to +II and back.

The oxidative addition is considered to be the rate determining step of the catalytic cycle. It is favoured when the C–halide bond is electron poor and/or the palladium centre is electron rich. The oxidative addition results in the formation of complex *cis*-**B** which isomerises immediately to the complex *trans*-**B**. The latter undergoes then a transmetalation process in which the halide is exchanged for the organic moiety of the organoboron compound. The product of this transmetalation step is complex *cis*-**C** which isomerises to complex *trans*-**C**. Due to the fact that only the *cis*-isomer can undergo reductive elimination of the coupling product, it is incessantly consumed and the equilibrium of the isomerisation between *cis*-**C** and *trans*-**C** is not reached. Once the coupling product is reductively eliminated the catalytically active species is regenerated.

It has been observed, however, that the oxidation state of palladium in the precatalyst is not crucial for the catalytic activity of the different palladium complexes presented in the literature. It is believed that the catalytically active species differs from the initial palladium compound. The active species is duly formed in the reaction mixture with the exact structure or formula being not fully recognized. In the case of *N*-heterocyclic carbene and pincer complexes recently evidence was presented that these ligands are merely pre-catalysts generating some forms of metallic palladium(0) ("nanoparticles") which actually are involved in the catalytic process.^{95,119–122}

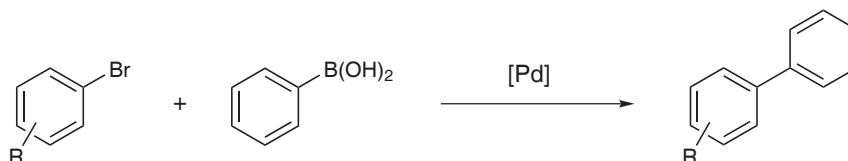
In this context the ligands of the initially used palladium compound play a decisive role. They should not bind too strong to the palladium centre so as to deactivate the catalyst but be labile enough to allow for the formation of the catalytically active species.



Scheme 3.33: General mechanism of the Suzuki-Miyaura coupling

Moreover, if the ligands show a far too high lability they are not capable of stabilising the palladium centre by generating a favourable steric and electronic environment.

Palladium complexes containing α - and β -diimine ligands are excellent catalysts for the Suzuki-Miyaura coupling.^{123,124} Based on these findings we were interested in whether palladium complexes containing monodentate imine as well as amine ligands exhibit similar reactivities in C–C bond forming reactions. Accordingly, the catalytic activity of the complexes $\text{Pd}(\text{SN-Mes})_2\text{Cl}_2$, $\text{Pd}(\text{SN}^{\text{nPr}})_2\text{Cl}_2$, $\text{Pd}(\text{SN-PhEt})_2\text{Cl}_2$, and $\text{Pd}(\text{SN}^{\text{H-Ph}})_2\text{Cl}_2$ for the coupling of various aryl bromides with phenyl boronic acid was investigated.



Scheme 3.34: The Suzuki-Miyaura coupling of aryl bromides with phenyl boronic acid

The model reaction used in this study is depicted in Scheme 3.34. In a typical procedure 1.00 mmol of the substrate, 1.50 mmol of phenyl boronic acid and 2.00 mmol of Cs_2CO_3 were suspended in 5 mL of anhydrous 1,4-dioxane, charged with the respective amount of catalyst—in the solid state or, in the case of lower catalyst loadings, in solution—and stirred at 110°C for 18 h (Table 3.11), these conditions have not been optimized. The mixture was cooled to room temperature and diluted with 10 mL of a 2N aqueous NaOH solution. The aqueous phase was extracted three times with dichloromethane, dried over Na_2SO_4 and evaporated to dryness. The crude product was purified via column chromatography over silica gel (PE:EE 20:1).

Reaction time	18 h
Temperature	110 °C
Solvent	1,4-dioxane
Arylbromide	1.0 eq.
Phenyl boronic acid	1.5 eq.
Cs_2CO_3	2.0 eq.
Catalyst	1 mol%

Table 3.11: Reaction conditions for the Suzuki-Miyaura coupling

The results of the catalytic reactions are summarized in Table 3.12. The nature of the substituent on the aryl bromide is the determining factor considering the ease of the oxidative addition in the catalytic cycle. As outlined before this step is facilitated when

the substrates bear electron-poor C–halide bonds. Regarding ease of oxidative addition the substrates are classified as “activated”, “neutral”, and deactivated.

Entry	Substrate	Catalyst	Yield (%)
1	4-bromoacetophenone	$\text{Pd}(\text{SN-Mes})_2\text{Cl}_2$	> 99
2	4-bromoacetophenone	$\text{Pd}(\text{SN-}^n\text{Pr})_2\text{Cl}_2$	> 99
3	4-bromoacetophenone	$\text{Pd}(\text{SN-PhEt})_2\text{Cl}_2$	93
4	4-bromoacetophenone	$\text{Pd}(\text{SN}^{\text{H}}\text{-Ph})_2\text{Cl}_2$	> 99
5	1-bromo-4-nitrobenzene	$\text{Pd}(\text{SN-Mes})_2\text{Cl}_2$	97
6	1-bromo-4-nitrobenzene	$\text{Pd}(\text{SN-}^n\text{Pr})_2\text{Cl}_2$	95
7	1-bromo-4-nitrobenzene	$\text{Pd}(\text{SN-PhEt})_2\text{Cl}_2$	94
8	4-bromoanisole	$\text{Pd}(\text{SN-Mes})_2\text{Cl}_2$	96
9	4-bromoanisole	$\text{Pd}(\text{SN-}^n\text{Pr})_2\text{Cl}_2$	29
10	4-bromoanisole	$\text{Pd}(\text{SN-PhEt})_2\text{Cl}_2$	16
11	4-bromoanisole	$\text{Pd}(\text{SN}^{\text{H}}\text{-Ph})_2\text{Cl}_2$	35

Table 3.12: Yields of the Suzuki-Miyaura coupling of aryl halides with phenyl boronic acid catalysed by $\text{Pd}(\text{SN-R})_2\text{Cl}_2$ complexes (catalyst loading was 1 mol % for all experiments)

The coupling of the electronically activated substrate 4-bromoacetophenone with phenyl boronic acid proceeds with all catalysts resulting in yields > 93% (entries 1–4). Likewise, the coupling of the “neutral” substrate 1-bromo-4-nitrobenzene—which was only tested with the imine containing complexes—affords the in yields > 94 % (entries 5–7). When it comes to the deactivated 4-bromoanisole the coupling product 4-methoxybiphenyl is obtained in 96 % ($\text{Pd}(\text{SN-Mes})_2\text{Cl}_2$), 29 % ($\text{Pd}(\text{SN-}^n\text{Pr})_2\text{Cl}_2$), 16 % ($\text{Pd}(\text{SN-PhEt})_2\text{Cl}_2$), and 35 % ($\text{Pd}(\text{SN}^{\text{H}}\text{-Ph})_2\text{Cl}_2$) isolated yields (entries 8–11).

Based on these findings the catalytic activity of the most promising catalyst, $\text{Pd}(\text{SN-Mes})_2\text{Cl}_2$, which showed satisfactory results even in the coupling of the deactivated substrate was further investigated with respect to catalyst loadings and substrates, the results being summarised in Table 3.13. It was observed that the activated 4-bromoacetophenone could be successfully coupled with a catalyst loading of down to 0.01 mol % (entry 2). Further reduction of the catalyst loading to 0.001 mol % resulted in almost no conversion (entry 3). For the “neutral” and deactivated substrates the limit of catalyst loadings which result in acceptable yields is 0.1 mol % (entries 4–7).

It has also been observed that the reaction temperature is crucial: In the coupling of bromobenzene a lowering of the temperature by 20 °C results in a dramatic dropping of the isolated yield (31 *vs.* 87 %, entries 8 and 9). The coupling of bromobenzene and of 2-bromopyridine with a catalyst loading of 1 mol % proceeded with only moderate

yields so that no further investigations with smaller amounts of catalyst were carried out (entries 9 and 10). Finally, attempts to couple 4-chloroacetophenone with phenyl boronic acid resulted in almost no conversion (entry 11).

Entry	Substrate	Mol %	Yield (%)
1	4-bromoacetophenone	0.1	> 99
2	4-bromoacetophenone	0.01	96
3	4-bromoacetophenone	0.001	4
4	4-bromoanisole	0.1	72
5	4-bromoanisole	0.01	20
6	1-bromo-4-nitrobenzene	0.1	97
7	1-bromo-4-nitrobenzene	0.01	0
8	bromobenzene	1	31 ^a
9	bromobenzene	1	87
10	2-bromopyridine	1	77
11	4-chloroacetophenone	1	5

^athe reaction was performed at 90 °C

Table 3.13: Yields of the Suzuki-Miyaura coupling of aryl halides with phenyl boronic acid catalysed by Pd(SN-Mes)₂Cl₂

While it is difficult to establish a clear trend in the catalytic activity of these complexes, on average, the complex Pd(SN-Mes)₂Cl₂ shows higher activity than the other complexes. This is especially apparent in the coupling of the electronically deactivated and thus more challenging substrate 4-bromoanisole with phenyl boronic acid. This reactivity trend may suggest that the bulkier mesityl substituent renders the catalyst more active. In addition to what has been said about the catalytically active compound the formation of metallic palladium(0) species which actually take part in the catalytic process cannot be excluded since in some cases the formation of palladium black was observed.

4 Summary

In order to prepare new ligands with different properties the concept of PNP ligands was extended to *N*-heterocyclic diamines other than pyridine. These new PNP ligands are easily prepared from commercially available and inexpensive 2,6-diamino-4-phenyl-1,3,5-triazine and 2,6-diamino-pyrimidine which can be varied in modular fashion by choosing the appropriate monochloro phosphine or phosphite R_2PCl . The latter, in turn, is easily accessible in high yields from a large array of both achiral and chiral diols and PCl_3 .

$Mo(CO)_3(CH_3CN)_3$ reacts with these PNP ligands to give neutral octahedral tricarbonyl complexes. Upon reaction with bromine hepta-coordinated species are obtained. This methodology can also be applied successfully to the synthesis of bidentate PN ligands. In this case 2-aminopyridine and the chlorophosphine or -phosphite were reacted in equimolar amounts. When treated with $Mo(CO)_6$ neutral octahedral tetracarbonyl complexes are obtained which show interesting reactivities towards substrates such as allyl bromide or iodine.

Iron(II) PNP^T and PNP^P complexes could be prepared starting from $[Fe(H_2O)_6](BF_4)_2$ as precursor: when $[Fe(H_2O)_6](BF_4)_2$ and the ligands were reacted in equimolar amounts, octahedral, diamagnetic, iron(II) tris(acetonitrile) PNP complexes were obtained. The acetonitrile ligands in these complexes are labile and can be substituted by bidentate nitrogen donor ligands or carbon monoxide. Exemplarily, one of these the complexes was further investigated in terms of reactivity and catalytic applicability. A general and efficient protocol for the coupling of aromatic aldehydes with ethyl diazoacetate has been developed.

New palladium(II) complexes containing *N*-(2-thienylmethylene)-aniline and *N*-(2-thienylmethyl)-aniline derived ligands were successfully prepared. These complexes were found to be active as catalysts for the Suzuki-Miyaura coupling of aryl bromides with phenyl boronic acid and are comparable to related α - and β -diimine systems, thus representing an interesting alternative to existing catalytic systems. Qualitatively, it was found that complexes with imine ligands featuring sterically demanding substituents such as mesityl are clearly better catalysts.

5 Experimental

5.1 General remarks

All reactions involving organometallic compounds were performed under an inert atmosphere of argon using standard Schlenk techniques.

Reagents and solvents were purchased from Aldrich, Fluka, and Merck and used as received.

Anhydrous solvents were dried and purified according to standard procedures.¹²⁵

Deuterated solvents were purchased from Aldrich and Eurisotop, degassed using the freeze-pump-thaw technique and stored over 4 Å molecular sieves.

NMR spectra were recorded on a Bruker AVANCE-250 spectrometer, the resonance frequencies being 250.13 (^1H), 62.86 (^{13}C), and 101.26 MHz (^{31}P), respectively. Chemical shifts are reported as δ -values with the solvent or TMS (^1H and ^{13}C) and 85 % H_3PO_4 (^{31}P) as standard. Signal assignments were confirmed by 135-DEPT experiments.

IR spectra were recorded on a Perkin Elmer 16PC-IR spectrometer.

***n*-Butyl lithium** was purchased from Aldrich as a 1.6 M solution in *n*-hexane. The actual concentration was determined as follows:¹²⁶ A small amount of 1,10-phenanthroline was dissolved in Et_2O and treated with 0.70 mL of *n*-BuLi. The brown solution was titrated with a 2.06 M solution of *tert*.-BuOH in toluene until decolouration occurred.

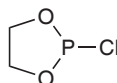
Thin layer chromatography was accomplished on silica gel coated aluminium foil 60 F₂₅₄ (Merck). Spot detection was performed in UV light ($\lambda = 254 \text{ nm}$) and by bathing the silica gel plates in molybdate phosphorous acid (5 % solution in EtOH) and heating.

X-ray structure determination. X-ray data were collected on a Bruker Smart CCD area detector diffractometer using graphite-monochromated Mo K α radiation with the wavelength $\lambda = 0.71073 \text{ \AA}$ and 0.3° ω -scan frames covering complete spheres of the reciprocal space. Corrections for absorption, $\lambda/2$ -effects, and crystal decay were applied using SADABS.¹²⁷ The structures were solved by direct methods using the program SHELXS97.¹²⁸ Structure refinement on F^2 was carried out with the program SHELXL97.¹²⁹ All non-hydrogen atoms were refined anisotropically. Hydrogen atoms were inserted in idealised positions and were refined riding with the atoms they were bound to. Badly disordered solvents were squeezed with the program PLATON prior to final refinement.¹³⁰

Computational details. DFT calculations were performed employing the Gaussian03 software package on the Silicon Graphics Origin 2000 of the Vienna University of Technology.¹³¹ The geometry and energy of the model complexes and the transition states were optimised at the B3LYP level with the Stuttgart/Dresden ECP (SDD) basis set^{132–134} to describe the electrons of the metal centres. For the C, N, P, Cl, and H atoms the 6-31g** basis set was employed.^{135–141} A vibrational analysis was performed to confirm that the structures of the model compounds have no imaginary frequency. All geometries were optimised without symmetry constraints. Solvation effects were evaluated with the DPCM method.^{142–145}

5.2 Building blocks and precursors

2-Chloro-1,3,2-dioxaphospholane (ETOL-PCI)



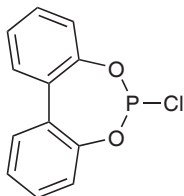
Under inert atmosphere anhydrous ethylene glycol (6.4 mL, 115 mmol) was added dropwise to a solution of PCl₃ (10.0 mL, 115 mmol) in CH₂Cl₂ so that gentle refluxing took place. After complete addition of ethylene glycol the reaction flask was adapted for distillation. First the solvent was removed at normal pressure and then ETOL-PCI was distilled under reduced pressure.

Yield: 9.5 g (65 %) colourless oil; C₂H₄ClO₂P; MW: 126.48; 18.99 % C, 3.19 % H.

¹H NMR (δ , CDCl₃, 20 °C): 4.41 (s, 2H, CH₂–CH₂), 4.25–4.19 (m, 2H, CH₂–CH₂).

$^{31}\text{P}\{^1\text{H}\}$ NMR (δ , CDCl_3 , 20 °C): 169.0.

2-Chlorodibenzo[*d,f*]-1,3,2-dioxaphosphepine (BIPOL-PCl)



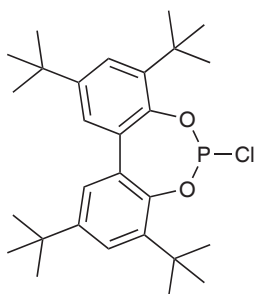
2,2-Biphenol (10.00 g, 53.71 mmol) was cooled to 0 °C under inert atmosphere and treated with NMP (0.53 g, 5.37 mmol) and PCl_3 (25.81 g, 188.00 mmol). The mixture was then stirred for 3 h at 80 °C; subsequently the excess of PCl_3 was removed under vacuum. Bulb-to-bulb distillation (200 °C, 10^{-4} mbar) of the crude product gave a bright yellow oil which crystallised in the refrigerator.

Yield: 11.75 g (87 %) white microcrystalline solid; $\text{C}_{12}\text{H}_8\text{ClO}_2\text{P}$; MW = 250.62; 57.51 % C, 3.22 % H.

^1H NMR (δ , CDCl_3 , 20 °C): 7.58–7.22 (m, 8H)

$^{31}\text{P}\{^1\text{H}\}$ NMR (δ , CDCl_3 , 20 °C): 179.6.

2-Chloro-4,6,9,11-tetra-*tert*-butyldibenzo[*d,f*]-1,3,2-dioxaphosphepine (*t*BuBIPOL-PCl)



NEt_3 (6.88 mL, 49.4 mmol) was added dropwise to a suspension of 2,4,7,9-tetra-*tert*-butyl-2,2-biphenyl (8.29 g, 20.2 mmol) in 50 mL of toluene. The mixture was cooled to

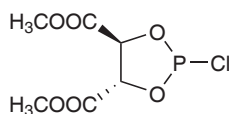
0 °C and PCl_3 (1.8 mL, 21.1 mmol) was added dropwise. A white solid was formed immediately. The mixture was allowed to reach RT and stirred overnight. Insoluble materials were filtered off, the solvent was removed under vacuum and the product was dried.

Yield: 7.57 g (79 %) pale yellow solid; $\text{C}_{28}\text{H}_{40}\text{ClO}_2\text{P}$; MW = 475.05; 70.79 % C, 8.49 % H.

^1H NMR (δ , CDCl_3 , 20 °C): 7.49–7.21 (m, 4H, Ph), 1.50 and 1.38 (2s, 36H, CH_3).

$^{31}\text{P}\{^1\text{H}\}$ NMR (δ , CDCl_3 , 20 °C): 173.0.

(4S, 5S)-2-Chloro-1,3,2-dioxaphospholane-4-5-dicarboxylic acid, dimethylester (TAR^{Me}-PCl)



A mixture of D-(–)-methyl tartrate (10.0 g, 56.1 mmol), PCl_3 (14.7 mL, 168.4 mmol) and NMP (0.5 mL, 5.6 mmol) were refluxed for 30 min. (due to heavy HCl formation, the reflux condenser was connected to the extractor hood). After removal of excess PCl_3 from the orange residue, the product was purified by bulb-to-bulb distillation (150 °C, 10^{-4} mbar, 30 min.).

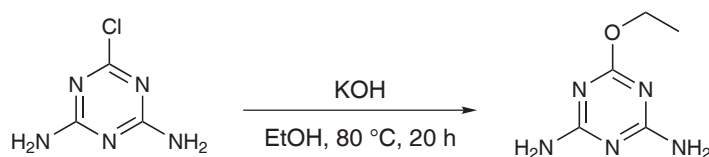
Yield: 11.2 g (82 %) colourless oil; $\text{C}_6\text{H}_8\text{ClO}_6\text{P}$; MW: 242.55; 29.71 % C, 3.32 % H.

^1H NMR (δ , CDCl_3 , 20 °C): 5.45 (d, J = 6.2 Hz, 1H, CH), 5.00 (dd, J_1 = 6.2 Hz, J_2 = 9.6 Hz, 1H, CH), 3.83 (s, 6H, COOCH_3).

$^{31}\text{P}\{^1\text{H}\}$ NMR (δ , CDCl_3 , 20 °C): 176.3.

2,6-Diamino-4-ethoxy-1,3,5-triazine

2,6-Diamino-4-chlor-1,3,5-triazine (3.0 g, 20.6 mmol) was suspended in 40 mL of EtOH, treated with KOH (1.27 g, 22.7 mmol) and refluxed for 20 h. The hot solution was then filtered and left in the refrigerator overnight. The supernatant was decanted and the white solid was dried *in vacuo*.

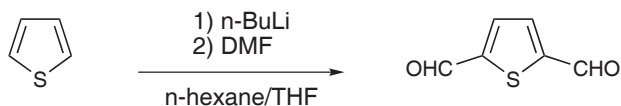


Yield: 2.62 g (82 %) white solid; $C_5H_9N_5O$; MW: 155.16; 38.71 % C, 5.85 % H, 45.14 % N.

1H NMR (δ , d^6 -DMSO, 20 °C): 6.66 (s, 4H, NH), 4.21 (s, 2H, CH_2-CH_3), 1.25 (s, 3H, CH_2-CH_3).

$^{13}C\{^1H\}$ NMR (δ , d^6 -DMSO, 20 °C): 171.0 (triaz⁴), 68.7 (triaz^{2,6}), 61.6 (CH_2-CH_3), 14.9 (CH_2-CH_3).

2,5-Thiophenedicarboxaldehyde



A solution of freshly distilled thiophene (8 mL, 100 mmol) and TMEDA (18 mL, 120 mmol) in 30 mL of anhydrous n -hexane was cooled to 0 °C and treated with $n-BuLi$ (48 mL of a 2.5 M solution in n -hexane, 120 mmol). Upon completion of the addition the solution was heated to reflux for 30 min. After reaching room temperature again the mixture was diluted with 120 mL of anhydrous THF and then cooled to -40 °C. The reaction was now quenched with DMF (21 mL, 270 mmol) while the temperature was kept between -45 °C and -30 °C. Then the cooling bath was removed and the solution stirred for 2 hours at room temperature.

The reaction mixture was diluted with 1 L H_2O and 100 mL HCl and neutralised with solid $NaHCO_3$. The aqueous phase was extracted four times with Et_2O , the combined organic layers were dried over Na_2SO_4 , filtered and the solvent removed. The crude product was recrystallised from THF/ Et_2O 4:1.

Yield: 10.9 g (78 %) light brown solid; $C_6H_4O_2S$; MW: 140.16; 51.42 % C, 2.88 % H.

1H NMR (δ , $CDCl_3$, 20 °C): 10.03 (s, 2H, CHO), 7.45 (s, 2H, thiophene^{3,4}).

Mo(CO)₃(CH₃CN)₃

Mo(CO)₆ (0.60 g, 2.27 mmol) was suspended in 15 mL anhydrous CH₃CN and heated to reflux for 4 h resulting in a pale yellow solution which darkened quite fast when traces of oxygen were present. Due to the high air sensitivity of the product it was not isolated but reacted *in situ* with the respective ligands.

Yield: (*product not isolated*) white solid; C₉H₉MoN₃O₃; MW: 303.13; 35.66 % C, 2.99 % H, 13.86 % N.

Pd(cod)Cl₂¹⁴⁶

1,5-cyclooctadiene (10 mL, 84.6 mmol) was added dropwise to a suspension of PdCl₂ (5.0 g, 28.2 mmol) in 150 mL MeOH, whereupon a yellow solid precipitated. The reaction mixture was stirred overnight at room temperature, filtered, and the resulting yellow solid was washed with MeOH and dried *in vacuo*.

Yield: 7.29 g (91 %) yellow solid; C₈H₁₂Cl₂Pd; MW: 285.50; 33.66 % C, 4.24 % H.

¹H NMR (δ, CDCl₃, 20 °C): 6.32 (s, 4H, CH=CH), 2.92 (m, 4H, CH₂–CH₂), 2.57 (m, 4H, CH₂–CH₂).

[Fe(H₂O)₆](BF₄)₂⁷⁰

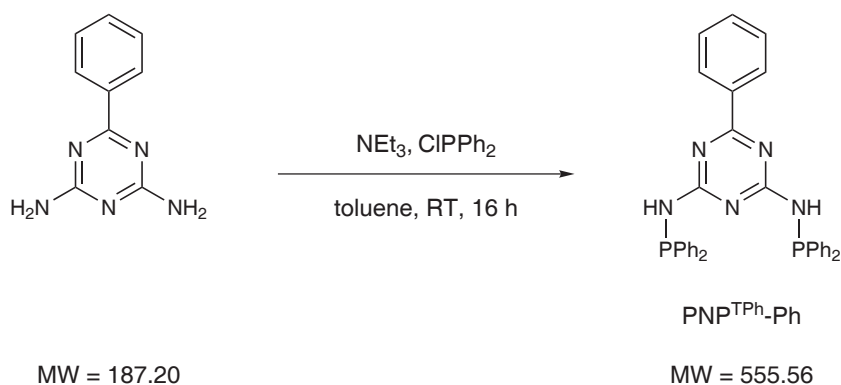
HBFe₄ (25 mL of a 48 % solution in H₂O, 0.14 mol) was added dropwise under ice cooling to a suspension of iron powder (5 g, 90 mmol) in 100 mL H₂O. The reaction mixture was stirred at room temperature overnight and then filtered twice. The solvent was evaporated under vacuum until crystallisation set in and the mixture was allowed to stand in the refrigerator overnight. The resulting colourless to pale green crystals were filtered, washed with Et₂O and dried under vacuum.

Yield: 24 g (79 %) colourless to pale green crystals; H₁₂B₂F₈FeO₆; MW: 337.54.

5.3 Ligands

5.3.1 PNP^T ligands

N,N'-Bis(diphenylphosphino)-2,6-diamino-4-phenyl-1,3,5-triazine (PNP^{TPh}-Ph)



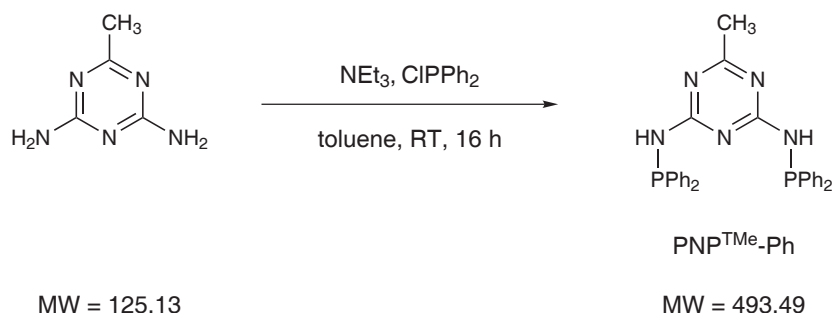
A suspension of 2,6-diamino-4-phenyl-1,3,5-triazine (0.50 g, 2.67 mmol) in 30 mL THF was treated with NEt₃ (0.82 mL, 5.88 mmol). After cooling to 0 °C a solution of ClPPh₂ (0.96 mL, 5.34 mmol) in 20 mL THF was added dropwise. The suspension was warmed up to room temperature and stirred for 16 h. After that, the precipitate was filtered off and the solvent removed under vacuum. The remaining white solid was used without further purification.

Yield: 1.41 g (95 %) white solid; C₃₃H₂₇N₅P₂; MW: 555.56; 71.34 % C, 4.90 % H, 12.61 % N.

¹H NMR (δ, C₆D₆, 20 °C): 7.44–7.03 (m, 25H, Ph and PPh), 6.33 (s, 2H, NH).

¹³C{¹H} NMR (δ, C₆D₆, 20 °C): 171.9 (triaz⁴), 168.7 (dd, *J*_{CP} = 17.0 Hz, *J*_{CP} = 2.8 Hz, triaz^{2,6}), 139.6 (d, *J*_{CP} = 15.6 Hz, PPh¹), 136.7 (Ph¹), 131.7 (d, *J*_{CP} = 22.1 Hz, PPh^{2,6}), 131.7 (Ph⁴), 129.1 (PPh⁴), 128.5 (d, *J*_{CP} = 6.9 Hz, PPh^{3,5}), 128.2 and 128.1 (Ph^{2,3,5,6}).

³¹P{¹H} NMR (δ, C₆D₆, 20 °C): 29.06.



N,N'-Bis(diphenylphosphino)-2,6-diamino-4-methyl-1,3,5-triazine (PNP^{TM_e}-Ph)

This ligand was prepared analogously to PNP^{TPh}-Ph with 2,6-diamino-4-methyl-1,3,5-triazine (1.00 g, 7.99 mmol), ClPPh₂ (2.87 mL, 15.98 mmol), and NEt₃ (2.23 mL, 15.98 mmol) as the starting materials.

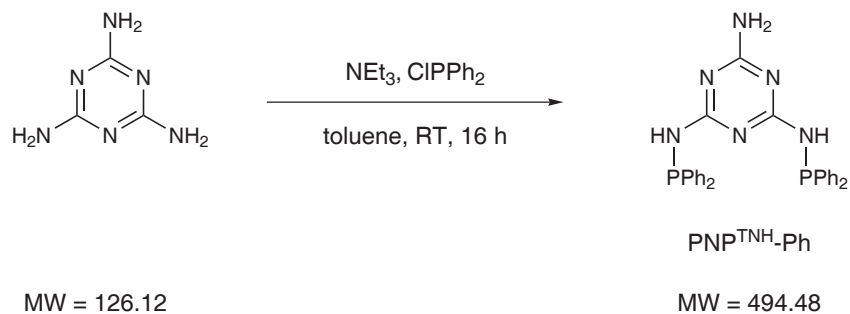
Yield: 3.66 g (93 %); C₂₈H₂₅N₅P₂; MW: 493.49; 68.15 % C, 5.11 % H, 14.19 % N.

¹H NMR (δ, CDCl₃, 20 °C): 7.81–7.22 (m, 20H, Ph), 5.96 (bs, 2H, NH), 2.27 (s, 3H, CH₃).

¹³C{¹H} NMR (δ, CDCl₃, 20 °C): 176.6 (d, *J*_{CP} = 11.0 Hz, triaz⁴), 167.6 (d, *J*_{CP} = 17.0 Hz, triaz^{2,6}), 138.6 (d, *J*_{CP} = 13.8 Hz, Ph¹), 131.6 (d, *J*_{CP} = 21.5 Hz, Ph^{2,6}), 129.5 (Ph⁴), 128.6 (d, *J*_{CP} = 6.5 Hz, Ph^{3,5}), 25.6 (CH₃).

³¹P{¹H} NMR (δ, CDCl₃, 20 °C): 27.64.

N,N'-Bis(diphenylphosphino)-2,4,6-triamino-1,3,5-triazine (PNP^{TNH}-Ph)



This ligand was prepared analogously to $\text{PNP}^{\text{TPh}}\text{-Ph}$ with 2,4,6-triamino-1,3,5-triazine (melamine, 0.50 g, 3.96 mmol), ClPPh_2 (1.42 mL, 7.93 mmol), and NEt_3 (1.16 mL, 8.325 mmol) as the starting materials.

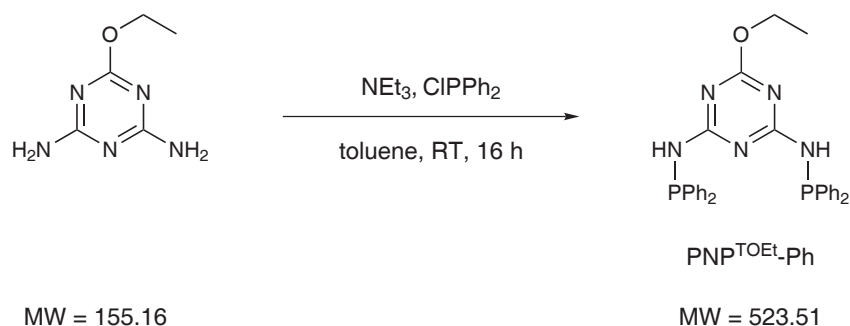
Yield: 1.26 g (64 %); $\text{C}_{27}\text{H}_{24}\text{N}_6\text{P}_2$; MW: 494.48; 65.58 % C, 4.89 % H, 17.00 % N.

^1H NMR (δ , CDCl_3 , 20 °C): 7.75–7.12 (m, 20H, Ph), 5.65 (bs, 2H, NH), NH_2 not observed.

$^{13}\text{C}\{^1\text{H}\}$ NMR (δ , CDCl_3 , 20 °C): 171.9 (triaz^4), 168.7 (d, $J_{\text{CP}} = 17.0$ Hz, $\text{triaz}^{2,6}$), 138.7 (d, $J_{\text{CP}} = 13.0$ Hz, Ph^1), 131.7 (d, $J_{\text{CP}} = 21.5$ Hz, $\text{Ph}^{2,6}$), 129.4 (Ph^4), 128.5 (d, $J_{\text{CP}} = 6.9$ Hz, $\text{Ph}^{3,5}$).

$^{31}\text{P}\{^1\text{H}\}$ NMR (δ , CDCl_3 , 20 °C): 27.29.

N,N'-Bis(diphenylphosphino)-2,6-diamino-4-ethoxy-1,3,5-triazine ($\text{PNP}^{\text{TOEt}}\text{-Ph}$)



A suspension of 2,6-diamino-4-ethoxy-1,3,5-triazine (1.50 g, 9.67 mmol) in 50 mL toluene was treated with NEt_3 (2.69 mL, 19.33 mmol). After cooling to 0 °C ClPPh_2 (3.47 mL, 19.33 mmol) was added dropwise. The suspension was heated to reflux and stirred for 16 h. Then the mixture was allowed to reach room temperature, the precipitate was filtered off and the solvent removed under vacuum. The remaining white solid was dried *in vacuo*.

Yield: 4.61 g (92 %); $\text{C}_{29}\text{H}_{27}\text{N}_5\text{OP}_2$; MW: 523.51; 66.53 % C, 5.20 % H, 13.38 % N.

^1H NMR (δ , CDCl_3 , 20 °C): 7.62–7.16 (m, 20H, Ph), 5.45 (bs, 2H, NH), 3.97–3.87 (m, 2H, O-CH_2), 1.09–1.00 (m, 3H, CH_3).

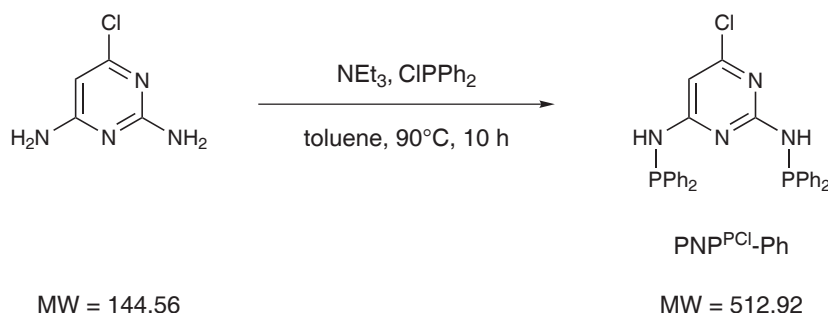
$^{13}\text{C}\{^1\text{H}\}$ NMR (δ , CDCl_3 , 20 °C): 169.1 (triaz^4), 166.8 ($\text{triaz}^{2,6}$), 138.6 (Ph^1), 131.4 (Ph^4),

130.6 (d, $J_{CP} = 11.5$ Hz, Ph^{2,6}), 128.9 (d, $J_{CP} = 12.9$ Hz, Ph^{3,5}), 62.8 (O-CH₂), 39.9 (CH₃).

³¹P{¹H} NMR (δ, CDCl₃, 20 °C): 29.88.

5.3.2 PNP^P ligands

N,N'-Bis(diphenylphosphino)-2,6-diamino-4-chloropyrimidine (PNP^{PCl}-Ph)



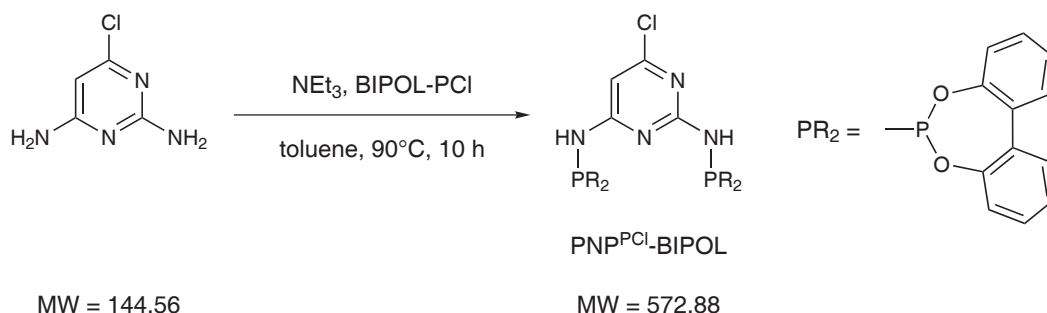
This ligand was prepared analogously to PNP^{TOEt}-Ph with 2,6-diamino-4-chloropyrimidine (1.00 g, 6.92 mmol), ClPPh₂ (2.48 mL, 13.84 mmol), and NEt₃ (2.12 mL, 15.22 mmol) as the starting materials.

Yield: 3.15 g (89 %) yellow solid; C₂₈H₂₃ClN₄P₂; MW: 512.92; 65.57 % C, 4.52 % H, 10.92 % N.

¹H NMR (δ, CDCl₃, 20 °C): 7.60–7.03 (m, 20H, Ph), 6.73 (bs, 1H, N), 6.07 (d, $J = 7.7$ Hz, 1H, NH), pyrimidine⁵ not observed.

¹³C{¹H} NMR (δ, CDCl₃, 20 °C): 166.0 (pyrimidine⁶), 162.3 (pyrimidine⁴), 158.8 (pyrimidine²), 139.1 (d, $J_{CP} = 13.3$ Hz, Ph¹), 131.2 (Ph⁴), 130.7 (d, $J_{CP} = 11.5$ Hz, Ph^{2,6}), 128.9 (d, $J_{CP} = 12.9$ Hz, Ph^{3,5}), 95.7 (pyrimidine⁵).

³¹P{¹H} NMR (δ, CDCl₃, 20 °C): 27.97.



N,N'-Bis(dibenzo[*d,f*]-1,3,2-dioxaphosphepine-1-yl)-2,6-diamino-4-chloropyrimidine (PNP^{PCl}-BIPOL)

This ligand was prepared analogously to PNP^{TOEt}-Ph with 2,6-diamino-4-chloropyrimidine (1.00 g, 6.92 mmol), BIPOL-PCl (3.47 g, 13.84 mmol), and NEt₃ (2.12 mL, 15.22 mmol) as the starting materials.

Yield: 2.66 g (67 %) yellow solid; C₂₈H₁₉ClN₄O₄P₂; MW: 572.88; 58.70 % C, 3.34 % H, 9.78 % N.

¹H NMR (δ, CDCl₃, 20 °C): 7.36–6.98 (m, 16H, Ph), 6.51 (d, *J* = 6.8 Hz, 1H, NH), 6.34 (d, *J* = 4.6 Hz, 1H, NH), pyrimidine⁵ not observed.

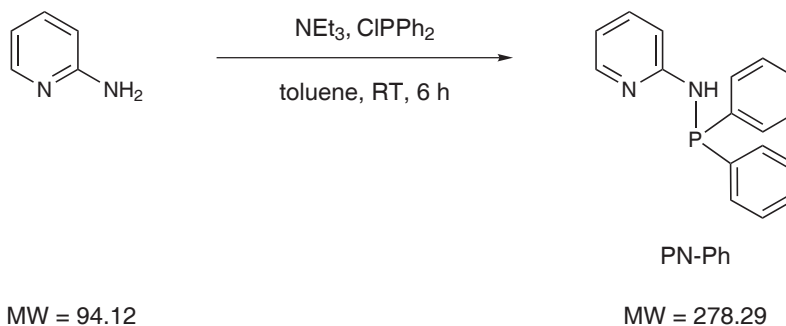
¹³C{¹H} NMR (δ, CDCl₃, 20 °C): 165.0, 160.9, 160.7 (pyrimidine^{2,4,6}), 149.4 (Ph), 149.3 (d, *J*_{CP} = 7.4 Hz, Ph), 146.5 (d, *J*_{CP} = 10.1 Hz, Ph), 131.6 (d, *J*_{CP} = 2.8 Hz, Ph), 131.3 (d, *J*_{CP} = 2.8 Hz, Ph), 130.3 (d, *J*_{CP} = 1.4 Hz, Ph), 130.2 (d, *J*_{CP} = 1.8 Hz, Ph), 130.0 (d, *J*_{CP} = 1.8 Hz, Ph), 129.9, 129.4, 129.3, and 129.1 (Ph), 128.6 (d, *J*_{CP} = 1.8 Hz, Ph), 128.3 (Ph), 126.9 (d, *J*_{CP} = 1.8 Hz, Ph), 125.7, 125.5, and 122.1 (Ph), 121.7 (d, *J*_{CP} = 3.7 Hz, Ph), 95.8 (pyrimidine⁵).

³¹P{¹H} NMR (δ, CDCl₃, 20 °C): 146.06 (d, *J* = 42.2 Hz).

5.3.3 PN ligands

N-(Diphenylphosphino)-2-aminopyridine (PN-Ph)

2-aminopyridine (1.0 g, 10.6 mmol) and NEt₃ (1.63 mL, 11.7 mmol) were dissolved in 30 mL of anhydrous toluene and cooled to 0 °C. ClPPh₂ (1.91 mL, 10.6 mmol) was added



dropwise. The reaction mixture was allowed to reach room temperature, stirred for 6 h and filtered. The solvent was removed and the crude product dried *in vacuo*.

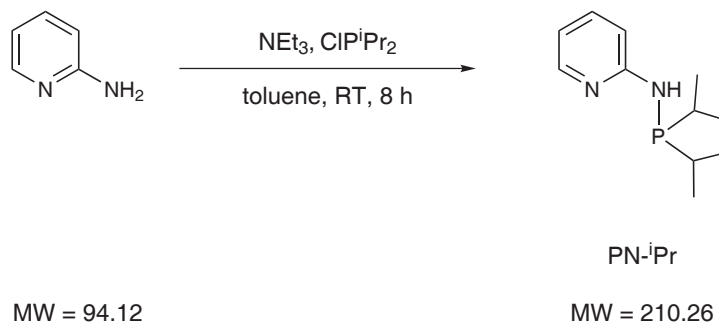
Yield: 2.30 g (78 %) pale yellow solid; $\text{C}_{17}\text{H}_{15}\text{N}_2\text{P}$; MW: 278.29; 73.37 % C, 5.43 % H, 10.07 % N.

$^1\text{H NMR}$ (δ , CDCl_3 , 20 °C): 7.93 (d, $J = 4.6$ Hz, 1H, py^6), 7.51–7.42 (m, 5H, Ph), 7.36–7.33 (m, 6H, Ph and py^4), 7.06 (d, $J = 8.2$ Hz, 1H, py^3), 6.64 (dd, $J_1 = 6.4$ Hz, $J_2 = 5.2$ Hz, 1H, py^5), 5.93 (d, $J = 8.4$ Hz, 1H, NH).

$^{13}\text{C}\{^1\text{H}\}$ NMR (δ , CDCl_3 , 20 °C): 158.7 (d, $J_{\text{CP}} = 20.7$ Hz, py^2), 148.1 (d, $J_{\text{CP}} = 1.5$ Hz, py^6), 139.6 (d, $J_{\text{CP}} = 11.1$ Hz, Ph^1), 137.82 (d, $J_{\text{CP}} = 2.3$ Hz, py^4), 131.3 (d, $J_{\text{CP}} = 20.7$ Hz, $\text{Ph}^{2,6}$), 129.2 (Ph^4), 128.6 (d, $J_{\text{CP}} = 6.9$ Hz, $\text{Ph}^{3,5}$), 115.0 (py^5), 108.9 (d, $J_{\text{CP}} = 15.7$ Hz, py^3).

$^{31}\text{P}\{^1\text{H}\}$ NMR (δ , CDCl_3 , 20 °C): 27.45.

N-(Di-*iso*-propylphosphino)-2-aminopyridine (PN-*i*Pr)



This compound was prepared analogously to PN-Ph with 2-aminopyridine (1.0 g, 10.6 mmol), NEt₃ (1.63 mL, 11.7 mmol), and ClP^{*i*}Pr₂ (1.69 mL, 10.6 mmol) as the starting materials.

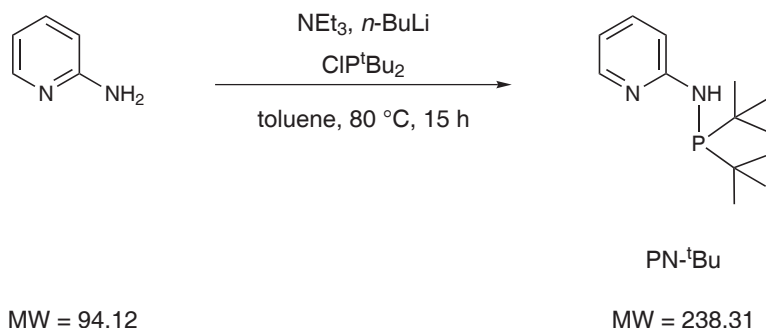
Yield: 2.05 g (92 %) pale yellow solid; C₁₁H₁₉N₂P; MW: 210.26; 62.84 % C, 9.11 % H, 13.32 % N.

¹H NMR (δ, CDCl₃, 20 °C): 7.97 (d, *J* = 4.9 Hz, 1H, py⁶), 7.38 (dt, *J*₁ = 7.7 Hz, *J*₂ = 1.6 Hz, 1H, py⁴), 7.05 (d, *J* = 8.5 Hz, 1H, py³), 6.57 (vt, *J* = 6.1 Hz, 1H, py⁵), 4.94 (d, *J* = 10.4 Hz, 1H, NH), 1.73 (dh, *J*₁ = 7.0 Hz, *J*₂ = 2.1 Hz, 2H, CH(CH₃)₂), 1.05–0.96 (m, 12H, CH(CH₃)₂).

¹³C{¹H} NMR (δ, CDCl₃, 20 °C): 160.7 (d, *J*_{CP} = 19.6 Hz, py²), 147.5 (d, *J*_{CP} = 1.2 Hz, py⁶), 137.6 (d, *J*_{CP} = 2.0 Hz, py⁴), 114.1 (py⁵), 108.9 (d, *J*_{CP} = 18.0 Hz, py³), 26.3 (d, *J*_{CP} = 11.1 Hz, CH(CH₃)₂), 18.6 (d, *J*_{CP} = 19.5 Hz, CH(CH₃)₂), 17.0 (d, *J*_{CP} = 7.7 Hz, CH(CH₃)₂).

³¹P{¹H} NMR (δ, CDCl₃, 20 °C): 49.96.

N-(Di-*tert*-butylphosphino)-2-aminopyridine (PN-^{*t*}Bu)



A solution of 2-aminopyridine (0.50 g, 5.31 mmol) and NEt₃ (0.81 mL, 5.844 mmol) in 10 mL of anhydrous toluene was cooled to 0 °C and treated with *n*-BuLi (5.31 mmol, 2.3 mL of a 2.3 M solution in *n*-hexane). After 15 min. of stirring at this temperature ClP^{*t*}Bu₂ (1.01 mL, 5.31 mmol) was added dropwise. The solution was then heated to 80 °C and stirred for 15 h, filtered and the solvent removed under vacuum.

Yield: 0.86 g (68 %) yellow oil; C₁₃H₂₃N₂P; MW: 238.31; 65.52 % C, 9.73 % H, 11.76 % N.

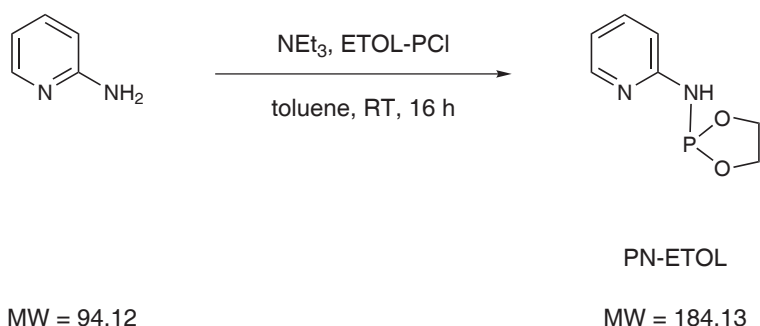
¹H NMR (δ, CDCl₃, 20 °C): 8.03 (d, *J* = 4.1 Hz, 1H, py⁶), 7.43 (vt, *J* = 7.9 Hz, 1H, py⁴), 7.13 (d, *J* = 8.4 Hz, 1H, py³), 6.62 (vt, *J* = 5.9 Hz, 1H, py⁵), 5.02 (d, *J* = 9.6 Hz, 1H, NH),

1.16 and 1.11 (2s, 9H each, C(CH₃)₃).

¹³C{¹H} NMR (δ, CDCl₃, 20 °C): 160.9 (d, *J*_{CP} = 18.2 Hz, py²), 147.9 (d, *J*_{CP} = 0.8 Hz, py⁶), 137.6 (d, *J*_{CP} = 1.5 Hz, py⁴), 114.2 (d, *J*_{CP} = 0.8 Hz, py⁵), 109.0 (d, *J*_{CP} = 18.4 Hz, py³), 34.2 and 33.9 (2s, C(CH₃)₃), 28.2 and 27.9 (2s, C(CH₃)₃).

³¹P{¹H} NMR (δ, CDCl₃, 20 °C): 61.19.

N-(1,3,2-Dioxaphospholane-1-yl)-2-aminopyridine (PN-ETOL)



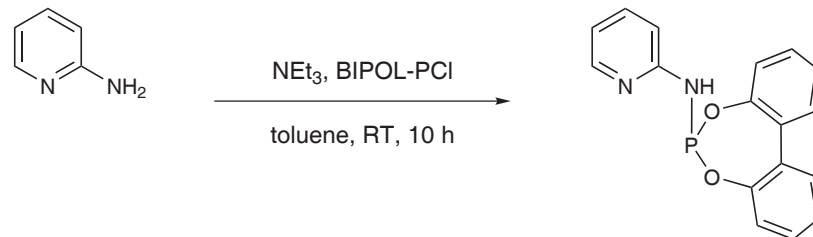
A solution of 2-aminopyridine (0.50 g, 5.31 mmol) in 15 mL of anhydrous toluene was treated with NEt₃ (0.81 mL, 5.84 mmol) and cooled to 0 °C. 2-chloro-1,3,2-dioxaphospholane (ETOL-PCl, 0.48 mL, 5.31 mmol) dissolved in 5 mL toluene was added dropwise. The mixture was allowed to reach room temperature and stirred for 16 h, filtered and the solvent removed under vacuum.

Yield: 0.83 g (85 %) white solid; C₇H₉N₂O₂P; MW: 184.13; 45.66 % C, 4.93 % H, 15.21 % N.

¹H NMR (δ, CDCl₃, 20 °C): 8.03 (d, *J* = 4.1 Hz, 1H, py⁶), 7.43 (td, *J*₁ = 7.7 Hz, *J*₂ = 1.5 Hz, 1H, py⁴), 6.79–6.74 (m, 2H, py^{3,5}), 6.06 (s, 1H, NH), 4.22–4.10 (m, 2H, CH₂–CH₂), 4.03–3.94 (m, 2H, CH₂–CH₂).

¹³C{¹H} NMR (δ, CDCl₃, 20 °C): 155.9 (d, *J*_{CP} = 13.8 Hz, py²), 148.1 (d, *J*_{CP} = 1.2 Hz, py⁶), 137.9 (d, *J*_{CP} = 1.5 Hz, py⁴), 116.1 (s, py⁵), 109.7 (d, *J*_{CP} = 10.7 Hz, py³), 63.6 (s, CH₂–CH₂), 63.5 (s, CH₂–CH₂).

³¹P{¹H} NMR (δ, CDCl₃, 20 °C): 61.19.

N-(Dibenzo[d,f]-1,3,2-dioxaphosphepine-1-yl)-2-aminopyridine (PN-BIPOL)

MW = 94.12

PN-BIPOL

MW = 308.27

This compound was prepared analogously to PN-Ph with 2-aminopyridine (0.80 g, 8.6 mmol), NEt₃ (1.20 mL, 8.6 mmol), and BIPOL-PCl (2-chlorodibenzo[d,f]-1,3,2-dioxaphosphepine, 2.2 g, 8.6 mmol) as the starting materials.

Yield: 2.46 g (92 %) white solid; C₁₇H₁₃N₂O₂P; MW: 308.27; 66.24 % C, 4.25 % H, 9.09 % N.

¹H NMR (δ, CDCl₃, 20 °C): 8.12 (d, *J* = 5.0 Hz, 1H, py⁶), 7.54–7.47 (m, 3H, Ph and py⁴), 7.39–7.24 (m, 6H, Ph), 6.84–6.79 (m, 2H, py³ and py⁵), 6.38 (s, 1H, NH).

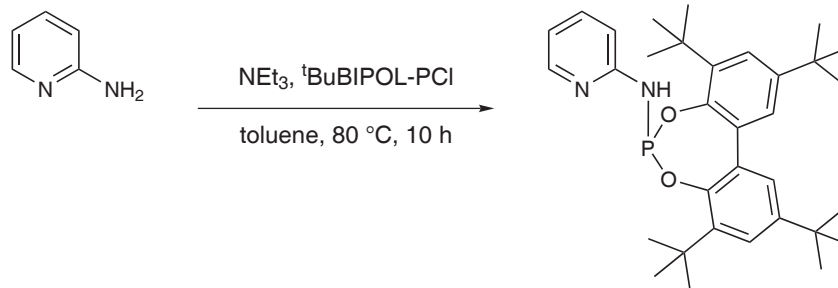
¹³C{¹H} NMR (δ, CDCl₃, 20 °C): 155.4 (d, *J*_{CP} = 16.9 Hz, py²), 149.6 (d, *J*_{CP} = 4.2 Hz, Ph), 148.3 (py⁶), 138.0 (d, *J*_{CP} = 1.6 Hz, py⁴), 131.6 (d, *J*_{CP} = 3.1 Hz, Ph), 129.8 (d, *J*_{CP} = 1.1 Hz, Ph), 129.2 (Ph), 125.3 (Ph), 122.2 (d, *J*_{CP} = 1.5 Hz, Ph), 116.6 (py⁵), 110.2 (d, *J*_{CP} = 11.1 Hz, py³).

³¹P{¹H} NMR (δ, CDCl₃, 20 °C): 147.32.

N-(3,5,8,10-Tetra-*tert*-butyldibenzo[d,f]-1,3,2-dioxaphosphepine-1-yl)-2-aminopyridine (PN-^tBuBIPOL)

To a solution of 2-aminopyridine (0.80 mg, 8.4 mmol) in 20 mL toluene NEt₃ (1.2 mL, 8.4 mmol) and ^tBuBIPOL-PCl (2-chloro-4,6,9,11-tetra-*tert*-butyldibenzo[d,f]-1,3,2-dioxaphosphepine, 4.0 g, 8.4 mmol) were added at 0 °C. The reaction mixture was allowed to reach room temperature and then refluxed for 10 h. The solution was then filtered and the solvent removed under vacuum.

Yield: 0.99 g (88 %) white solid; C₃₃H₄₅N₂O₂P; MW: 532.70; 74.41 % C, 8.51 % H, 5.26 % N.

PN-^tBuBIPOL

MW = 94.12

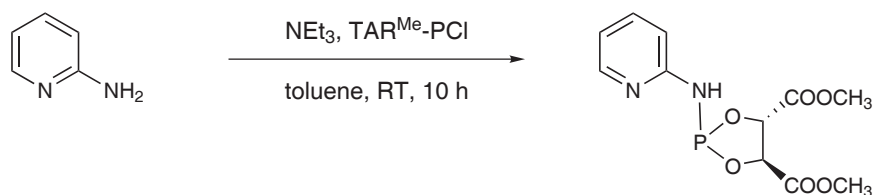
MW = 532.70

¹H NMR (δ, CDCl₃, 20 °C): 8.17 (d, *J* = 4.0 Hz, 1H, py⁶), 7.93 (d, *J* = 4.7 Hz, py⁴), 7.43 (d, *J* = 2.4 Hz, 2H, Ph), 6.89 (d, *J* = 8.2 Hz, 1H, py³), 6.78 (dd, *J*₁ = 6.8 Hz, *J*₂ = 5.4 Hz, 1H, py⁵), 6.62 (vt, *J* = 6.5 Hz, 1H, Ph), 6.55 (d, *J* = 8.4 Hz, 1H, Ph), 6.15 (s, 1H, NH), 1.37–1.19 (m, 36H, C(CH₃)₃).

¹³C{¹H} NMR (δ, CDCl₃, 20 °C): 156.3 (Ph), 155.7 (d, *J*_{CP} = 17.2 Hz, py²), 148.3 (py⁶), 146.6 (Ph), 137.7 (py⁴), 133.2 (d, *J*_{CP} = 18.2 Hz, Ph), 126.3 (Ph), 124.3 (Ph), 112.1 (py⁵), 112.1 (Ph), 110.1 (d, *J*_{CP} = 14.4 Hz, py³), 35.5 (C(CH₃)₃), 34.7 (C(CH₃)₃), 31.6 (C(CH₃)₃), 31.3 (C(CH₃)₃).

³¹P{¹H} NMR (δ, CDCl₃, 20 °C): 140.89.

(4*S*, 5*S*)-1-(2-Aminopyridyl)-1,3,2-dioxaphospholane-4-5-dicarboxylic acid, dimethylester (PN-TAR^{Me})

PN-TAR^{Me}

MW = 94.12

MW = 300.21

This compound was prepared analogously to PN-Ph with 2-aminopyridine (0.50 g, 5.31 mmol), NEt_3 (0.81 mL, 5.84 mmol), and $\text{TAR}^{\text{Me}}\text{-PCl}$ ((4*S*, 5*S*)-2-chloro-1,3,2-dioxaphospholane-4-5-dicarboxylic acid, dimethylester, 1.29 g, 5.31 mmol) as the starting materials.

Yield: 1.37 g (86 %) white solid; $\text{C}_{11}\text{H}_{13}\text{N}_2\text{O}_6\text{P}$; MW: 300.21; 44.01 % C, 4.36 % H, 9.33 % N.

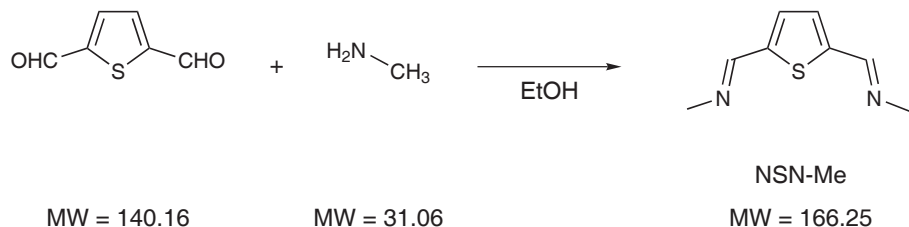
$^1\text{H NMR}$ (δ , CDCl_3 , 20 °C): 8.13 (d, $J = 4.1$ Hz, 1H, py^6), 7.48 (dt, $J_1 = 7.7$ Hz, $J_2 = 1.5$ Hz, 1H, py^4), 6.80 (dd, $J_1 = 6.8$ Hz, $J_2 = 5.4$ Hz, 1H, py^5), 6.70 (d, $J = 8.2$ Hz, py^3), 6.60 (s, 1H, NH), 5.09 (dd, $J_1 = 5.2$ Hz, $J_2 = 1.3$ Hz, 1H, CH), 4.84 (dd, $J_1 = 10.0$ Hz, $J_2 = 5.2$ Hz, 1H, CH), 3.83 (s, 3H, COOCH_3), 3.81 (s, 3H, COOCH_3).

$^{13}\text{C}\{^1\text{H}\}$ NMR (δ , CDCl_3 , 20 °C): 171.3 (COOCH_3), 169.1 (d, $J_{\text{CP}} = 4.3$ Hz, COOCH_3), 154.9 (d, $J_{\text{CP}} = 11.5$ Hz, py^2), 147.9 (py^6), 138.0 (py^4), 116.6 (py^5), 110.3 (d, $J_{\text{CP}} = 6.7$ Hz, py^3), 77.2 (CH), 77.0 (CH), 53.3 (COOCH_3), 53.1 (COOCH_3).

$^{31}\text{P}\{^1\text{H}\}$ NMR (δ , CDCl_3 , 20 °C): 142.58.

5.3.4 NSN ligands

2,5-Bis(methyliminomethyl)thiophene (NSN-Me)



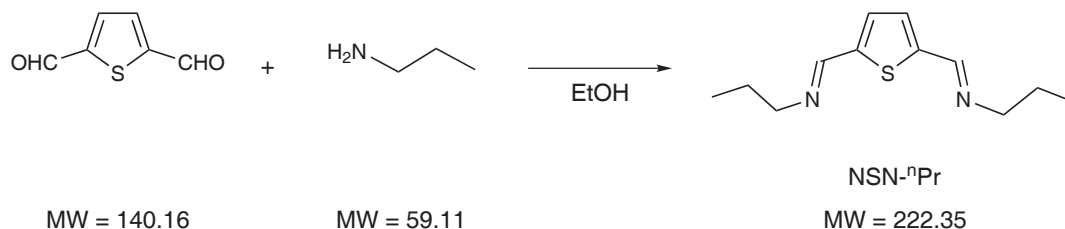
A solution of 2,5-thiophenecarboxaldehyde (0.50 g, 3.57 mmol) in 8 mL of EtOH was treated with methylamine (0.60 mL of a 40 % solution in H_2O) and the resulting orange solution was stirred for 15 at room temperature. Removal of the solvent afforded the crude product which was then dried *in vacuo*.

Yield: 0.56 g (94 %) off-white solid; $\text{C}_8\text{H}_{10}\text{N}_2\text{S}$; MW: 166.25; 57.80 % C, 6.06 % H, 16.85 % N.

$^1\text{H NMR}$ (δ , CDCl_3 , 20 °C): 8.29 (d, $J = 1.6$ Hz, 2H, $\text{N}=\text{CH}$), 7.21 (s, 2H, thiophene^{3,4}), 3.46 (d, $J = 1.6$ Hz, 6H, CH_3).

$^{13}\text{C}\{^1\text{H}\}$ NMR (δ , CDCl_3 , 20 °C): 155.5 (N=CH), 144.5 (thiophene^{2,5}), 129.7 (thiophene^{3,4}), 48.0 (CH_3).

2,5,-Bis(1-propyliminomethyl)thiophene (NSN-ⁿPr)



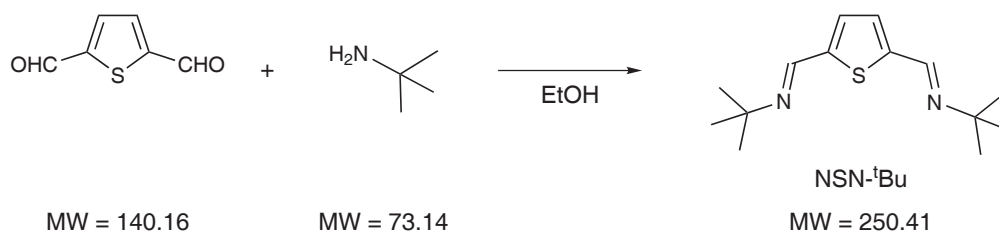
This compound was prepared analogously to NSN-Me with 2,5-thiophenecarboxaldehyde (0.50 g, 3.57 mmol) and *n*-propylamine (0.60 mL, 7.31 mmol) as the starting materials.

Yield: 0.76 g (96 %) off-white solid; $\text{C}_{12}\text{H}_{18}\text{N}_2\text{S}$; MW: 222.35; 64.82 % C, 8.16 % H, 12.60 % N.

^1H NMR (δ , CDCl_3 , 20 °C): 8.29 (s, 2H, N=CH), 7.23 (s, 2H, thiophene^{3,4}), 3.53 (t, J = 6.9 Hz, 4H, N- CH_2), 1.76-1.62 (m, 4H, CH_2 - CH_3), 0.92 (t, J = 7.4 Hz, 6H, CH_3).

$^{13}\text{C}\{^1\text{H}\}$ NMR (δ , CDCl_3 , 20 °C): 153.7 (N=CH), 144.7 (thiophene^{2,5}), 129.5 (thiophene^{3,4}), 63.1 (N- CH_2), 23.9 (CH_2 - CH_3), 11.8 (CH_3).

2,5,-Bis(*tert*.-butyliminomethyl)thiophene (NSN-^tBu)



A solution of 2,5-thiophenecarboxaldehyde (0.21 g, 1.50 mmol) in 8 mL of anhydrous EtOH was treated with *tert*.-butylamine (0.35 mL, 3.30 mmol) and stirred overnight at

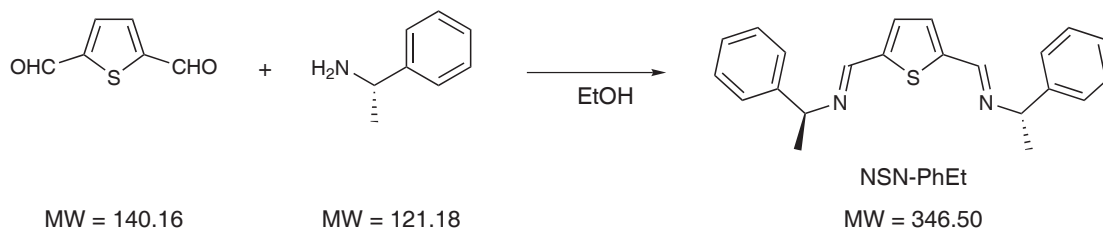
room temperature. Upon removal of the solvent an off-white solid precipitated which was collected on a glass frit and dried *in vacuo*.

Yield: 0.34 g (91 %) off-white solid; $C_{14}H_{22}N_2S$; MW: 250.41; 67.15 % C, 8.86 % H, 11.19 % N.

1H NMR (δ , $CDCl_3$, 20 °C): 8.28 (s, N=CH), 7.21 (s, 2H, thiophene^{3,4}), 1.26 (s, 18H, CH_3).

$^{13}C\{^1H\}$ NMR (δ , $CDCl_3$, 20 °C): 148.3 (N=CH), 146.0 (thiophene^{2,5}), 128.9 (thiophene^{3,4}), 57.4 ($C(CH_3)_3$), 29.6 ($C(CH_3)_3$).

S-2,5,-Bis((methyl)(phenyl)methyliminomethyl)thiophene (NSN-PhEt)

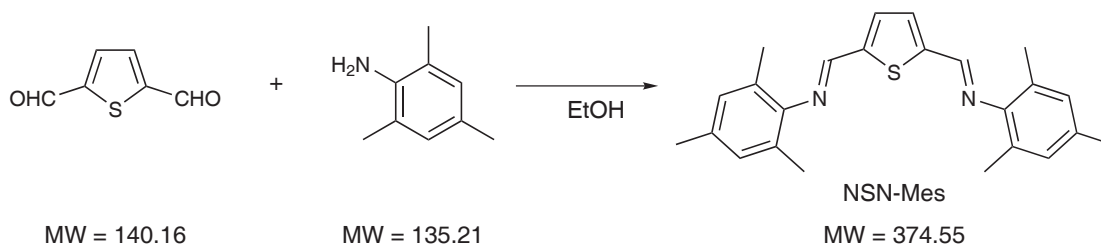


This ligand was prepared analogously to NSN-Me with 2,5-thiophenecarboxaldehyde (0.38 g, 2.68 mmol) and S-(−)-1-phenylethylamine (0.76 mL, 5.89 mmol) as the starting materials. The crude product was washed twice with small amounts of EtOH and dried *in vacuo*.

Yield: 0.76 g (82 %) off-white solid; $C_{22}H_{22}N_2S$; MW: 346.50; 76.26 % C, 6.40 % H, 8.08 % N.

1H NMR (δ , $CDCl_3$, 20 °C): 8.39 (s, 2H, N=CH), 7.44–7.23 (m, 12H, thiophene^{3,4} and Ph), 4.58–4.50 (m, 2H, $C(H)CH_3$), 1.60 and 1.57 (2s, 3H each, $C(H)CH_3$).

$^{13}C\{^1H\}$ NMR (δ , $CDCl_3$, 20 °C): 152.4 (N=CH), 145.2 and 145.0 (thiophene^{2,5} and Ph¹), 129.9 (thiophene^{3,4}), 128.4 and 126.6 (Ph^{2,6} and Ph^{3,5}), 126.9 (Ph⁴), 69.4 ($C(H)CH_3$), 25.1 ($C(H)CH_3$).



2,5-Bis((2,4,6-trimethylphenyl)iminomethyl)thiophene (NSN-Mes)

A solution of 2,5-thiophenecarboxaldehyde (1.00 g, 7.14 mmol) in 15 mL of anhydrous EtOH was treated with 2,4,6-trimethylaniline (2.05 mL, 14.63 mmol). Upon stirring at room temperature overnight a yellow solid precipitated which was collected on a glass frit, washed with EtOH and dried *in vacuo*.

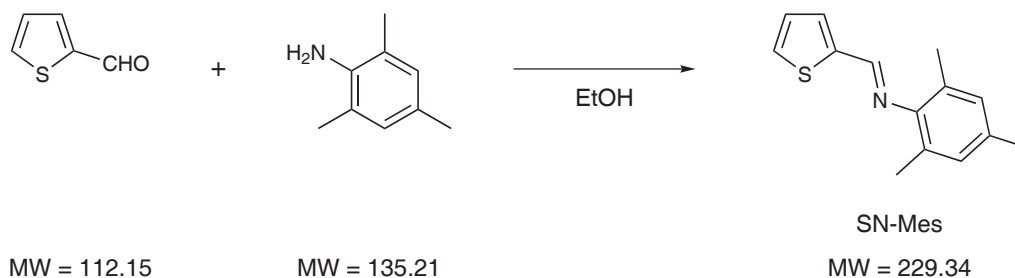
Yield: 2.58 g (97 %) yellow solid; $\text{C}_{24}\text{H}_{26}\text{N}_2\text{S}$; MW: 374.55; 76.96 % C, 7.00 % H, 7.48 % N.

^1H NMR (δ , CDCl_3 , 20 °C): 8.21 (s, 2H, $\text{N}=\text{CH}$), 7.34 (s, 2H, thiophene^{3,4}), 6.80 (s, 4H, $\text{Ph}^{3,5}$), 2.20 (s, 6H, Ph^4-CH_3), 2.07 (s, 12H, $\text{Ph}^{2,6}-\text{CH}_3$).

$^{13}\text{C}\{^1\text{H}\}$ NMR (δ , CDCl_3 , 20 °C): 155.3 ($\text{N}=\text{CH}$), 147.8 and 145.9 (thiophene^{2,5} and Ph^1), 133.4 (Ph^4), 131.3 (thiophene^{3,4}), 128.7 ($\text{Ph}^{3,5}$), 127.3 ($\text{Ph}^{2,6}$), 20.7 (Ph^4-CH_3), 18.2 ($\text{Ph}^{2,6}-\text{CH}_3$).

5.3.5 SN imine ligands

2,4,6-Trimethyl-N-(2-thienylmethylene)-aniline (SN-Mes)



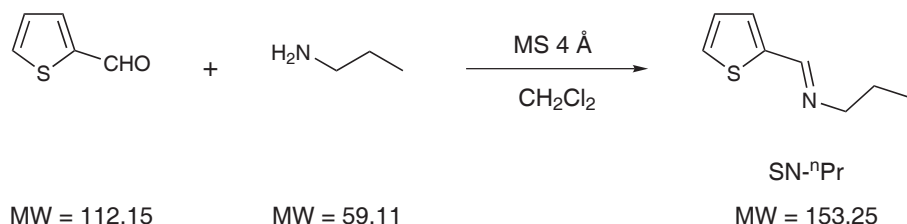
A solution of 2-thiophenecarboxaldehyde (1.25 mL, 13.38 mmol) in 50 mL EtOH was treated with 2,4,6-trimethylaniline (1.88 mL, 13.38 mmol). The solution was stirred for 15 h at room temperature. Upon removal of the solvent a yellow solid was obtained which was purified by recrystallisation from PE:EE.

Yield: 2.19 g (71 %) yellow solid; $C_{14}H_{15}NS$; MW: 229.34; 73.32 % C, 6.59 % H, 6.11 % N.

1H NMR (δ , $CDCl_3$, 20 °C): 8.32 (s, 1H, $N=CH$), 7.54 (d, $J = 5.1$ Hz, 1H, thiophene), 7.45 (d, $J = 3.5$ Hz, 1H, thiophene), 7.17 (dd, $J_1 = 4.9$ Hz, $J_2 = 3.8$ Hz, 1H, thiophene⁴), 6.91 (s, 2H, $Ph^{3,5}-H$), 2.32 (s, 3H, Ph^4-CH_3), 2.18 (s, 6H, $Ph^{2,6}-CH_3$).

$^{13}C\{^1H\}$ NMR (δ , $CDCl_3$, 20 °C): 155.6 ($N=CH$), 147.9 and 142.6 (thiophene² and Ph^1), 133.0 and 127.3 ($Ph^{2,6}$ and Ph^4), 131.6, 129.9, and 127.6 (thiophene^{3,4,5}), 128.6 ($Ph^{3,5}$), 20.7 (Ph^4-CH_3), 18.2 ($Ph^{2,6}-CH_3$).

***N*-(2-Thienylmethylene)-1-propaneamine (SN-ⁿPr)**

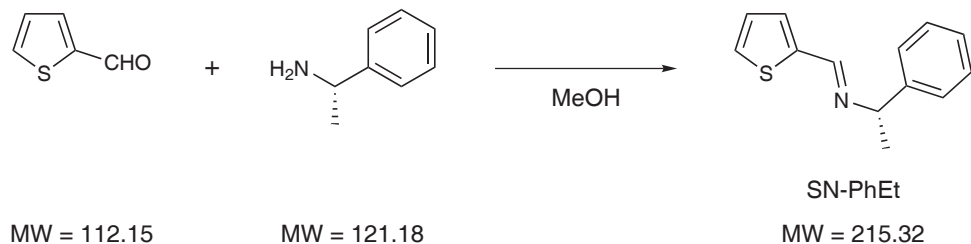


A solution of 2-thiophenecarboxaldehyde (1.25 mL, 13.38 mmol) and 1-propaneamine (1.10 mL, 13.38 mmol) in 20 mL of CH_2Cl_2 was charged with 4 Å molecular sieve and stirred at room temperature overnight. The suspension was filtered over Celite to remove traces of molecular sieve, the solvent removed and the product dried *in vacuo*.

Yield: 1.95 g (95 %) orange oil; $C_8H_{11}NS$; MW: 153.25; 62.70 % C, 7.23 % H, 9.14 % N.

1H NMR (δ , $CDCl_3$, 20 °C): 8.35 (s, 1H, $N=CH$), 7.37 (d, $J = 5.1$ Hz, 1H, thiophene), 7.28 (dd, $J_1 = 3.6$ Hz, $J_2 = 0.9$ Hz, 1H, thiophene), 7.06 (dd, $J_1 = 4.9$ Hz, $J_2 = 3.6$ Hz, 1H, thiophene⁴), 3.53 (dd, $J_1 = 7.0$ Hz, $J_2 = 1.2$ Hz, 2H, $N-CH_2$), 1.68-1.64 (m, 2H, CH_2-CH_3), 0.93 (t, $J = 7.4$ Hz, 3H, CH_3).

$^{13}C\{^1H\}$ NMR (δ , $CDCl_3$, 20 °C): 154.0 ($N=CH$), 142.6 (thiophene²), 130.1, 128.5, and 127.3 (thiophene^{3,4,5}), 63.2 ($N-CH_2$), 24.0 (CH_2-CH_3), 11.8 (CH_3).

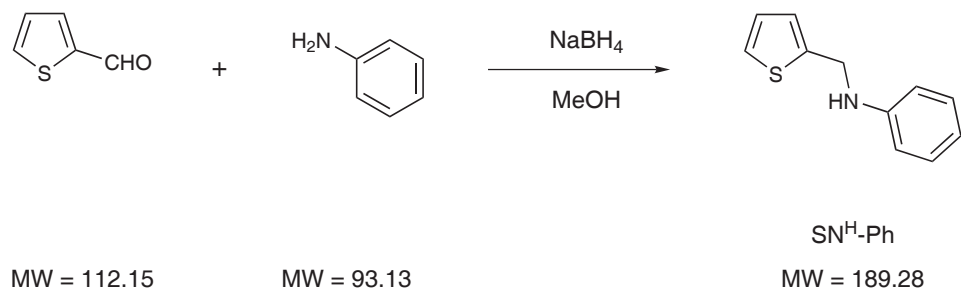
S-(–)-N-(2-Thienylmethylene)-1-phenylethylamine (SN-PhEt)

A solution of 2-thiophenecarboxaldehyde (0.5 mL, 5.35 mmol) and S-(–)-1-phenylethylamine (1.38 mL, 10.17 mmol) in MeOH was stirred at room temperature for 16 h. The solvent was removed and the crude product was purified by bulb-to-bulb distillation.

Yield: 1.07 g (93 %) brown oil; $\text{C}_{13}\text{H}_{13}\text{NS}$; MW: 215.32; 72.52 % C, 6.09 % H, 6.51 % N.

^1H NMR (δ , CDCl_3 , 20 °C): 8.46 (s, 1H, $\text{N}=\text{CH}$), 7.45–7.31 (m, 7H, thiophene^{3,4,5} and $\text{Ph}^{2,3,5,6}$), 7.08 (t, $J = 3.8$ Hz, 1H, Ph^4), 4.55 (q, $J = 6.4$ Hz, 1H, $\text{C}(\text{H})\text{CH}_3$), 1.62 (d, $J = 6.5$ Hz, 1H, $\text{C}(\text{H})\text{CH}_3$).

$^{13}\text{C}\{^1\text{H}\}$ NMR (δ , CDCl_3 , 20 °C): 152.8 ($\text{N}=\text{CH}$), 145.0 and 142.8 (thiophene² and Ph^1), 130.4, 128.9, 127.3, and 126.9 (thiophene^{3,4,5} and Ph^4), 128.5 and 126.7 ($\text{Ph}^{2,6}$ and $\text{Ph}^{3,5}$), 69.2 ($\text{C}(\text{H})\text{CH}_3$), 24.8 ($\text{C}(\text{H})\text{CH}_3$).

5.3.6 SN amine ligands**N-(2-Thienylmethyl)-aniline ($\text{SN}^{\text{H}}\text{-Ph}$)**

2-Thiophenecarboxaldehyde (0.83 mL, 8.92 mmol) and aniline (0.81 mL, 8.92 mmol) were

mixed while cooling with an ice bath. The mixture was diluted with 20 mL of anhydrous MeOH and stirring was continued for 50 min. NaBH₄ (0.34 g, 8.92 mmol) was added in portions to the cooled solution and the reaction was allowed to stir at room temperature for 15 h.

The solvent was removed and the residue diluted with 40 mL of H₂O. The aqueous phase was extracted three times with Et₂O, the combined organic layers were dried over Na₂SO₄, filtered and the solvent removed. The crude product was purified by column chromatography (SiO₂, eluent PE:EE 10:1).

Yield: 1.63 g (97 %) yellow oil; C₁₁H₁₁NS; MW: 189.28; 69.80 % C, 5.86 % H, 7.40 % N.

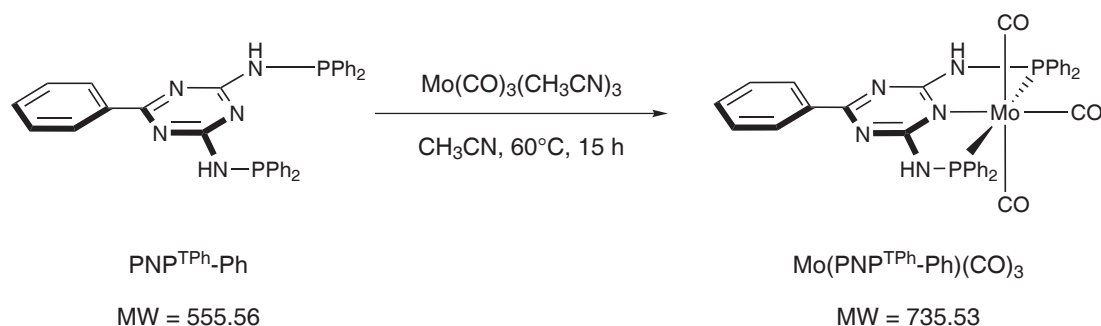
¹H NMR (δ, CDCl₃, 20 °C): 7.34–7.26 (m, 3H, thiophene⁵ and Ph^{3,5}), 7.11–7.05 (m, 2H, thiophene^{3,4}), 6.86 (t, *J* = 7.3 Hz, 1H, Ph⁴), 6.76 (d, *J* = 7.6 Hz, 2H, Ph^{2,6}).

¹³C{¹H} NMR (δ, CDCl₃, 20 °C): 147.7 (Ph¹), 143.1 (thiophene²), 129.4 (Ph^{3,5}), 127.0, 125.1, and 124.7 (thiophene^{3,4,5}), 118.2 (Ph⁴), 113.3 (Ph^{2,6}), 43.6 (N–CH₂).

5.4 Molybdenum complexes

5.4.1 Molybdenum PNP^T complexes

Mo(PNP^{TPh}-Ph)(CO)₃

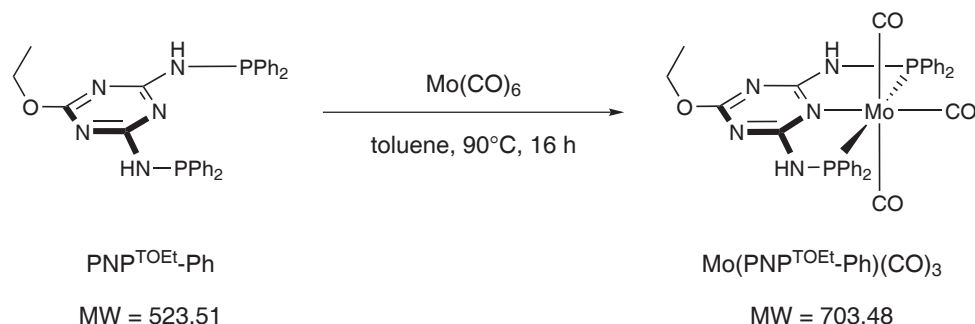


Mo(CO)₆ (0.30 mg, 0.88 mmol) was refluxed in 10 mL of CH₃CN for 2 h. The yellow solution was cooled to room temperature and PNP^{TPh}-Ph (232 mg, 0.47 mmol) was added. The mixture was stirred for 8 h at room temperature. Removal of the solvent afforded

130.2 (PPh⁴), 128.4 (t, J_{CP} = 5.2 Hz, PPh^{3,5}), 25.0 (CH₃).

³¹P{¹H} NMR (δ, CD₂Cl₂, 20 °C): 105.13.

Mo(PNP^{TOEt}-Ph)(CO)₃



PNP^{TOEt}-Ph (0.350 g, 0.669 mmol) was dissolved in 10 mL of anhydrous toluene, treated with Mo(CO)₆ (0.176 g, 0.669 mmol) and stirred at 90 °C for 16 h. After cooling to room temperature the solvent was removed and the crude product was purified by flash chromatography (neutral Al₂O₃, eluent CH₂Cl₂).

Yield: 0.322(68 %) yellow solid; C₃₂H₂₇MoN₅O₄P₂; MW: 703.48; 54.64 % C, 3.87 % H, 9.96 % N.

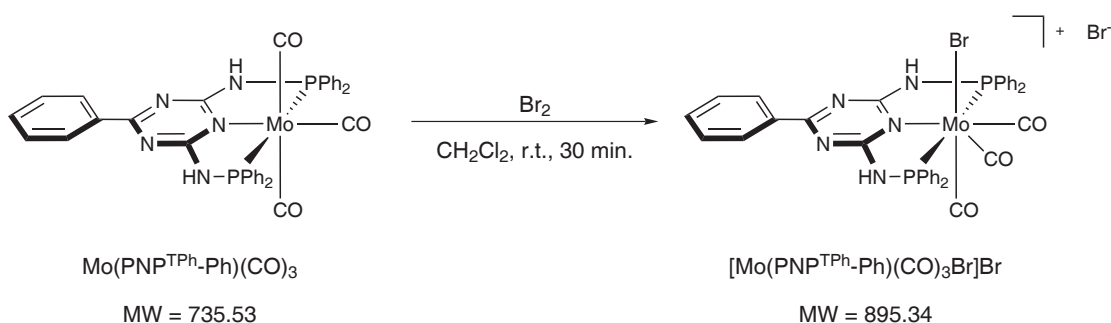
¹H NMR (δ, CD₂Cl₂, 20 °C): 7.66–7.44 (m, 20H, Ph), 7.31 (bs, 2H, NH), 4.16 (q, J = 7.1 Hz, 2H, CH₂–CH₃), 1.19 (t, J = 7.0 Hz 3H, CH₂–CH₃).

¹³C{¹H} NMR (δ, CD₂Cl₂, 20 °C): 226.4 (t, J_{CP} = 5.7 Hz, CO), 210.8 (t, J_{CP} = 10.1 Hz, CO), 170.4 (t, J_{CP} = 13.2 Hz, triaz^{2,6}), 168.8 (t, J_{CP} = 2.3 Hz, triaz⁴), 139.0 (t, J_{CP} = 19.3 Hz, PPh¹), 130.6 (t, J_{CP} = 7.8 Hz, PPh^{2,6}), 130.1 (PPh⁴), 128.4 (t, J_{CP} = 5.2 Hz, PPh^{3,5}), 64.03 (CH₂–CH₃), 13.96 (CH₂–CH₃).

³¹P{¹H} NMR (δ, CD₂Cl₂, 20 °C): 105.72.

[Mo(PNP^{TPh}-Ph)(CO)₃Br]Br

To a solution of PNP^{TPh}-Ph (0.300 g, 0.408 mmol) in 10 mL of CH₂Cl₂ Br₂ (21 μL, 0.408 mmol) was added at room temperature. After 30 min. solvent was removed and the



product was dried *in vacuo*.

Yield: 0.335 g (92 %) orange solid; $\text{C}_{36}\text{H}_{27}\text{Br}_2\text{MoN}_5\text{O}_3\text{P}_2$; MW: 895.34; 48.29 % C, 3.04 % H, 7.82 % N.

$^1\text{H NMR}$ (δ , CD_2Cl_2 , 20 °C): 8.38–8.34 (m, 2H, NH), 7.73–7.63 (m, 7H, Ph), 7.58–7.45 (m, 18H, Ph).

$^{13}\text{C}\{^1\text{H}\}$ NMR (δ , CD_2Cl_2 , 20 °C): 210.4 (d, $J_{\text{CP}} = 18.8$ Hz, CO), 206.0 (d, $J_{\text{CP}} = 10.1$ Hz, CO), 173.5 (triaz⁴), 168.4 (t, $J_{\text{CP}} = 10.3$ Hz, triaz^{2,6}), 138.6 (t, $J_{\text{CP}} = 19.8$ Hz, PPh¹), 135.3 (Ph¹), 132.4 (Ph⁴), 131.0 (Ph^{2,6}), 130.7 (t, $J_{\text{CP}} = 15.4$ Hz, PPh^{2,6}), 130.5 (PPh⁴), 129.1 (Ph^{3,5}), 128.6 (t, $J_{\text{CP}} = 5.1$ Hz, PPh^{3,5}).

$^{31}\text{P}\{^1\text{H}\}$ NMR (δ , CD_2Cl_2 , 20 °C): 116.27.

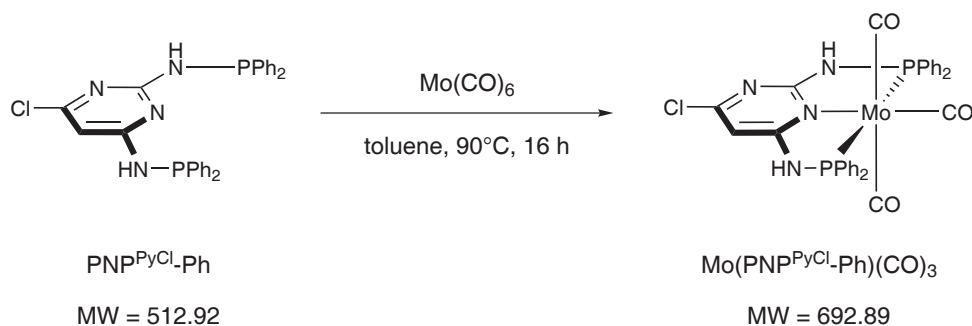
5.4.2 Molybdenum PNP^P complexes

Mo(PNP^{PCl}-Ph)(CO)₃

This complex was prepared analogously to $\text{Mo(PNP}^{\text{TOEt}}\text{-Ph)(CO)}_3$ with PNP^{PCl}-Ph (0.500 g, 0.975 mmol) and Mo(CO)_6 (0.257 g, 0.975 mmol) as the starting materials.

Yield: 0.367 g (54 %) yellow solid; $\text{C}_{31}\text{H}_{23}\text{ClMoN}_4\text{O}_3\text{P}_2$; MW: 692.89; 53.74 % C, 3.35 % H, 8.09 % N.

$^1\text{H NMR}$ (δ , CD_2Cl_2 , 20 °C): 7.69–7.45 (m, 20H, Ph), 6.92 (d, $J = 5.2$ Hz, 1H, NH), 6.80 (d, $J = 5.4$ Hz, 1H, NH), 6.42 (s, 1H, pyrimidine⁵).

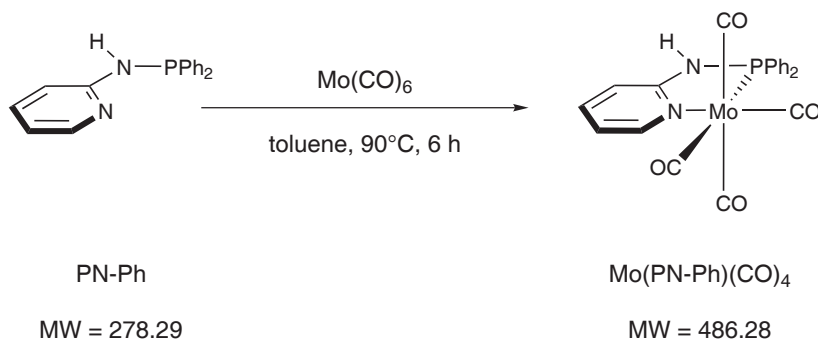


$^{13}\text{C}\{^1\text{H}\}$ NMR (δ , CD_2Cl_2 , 20 $^\circ\text{C}$): 227.0 (vt, $J_{\text{CP}} = 5.2$ Hz, CO), 210.4 (vt, $J_{\text{CP}} = 10.1$ Hz, CO), 205.8 (d, $J_{\text{CP}} = 65.2$ Hz, CO), 164.8 (dd, $J_{\text{CP}} = 21.3$ Hz, $J_{\text{CP}} = 6.3$ Hz, pyrimidine), 164.1 (d, $J_{\text{CP}} = 2.9$ Hz, pyrimidine), 159.0 (d, $J_{\text{CP}} = 2.9$ Hz, pyrimidine), 139.7 (d, $J_{\text{CP}} = 1.7$ Hz, Ph^1), 132.3 (d, $J_{\text{CP}} = 11.5$ Hz, Ph^4), 130.6 (dd, $J_{\text{CP}} = 14.9$ Hz, $J_{\text{CP}} = 11.5$ Hz, $\text{Ph}^{2,6}$), 128.9 (dd, $J_{\text{CP}} = 10.9$ Hz, $J_{\text{CP}} = 8.6$ Hz, $\text{Ph}^{3,5}$), 95.8 (d, $J_{\text{CP}} = 7.4$ Hz, pyrimidine⁵).

$^{31}\text{P}\{^1\text{H}\}$ NMR (δ , CD_2Cl_2 , 20 $^\circ\text{C}$): 102.09.

5.4.3 Molybdenum PN complexes

Mo(PN-Ph)(CO)₄



A mixture of PN-Ph (0.50 g, 1.80 mmol) and Mo(CO)_6 (0.46 g, 1.80 mmol) was stirred in toluene at 90 $^\circ\text{C}$. After 6 h the solvent was removed and the crude product was purified by flash chromatography (neutral Al_2O_3 , eluent CH_2Cl_2).

Yield: 0.59 g (68 %) yellow solid; $\text{C}_{21}\text{H}_{15}\text{MoN}_2\text{O}_4\text{P}$; MW: 486.28; 51.87 % C, 3.11 % H,

5.76 % N.

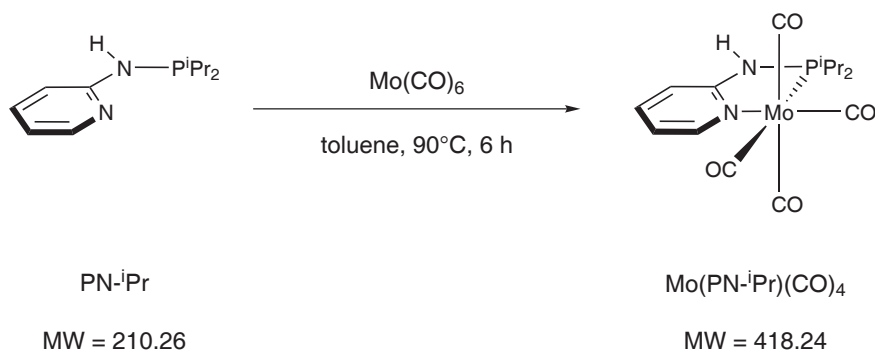
^1H NMR (δ , CD_2Cl_2 , 20 °C): 8.51 (d, J = 5.4 Hz, 1H, py^6), 7.66–7.50 (m, 11H, py^4 and Ph), 6.91 (d, J = 8.4 Hz, 1H, py^3), 6.69 (t, J = 6.6 Hz, 1H, py^5), 6.18 (d, J = 5.8 Hz, 1H, NH).

$^{13}\text{C}\{^1\text{H}\}$ NMR (δ , CD_2Cl_2 , 20 °C): 220.7 (d, J_{CP} = 7.0 Hz, CO), 216.1 (d, J_{CP} = 34.9 Hz, CO), 208.1 (d, J_{CP} = 9.5 Hz, CO), 160.0 (d, J_{CP} = 15.5 Hz, py^2), 153.6 (d, J_{CP} = 4.5 Hz, py^6), 139.0 (py^4), 137.7 (d, J_{CP} = 39.4 Hz, Ph^1), 130.6 (d, J_{CP} = 15.5 Hz, $\text{Ph}^{2,6}$), 130.6 (d, J_{CP} = 2.0 Hz, Ph^4), 128.7 (d, J_{CP} = 10.0 Hz, $\text{Ph}^{3,5}$), 115.7 (py^5), 111.2 (d, J_{CP} = 6.0 Hz, py^3).

$^{31}\text{P}\{^1\text{H}\}$ NMR (δ , CD_2Cl_2 , 20 °C): 87.50.

IR (ATR, cm^{-1}): 2075 (s, $\nu_{\text{C=O}}$), 1895 (s, $\nu_{\text{C=O}}$), 1807 (s, $\nu_{\text{C=O}}$).

Mo(PN-*i*Pr)(CO)₄



PN-*i*Pr (0.50 g, 2.39 mmol) was dissolved in 10 mL of anhydrous toluene and treated with Mo(CO)_6 (0.63 g, 2.39 mmol). The mixture was stirred at 90 °C for 6 h, then the solvent was removed. The crude product was dried *in vacuo*.

Yield: 0.66 g (66 %) yellow solid; $\text{C}_{15}\text{H}_{19}\text{MoN}_2\text{O}_4\text{P}$; MW: 418.24; 43.08 % C, 4.58 % H, 6.70 % N.

^1H NMR (δ , CD_2Cl_2 , 20 °C): 8.41 (d, J = 4.9 Hz, 1H, py^6), 7.49 (vt, J = 7.3 Hz, 1H, py^4), 6.75 (d, J = 8.2 Hz, 1H, py^3), 6.58 (vt, J = 6.2 Hz, 1H, py^5), 5.45 (d, J = 4.4 Hz, 1H, NH), 2.44–2.23 (m, 2H, $\text{CH(CH}_3)_2$), 1.34–1.20 (m, 12H, $\text{CH(CH}_3)_2$).

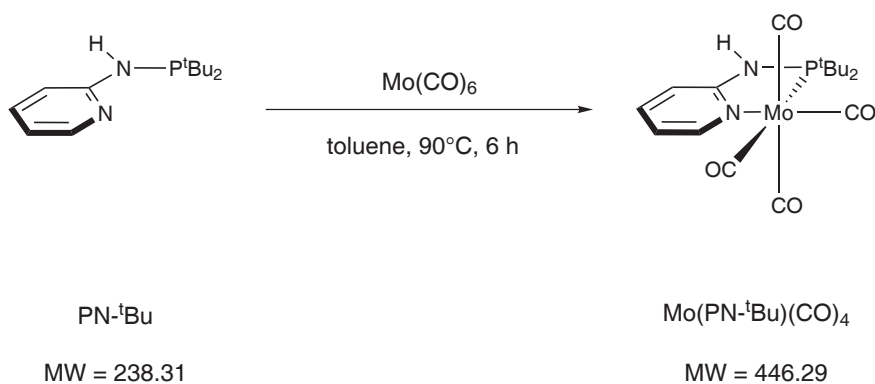
$^{13}\text{C}\{^1\text{H}\}$ NMR (δ , CD_2Cl_2 , 20 °C): 221.5 (d, J_{CP} = 7.0 Hz, CO), 215.7 (d, J_{CP} = 33.4 Hz, CO), 209.6 (d, J_{CP} = 9.5 Hz, CO), 161.0 (d, J_{CP} = 12.0 Hz, py^2), 153.4 (d, J_{CP} = 4.5 Hz, py^6), 138.8

(py⁴), 114.8 (py⁵), 110.6 (d, $J_{CP} = 5.0$ Hz, py³), 30.6 and 30.3 (2s, CH(CH₃)₂), 18.2 and 18.1 (2s, CH(CH₃)₂).

³¹P{¹H} NMR (δ, CD₂Cl₂, 20 °C): 114.44.

IR (ATR, cm⁻¹): 2019 (s, ν_{C=O}), 1879 (s, ν_{C=O}), 1818 (s, ν_{C=O}).

Mo(PN-^tBu)(CO)₄



This compound was prepared analogously to Mo(PN-ⁱPr)(CO)₄ with PN-^tBu (0.41 g, 1.74 mmol) and Mo(CO)₆ (0.46 g, 1.74 mmol) as the starting materials.

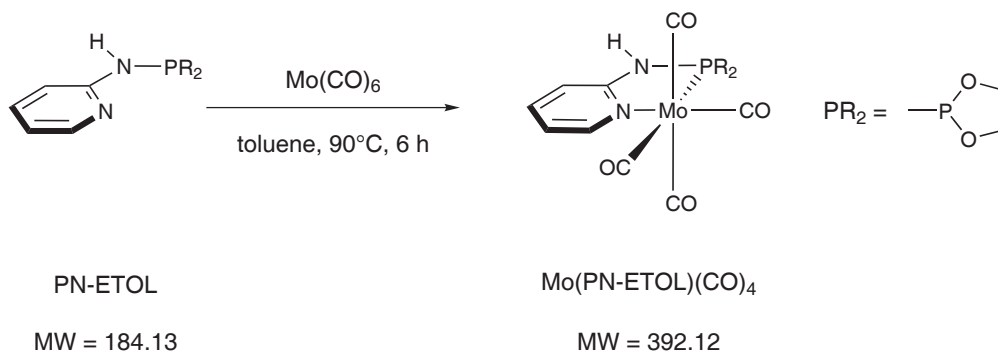
Yield: 0.57 g (74 %) yellow solid; C₁₇H₂₃MoN₂O₄P; MW: 446.29; 45.75 % C, 5.19 % H, 6.28 % N.

¹H NMR (δ, CD₂Cl₂, 20 °C): 8.39 (d, $J = 5.4$ Hz, 1H, py⁶), 7.49 (vt, $J = 7.6$ Hz, 1H, py⁴), 6.87 (d, $J = 8.2$ Hz, 1H, py³), 6.59 (vt, $J = 6.3$ Hz, 1H, py⁵), 5.54 (d, $J = 3.9$ Hz, 1H, NH), 1.42 and 1.36 (2s, 9H each, C(CH₃)₃).

¹³C{¹H} NMR (δ, CD₂Cl₂, 20 °C): 222.2 (d, $J_{CP} = 6.9$ Hz, CO), 216.4 (d, $J_{CP} = 34.9$ Hz, CO), 211.4 (d, $J_{CP} = 8.3$ Hz, CO), 161.5 (d, $J_{CP} = 10.6$ Hz, py²), 153.2 (d, $J_{CP} = 4.6$ Hz, py⁶), 138.9 (py⁴), 115.0 (py⁵), 111.1 (d, $J_{CP} = 4.6$ Hz, py³), 37.7 (d, $J_{CP} = 9.2$ Hz, C(CH₃)₃), 28.8 and 28.7 (2 s, C(CH₃)₃).

³¹P{¹H} NMR (δ, CD₂Cl₂, 20 °C): 127.89.

IR (ATR, cm⁻¹): 2010 (s, ν_{C=O}), 1903 (s, ν_{C=O}), 1880 (s, ν_{C=O}), 1812 (s, ν_{C=O}).

Mo(PN-ETOL)(CO)₄

This compound was prepared analogously to Mo(PN-ⁱPr)(CO)₄ with PN-ETOL (0.37 g, 2.02 mmol) and Mo(CO)₆ (0.53 g, 2.02 mmol) as the starting materials.

Yield: 0.63 g (80 %) yellow solid; C₁₁H₉MoN₂O₆P; MW: 392.12; 33.69 % C, 2.31 % H, 7.14 % N.

¹H NMR (δ, CD₂Cl₂, 20 °C): 8.42 (d, *J* = 4.7 Hz, 1H, py⁶), 7.56 (vt, *J* = 7.5 Hz, 1H, py⁴), 6.75–6.69 (m, 3H, py^{3,5}, NH), 4.35–4.30 (m, 4H, CH₂–CH₂).

¹³C{¹H} NMR (δ, CD₂Cl₂, 20 °C): 219.1 (d, *J*_{CP} = 11.5 Hz, CO), 214.8 (d, *J*_{CP} = 53.4 Hz, CO), 206.1 (d, *J*_{CP} = 13.2 Hz, CO), 157.8 (d, *J*_{CP} = 19.0 Hz, py²), 153.4 (d, *J*_{CP} = 5.2 Hz, py⁶), 139.1 (py⁴), 116.3 (py⁵), 110.9 (d, *J*_{CP} = 5.7 Hz, py³), 65.5 (d, *J*_{CP} = 7.5 Hz, CH₂–CH₂).

³¹P{¹H} NMR (δ, CD₂Cl₂, 20 °C): 180.27.

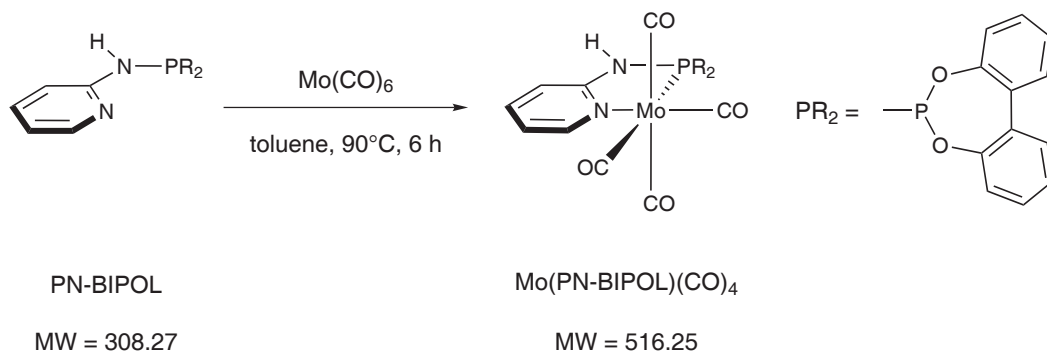
IR (ATR, cm^{−1}): 2025 (s, ν_{C=O}), 1920 (s, ν_{C=O}), 1887 (s, ν_{C=O}), 1850 (s, ν_{C=O}).

Mo(PN-BIPOL)(CO)₄

This compound was prepared analogously to Mo(PN-ⁱPr)(CO)₄ with PN-BIPOL (0.76 g, 2.45 mmol) and Mo(CO)₆ (0.65 g, 2.45 mmol) as the starting materials.

Yield: 1.03 g (81 %) yellow solid; C₂₁H₁₃MoN₂O₆P; MW: 516.25; 48.86 % C, 2.54 % H, 5.43 % N.

¹H NMR (δ, CD₂Cl₂, 20 °C): 8.52 (d, *J* = 4.7 Hz, 1H, py⁶), 7.64–7.08 (m, 9H, py⁴ and Ph), 6.82–6.79 (m, 2H, py³ and py⁵), 6.60–6.52 (m, 1H, NH).

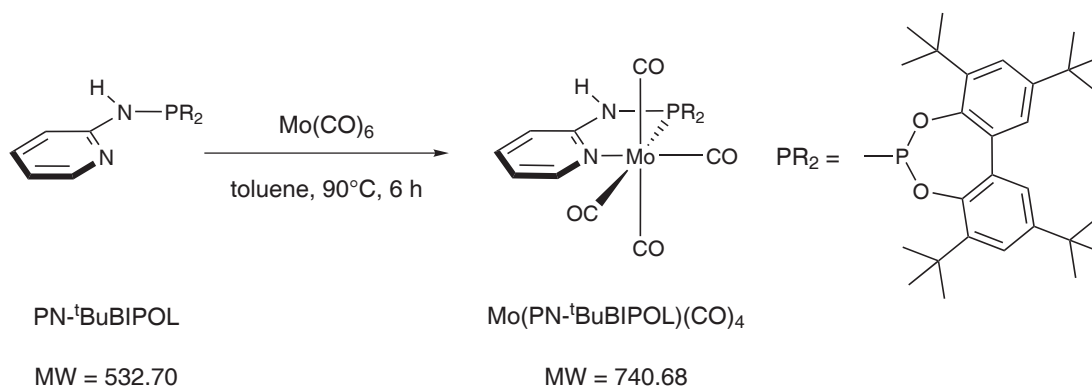


¹³C{¹H} NMR (δ, CD₂Cl₂, 20 °C): 218.5 (d, *J*_{CP} = 10.9 Hz, CO), 214.4 (d, *J*_{CP} = 55.7 Hz, CO), 206.2 (d, *J*_{CP} = 13.8 Hz, CO), 157.8 (d, *J*_{CP} = 20.7 Hz, py²), 153.9 (d, *J*_{CP} = 4.6 Hz, py⁶), 148.8 (d, *J*_{CP} = 9.2 Hz, Ph¹), 139.4 (py⁴), 130.3 (d, *J*_{CP} = 2.3 Hz, Ph²), 129.9 (d, *J*_{CP} = 1.7 Hz, Ph), 129.8 (d, *J*_{CP} = 1.7 Hz, Ph), 126.2 (d, *J*_{CP} = 1.7 Hz, Ph), 121.9 (d, *J*_{CP} = 2.9 Hz, Ph), 116.8 (py⁵), 111.2 (d, *J*_{CP} = 6.9 Hz, py³).

³¹P{¹H} NMR (δ, CD₂Cl₂, 20 °C): 186.37.

IR (ATR, cm⁻¹): 2022 (s, ν_{C=O}), 1944 (s, ν_{C=O}), 1885 (s, ν_{C=O}), 1860 (s, ν_{C=O}).

Mo-PN-^tBuBIPOL(CO)₄



This compound was prepared analogously to Mo(PN-ⁱPr)(CO)₄ with PN-^tBuBIPOL (0.381 g, 0.728 mmol) and Mo(CO)₆ (0.192 g, 0.728 mmol) as the starting materials.

Yield: 0.352 g (65 %) dark yellow solid; C₃₇H₄₅MoN₂O₆P; MW: 740.68; 60.00 % C, 6.12 % H,

3.78 % N.

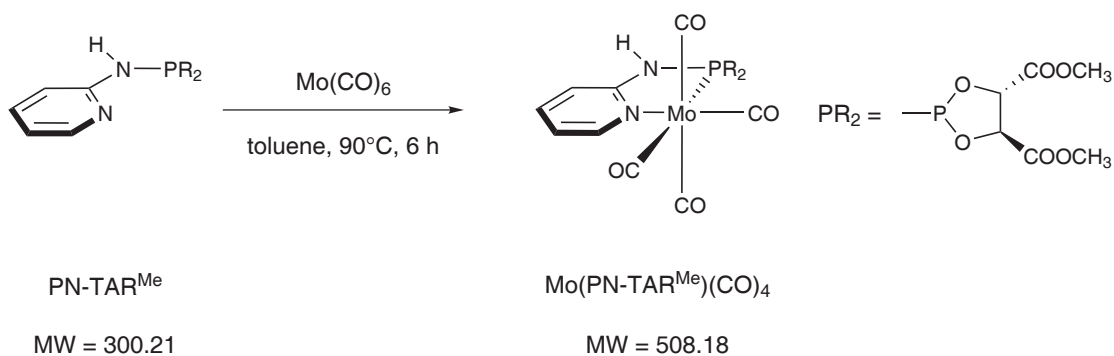
^1H NMR (δ , CD_2Cl_2 , 20 °C): 8.52 (s, 1H, py^6), 7.55–7.12 (m, 5H, py^4 and Ph), 6.74–6.59 (m, 3H, py^3 , py^5 , and NH), 1.54–1.24 (m, 36H, $\text{C}(\text{CH}_3)_3$).

$^{13}\text{C}\{^1\text{H}\}$ NMR (δ , CD_2Cl_2 , 20 °C): 219.2 (d, $J_{\text{CP}} = 10.9$ Hz, CO), 215.2 (d, $J_{\text{CP}} = 56.9$ Hz, CO), 206.7 (d, $J_{\text{CP}} = 12.1$ Hz, CO), 157.5 (d, $J_{\text{CP}} = 19.5$ Hz, py^2), 153.7 (d, $J_{\text{CP}} = 4.6$ Hz, py^6), 147.6 (Ph^1), 145.7 (d, $J_{\text{CP}} = 10.9$ Hz, Ph), 140.6 (d, $J_{\text{CP}} = 3.4$ Hz, Ph), 139.4 (d, $J_{\text{CP}} = 3.4$ Hz, py^4), 131.6 (d, $J_{\text{CP}} = 2.9$ Hz, Ph^2), 127.2 (Ph), 124.9 (Ph), 116.4 (py^5), 111.0 (d, $J_{\text{CP}} = 6.3$ Hz, py^3), 35.4 ($\text{C}(\text{CH}_3)_3$), 34.6 ($\text{C}(\text{CH}_3)_3$), 31.2 ($\text{C}(\text{CH}_3)_3$), 30.9 ($\text{C}(\text{CH}_3)_3$).

$^{31}\text{P}\{^1\text{H}\}$ NMR (δ , CD_2Cl_2 , 20 °C): 183.90.

IR (ATR, cm^{-1}): 2028 (s, $\nu_{\text{C=O}}$), 1959 (s, $\nu_{\text{C=O}}$), 1915 (s, $\nu_{\text{C=O}}$), 1877 (s, $\nu_{\text{C=O}}$).

Mo(PN-TAR^{Me})(CO)₄



This compound was prepared analogously to $\text{Mo(PN-}^i\text{Pr)(CO)}_4$ with PN-TAR^{Me} (0.40 g, 1.33 mmol) and Mo(CO)_6 (0.35 g, 1.33 mmol) as the starting materials.

Yield: 0.51 g (75 %) yellow solid; $\text{C}_{15}\text{H}_{13}\text{MoN}_2\text{O}_{10}\text{P}$; MW: 508.18; 35.45 % C, 2.58 % H, 5.51 % N.

^1H NMR (δ , CD_2Cl_2 , 20 °C): 8.44 (bs, 1H, py^6), 7.59 (bs, 2H, py^4 and py^3), 6.84–6.74 (m, 2H, py^5 and NH), 5.33–5.10 (m, 2H, CH), 3.93 (s, 3H, COOCH_3), 3.90 (s, 3H, COOCH_3).

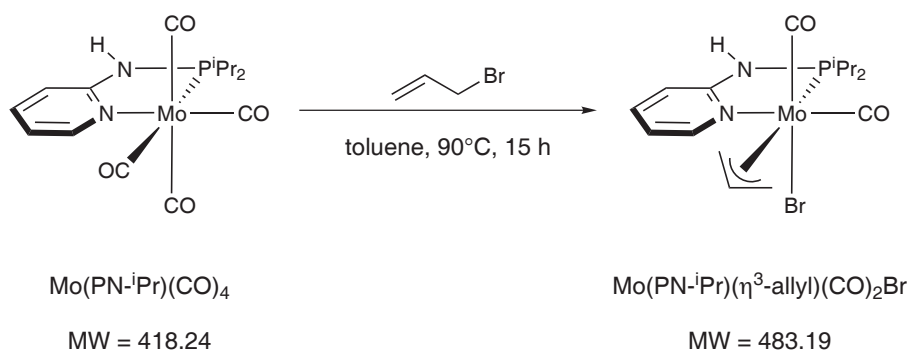
$^{13}\text{C}\{^1\text{H}\}$ NMR (δ , CD_2Cl_2 , 20 °C): 218.5 (d, $J_{\text{CP}} = 11.5$ Hz, CO), 214.8 (d, $J_{\text{CP}} = 55.7$ Hz, CO), 205.8 (d, $J_{\text{CP}} = 13.8$ Hz, CO), 205.6 (d, $J_{\text{CP}} = 13.8$ Hz, CO), 170.9 (s, COOCH_3), 168.3

(d, $J_{CP} = 2.3$ Hz, COOCH₃), 157.4 (d, $J_{CP} = 20.1$ Hz, py²), 153.3 (d, $J_{CP} = 5.2$ Hz, py⁶), 139.2 (py⁴), 116.6 (py⁵), 111.4 (d, $J_{CP} = 6.3$ Hz, py³), 78.1 (d, $J_{CP} = 8.0$ Hz, CH), 76.7 (d, $J_{CP} = 10.3$ Hz, CH), 53.8 (s, COOCH₃), 53.7 (s, COOCH₃).

³¹P{¹H} NMR (δ, CD₂Cl₂, 20 °C): 192.57.

IR (ATR, cm⁻¹): 2030 (s, ν_{C=O}), 1900 (s, ν_{C=O}), 1857 (s, ν_{C=O}).

Mo(PN-ⁱPr)(η³-allyl)(CO)₂Br



A solution of Mo(PN-ⁱPr)(CO)₄ (0.23 g, 0.54 mmol) in 10 mL of anhydrous toluene was treated with excess allyl bromide (51 μl, 0.60 mmol) and heated to 90 °C for 15 h. After removal of the solvent the crude product was washed twice with *n*-pentane and dried *in vacuo*.

Yield: 0.22 g (82 %) orange solid; C₁₆H₂₄BrMoN₂O₂P; MW: 483.19; 39.77 % C, 5.01 % H, 5.80 % N.

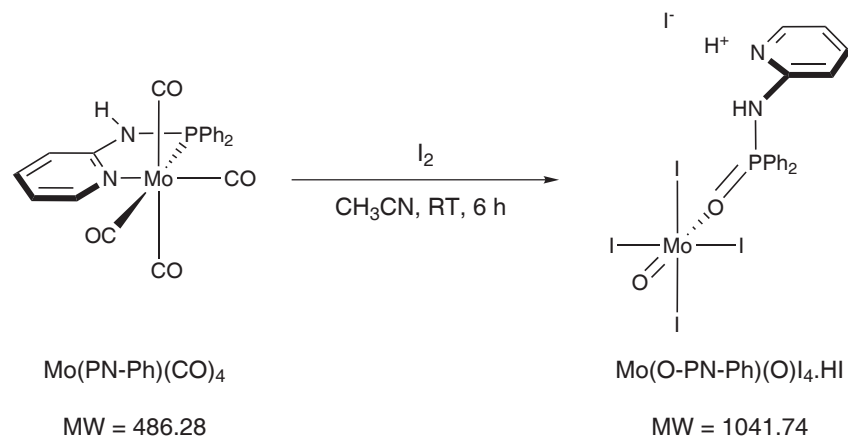
¹H NMR (δ, CD₂Cl₂, 20 °C): 7.96 (d, $J = 5.2$ Hz, 1H, py⁶), 7.49 (vt, $J = 7.5$ Hz, 1H, py⁴), 6.83–6.76 (m, 2H, py³ and py⁵), 5.70 (d, $J = 5.4$ Hz, 1H, NH), 4.37–4.24 (m, 1H, allyl-CH), 4.10 (bs, 1H, allyl-CH₂), 3.58 (bs, 1H, allyl-CH₂), 3.14–2.98 (m, 1H, CH(CH₃)₂), 2.88–2.72 (m, 1H, CH(CH₃)₂), 1.81 (d, $J = 9.5$ Hz, 1H, allyl-CH₂), 1.70–1.61 (m, 4H, allyl-CH₂ and CH₃), 1.49–1.33 (m, 9H, CH₃).

¹³C{¹H} NMR (δ, CD₂Cl₂, 20 °C): 226.3 (d, $J_{CP} = 13.2$ Hz, CO), 223.1 (d, $J_{CP} = 8.0$ Hz, CO), 160.7 (d, $J_{CP} = 10.9$ Hz, py²), 147.9 (py⁶), 138.7 (py⁴), 120.6 (allyl-CH), 115.7 (py⁵), 111.5 (d, $J_{CP} = 5.7$ Hz, py³), 77.2 (allyl-CH₂), 62.0 (allyl-CH₂), 29.3 (d, $J_{CP} = 20.1$ Hz, CH(CH₃)₂), 27.9 (d, $J_{CP} = 22.4$ Hz, CH(CH₃)₂), 19.3 (d, $J_{CP} = 8.0$ Hz, CH(CH₃)₂), 17.3 (d, $J_{CP} = 4.3$ Hz, CH(CH₃)₂).

$^{31}\text{P}\{^1\text{H}\}$ NMR (δ , CD_2Cl_2 , 20 °C): 96.54.

IR (ATR, cm^{-1}): 1929 (s, $\nu_{\text{C=O}}$), 1854 (s, $\nu_{\text{C=O}}$), 1838 (s, $\nu_{\text{C=O}}$).

Mo(O-PN-Ph)(O)I₄



Mo(PN-Ph)(CO)_4 (0.185 g, 0.380 mmol) was dissolved in 10 mL of CH_3CN and treated with I_2 (92 mg, 0.361 mmol) whereupon gas evolution was observed. Stirring was then continued for 6 h and afterwards the solvent was removed and the product dried *in vacuo*.

Yield: 0.150 g (38 %) dark brown solid; $\text{C}_{17}\text{H}_{16}\text{I}_5\text{MoN}_2\text{O}_2\text{P}$; MW: 1041.74; 19.60 % C, 1.55 % H, 2.69 % N.

^1H NMR (δ , CDCl_3 , 20 °C): 9.70 (s, 1H, NH), 7.90–6.78 (m, 14H, $\text{py}^{3,4,5,6}$ and Ph).

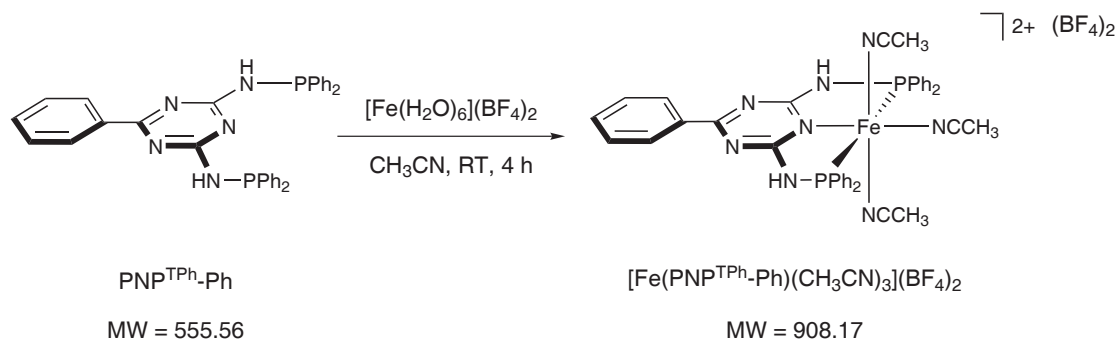
$^{13}\text{C}\{^1\text{H}\}$ NMR (δ , CDCl_3 , 20 °C): 159.2 (d, $J_{\text{CP}} = 10.9$ Hz, py^2), 154.5 (py^6), 142.0 (py^4), 132.2 (Ph), 131.8 (Ph), 129.0 (Ph), 128.8 (Ph), 117.8 and 117.6 (py^3 and py^5), Ph^1 not observed.

$^{31}\text{P}\{^1\text{H}\}$ NMR (δ , CDCl_3 , 20 °C): 99.32.

5.5 Iron complexes

5.5.1 Iron PNP^T complexes

[Fe(PNP^{TPh}-Ph)(CH₃CN)₃](BF₄)₂



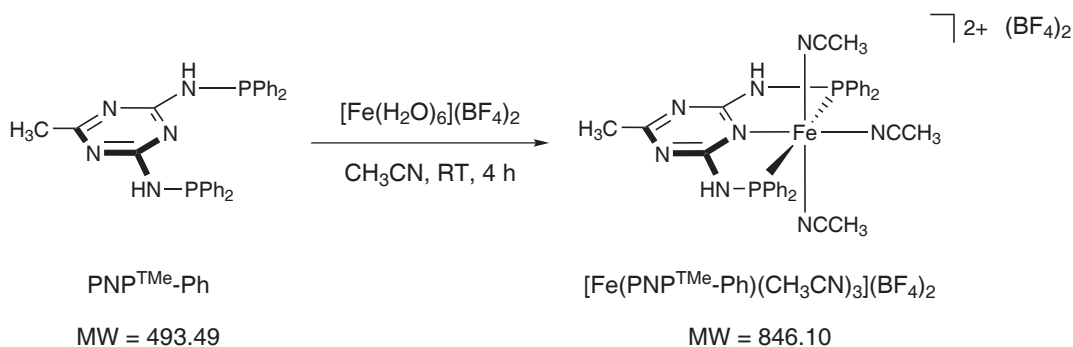
A solution of PNP^{TPh}-Ph (400 mg, 0.72 mmol) and [Fe(H₂O)₆](BF₄)₂ (0.242 g, 0.72 mmol) in 15 mL CH₃CN was stirred at room temperature for 4 h. The solvent was removed under vacuum and the remaining solid washed twice with Et₂O. The crude product was purified by flash chromatography (neutral Al₂O₃, eluent CH₃CN).

Yield: 582 mg (89 %) brown solid; C₃₉H₃₆B₂F₈FeN₈P₂; MW: 908.17; 51.58 % C, 4.00 % H, 12.34 % N.

¹H NMR (δ, CD₃CN, 20 °C): 8.11 (s, 2H, NH), 7.98–7.18 (m, 25H, Ph and PPh), 1.97 (s, 9H, CH₃CN).

¹³C{¹H} NMR (δ, CD₃CN, 20 °C): 174.8 (t, *J*_{CP} = 13.8 Hz, triaz^{2,6}), 170.7 (triaz⁴), 135.9 (Ph¹), 133.4 (t, *J*_{CP} = 23.2 Hz, PPh¹), 132.1 (PPh⁴), 131.2 (t, *J*_{CP} = 6.2 Hz, PPh^{2,6}), 130.8 (Ph⁴), 129.3 (t, *J*_{CP} = 5.1 Hz, PPh^{3,5}), 128.3 and 128.2 (Ph^{2,3,5,6}), 0.8 (CH₃CN), CH₃CN not observed.

³¹P{¹H} NMR (δ, CD₃CN, 20 °C): 98.48.



[Fe(PNP^{TMe}-Ph)(CH₃CN)₃](BF₄)₂

This complex was prepared analogously to the *p*-phenyl derivative [Fe(PNP^{TPh}-Ph)(CH₃CN)₃](BF₄)₂ with PNP^{TMe}-Ph (0.600 g, 1.22 mmol) and [Fe(H₂O)₆](BF₄)₂ (0.410 g, 1.22 mmol) as the starting materials.

Yield: 0.792 g (77 %) brown solid; C₃₄H₃₄B₂F₈FeN₈P₂; MW: 846.10; 48.27 % C, 4.05 % H, 13.24 % N.

¹H NMR (δ, CD₃CN, 20 °C): 8.88 (s, 2H, NH), 7.55 (bs, 20H, Ph), 3.33 (s, 3H, CH₃), 1.94 (s, 9H, CH₃CN).

¹³C{¹H} NMR (δ, CD₃CN, 20 °C): 178.6 (triaz^{2,6}), 174.4 (triaz⁴), 137.2 (Ph¹), 131.9 (Ph⁴), 131.2 (Ph^{2,6}), 129.4 (Ph^{3,5}), 33.9 (CH₃), 2.1 (CH₃CN), CH₃CN not observed.

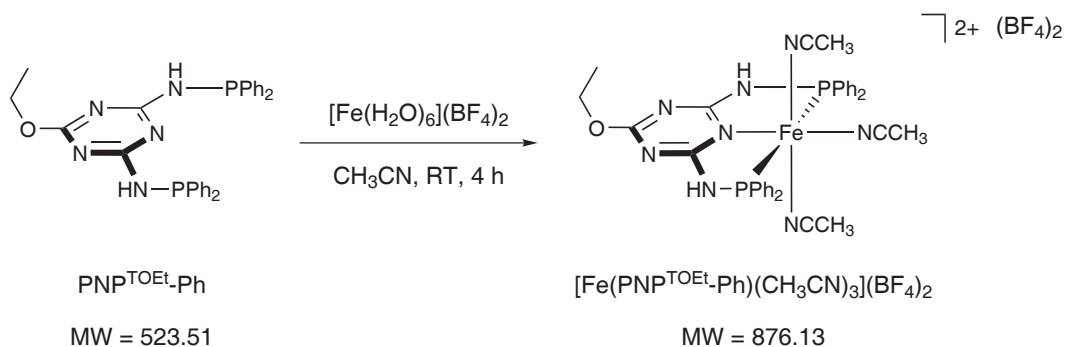
³¹P{¹H} NMR (δ, CD₃CN, 20 °C): 101.06.

[Fe(PNP^{TOEt}-Ph)(CH₃CN)₃](BF₄)₂

This complex was prepared analogously to the *p*-phenyl derivative [Fe(PNP^{TPh}-Ph)(CH₃CN)₃](BF₄)₂ with PNP^{TOEt}-Ph (0.600 g, 1.15 mmol) and [Fe(H₂O)₆](BF₄)₂ (0.385 g, 1.15 mmol) as the starting materials.

Yield: 0.822 g (82 %) brown solid; C₃₅H₃₆B₂F₈FeN₈OP₂; MW: 876.13; 47.98 % C, 4.14 % H, 12.79 % N.

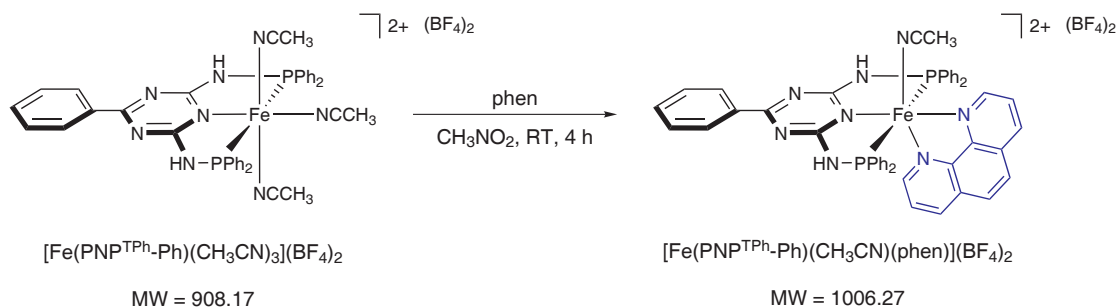
¹H NMR (δ, CD₃CN, 20 °C): 8.79 (s, 2H, NH), 7.77 (bs, 7H, Ph), 7.54 (bs, 13H, Ph), 3.31 (s, 2H, O-CH₂), 1.97 (s, 9H, CH₃CN), 1.01 (s, 3H, CH₃).



$^{13}\text{C}\{^1\text{H}\}$ NMR (δ , CD_3CN , 20 °C): 178.7 (triaz^{2,6}), 172.9 (triaz⁴), 137.3 (Ph¹), 132.0 (Ph⁴), 131.2 (t, J_{CP} = 6.6 Hz, Ph^{2,6}), 129.4 (t, J_{CP} = 5.1 Hz, Ph^{3,5}), 65.3 (O-CH₂), 14.6 (CH₃), 1.2 (CH₃CN), CH₃CN not observed.

$^{31}\text{P}\{^1\text{H}\}$ NMR (δ , CD_3CN , 20 °C): 101.05.

$[\text{Fe}(\text{PNP}^{\text{TPh}}\text{-Ph})(\text{CH}_3\text{CN})(\text{phen})](\text{BF}_4)_2$



$[\text{Fe}(\text{PNP}^{\text{TPh}}\text{-Ph})(\text{CH}_3\text{CN})_3](\text{BF}_4)_2$ (0.400 g, 0.440 mmol) was dissolved in 10 mL of anhydrous CH_3NO_2 and treated with 1,10-phenanthroline (79 mg, 0.440 mmol) whereupon the colour of the solution changed to red immediately. The mixture was stirred at room temperature for 4 h, then the solvent was removed. The product was washed with Et_2O and dried *in vacuo*.

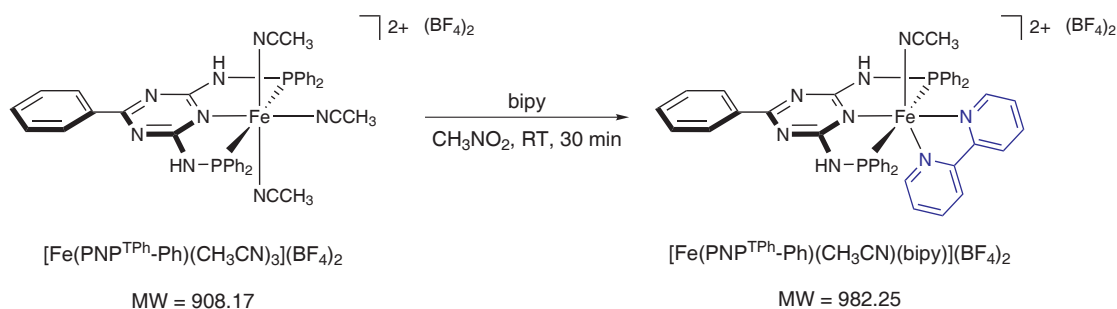
Yield: 0.343 g (77 %) red solid; $\text{C}_{47}\text{H}_{38}\text{B}_2\text{F}_8\text{FeN}_8\text{P}_2$; MW: 1006.27; 56.10 % C, 3.81 % H, 11.14 % N.

^1H NMR (δ , CD_3NO_2 , 20 °C): 8.51–8.28 (m, 4H, phen, NH), 8.13–7.84 (m, 9H, Ph and phen), 7.64–7.02 (m, 18H, Ph and phen), 6.52–6.45 (m, 4H, Ph), 1.73 (s, 3H, CH_3).

$^{13}\text{C}\{^1\text{H}\}$ NMR (δ , CD_3NO_2 , 20 °C): 172.5 (t, $J_{\text{CP}} = 13.8$ Hz, triaz^{2,6}), 169.7 (triaz⁴), 153.4, 152.2, 149.3, 147.5, 145.9, 145.0 (phen), 136.0 (PPh^1), 134.8 (phen), 128.6 (t, $J_{\text{CP}} = 6.3$ Hz, $\text{PPh}^{2,6}$), 127.5 (PPh^4), 126.7 (t, $J_{\text{CP}} = 4.8$ Hz, $\text{PPh}^{2,5}$), 126.3, 125.4, 123.2 (phen), 0.57 (CH_3CN), CH_3CN not observed.

$^{31}\text{P}\{^1\text{H}\}$ NMR (δ , CD_3NO_2 , 20 °C): 95.23.

$[\text{Fe}(\text{PNP}^{\text{TPh}}\text{-Ph})(\text{CH}_3\text{CN})(\text{bipy})](\text{BF}_4)_2$



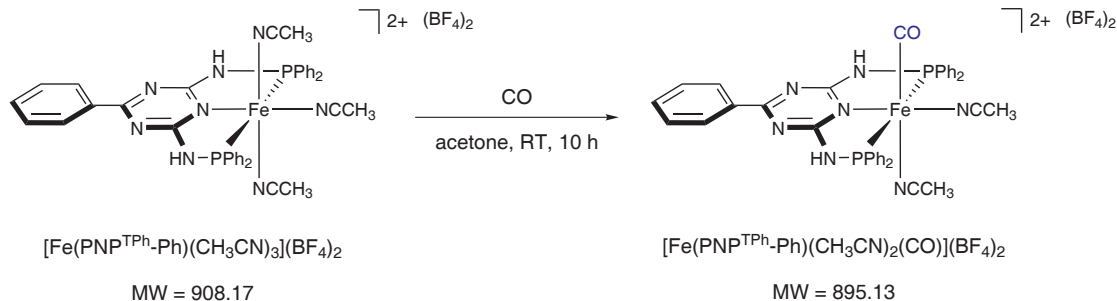
$[\text{Fe}(\text{PNP}^{\text{TPh}}\text{-Ph})(\text{CH}_3\text{CN})_3](\text{BF}_4)_2$ (0.400 g, 0.440 mmol) was dissolved in 10 mL of anhydrous CH_3NO_2 and treated with 2,2'-bipyridine (69 mg, 0.440 mmol) whereupon the colour of the solution changed to red immediately. The mixture was stirred at room temperature for 30 min., then the solvent was removed. The product was washed with Et_2O and dried *in vacuo*.

Yield: 0.420 g (97 %) red solid; $\text{C}_{45}\text{H}_{38}\text{B}_2\text{F}_8\text{FeN}_8\text{P}_2$; MW: 982.25; 55.03 % C, 3.90 % H, 11.41 % N.

^1H NMR (δ , CD_3NO_2 , 20 °C): 7.52 (bs, 35H, Ph, PPh, bipy, NH), 1.72 (s, 3H, CH_3).

$^{13}\text{C}\{^1\text{H}\}$ NMR (δ , CD_3NO_2 , 20 °C): 171.9 (triaz), 168.3 (triaz), 156.9, 151.6 (bipy), 136.1 (PPh^1), 134.5 (bipy), 128.4 ($\text{PPh}^{2,6}$), 127.1 (PPh^4), 126.5 ($\text{PPh}^{2,5}$), 124.8, 121.3 (bipy), 0.6 (CH_3CN), CH_3CN not observed.

$^{31}\text{P}\{^1\text{H}\}$ NMR (δ , CD_3NO_2 , 20 °C): 95.96.

[Fe(PNP^{TPh}-Ph)(CH₃CN)₂(CO)](BF₄)₂

Carbon monoxide was bubbled through a solution of $[\text{Fe}(\text{PNP}^{\text{TPh}}\text{-Ph})(\text{CH}_3\text{CN})_3](\text{BF}_4)_2$ (0.300 g, 0.330 mmol) in acetone for 15 min. The mixture was stirred under CO atmosphere at room temperature for 15 h. Then the solvent was removed and the crude product was washed with Et₂O and dried *in vacuo*.

Yield: 0.241 g (82 %) brown solid; C₃₈H₃₃B₂F₈FeN₇OP₂; MW: 895.13; 50.99 % C, 3.72 % H, 10.95 % N.

¹H NMR (δ, CD₃NO₂, 20 °C): 8.68–8.47 (m, 2H, NH), 7.46–7.34 (bs, 25H, Ph and PPh), 2.07 (s, 3H, CH₃).

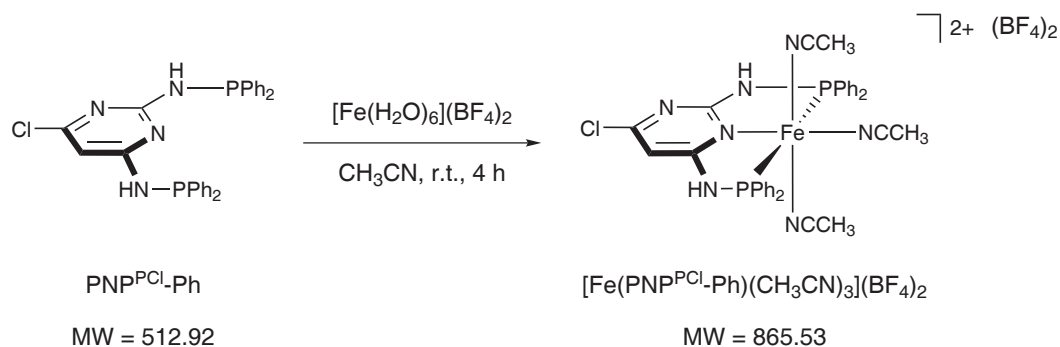
¹³C{¹H} NMR (δ, CD₃NO₂, 20 °C): 213.7 (CO), 176.5 (triaz), 170.7 (triaz), 140.2 (PPh¹), 131.6–125.4 (Ph and PPh), 4.3 (CH₃CN), CH₃CN not observed.

³¹P{¹H} NMR (δ, CD₃NO₂, 20 °C): 98.6.

5.5.2 Iron PNP^P complexes**[Fe(PNP^{PCl}-Ph)(CH₃CN)₃](BF₄)₂**

This complex was prepared analogously to the triazine-based derivative $[\text{Fe}(\text{PNP}^{\text{TPh}}\text{-Ph})(\text{CH}_3\text{CN})_3](\text{BF}_4)_2$ with PNP^{PCl}-Ph (0.300 g, 0.585 mmol) and $[\text{Fe}(\text{H}_2\text{O})_6](\text{BF}_4)_2$ (0.197 g, 0.585 mmol) as the starting materials.

Yield: 0.385 g (76 %) brown solid; C₃₄H₃₂B₂ClF₈FeN₇P₂; MW: 865.53; 47.18 % C, 3.73 % H, 11.33 % N.

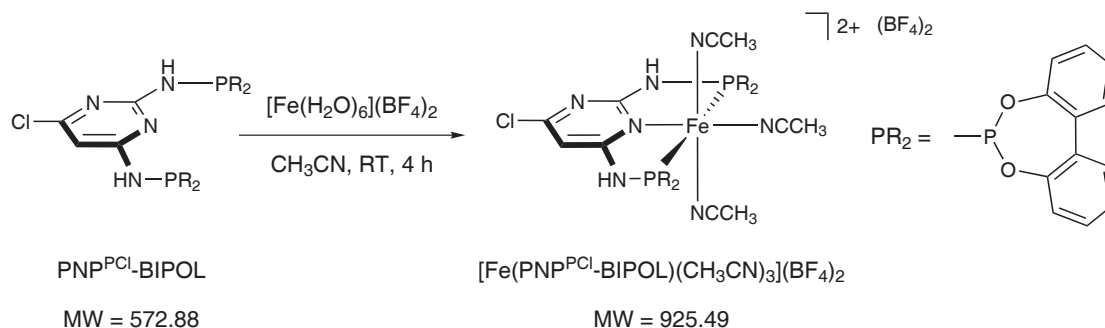


$^1\text{H NMR}$ (δ , CD_3CN , 20 °C): 8.96 (bs, 1H, NH), 8.46 (bs, 1H, NH), 8.01–7.29 (m, 20H, Ph), 6.88 (bs, 1H, pyrimidine⁵), 1.98 (s, 9H, CH_3CN).

$^{13}\text{C}\{^1\text{H}\}$ NMR (δ , CD_3CN , 20 °C): 168.2 (d, $J_{\text{CP}} = 13.8$ Hz, pyrimidine), 164.7 and 159.7 (pyrimidine), 135.2 (Ph^1), 129.6 (d, $J_{\text{CP}} = 3.4$ Hz, Ph^4), 128.7 (d, $J_{\text{CP}} = 13.2$ Hz, $\text{Ph}^{2,6}$), 127.0 (d, $J_{\text{CP}} = 9.8$ Hz, $\text{Ph}^{3,5}$), 95.8 (pyrimidine⁵), 0.2 (2s, CH_3CN), CH_3CN not observed.

$^{31}\text{P}\{^1\text{H}\}$ NMR (δ , CD_3CN , 20 °C): 99.29.

$[\text{Fe}(\text{PNP}^{\text{PCL}}\text{-BIPOL})(\text{CH}_3\text{CN})_3](\text{BF}_4)_2$



This complex was prepared analogously to the triazine-based derivative $[\text{Fe}(\text{PNP}^{\text{TPh}}\text{-Ph})(\text{CH}_3\text{CN})_3](\text{BF}_4)_2$ with $\text{PNP}^{\text{PCL}}\text{-BIPOL}$ (0.300 g, 0.524 mmol) and $[\text{Fe}(\text{H}_2\text{O})_6](\text{BF}_4)_2$ (0.177 g, 0.524 mmol) as the starting materials.

Yield: 0.346 g (71 %) brown solid; $\text{C}_{34}\text{H}_{28}\text{B}_2\text{ClF}_8\text{FeN}_7\text{O}_4\text{P}_2$; MW: 925.49; 44.12 % C, 3.05 % H, 10.59 % N.

^1H NMR (δ , CD_3NO_2 , 20 °C): 7.87 (bs, 4H, Ph), 7.66–7.59 (m, 12H, Ph), 7.30 (d, J = 7.0 Hz, 1H, NH), 7.07–6.99 (m, 1h, NH), 6.85 (s, 1H, pyrimidine⁵), 2.00 1.97 (s, 9H, CH_3CN).

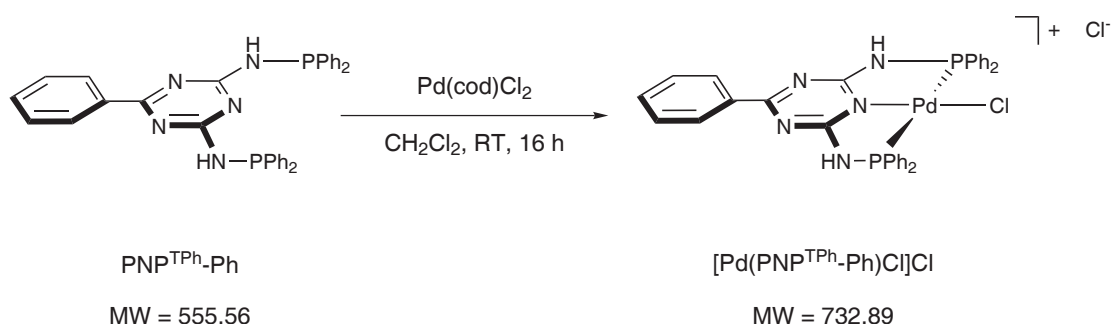
$^{13}\text{C}\{^1\text{H}\}$ NMR (δ , CD_3NO_2 , 20 °C): 176.9, 169.7, and 165.4 (pyrimidine), 146.1 (Ph), 136.3, 134.3, 129.1, 128.2, 127.1, 125.3, 119.3 (Ph), 97.4 (pyrimidine⁵), 1.1 and 0.2 (2s, CH_3CN), CH_3CN not observed.

$^{31}\text{P}\{^1\text{H}\}$ NMR (δ , CD_3NO_2 , 20 °C): 181.05, 176.73.

5.6 Palladium complexes

5.6.1 Palladium PNP^{T} complexes

$[\text{Pd}(\text{PNP}^{\text{TPh-Ph}})\text{Cl}]\text{Cl}$



A solution of $\text{PNP}^{\text{TPh-Ph}}$ (300 mg, 0.54 mmol) in 10 mL of CH_2Cl_2 was treated with Pd(cod)Cl_2 (154 mg, 0.54 mmol) and stirred at room temperature for 16 h. The solvent was removed under vacuum and the product washed twice with Et_2O .

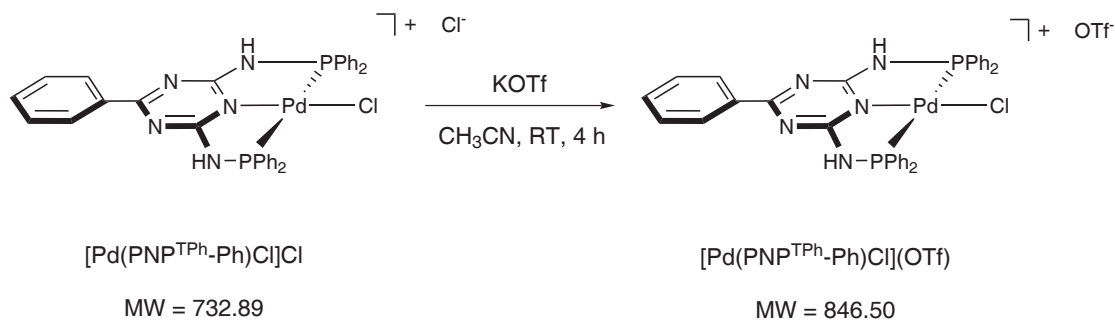
Yield: 345 mg (87 %) yellow solid; $\text{C}_{33}\text{H}_{27}\text{Cl}_2\text{N}_5\text{P}_2\text{Pd}$; MW: 732.89; 54.08 % C, 3.71 % H, 9.56 % N.

^1H NMR (δ , CD_3NO_2 , 20 °C): 8.43–7.08 (m, 27H, NH and Ph).

$^{13}\text{C}\{^1\text{H}\}$ NMR Due to the bad solubility of this compound no $^{13}\text{C}\{^1\text{H}\}$ NMR has been taken.

$^{31}\text{P}\{^1\text{H}\}$ NMR (δ , CD_3NO_2 , 20 °C): 62.69.

[Pd(PNP^{TPh}-Ph)Cl](OTf)



A suspension of $[\text{Pd}(\text{PNP}^{\text{TPh}}\text{-Ph})\text{Cl}]\text{Cl}$ (200 mg, 0.27 mmol) in 10 mL of CH_3CN was treated with KOTf (52 mg, 0.27 mmol) and stirred at room temperature for 4 h. The solvent was removed under vacuum and the product washed twice with Et_2O .

Yield: 212 mg (92 %) yellow solid; $\text{C}_{34}\text{H}_{27}\text{ClF}_3\text{N}_5\text{O}_3\text{P}_2\text{PdS}$; MW: 846.50; 48.24 % C, 3.21 % H, 8.27 % N.

^1H NMR (δ , CDCl_3 , 20 °C): 8.27 (d, J = 7.1 Hz, 2H, NH), 8.14–7.20 (m, 25H, Ph and PPh).

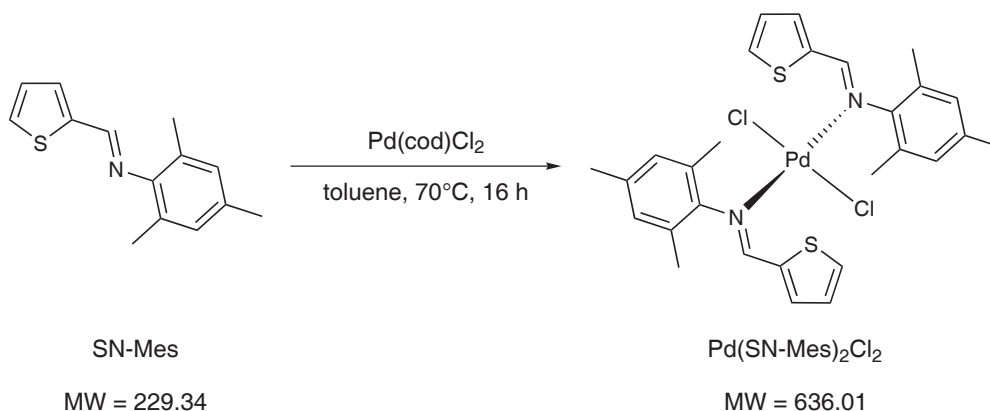
$^{13}\text{C}\{^1\text{H}\}$ NMR (δ , CDCl_3 , 20 °C): 173.1 (triaz⁴), 168.5 (t, J_{CP} = 11.9 Hz, triaz^{2,6}), 135.6 (Ph¹), 133.1 (PPh⁴), 132.5 (t, J_{CP} = 8.3 Hz, PPh^{2,6}), 131.0 (Ph⁴), 129.5 (t, J_{CP} = 6.2 Hz, PPh^{3,5}), 129.9 and 128.2 (Ph^{2,3,5,6}), PPh¹ and OSO_2CF_3 not observed.

$^{31}\text{P}\{^1\text{H}\}$ NMR (δ , C_6D_6 , 20 °C): 60.72.

5.6.2 Palladium SN imine complexes

Pd(SN-Mes)₂Cl₂

A solution of 2,4,6-trimethyl-N-(2-thienylmethylene)-aniline (0.40 g, 1.74 mmol) in 10 mL of anhydrous toluene was treated with $\text{Pd}(\text{cod})\text{Cl}_2$ (0.25 g, 0.87 mmol) and stirred at



70 °C for 16 h. The solvent was removed and the crude product washed three times with Et₂O and dried *in vacuo*.

Yield: 0.48 g (87 %) yellow solid; C₂₈H₃₀Cl₂N₂PdS₂; MW: 636.01; 52.88 % C, 4.75 % H, 4.40 % N.

¹H NMR (δ, CDCl₃, 20 °C): 9.09 (d, *J* = 1.3 Hz, 1H, N=CH), 7.53 (dd, *J*₁ = 3.8 Hz, *J*₂ = 1.1 Hz, 1H, thiophene), 7.44 (dt, *J*₁ = 5.1 Hz, *J*₂ = 1.2 Hz, 1H, thiophene), 7.00 (dd, *J*₁ = 5.0 Hz, *J*₂ = 3.9 Hz, 1H, thiophene⁴), 6.94 (s, 2H, Ph^{3,5}), 2.32 (s, 6H, Ph^{2,6}-CH₃), 2.31 (s, 3H, Ph⁴-CH₃).

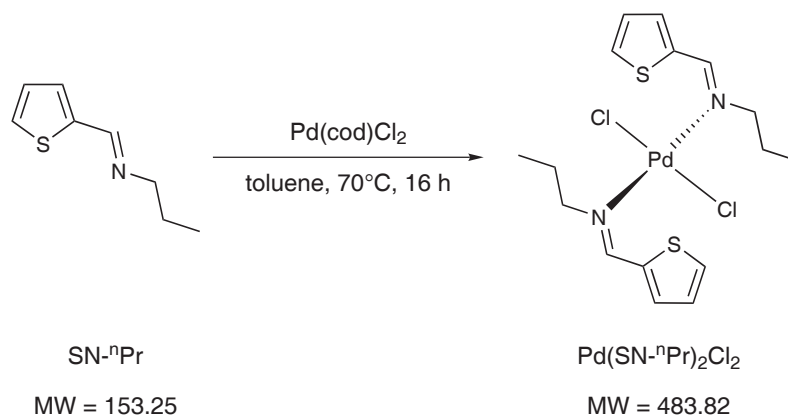
¹³C{¹H} NMR (δ, CDCl₃, 20 °C): 165.5 (N=CH), 142.4 and 137.7 (thiophene² and Ph¹), 139.6, 136.4, and 126.8 (thiophene^{3,4,5}), 134.5 (Ph⁴), 131.3 (Ph^{2,6}), 130.3 (Ph^{3,5}), 21.2 (Ph⁴-CH₃), 19.4 (Ph^{2,6}-CH₃).

Pd(SN-ⁿPr)₂Cl₂

This complex has been prepared analogously to Pd(SN-Mes)₂Cl₂ with SN-ⁿPr (0.30 g, 1.96 mmol) and Pd(cod)Cl₂ (0.28 g, 0.98 mmol) as the starting materials.

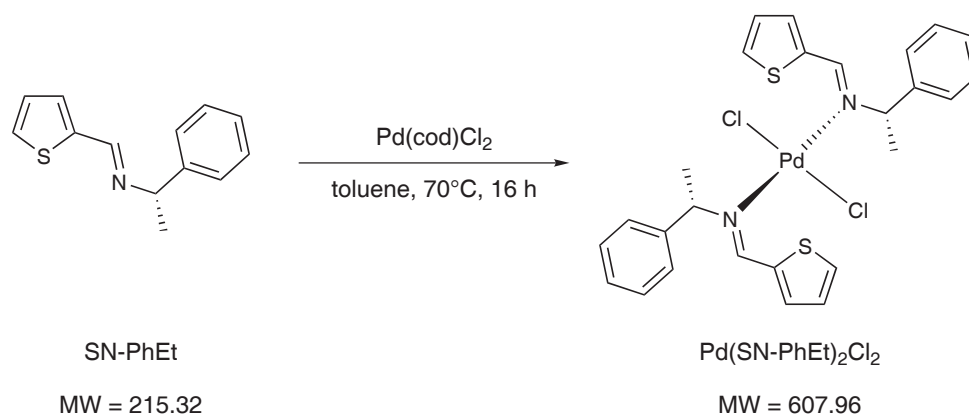
Yield: 0.40 g (85 %) yellow solid; C₁₆H₂₂Cl₂N₂PdS₂; MW = 483.82; 39.72 % C, 4.58 % H, 5.79 % N.

¹H NMR (δ, CDCl₃, 20 °C): 8.03 (s, 1H, N=CH), 7.84 (d, *J* = 5.1 Hz, 1H, thiophene), 7.65 (dd, *J*₁ = 3.8 Hz, *J*₂ = 1.0 Hz, 1H, thiophene), 7.22 (dd, *J*₁ = 4.9 Hz, *J*₂ = 3.8 Hz, 1H, thiophene⁴), 4.00 (t, *J* = 7.5 Hz, 2H, N-CH₂), 2.36-2.21 (m, 2H, CH₂-CH₃), 1.06 (t, *J* = 7.3 Hz, 3H, CH₃).



$^{13}\text{C}\{^1\text{H}\}$ NMR (δ , CDCl_3 , 20 $^\circ\text{C}$): 161.2 (N=CH), 138.5, 134.2, and 127.3 (thiophene^{3,4,5}), 136.3 (thiophene²), 67.0 (N-CH₂), 22.9 (CH₂-CH₃), 11.6 (CH₃).

Pd(SN-PhEt)₂Cl₂



This complex has been prepared analogously to Pd(SN-Mes)₂Cl₂ with SN-PhEt (0.41 g, 1.90 mmol) and Pd(cod)Cl₂ (0.27 g, 0.95 mmol) as the starting materials.

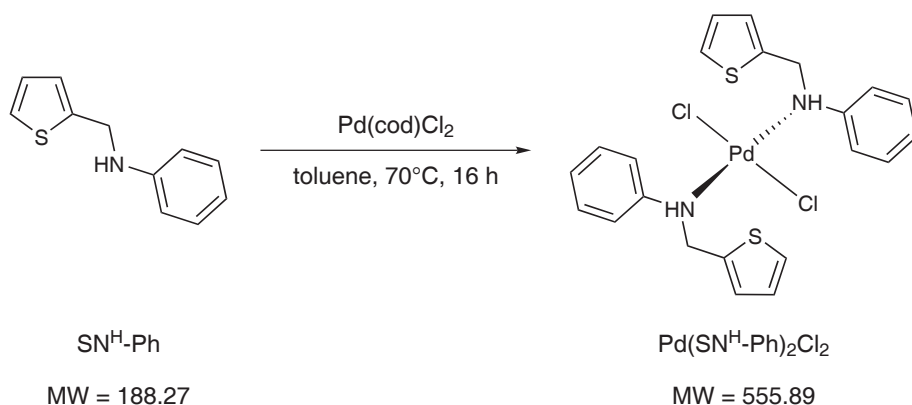
Yield: 0.49 g (85 %); C₂₆H₂₆Cl₂N₂PdS₂; MW: 607.96; 51.37 % C, 4.31 % H, 4.61 % N.

^1H NMR (δ , CDCl_3 , 20 $^\circ\text{C}$): 7.80 (d, J = 4.9 Hz, 1H, thiophene), 7.75 (s, 1H, N=CH), 7.70-7.65 (m, 2H, thiophene and Ph), 7.45-7.31 (m, 4H, Ph), 7.15 (dd, J_1 = 4.9 Hz, J_2 = 3.8 Hz, 1H, thiophene⁴), 6.22 (q, J = 6.9 Hz, 1H, C(H)CH₃), 2.12 (d, J = 7.0 Hz, 1H, C(H)CH₃).

$^{13}\text{C}\{^1\text{H}\}$ NMR (δ , CDCl_3 , 20 °C): 162.1 (N=CH), 139.4 and 136.8 (thiophene² and Ph¹), 138.6, 134.4, and 127.2 (thiophene^{3,4,5}), 128.9, 128.8, and 128.4 (Ph^{2,3,4,5,6}), 69.3 (C(H)CH₃), 19.9 (C(H)CH₃).

5.6.3 Palladium SN amine complexes

$\text{Pd}(\text{SN}^{\text{H}}\text{-Ph})_2\text{Cl}_2$

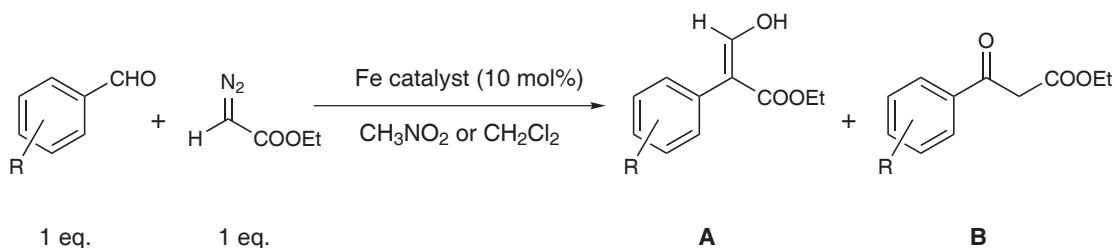


This complex has been prepared analogously to $\text{Pd}(\text{SN-Mes})_2\text{Cl}_2$ with $\text{SN}^{\text{H}}\text{-Ph}$ (0.30 g, 1.59 mmol) and $\text{Pd}(\text{cod})\text{Cl}_2$ (0.23 g, 0.80 mmol) as the starting materials.

Yield: 0.13 g (81 %); $\text{C}_{22}\text{H}_{22}\text{Cl}_2\text{N}_2\text{PdS}_2$; MW: 555.89; 47.53 % C, 3.99 % H, 5.04 % N.

^1H NMR (δ , CDCl_3 , 20 °C): 7.43–7.25 (m, 5H, thiophene and Ph), 7.21–7.15, 7.04–6.99, and 6.88–6.81 (m, 3H, thiophene and Ph), 5.27 (d, J = 6.3 Hz, 1H, NH), 4.94–4.78 and 4.26–4.18 (m, 2H, N-CH₂).

$^{13}\text{C}\{^1\text{H}\}$ NMR (δ , CDCl_3 , 20 °C): 143.8 (Ph¹), 135.9 (thiophene²), 129.5 (Ph^{3,5}), 129.1, 126.8, 126.7, and 126.6 (thiophene^{3,4,5} and Ph⁴), 122.0 and 121.9 (Ph² and Ph⁶), 51.7 (N-CH₂).



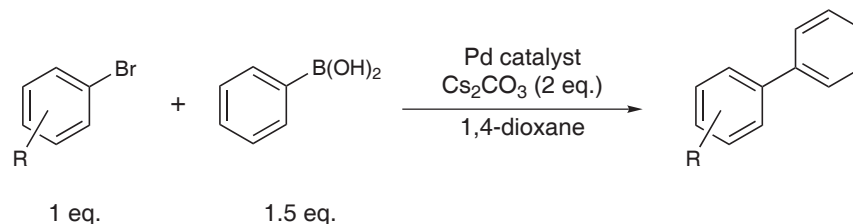
5.7 Catalytic reactions

5.7.1 Iron(II) catalysed coupling of aromatic aldehydes with EDA

General procedure

The catalyst (10 mol%) was dissolved in either CH_3NO_2 or CH_2Cl_2 at room temperature. Aldehyde (1 eq.) and EDA (1 eq.) were added and the reaction mixture was stirred for 16 h. The solvent was removed and the crude product was purified by flash chromatography (SiO_2 , eluent PE:EE 5:1).

5.7.2 Palladium(II) catalysed Suzuki-Miyaura coupling



General procedure

The substrate (1.00 mmol), phenyl boronic acid (1.50 mmol), and Cs_2CO_3 (2.00 mmol) were suspended in 5 mL of anhydrous 1,4-dioxane, charged with the respective amount of catalyst, and stirred at 110 °C for 18 h. After that, the mixture was cooled to room temperature and diluted with 10 mL of a 2N aqueous NaOH solution. The aqueous phase

was extracted three times with CH_2Cl_2 , dried over Na_2CO_3 , and evaporated to dryness. The crude product was purified via column chromatography (SiO_2 , PE:EE 20:1).

Appendix A: List of abbreviations

Ac	acetyl
AN	acetonitrile
BArF [−]	tetrakis[(3,5-trifluoromethyl)phenyl]borate
bipy	2,2'-bipyridine
<i>tert.</i> -BuOH	<i>tert.</i> -butanol
cod	1,5-cyclooctadiene
Cp	cyclopentadienyl
Cy	cyclohexyl
DEPT	Distortionless Enhancement by Polarisation Transfer
DME	1,2-dimethoxyethane
DMF	<i>N,N</i> -dimethyl formamide
DMSO	dimethyl sulfoxide
EDA	ethyl diazoacetate (N ₂ C(H)COOEt)
EE	ethyl acetate
Et ₂ O	diethyl ether
EtOH	ethanol
iPr	<i>iso</i> -propyl
Hz	Hertz
MeOH	methanol
MS	molecular sieve 4 Å
nbd	norbornadiene
NBS	<i>N</i> -bromosuccinimide
n. d.	not determined
NEt ₃	triethylamine
NMP	<i>N</i> -methylpyrrolidone
OTf	trifluoro methane sulfonate ([−] OSO ₂ CF ₃)
PE	petroleum ether
Ph	phenyl
phen	1,10-phenanthroline
pip	piperidine
py	pyridine
RT	room temperature
terpy	2,2':6',2''-terpyridine
THF	tetrahydrofuran
TMEDA	<i>N,N,N',N'</i> -tetramethylethylenediamine
TMS	tetramethylsilane
triaz	1,3,5-triazine

Table A.1: List of abbreviations

Appendix B: Crystallographic data

Property	Mo(PN-Ph)(CO) ₄ · CH ₂ Cl ₂	Mo(PN- ⁱ Pr)(CO) ₄	Mo(PN- ^t Bu)(CO) ₄
Formula	C ₂₂ H ₁₇ Cl ₂ MoN ₂ O ₄ P	C ₁₅ H ₁₉ MoN ₂ O ₄ P	C ₁₇ H ₂₃ MoN ₂ O ₄ P
FW	571.19	418.24	446.29
Crystal size (mm)	0.65 × 0.45 × 0.40	0.54 × 0.40 × 0.38	0.58 × 0.55 × 0.53
Crystal system	triclinic	monoclinic	orthorhombic
Space group	<i>P</i> 1 (no. 2)	<i>C</i> 2/ <i>c</i> (no. 15)	<i>P</i> 2 ₁ 2 ₁ 2 ₁ (no. 19)
<i>a</i> (Å)	8.8999(2)	20.9340(3)	9.0235(2)
<i>b</i> (Å)	11.4108(2)	10.3981(2)	13.3324(2)
<i>c</i> (Å)	13.3360(2)	16.8091(3)	16.0575(3)
α (°)	108.0050(10)	90	90
β (°)	94.3900(10)	99.1730(10)	90
γ (°)	109.6680(10)	90	90
<i>V</i> (Å ³)	1187.96(4)	3612.11(11)	1931.80(6)
<i>Z</i>	2	8	4
ρ_{calc} (g cm ⁻³)	1.597	1.538	1.534
<i>T</i> (K)	100(2)	100(2)	100(2)
μ (mm ⁻¹) (Mo K α)	0.875	0.834	0.785
<i>F</i> (000)	572	1696	912
θ for data coll. (°)	2.48–30.00	2.19–30.00	2.54–30.00
Compl. to $\theta = 30^\circ$	99.2 %	99.6 %	99.7 %
No. of rflns measured	24509	23511	24308
No. of unique rflns	6884	5266	5613
No. of params	266	215	235
R_1 ($I > 2\sigma(I)$) ^a	0.0227	0.0185	0.0144
ωR_2 ($I > 2\sigma(I)$) ^b	0.0608	0.0485	0.0386
R_1 (all data) ^a	0.0237	0.0193	0.0146
ωR_2 (all data) ^b	0.0615	0.0489	0.0388
Largest diff. peak and hole (eÅ ⁻³)	−0.401/0.656	−0.321/0.558	−0.41/0.26

$$^a R_1 = \frac{\sum ||F_0| - |F_c||}{\sum |F_0|} \quad ^b \omega R_2 = \left[\frac{\sum (\omega(F_0^2 - F_c^2)^2)}{\sum (\omega(F_0^2)^2)} \right]^{\frac{1}{2}}$$

Table B.1: Details for the structure determination of the complexes Mo(PN-Ph)(CO)₄, Mo(PN-ⁱPr)(CO)₄, and Mo(PN-^tBu)(CO)₄

Property	Mo(PN-ETOL)(CO) ₄	Mo(PN- ⁱ Pr)(η^3 -allyl)(CO) ₂ Br	Mo(O-PN-Ph)(O)I ₄
Formula	C ₁₁ H ₉ MoN ₂ O ₆ P	C ₁₆ H ₂₄ BrMoN ₂ O ₂ P	C ₂₂ H ₂₂ I ₅ MoN ₄ O ₂ P
FW	392.11	483.19	1135.85
Crystal size (mm)	0.59 × 0.12 × 0.11	0.56 × 0.24 × 0.22	0.30 × 0.26 × 0.12
Crystal system	monoclinic	monoclinic	monoclinic
Space group	<i>P</i> 2 ₁ / <i>c</i> (no. 14)	<i>C</i> 2/ <i>c</i> (no. 15)	<i>P</i> 2 ₁ / <i>c</i> (no. 14)
<i>a</i> (Å)	8.7014(6)	33.2832(16)	9.4393(4)
<i>b</i> (Å)	12.4996(8)	8.5131(4)	17.6516(8)
<i>c</i> (Å)	13.2883(9)	13.7154(7)	18.7111(8)
α (°)	90	90	90
β (°)	92.3850(10)	101.252(2)	94.2330(10)
γ (°)	90	90	90
<i>V</i> (Å ³)	1444.04(17)	3811.5(3)	3109.1(2)
<i>Z</i>	4	8	4
ρ_{calc} (g cm ⁻³)	1.804	1.684	2.427
<i>T</i> (K)	100(2)	100(2)	100(2)
μ (mm ⁻¹) (Mo K α)	1.046	2.878	5.464
<i>F</i> (000)	776	1936	2080
θ for data coll. (°)	3.07–30.00	2.50–30.01	2.18–30.02
Compl. to $\theta = 30^\circ$	99.4 %	99.5 %	99.5 %
No. of rflns measured	19512	26966	40731
No. of unique rflns	4187	5533	9043
No. of params	190	217	316
<i>R</i> ₁ (<i>I</i> > 2 σ (<i>I</i>)) ^a	0.0267	0.0232	0.0233
ωR_2 (<i>I</i> > 2 σ (<i>I</i>)) ^b	0.0641	0.0576	0.0550
<i>R</i> ₁ (all data) ^a	0.0314	0.0272	0.0271
<i>R</i> ₁ (all data) ^a	0.0674	0.0590	0.0565
Largest diff. peak and hole (eÅ ⁻³)	−0.969/1.136	−0.578/0.690	−1.342/1.776

$$^a R_1 = \frac{\sum ||F_0| - |F_c||}{\sum |F_0|} \quad ^b \omega R_2 = \left[\frac{\sum (\omega(F_0^2 - F_c^2)^2)}{\sum (\omega(F_0^2)^2)} \right]^{\frac{1}{2}}$$

Table B.2: Details for the structure determination of the complexes Mo(PN-ETOL)(CO)₄, Mo(PN-ⁱPr)(η^3 -allyl)(CO)₂Br, and Mo(O-PN-Ph)(O)I₄

Property	[Fe(PNP ^{TPh} -Ph)(AN) ₃] (BF ₄) ₂ · 3 C ₂ H ₄ Cl ₂ · H ₂ O	[Fe(PNP ^{TMe} -Ph)(AN) ₃] (BF ₄) ₂	[Fe(PNP ^{TOEt} -Ph)(AN) ₃] (BF ₄) ₂
Formula	C ₄₅ H ₅₀ B ₂ Cl ₆ F ₈ FeN ₈ OP ₂	C ₃₄ H ₃₄ B ₂ F ₈ FeN ₈ P ₂	C ₃₉ H ₄₂ B ₂ F ₈ FeN ₁₀ OP ₂
FW	1223.04	846.10	958.24
Crystal size (mm)	0.54 × 0.27 × 0.16	0.60 × 0.50 × 0.40	0.58 × 0.36 × 0.30
Crystal system	triclinic	monoclinic	triclinic
Space group	<i>P</i> 1 (no. 2)	<i>P</i> 2 ₁ /c (no. 14)	<i>P</i> 1 (no. 2)
<i>a</i> (Å)	11.6591(6)	8.9596(8)	8.8548(4)
<i>b</i> (Å)	11.6700(2)	20.6865(19)	13.8402(7)
<i>c</i> (Å)	22.4063(11)	20.8578(19)	20.1352(10)
α (°)	94.318(1)	90	71.399(1)
β (°)	90.115(1)	96.5790(10)	82.731(1)
γ (°)	115.918(1)	90	72.789(1)
<i>V</i> (Å ³)	2732.2(2)	3840.4(6)	2232.6(2)
<i>Z</i>	2	4	2
ρ_{calc} (g cm ⁻³)	1.487	1.463	1.425
<i>T</i> (K)	100(2)	100(2)	100(2)
μ (mm ⁻¹) (Mo K α)	0.698	0.552	0.487
<i>F</i> (000)	1248	1728	984
θ for data coll. (°)	2.08–30.00	2.49–30.05	2.51–30.01
Compl. to $\theta = 30^\circ$	99.3 %	99.3 %	99.2 %
No. of rflns measured	50406	38125	26262
No. of unique rflns	15866	11189	12688
No. of params	737	527	573
<i>R</i> ₁ (<i>I</i> > 2 σ (<i>I</i>)) ^a	0.0373	0.0648	0.0381
ωR_2 (<i>I</i> > 2 σ (<i>I</i>)) ^b	0.0987	0.1438	0.0979
<i>R</i> ₁ (all data) ^a	0.0441	0.0784	0.0443
ωR_2 (all data) ^b	0.1044	0.1509	0.1024
Largest diff. peak and hole (eÅ ⁻³)	−0.826/0.716	−0.868/0.996	−0.437/0.735

^a $R_1 = \frac{\sum ||F_0| - |F_c||}{\sum |F_0|}$ ^b $\omega R_2 = \left[\frac{\sum (\omega(F_0^2 - F_c^2)^2)}{\sum (\omega(F_0^2)^2)} \right]^{\frac{1}{2}}$

 Table B.3: Details for the structure determination of the complexes [Fe(PNP^{TPh}-Ph)(AN)₃](BF₄)₂, [Fe(PNP^{TMe}-Ph)(AN)₃](BF₄)₂, and [Fe(PNP^{TOEt}-Ph)(AN)₃](BF₄)₂

Property	[Pd(PNP-Ph)Cl]Cl · C ₂ H ₄ Cl ₂ · H ₂ O	Pd(SN-Mes) ₂ Cl ₂ · C ₂ H ₄ Cl ₂	Pd(SN- ⁿ Pr) ₂ Cl ₂ · C ₂ H ₄ Cl ₂	Pd(SN ^H -Ph) ₂ Cl ₂
Formula	C ₃₁ H ₃₁ Cl ₄ N ₃ OP ₂ Pd	C ₃₀ H ₃₄ Cl ₄ N ₂ PdS ₂	C ₁₈ H ₂₆ Cl ₄ N ₂ PdS ₂	C ₂₂ H ₂₂ Cl ₂ N ₂ PdS ₂
FW	771.73	734.91	582.73	555.84
Crystal size (mm)	0.40 × 0.30 × 0.27	0.63 × 0.38 × 0.17	0.29 × 0.24 × 0.20	0.25 × 0.22 × 0.18
Crystal system	triclinic	monoclinic	monoclinic	monoclinic
Space group	<i>P</i> 1 (no. 2)	<i>C</i> 2/ <i>c</i> (no. 15)	<i>P</i> 2 ₁ / <i>c</i> (no. 14)	<i>P</i> 2 ₁ / <i>c</i> (no. 14)
<i>a</i> (Å)	10.7915(19)	14.0954(6)	8.8537(3)	6.4398(7)
<i>b</i> (Å)	12.2186(11)	10.3528(4)	13.4687(5)	7.8355(8)
<i>c</i> (Å)	13.5664(12)	21.8652(9)	10.9671(4)	21.922(2)
α (°)	69.0720(10)	90	90	90
β (°)	89.2750(10)	98.874(1)	111.226(1)	91.983(2)
γ (°)	84.6070(10)	90	90	90
<i>V</i> (Å ³)	1663.0(3)	3152.5(2)	1219.08(8)	1105.5(2)
<i>Z</i>	2	4	2	2
ρ_{calc} (g cm ⁻³)	1.541	1.548	1.587	1.670
<i>T</i> (K)	297(2)	173(2)	223(2)	100(2)
μ (mm ⁻¹) (Mo K α)	1.005	1.084	1.378	1.282
<i>F</i> (000)	780	1496	588	560
θ for data coll. (°)	2.46–28.32	2.45–29.99	2.47–29.98	2.76–29.99
Compl. to $\theta = 30^\circ$	99.3 %	99.4 %	99.6 %	99.6 %
No. of rflns measured	22229	28633	13449	8641
No. of unique rflns	8236	4577	3537	3192
No. of params	392	191	122	133
<i>R</i> ₁ (<i>I</i> > 2 σ (<i>I</i>)) ^a	0.0349	0.0261	0.0225	0.0411
ωR_2 (<i>I</i> > 2 σ (<i>I</i>)) ^b	0.0835	0.0673	0.0572	0.0809
<i>R</i> ₁ (all data) ^a	0.0467	0.0276	0.0250	0.0448
<i>R</i> ₁ (all data) ^a	0.0896	0.0683	0.0587	0.0820
Largest diff. peak and hole (eÅ ⁻³)	−0.458/0.945	−0.85/0.67	−0.62/0.87	−0.59/0.66

^a $R_1 = \frac{\sum ||F_0| - |F_c||}{\sum |F_0|}$ ^b $\omega R_2 = \left[\frac{\sum (\omega(F_0^2 - F_c^2)^2)}{\sum (\omega(F_0^2)^2)} \right]^{\frac{1}{2}}$

Table B.4: Details for the structure determination of the complexes [Pd(PNP-Ph)Cl]Cl, Pd(SN-Mes)₂Cl₂, Pd(SN-ⁿPr)₂Cl₂, and Pd(SN^H-Ph)₂Cl₂

References

1. Moulton, C. J.; Shaw, B. L. *J. C. S. Dalton* **1976**, 1020.
2. van Koten, G.; Timmer, K.; Noltes, J. G.; Spek, A. L. *J. Chem. Soc. Chem. Commun.* **1978**, 250.
3. Albrecht, M.; van Koten, G. *Angew. Chem. Int. Ed.* **2001**, 40, 3750.
4. van der Boom, M. E.; Milstein, D. *Chem. Rev.* **2003**, 103, 1759.
5. Singleton, J. T. *Tetrahedron* **2003**, 59, 1837.
6. Peveling, K.; Henn, M.; Loew, C.; Mehring, M.; Schuermann, M.; Costisella, B.; Jurkschat, K. *Organometallics* **2004**, 23, 1501.
7. Yao, Q.; Sheets, M. *J. Org. Chem.* **2006**, 71, 5384.
8. van Manen, H.-J.; Nakashima, K.; Shinkai, S.; Kooijman, H.; Spek, A. L.; van Veggel, F. C. J. M.; Reinhoudt, D. N. *Eur. J. Inorg. Chem.* **2000**, 2533.
9. Castonguay, A.; Sui-Seng, C.; Zaragarina, D.; Beauchamp, A. L. *Organometallics* **2006**, 25, 602.
10. Danopoulos, A. A.; Tulloch, A. A. D.; Winston, S.; Eastham, G.; Hursthouse, M. B. *Dalton Trans.* **2003**, 1009.
11. Churrua, F.; SanMartin, R.; Tellitu, I.; Dominguez, E. *Tetrahedron Lett.* **2006**, 47, 3233.
12. Benito-Garagorri, D.; Becker, E.; Wiedermann, J.; Lackner, W.; Pollak, M.; Meriter, K.; Kisala, J.; Kirchner, K. *Organometallics* **2006**, 25, 1900.
13. Tolman, C. A. *Chem. Rev.* **1977**, 77, 313.

14. Olazábal, C. A.; Gabba, F. P.; Cowley, A. H.; Carrano, C. J.; Mokry, L. M.; Bond, M. R. *Organometallics* **1994**, *13*, 412.
15. Carré, F.; Chuit, C.; Corriu, J. P.; Fanta, A.; Mehdi, A.; Reyé, C. *Organometallics* **1995**, *14*, 194.
16. Contel, M.; Nobel, D.; Spek, A. L.; van Koten, G. *Organometallics* **2000**, *19*, 3288.
17. Chen, J.; Angelici, R. J. *Coord. Chem. Rev.* **2000**, 206–207, 63.
18. Angelici, R. J. *Coord. Chem. Rev.* **1990**, *105*, 61.
19. Angelici, R. J. *Organometallics* **2001**, *20*, 1259.
20. Chen, B.-L.; Mok, K.-F.; Ng, S.-C. *J. Chem. Soc., Dalton Trans.* **1998**, 2861.
21. Schirmer, W.; Flörke, U.; Haupt, H.-J. *Z. Anorg. Allg. Chem.* **1987**, *545*, 83.
22. Benito-Garagorri, D. *Synthesis, characterization and catalytic activity of P–N bond containing transition metal pincer complexes*, Thesis, Vienna University of Technology, 2007.
23. Pollak, M. “Synthese neuer N-alkylierter PNP-Pincer-Liganden und katalytische Anwendung ihrer Übergangsmetallkomplexe”, Master’s thesis, Vienna University of Technology, 2006.
24. Lucas, H. J.; Mitchell, Jr., F. W.; Scully, C. N. *J. Am. Chem. Soc.* **1950**, *72*, 5491.
25. Lot, O.; Suisse, I.; Mortreux, A.; Agbossou, F. *J. Mol. Cat. A* **2000**, *164*, 125.
26. Kadyrov, R.; Heller, D.; Selke, R. *Tetrahedron: Asymmetry* **1998**, *9*, 329.
27. Feringa, B. L.; Hulst, R.; Rikers, R.; Brandsma, L. *Synthesis* **1988**, 316.
28. Roth, B.; Smith, J. M.; Hultquist, M. E. *J. Am. Chem. Soc.* **1951**, *73*, 2869.
29. Schirmer, W.; Flörke, U.; Haupt, H.-J. *Z. Anorg. Allg. Chem.* **1989**, *574*, 239.
30. Benito-Garagorri, D.; Kirchner, K. *Acc. Chem. Res.* **2008**, *41*, 201.
31. Biricik, N.; Fei, Z.; Scopelliti, R.; Dyson, P. J. *Helv. Chim. Acta* **2003**, *86*, 3281.
32. Smith, N. L.; Sisler, H. H. *J. Org. Chem.* **1961**, *26*, 5145.

-
33. Moutloali, R. M.; Nevondo, F. A.; Darkwa, J.; Iwuoha, E. I.; Henderson, W. J. *Organomet. Chem.* **2002**, 656, 262.
34. Ho, R. K. Y.; Livingstone, S. E. *Aust. J. Chem.* **1965**, 18, 659.
35. Brunner, H.; Reiter, B.; Riepl, G. *Chem. Ber.* **1984**, 117, 1330.
36. Himbert, G.; Diehl, K.; Schlindwein, H.-J. *Chem. Ber.* **1986**, 119, 3227.
37. Lang, H.-F.; Fanwick, P. E.; Walton, R. A. *Inorg. Chim. Acta* **2002**, 329, 1.
38. Knebel, W. J.; Angelici, R. J. *Inorg. Chim. Acta* **1973**, 7, 713.
39. Knebel, W. J.; Angelici, R. J. *Inorg. Chem.* **1974**, 13, 632.
40. Seidel, W.; Schöler, H. Z. *Chem.* **1967**, 7, 431.
41. Seidel, W. Z. *Chem.* **1967**, 7, 462.
42. Ainscough, E. W.; Peterson, L. K. *Inorg. Chem.* **1970**, 9, 2699.
43. Aucott, S. M.; Slawin, A. M. Z.; Woollins, J. D. *J. Chem. Soc., Dalton Trans.* **2000**, 2559.
44. Storhoff, B. N.; Lewis, Jr., H. C. *Coord. Chem. Rev.* **1977**, 23, 1.
45. Tate, D. P.; Knipple, W. R.; Augl, J. M. *Inorg. Chem.* **1962**, 1, 433.
46. Doney, J. J.; Bergman, R. J.; Heathcock, C. H. *J. Am. Chem. Soc.* **1985**, 107, 3724.
47. Hughes, R. P.; Klauui, W.; Reisch, J. W.; Mueller, A. *Organometallics* **1985**, 4, 1761.
48. Trofimenko, S. *J. Am. Chem. Soc.* **1967**, 89, 3904.
49. Trofimenko, S. *J. Am. Chem. Soc.* **1969**, 91, 588.
50. Enemark, J. H.; Marabella, P. J. *Organomet. Chem.* **1982**, 226, 57.
51. Shiu, K.-B.; Lee, J. Y.; Wang, Y.; Cheng, M.-C.; Wang, S.-L.; Liao, F.-L. *J. Organomet. Chem.* **1993**, 453, 211.
52. Schrock, R. R. *Topics in Organometallic Chemistry* **1998**, 1, 1.

53. Indictor, N.; Brill, W. F. *J. Org. Chem.* **1965**, *30*, 2074.
54. Mimoun, H.; Serée de Roch, I.; Sajus, L. *Bull. Soc. Chim.* **1969**, 1481.
55. Kuehn, F. E.; Zhao, J.; Herrmann, W. A. *Tetrahedron: Asymmetry* **2005**, *16*, 3469.
56. Schrock, R. R. *Acc. Chem. Res.* **2005**, *38*, 955.
57. Baker, P. K. *Chem. Soc. Rev.* **1998**, *27*, 125.
58. Lichtenberger, R. "Synthesis and reactivity of novel molybdenum and tungsten PNP pincer complexes", Master's thesis, Vienna University of Technology, 2006.
59. Douglas, W. M.; Ruff, J. K. *Synth. Inorg. Metal-Org. Chem.* **1972**, *2*, 151.
60. Douglas, W. M.; Ruff, J. K. *J. Chem. Soc. (A)* **1971**, 3558.
61. Höfler, M.; Marre, W. *Angew. Chem.* **1971**, *83*, 174.
62. Ainscough, E. W.; Brodie, A. M.; Wong, S. T. *J. C. S. Dalton* **1977**, 915.
63. Gibson, V. C.; Redshaw, C.; Solan, G. A. *Chem. Rev.* **2007**, *107*, 1745.
64. Small, B. L.; Brookhart, M.; Bennett, A. M. *J. Am. Chem. Soc.* **1998**, *120*, 4049.
65. Britovsek, G. J. P.; Bruce, M.; Gibson, V. C.; Kimberley, B. S.; Maddox, P. J.; Mastroianni, S.; McTavish, S. J.; Redshaw, C.; Solan, G. A.; Strömberg, S.; White, A. J. P.; Williams, D. J. *J. Am. Chem. Soc.* **1999**, *121*, 8728.
66. Bart, S. C.; Lobkovsky, E.; Chirik, P. J. *J. Am. Chem. Soc.* **2004**, *126*, 13794.
67. Bouwkamp, M. W.; Lobkovsky, E.; Chirik, P. J. *J. Am. Chem. Soc.* **2005**, *127*, 9660.
68. Bouwkamp, M. W.; Lobkovsky, E.; Chirik, P. J. *Inorg. Chem.* **2006**, *45*, 2.
69. Archer, A. M.; Bouwkamp, M. W.; Cortez, M.-P.; Lobkovsky, E.; Chirik, P. J. *Organometallics* **2006**, *25*, 4269.
70. Kirchner, K. *Outer-sphere Reaktionskinetik substitutionslabiler Eisenkomplexe in Acetonitril*, Thesis, Vienna University of Technology, 1987.
71. Bolm, C.; Legros, J.; Le Pailh, J.; Zani, L. *Chem. Rev.* **2004**, *104*, 6217.

-
72. Fürstner, A.; Leitner, A.; Méndez, M.; Krause, H. *J. Am. Chem. Soc.* **2002**, *124*, 13856.
73. Scheiper, B.; Bonnekessel, M.; Krause, H.; Fürstner, A. *J. Org. Chem.* **2004**, *69*, 3943.
74. Fürstner, A.; Martin, R.; Majima, K. *J. Am. Chem. Soc.* **2005**, *127*, 12236.
75. Seidel, G.; Leurich, D.; Fürstner, A. *J. Org. Chem.* **2004**, *69*, 3950.
76. Holmquist, C. R.; Roskamp, E. J. *J. Org. Chem.* **1989**, *54*, 3258.
77. Holmquist, C. R.; Roskamp, E. J. *Tetrahedron Lett.* **1992**, *33*, 1131.
78. Padwa, A.; Hornbuckle, S. F.; Zhang, Z.; Zhi, L. *J. Org. Chem.* **1990**, *55*, 5297.
79. Sudrik, S. G.; Balaji, B. S.; Singh, A. P.; Mitra, R. B.; Sonawane, H. R. *Synlett* **1996**, 369.
80. Nomura, K.; Iida, T.; Hori, K.; Yoshii, E. *J. Org. Chem.* **1994**, *59*, 488.
81. Mahmood, S. J.; Hossain, M. M. *J. Org. Chem.* **1998**, *63*, 3333.
82. Mahmood, S. J.; Brennan, C.; Hossain, M. M. *Synthesis* **2002**, 1807.
83. Albisson, D. A.; Bedford, R. B.; Lawrence, S. E.; Scully, P. N. *Chem. Commun.* **1998**, 2095.
84. Nelson, S. M.; Dahlhoff, W. V. *J. Chem. Soc. A* **1971**, *13*, 2184.
85. van Koten, G.; Jastrzebski, J. T. B. H.; Noltes, J. G. *J. Organomet. Chem.* **1978**, *148*, 233.
86. Creaser, C. S.; Kaska, W. C. *Inorg. Chim. Acta* **1978**, *30*, 325.
87. Tietze, L. F.; Ila, H.; Bell, H. P. *Chem. Rev.* **2004**, *104*, 3453.
88. Zeni, G.; Larock, R. C. *Chem. Rev.* **2004**, *104*, 2285.
89. Culkin, D. A.; Hartwig, J. F. *Acc. Chem. Res.* **2003**, *36*, 234.
90. Bellina, F.; Carpita, A.; Rossi, R. *Synthesis* **2004**, *15*, 2419.
91. Miyaura, N.; Suzuki, A. *Chem. Rev.* **1995**, *95*, 2457.

92. Littke, A. F.; Fu, G. C. *Angew. Chem. Int. Ed.* **2002**, *41*, 4176.
93. Dupont, J.; Pfeffer, M.; Spencer, J. *Eur. J. Inorg. Chem.* **2001**, 1917.
94. Beletskaya, I. P.; Cheprakov, A. V. *Chem. Rev.* **2000**, *100*, 3009.
95. Morales-Morales, D.; Redón, R.; Yung, C.; Jensen, C. M. *Chem. Commun.* **2000**, 1619.
96. Bedford, R. B.; Draper, S. M.; Scully, P. N.; Welch, S. L. *New J. Chem.* **2000**, *24*, 745.
97. Morales-Morales, D.; Grause, C.; Kasaoka, K.; Redón, R.; Cramer, R. E.; Jensen, C. M. *Inorg. Chim. Acta* **2000**, *300*, 958.
98. Ohff, M.; Ohff, A.; van der Boom, M. E.; Milstein, D. J. *Am. Chem. Soc.* **1997**, *119*, 11687.
99. Beletskaya, I. P.; Chuchurjukin, A. V.; Dijkstra, H. P.; van Klink, G. P. M.; van Koten, G. *Tetrahedron Lett.* **2000**, *41*, 1075.
100. Crisp, G. T. *Chem. Soc. Rev.* **1998**, *27*, 427.
101. Mas-Marza, E.; Segarra, A. M.; Claver, C.; Peris, E.; Fernández, E. *Tetrahedron Lett.* **2003**, *44*, 6595.
102. Denmark, S. E.; Stavenger, R. A.; Faucher, A. M.; Edwards, J. P. *J. Org. Chem.* **1997**, *62*, 3375.
103. Schlenk, C.; Kleij, A. W.; Frey, H.; van Koten, G. *Angew. Chem. Int. Ed.* **2000**, *39*, 3445.
104. Takenaka, K.; Uozumi, Y. *Org. Lett.* **2004**, *6*, 1833.
105. Lobana, T. S.; Bawa, G.; Hundal, G.; Pannu, A. P. S.; Butcher, R. J.; Liaw, B.-J.; Liu, C. W. *Polyhedron* **2007**, *26*, 4993.
106. Lu, W.; Chan, M. C. W.; Zhu, N.; Che, C.-M.; Li, C.; Hui, Z. *J. Am. Chem. Soc.* **2004**, *126*, 7639.
107. Constable, E. C.; Henney, R. P. G.; Raitby, P. R.; Sousa, L. R. *J. Chem. Soc. Dalton Trans.* **1992**, 2251.

-
108. Hwang, W.-S.; Lai, J.-H.; Wang, D.-L.; Chiang, M. Y. *J. Chin. Chem. Soc.* **1999**, *46*, 529.
109. Wiedermann, J.; Benito-Garagorri, D.; Kirchner, K.; Mereiter, K. *Acta Cryst.* **2006**, *E62*, m1106.
110. Weissman, H.; Milstein, D. *Chem. Commun.* **1999**, 1901.
111. Botella, L.; Nájera, C. *Angew. Chem. Int. Ed.* **2002**, *41*, 179.
112. Baleizão, C.; Corma, A.; García, H.; Leyva, A. *Chem. Commun.* **2003**, 606.
113. Vila, J. M.; Gayoso, M.; Pereira, M.; Torres, M. L.; Fernández, J. J.; Fernández, A.; Ortigueira, J. M. *J. Organomet. Chem.* **1996**, *506*, 165.
114. Bedford, R. B.; Blake, M. E.; Butts, C. P.; Holder, D. *Chem. Commun.* **2003**, 466.
115. Bedford, R. B. *Chem. Commun.* **2003**, 1787.
116. Bedford, R. B.; Cazin, C. S. J. *Chem. Commun.* **2001**, 1540.
117. Bedford, R. B.; Cazin, C. S. J.; Coles, S. J.; Gelbrich, T.; Horton, P. N.; Hursthouse, M. B.; Light, M. E. *Organometallics* **2003**, *22*, 987.
118. Biffis, A.; Zecca, M.; Basato, M. *J. Mol. Catal. A: Chem.* **2001**, *173*, 249.
119. Sommer, W. J.; Yu, K.; Sears, J. S.; Ji, Y.; Zheng, X.; Davis, R. J.; Sherrill, C. D.; Jones, C. W.; Weck, M. *Organometallics* **2005**, *24*, 4351.
120. Eberhard, M. R. *Org. Lett.* **2004**, *6*, 2125.
121. Viciu, M.; Kelly, R. A.; Stevens, E. D.; Naud, F.; Studer, M.; Nolan, S. P. *Org. Lett.* **2003**, *5*, 1479.
122. Trzeciak, A. M.; Ziółkowski, J. J. *Coord. Chem. Rev.* **2005**, *249*, 2308.
123. Grasa, G. A.; Hillier, A. C.; Nolan, S. P. *Org. Lett.* **2001**, *3*, 1077.
124. Domin, D.; Benito-Garagorri, D.; Mereiter, K.; Fröhlich, J.; Kirchner, K. *Organometallics* **2005**, *24*, 3957.
125. Perrin, D. D.; Armarego, W. L. F. *Purification of laboratory chemicals*, 3rd ed.; Pergamon Press, New York: 1988.

126. Watson, S. C.; Eastham, J. F. *J. Organomet. Chem.* **1967**, *9*, 165.
127. Sheldrick, G. M. *SADABS: Program for absorption correction*; University of Göttingen, Germany: 1996.
128. Sheldrick, G. M. *SHELXS97: Program for the solution of crystal structures*; University of Göttingen, Germany: 1997.
129. Sheldrick, G. M. *SHELXL97: Program for crystal structure refinement*; University of Göttingen, Germany: 1997.
130. Spek, A. L. *PLATON: A multipurpose crystallographic tool*; University of Utrecht, The Netherlands: 2004.
131. Frisch, M. J. *et al. Gaussian 03, Revision C.02*; Gaussian, Inc., Wallingford, CT: 2004.
132. Haeusermann, U.; Dolg, M.; Stoll, H.; Preuss, H. *Mol. Phys.* **1993**, *78*, 1211.
133. Kuechle, W.; Dolg, M.; Stoll, H.; Preuss, H. *J. Chem. Phys.* **1994**, *100*, 7535.
134. Leininger, T.; Nicklass, A.; Stoll, H.; Dolg, M.; Schwerdtfeger, P. *J. Chem. Phys.* **1996**, *105*, 1052.
135. McLean, A. D.; Chandler, G. S. *J. Chem. Phys.* **1980**, *72*, 5639.
136. Krishnan, R.; Binkley, J. S.; Seeger, R.; Pople, J. A. *J. Chem. Phys.* **1980**, *72*, 650.
137. Wachters, A. H. *J. Chem. Phys.* **1970**, *52*, 1033.
138. Hay, P. J. *J. Chem. Phys.* **1977**, *66*, 4377.
139. Raghavachari, K.; Trucks, G. J. *J. Chem. Phys.* **1989**, *91*, 1062.
140. Binning, R. C.; Curtiss, L. A. *J. Comput. Chem.* **1995**, *103*, 6104.
141. McGrath, M. P.; Radom, L. *J. Chem. Phys.* **1991**, *94*, 511.
142. Miertus, S.; Scrocco, E.; Tomasi, J. *J. Chem. Phys.* **1981**, *55*, 117.
143. Pascual-Ahuir, J. L.; Silla, E.; Tomasi, J.; Bonaccorsi, R. *J. Comput. Chem.* **1987**, *8*, 778.
144. Floris, F.; Tomasi, J. *J. Comput. Chem.* **1989**, *10*, 616.

145. Tomasi, J.; Persico, M. *Chem. Rev.* **1994**, *94*, 2027.
146. Drew, D.; Doyle, J. R. *Inorg. Synth.* **1990**, *28*, 346.

Lebenslauf

DI Julia Wiedermann

Ulmenweg 11

2301 Groß-Enzersdorf

Tel.: 01 58801 15343

E-Mail: jwiedermann@ioc.tuwien.ac.at

Persönliche Informationen

Geburtsdatum	22. Oktober 1978
Geburtsort	Wien
Staatsbürgerschaft	Österreich
Familienstand	ledig
Fremdsprachen	Englisch fließend, Italienisch, Französisch

Ausbildung

September 2004–März 2008	Dissertation am Institut für Angewandte Synthesechemie, Abteilung Metallorganische Chemie
März 2004	zweite Diplomprüfung mit Auszeichnung bestanden
Februar 2003–Februar 2004	Diplomarbeit <i>Beiträge zur stereoselektiven Synthese von Salmeterol-Metaboliten</i> am Institut für Angewandte Synthesechemie, Abteilung Organische Chemie
Dezember 2000	erste Diplomprüfung
Juni 1997	Matura mit Auszeichnung bestanden
1989–1997	Neusprachliches Gymnasium

Publikationen

1. *Achiral and Chiral Transition Metal Complexes with Modularly Designed Tridentate PNP Pincer-Type Ligands Based on N-Heterocyclic Diamines* Benito-Garagorri, D.; Becker, E.; Wiedermann, J.; Lackner, W.; Pollak, M.; Mereiter, K.; Kisala, J.; Kirchner, K. *Organometallics* **2006**, 25, 1900-1913.
2. *[N,N'-Bis(diphenylphosphino)pyridine-2,6-diamine- κ^3 P,N¹,P']chloropalladium(II) chloride monohydrate 1,2-dichloroethane solvate* Wiedermann, J.; Benito-Garagorri, D.; Kirchner, K.; Mereiter, K. *Acta Crystallogr., Sect. E: Struct. Rep. Online* **2006**, E62, m1106-m1108.
3. *Palladium imine and amine complexes derived from 2-thiophenecarboxaldehyde as catalysts for the Suzuki cross-coupling of aryl bromides* Wiedermann, J.; Mereiter, K.; Kirchner, K. *J. Mol. Catal. A: Chem.* **2006**, 257, 67-72.
4. *Iron(II) Complexes Bearing Tridentate PNP Pincer-Type Ligands as Catalysts for the Selective Formation of 3-Hydroxyacrylates from Aromatic Aldehydes and Ethyldiazoacetate* Benito-Garagorri, D.; Wiedermann, J.; Pollak, M.; Mereiter, K.; Kirchner, K. *Organometallics* **2007**, 26, 217-222.